# Development of Prodrugs to Deliver Super-Potent Drugs to Prostate Tumors

Twum, Elvis

*Award date:*
2013

*Awarding institution:*
University of Bath

# DEVELOPMENT OF PRODRUGS TO DELIVER SUPER-POTENT DRUGS TO PROSTATE TUMOURS

Elvis Asare Twum

A thesis submitted for the degree of Doctor of Philosophy

University of Bath

Department of Pharmacy and Pharmacology

September 2013



Signed.....

Date.....

## Acknowledgement

I would like to express my sincere gratitude to my supervisors Prof Michael Threadgill, Dr Andrew Thompson and Dr Matthew Lloyd for their help during my PhD programme. A special thanks to Prof Michael Threadgill for giving me the opportunity to undertake this PhD project. It has been a privilege to work under his supervision.

I would also like to say thank you to Dr Amit Nathubhai and Dr Elizabeth O'Donovan for their support in the laboratory. I am grateful to Dr Anne Beauchard and Dr Richard Patterson for their assistance during my early days in the laboratory.

My appreciation goes towards Mulham Al-Muhammad and Mujeeb Zia for their assistance in undertaking the DNA alkylation assay. My gratitude to Wenyi Wang for her contributions towards my project.

I am grateful to Dr Timothy Woodman for his help with NMR data and all the contributions he made towards my project. Thanks to Dr Anneke Lubben for her help in solving complex mass spectrometry data. I will also like to thank Dr Pauline Wood for her immense help when I was undertaking the MTS assays. Thanks to Dr Ian Eggleston for allowing me to use his HPLC equipment during my project.

I am very grateful to Prostate Cancer UK for their sponsorship of this project.

# Abstract

Conventional treatments for prostate cancer have significant limitations making it difficult to control the disease. Cyclopropabenzindoles (CBI) are more biologically potent, stable and synthetically accessible analogues of cyclopropapyrroloindole (CPI) anti-tumour antibiotics, such as duocarmycin-SA and CC1065. A polymeric prodrug carrying a CBI drug attached to the polymeric backbone through a PSA-cleavable linker peptide has two modes of selectivity: activation by PSA and the EPR effect. To synthesise a 5-amino-*seco*-CBI analogue, 2,4-di-nitronaphthalen-1-ol gave di-Boc-1-iodonaphthalene-2,4-diamine in five steps (triflation, $S_NAr$ displacement with iodide, reduction (loss of iodine), protection and restoration of the iodine. For the amino-*seco*-CBI, it was important to discriminate between $N^2$ and $N^4$. Acidic removal of the Boc-group(s) resulted in deiodination. NMR investigations showed an unexpected Wheland-like cationic intermediate. $N^3$ of naphthalene-1,3-diamine was selectively trifluoroacetylated and $N^1$ was masked with Boc. Electrophilic iodination gave an orthogonally protected 1-iodonaphthalene-2,4-diamine. Allylation at the trifluoroacetamide was followed by free radical cyclisation with TEMPO trap. Removal of the trifluoroacetyl group allowed coupling to 5-(2-(dimethylamino)ethoxy)-*1H*-indole-2-carboxylic acid. Reductive removal of 2,2,6,6-tetramethylpiperidine, substitution of the exposed hydroxy group with chloride and removal of the Boc-group gave the amino-*seco*-CBI drug, 5-amino-1-chloromethyl-3-(5-(2-dimethylaminoethoxy)indole-2-carbonyl)-2,3-dihydro-1*H*-benz[*e*]indole. A DNA-melting assay confirmed that it binds very strongly to dsDNA causing a 13 deg. C increase in melting temperature. The drug was a highly potent cytotoxin *in vitro*, with $IC_{50}$ = 18 nM against LNCaP prostate cancer cells. The polymeric prodrug system involved the synthesis of the pentapeptide SSKLQ. The amide side chain of glutamine can be masked as the nitrile and this can be quantitatively hydrated to the γ-carboxamide of L-Gln with hydroperoxide. The pentapeptide was coupled to 4-methoxynaphthalen-1-amine and to poly(ethylene glycol) as a model polymeric prodrug system. Efficient release of the model drug from the polymeric prodrug by PSA will allow this polymeric prodrug system to be adopted for the synthesised amino-*seco*-CBI drug.

# Publications

Beauchard, A.; Twum, E. A.; Lloyd, M. D.; Threadgill, M. D. *S*-2-Amino-4-cyanobutanoic acid (β-cyanomethyl-L-Ala) as an atom-efficient solubilising synthon for L-glutamine. *Tetrahedron Lett*. **2011**, *52*, 5311-5314.

Twum, E. A.; Woodman, T. J.; Wang, W.; Threadgill, M. D. Observation by NMR of cationic Wheland-like intermediates in the de-iodination of protected 1-iodonaphthalene-2,4-diamines in acidic media. *Org. Biomol. Chem.* **2013**, *11*, 6208–6214.

# Contents

# List of Figures

# List of Tables



# List of Schemes

# Abbreviations

| | |
|---|---|
| AcOH | Acetic acid |
| ACT | α-1-Antichymotrypsin |
| ADEPT | Antibody-directed enzyme prodrug therapy |
| AMC | 7-Amino-4-methyl coumarin |
| A2M | α-2-Macroglobulin |
| API | α-1-Trypsin inhibitor |
| Aq | Aqueous |
| AR | Androgen receptors |
| Bn | Benzyl |
| Boc | *tert*-Butoxycarbonyl |
| $Boc_2O$ | Di-*tert*-butyl dicarbonate |
| BPH | Benign prostatic hyperplasia |
| $Bu^tO^-K^+$ | Potassium *tert*-butoxide |
| $Bu^t$ | *tert*-Butyl |
| CbBI | 1,2,10,11-Tetrahydro-9*H*-cyclobuta[*c*]benzo[*e*]indol-4-one |
| CBI | 1,2,9,9a-Tetrahydrocyclopropa[*c*]benz[*e*]indole-4-one |
| CBIn | 1,2,9,9a-Tetrahydro-1*H*-cyclopropa[*c*]benz[*e*]inden-4-one |
| CBQ | 5-Oxo-1,2,10,10a- tetrahydrobenzo[*f*]cyclopropa[*d*]quinoline-3(5*H*)-carboxylate |
| Cbz | Carboxybenzyl |
| CCBI | 7-Cyano-1,2,9,9a-tetrahydrocyclopropa[*c*]benz[*e*]indol-4-one |
| CI | 1,2,7,7a-Tetrahydrocyclopropa[1,2-c]indol-4-one |
| CNA | 6-Oxo-2,3,11,11a-tetrahydro-1*H*-cyclopropa[*c*]naphtho[2,1-b]azepine-4(6*H*)-carboxylate |
| CpG | Cytosine-phosphate diester-guanine |
| CPI | Cyclopropapyrroloindole |
| CZ | Central zone |
| DA | Duocarmycin A |
| DSA | Duocarmycin SA |
| DCC | N,N'-Dicyclohexylcarbodiimide |
| DCU | Dicyclohexylurea |
| DMA | Dimethylacetamide |
| DMAP | 4-Dimethylaminopyridine |

| | |
|---|---|
| DMEM | Dulbecco's Modified Eagle's Medium |
| DMF | Dimethylformamide |
| DMP | 2,2-Dimethoxypropane |
| dmP | 5,5-Dimethyl-L-proline |
| DKP | Diketopiperazines |
| Dmo | 5,5-Dimethyl-4-oxaproline |
| DMSO | Dimethylsulfoxide |
| Dmt | 5,5-Dimethyl-4-thiaproline |
| DRE | Digital rectal examination |
| dThd | Thymidine |
| EBRT | External beam radiotherapy |
| EDA | Ethylenediamine |
| EDC | 1-Ethyl-3-(3-dimethylaminopropyl)carbodiimide |
| EDTa | Ethylenediaminetetraacetic acid |
| EPR | Enhanced permeability and retention effect |
| ERG | v-ets avian erythroblastosis virus E26 oncogene homolog |
| $Et_3N$ | Triethylamine |
| $Et_2O$ | Diethylether |
| EtOAc | Ethylacetate |
| EtOH | Ethanol |
| ETV1 | ets variant 1 |
| FBS | Foetal bovine serum |
| $F_2CBI$ | 9,9-Difluoro-1,2,9,9a-tetrahydrocyclopropa(*c*)benzo(*e*)indol-4-one |
| Fmoc | 9-Fluorenylmethoxycarbonyl |
| fPSA | Free prostate-specific antigen |
| FSH | Follicle stimulating hormone |
| GDEPT | Gene directed enzyme prodrug therapy |
| Gln | Glutamine |
| GSTP1 | Glutathione S-transferase pi 1 |
| HATU | O-(7-azabenzotriazol-1-yl)-N,N,N′,N′-tetramethyluronium hexafluorophosphate |
| HiFU | High-frequency ultrasound |
| HOBt | Hydroxybenzotriazole |
| HPLC | High performance liquid chromatography |
| HPMA | N-(2-hydroxypropyl)methacrylamide |

| | |
|---|---|
| $IC_{50}$ | Concentration required for 50% inhibition of activity |
| IR | Infrared |
| *J* | Coupling constant |
| Leu | Leucine |
| LH | Luteinizing hormone |
| LHRH | Luteinizing hormone-releasing hormone |
| Lit | Literature |
| Lys | Lysine |
| MCBI | 7-methoxy-1,2,9,9a-tetrahydrocyclopropa[*c*]benz[*e*]indol-4-one |
| MeOH | Methanol |
| Mp | Melting point |
| Ms | Methanesulfonyl |
| *MSR1* | Macrophage scavenger receptor 1 |
| MTS | 3-(4,5-Dimethylthiazol-2-yl)-5-(3-carboxymethoxyphenyl)-2-(4-sulfophenyl)- 2*H*-tetrazolium, inner salt |
| c-MyC | Avian myelocytomatosis viral oncogene homolog |
| Mu | Morpholinocarbonyl |
| *m/z* | Mass to charge ratio (mass spectrometry) |
| NIS | N-Iodosuccinimide |
| PABA | 4-Aminobenzyl alcohol |
| PBS | Phosphate buffered saline |
| PCa | Prostate cancer |
| PEG | Poly(ethylene glycol) |
| PIA | Proliferative inflammatory atrophy |
| PMT | Prodrug monotherapy |
| PIN | Prostatic intraepithelial neoplasia |
| PSA | Prostate-specific antigen |
| PyBOP | Benzotriazol-1-yl-oxytripyrrolidinophosphonium hexafluorophosphate |
| PZ | Peripheral zone |
| $R_f$ | Retention factor |
| RNASEL | Ribonuclease L (2',5'-oligoisoadenylate synthetase-dependent) |
| RNS | Reactive nitrogen species |
| ROS | Reactive oxygenative species |
| RP | Reverse phase |
| Ser | Serine |

| | |
|---|---|
| SPB | Sodium phosphate buffer |
| TAPS | Tumour-activated prodrugs |
| TBHP | *tert*-Butyl hydroperoxide |
| TEMPO | (2,2,6,6-Tetramethylpiperidin-1-yl)oxyl |
| TFA | Trifluoroacetic acid |
| THF | Tetrahydrofuran |
| TLC | Thin layer chromatography |
| $T_m$ | Transition-melting temperature |
| TMI | Trimethoxyindole |
| TNM | Tumour, lymph nodes and metastasis |
| tPSA | Total prostate-specific antigen |
| TMPRSS2 | Transmembrane protease serine 2 |
| Tris | Tris(hydroxymethyl)aminomethane |
| TRUS | Trans-rectal ultrasound |
| TsOH- | *para*-Toluenesulfonic acid |
| TZ | Transition zone |
| UGS | Urogenital sinus |
| UV | Ultraviolet |
| VIS | Visible |

# 1 Introduction

The walnut-sized prostate gland is the site of two of the most commonly encountered medical problems in elderly men; benign prostatic hyperplasia (BPH) and prostate cancer (PCa). The prostate gland is part of the male reproductive system lying in front of the rectum just beneath the bladder and surrounding the upper part of the urethra.

## 1.1 Prostate development

The development of prostate gland starts around the $10^{th}$ week of gestation triggered by production of testosterone by the foetal testis around week 8. Binding of α-dihydrotestosterone to androgen receptors in surrounding mesenchymal tissue causes the initial growth of prostate buds from the urogenital sinus (UGS). These outgrowths undergo extensive morphogenesis during the latter days of foetal growth. Influence of androgens during the postnatal stage results in further differentiation and development of the secretory role of the prostate. The posterior part of the prostate is the glandular region, whilst the anterior section of the prostate is entirely fibromuscular in nature.[1] Up to 40% of PCa occurs in the anterior section of the prostate gland.[2]

## 1.2 Zones of the prostate

The prostate consists of four anatomical zones based on biological and histological concepts. The zones originate from the prostatic urethra and have different features.[3]

### 1.2.1 Peripheral zone

The peripheral zone (PZ) is the outermost area and consists of relatively small and round uniformly distributed acini. It has a fibromuscular stroma made up of a meshwork of loosely arranged smooth muscle fibres separated by numerous collagen fibres and irregular spaces. This zone consists of columnar secretory cells with small uniform basal nuclei and regular luminal border. The PZ makes up about 70% of the glandular part of the prostate. The majority of prostate carcinoma occurs in this zone. [3, 4]

### 1.2.2 Central zone

The epithelium of the central zone (CZ) consists of a stroma containing muscle fibres closely-packed together and extending to the borders of the acini. The acini in the central zone are large and relatively rectangular in cross section and are separated by the stroma. Irregularly

arranged secretory cells with large nuclei are seen in this zone. There are fewer stromal components in CZ compared to PZ and transition zone (TZ). About 25% of the glandular prostate that surrounds the ejaculatory duct is the central zone. The zone is said to be resistant to cancer and other disease.[3, 4]

### 1.2.3 Transition zone

The transition zone rests next to the urethra and its morphology resembles that of the peripheral zone. The acini are uniformly distributed and the stroma consists of compactly arranged smooth muscle and collagen fibres. The zone grows with age and is frequently the site for benign prostatic hyperplasia.[3, 4]

### 1.2.4 Periurethral zone

This zone contains underdeveloped small ducts and acini. Muscle and collagen fibres in the periurethral region are compactly arranged. It makes up just a small fraction of the transition zone.[3]

## 1.3 Functions of the prostate gland

The prostate gland has a range of functions including its participation in the control of urine output from the bladder through its mass and musculature. It also aids in the transmission of seminal fluid during ejaculation. As an exocrine gland, it contributes to the seminal plasma by secreting a thick, milky-white fluid which is liquefied by prostate-specific antigen (PSA), an enzyme also secreted by the prostate. The liquefied milky fluid becomes part of the semen. This fluid contains small molecules and enzymes like coagulase and fibrinolysin which help fertility and are involved in coagulation. Prostatic secretion reduces the acidity of urethra and helps to keep sperm viable. The secretion also help improves the motility of sperm. Prostatic acid phosphatase produced by the prostate is directly involved in the nutrition of sperm cells by hydrolysing phosphorylcholine to choline. The prostate helps with the rapid metabolism of testosterone to dihydrotestosterone and appears to be responsible for the high level of zinc in the seminal plasma which acts as an antibacterial agent helping to protect sperms.[5, 6]

## 1.4 Prostate conditions

The prostate gland is prone to a number of medical conditions but mainly, benign prostatic hyperplasia (BPH), prostatitis and prostate cancer (PCa).

### 1.4.1 Benign prostatic hyperplasia (BPH)

Benign prostatic hypertrophy is defined as an increased in number of parenchymal cells and occurs almost exclusively in the transition zone of the prostate gland.[7] The condition is associated with age and around 60% of men aged 60 years and above have a degree of prostate enlargement. Causes are unknown but BPH is thought to be associated with hormonal changes, food and lifestyle. Symptoms include increased urinary frequency and weakened urinary flow as the enlargement places pressure on the bladder and the urethra. Treatment options include lifestyle changes, medications and surgery. BPH does not necessarily increase one's chance of getting prostate cancer.[8-10]

### 1.4.2 Prostatitis

Prostatitis is the inflammation of the tissues of the prostate gland. This can be due to infection (acute) or idiopathic in origin (chronic). Infection is mainly due to *E. coli*. It is estimated that one in seven men will develop at least one episode of prostatitis in their lifetime. Unlike other prostate conditions, prostatitis affects men of all ages (~10%) with majority of incidence present in those in their 40s. Symptoms include pelvic pain and pain on urination. It is managed with medications (*e.g.* antibiotics and pain killers).[11-13]

### 1.4.3 Prostate cancer

In the UK, prostate cancer (PCa) is the most common cancer in men. Early intervention is critical for successful treatment but most men do not seek help until it is too late.[14]

#### 1.4.3.1 Incidence

There is a 40% lifetime risk of developing prostate cancer for a male born in the Western world. The risk of becoming symptomatic is, however, only 10%.[15] About 14% of male cancers are prostate cancers in developed countries compared to 4% of male cancers in less-developed countries. Prostate cancer is the most common solid tumour in Europe accounting for an incidence rate of 214 cases per 1000 men.[16] About 190,000 new cases of prostate cancer are recorded in Europe yearly.[17] There are 21,400 new cases of PCa diagnosed in the UK annually, a rate of 74 cases per 100,000.[15] In England and Wales, one in thirteen men is affected by prostate cancer.[18]

#### 1.4.3.1.1 Age-adjusted incidence

PCa is rare under the age of 40 and the incidence increases exponentially with age. Age-adjusted incidence rates vary worldwide, with the highest rate found in African Americans (185.4 per 100,000 person-years) whilst the lowest incidence is found in Asian countries (*e.g.* China, India, Thailand, Pakistan, and Shanghai; 3-7 per 100,000 person-years). Incidence rates in Europe vary (15-100 per 100,000 person-years) and are highest in Western Europe. Incidence data from African countries is sparse with incidence apparently ranging 2-37 per 100,000 person-years).[19, 20]

### 1.4.3.2 Mortality

Prostate cancer is the second most common cause of deaths in men in most developed countries.[16] Higher mortality rates are recorded in Western nations compared to the lower mortality in low-risk Asian countries (Figure 1)[20].

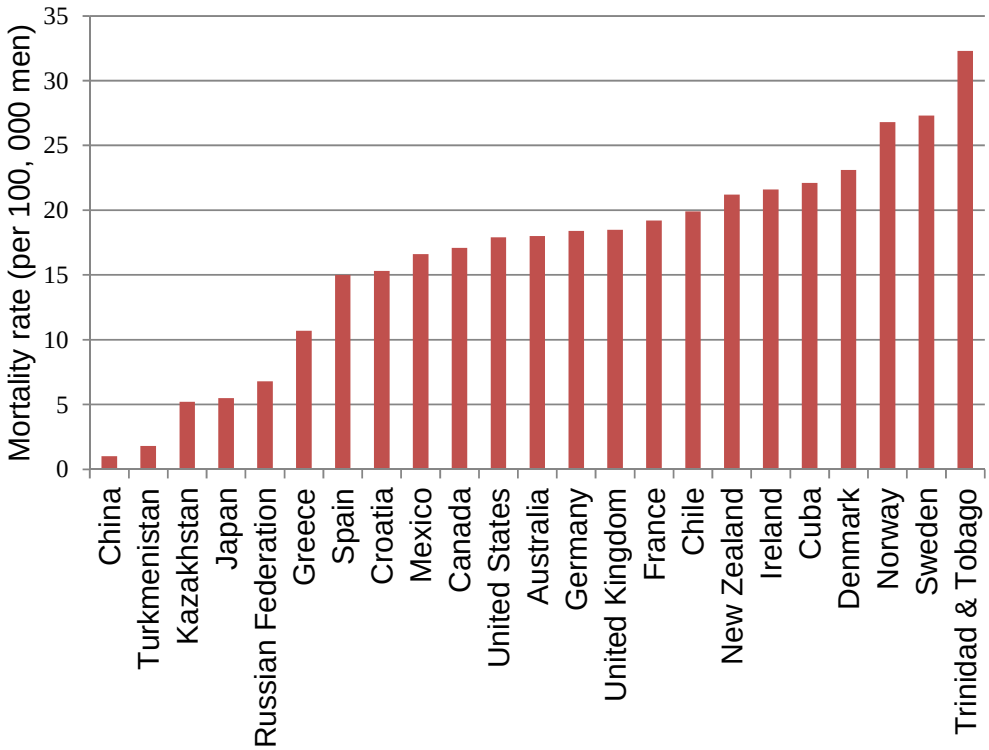


**Figure 1:** Age-adjusted prostate cancer mortality rates per 100,000 men in various countries for the year 2000.[20]

Carribean nations with large populations of men of African descent have the highest rate of mortality (30.3-47.9 per 100,000 person-years) and mortality in Asian countries (South Korea, Philippines and Japan) is the lowest (1.6-4.4 per 100,000 person-years).[19] The disease accounts for about 80,000 deaths per year in Europe.[17] There has been a slight increase in

death rate since 1985 in most countries.[16] Death rates have trebled in the last thirty years in England and Wales.[18]

#### 1.4.3.3 Aetiology

Seventy-seven loci suspected to be associated with PCa development have been identified.[21] Prostate cancer is thought to be due to a series of genetic mutational events which begins with the loss of tumour suppressive genes like p53 and p21. Mutation of p53 occurs in up to 64% and that of p21 up to 55% in prostate tumours. The gene, p73, which has significant homology with p53, also appears to be mutated in many prostate cancers. The most mutated tumour suppressor gene in prostate cancer is MMAC1 / p10 and this may be responsible for acquisition of the metastatic phenotype. Over-expression of mutant p53 and bcl-2 family proteins (regulates apoptosis), as well as amplification of the androgen receptor, appears to be related to the development of the hormone-refractory phenotype of prostate cancer.[18] The genes RNASEL and MSR1 are linked to some familial clusters of PCa. RNASEL encodes for a ribonuclease enzyme responsible for the degradation of cellular and viral DNA upon infection and MSR1 encodes for subunits of a macrophage scavenger. Four brothers with PCa were found to carry RNASEL alleles with the base substitution $795^{G\rightarrow T}$, whilst, in another four of the six affected brothers, it was found that they carried RNASEL alleles with a base substitution $3^{G\rightarrow A}$.[7] Defective MSR1 alleles have been found to be linked to familial PCa and also sporadic PCa cases.[7] Germline mutation in BRCA2, which has a tumour suppressor role, can also increase the relative risk of prostate cancer by 4.65.[21-23] It is estimated that between 0.8-2% of men with early-onset prostate cancer have BRCA2 mutation.[23] A genetic variant linked with prostate cancer in European and Africans has been identified on chromosome 8q24. This genetic variant occurs at high frequency in African Americans which could explain why the incidence of prostate cancer is high in this group of people. Other important aetiological factors include diet, pattern of sexual behaviour, alcohol, and ultraviolet radiation exposure.[17]

#### 1.4.3.4 Risk factors

A range of risk factors are implicated in the development of PCa. Some of these risk factors are modifiable (*e.g.* diet, exercise) whilst others are non- modifiable (*e.g.* age, family history).

#### 1.4.3.4.1 Age

Prostate cancer incidence increases exponentially with age, an increase faster than for other malignancies.[19] There is an increase in risk from 0.005% among individuals aged < 39 years to a risk of 2.2% for those aged 40-59 years and 19.7% in those aged 60-79 years. Studies suggests that a 50-year-old male has a lifetime risk of 42% for showing histological evidence of PCa, a 9.5% risk of developing the disease and a 2.9% risk of dying from the disease.[20]

#### 1.4.3.4.2 Family history and genetic susceptibility

The risk of PCa at least doubles if one first-line relative has the disease, increasing by 5-11-fold if two or more first-line relatives are affected. About 9% of individuals with PCa have true hereditary PCa which is defined as having three or more relatives affected or having at least two relatives who developed the disease before the age of 55.[16] Men with positive family history tend to be diagnosed earlier (~6 to 7 years) than those whose first degree relatives are not affected by the disease. Studies suggest that 5-10% of all PCa cases and up to 40% of PCa occurring in men < 55 years may be due to heredity.[20] Men with family history of breast cancer (mutated BRCA1 and BRCA2 genes) have been linked to an increased risk of PCa.[23]

#### 1.4.3.4.3 Diet and physical activities

Exercise has a tendency to decrease the risk of prostate cancer with smoking increasing the risk. The relationship with consumption of alcohol is, however, unknown. Body-mass index and lean body mass are positively correlated to the risk of prostate cancer. Intake of tomatoes (containing the antioxidant lycopenes) and cruciferous vegetables (containing the antioxidant sulforaphane) is found to reduce risk to the disease. Diets poor in selenium and Vitamin E can also increase the risk of PCa. Consumption of soya products with high concentrations of phyto-oestrogens has a protective effect against prostate cancer.[7, 17] Other environmental factors implicated in PCa are high intake of saturated fat and exposure to radiation.[18] Increased total fat intake, animal fat intake and consumption of red meat have been linked with increased risk of prostate cancer. Meats cooked at high temperatures or grilled on charcoal grills produce heterocyclic aromatic amine and polycyclic aromatic hydrocarbon carcinogens (*e.g.* 2-amino-1-methyl-6-phenylimidazo[4,5-b]pyridine) which caused prostate cancer when fed to rats.[24]

#### 1.4.3.4.4 Occupation

Studies have shown that farmers and other agricultural workers have a 7-12% increased risk of prostate cancer. This could be due to chemicals encountered in agriculture, such as fertilisers, solvents pesticides and herbicides which have a variety of poorly characterised effects. Furthermore, people working in heavy industries, rubber manufacturing and newspaper printing may be at increased risk, suggesting that exposure to certain chemicals or other factors may increase the risk of prostate cancer.[19]

#### 1.4.3.4.5 Sex steroid hormones

There is little evidence to suggest that overexposure to androgens causes human PCa. However, men castrated before puberty tend to have atrophic prostates, which are not prone to PCa.[7, 25] Relatively high levels of testosterone have been found in African-American men, which might explain the higher incidence of PCa compared to Caucasian men.[25] Studies in animals have demonstrated that testosterone can promote or even initiate the development of PCa. An explanation given is that through the action of aromatase, testosterone is converted to oestrogens which act as a carcinogen similar to its effect in the development of breast cancer. Supporting this is the fact that several countries with high rates of PCa also have a high breast cancer rates. Caucasians tend to have lower oestrogen levels, compared to African-Americans who have higher PCa rate. Administration of 17β-oestradiol to adult male Wistar rats increased prostatic inflammation.[7, 26]

#### 1.4.3.4.6 Infections and inflammation

Men with prostatitis display a relative risk of 1.3 towards developing PCa. Men at young ages with high levels of PSA, (probably indicating damage or dysfunction to the prostate epithelium by infection), tend to be at higher risk. A study has shown that men between 40-50 years whose PSA level is greater than 0.6 ng $mL^{-1}$ have a relative risk of 3.8 of developing PCa. When the prostate of mice is exposed to bacteria and viruses, this triggers immediate inflammatory response and subsequent PCa precursor lesions. Sexually transmitted diseases have been epidemiologically associated with increased risk to PCa. Epstein-Barr virus and the murine retrovirus XMRV have been detected in PCa cells and tissues.[7, 27] Other risk factors include ethnicity and high bone mass.[20]

### 1.4.3.5 Tumourigenesis

Figure 2 shows the different factors that influence the development of PCa.[7, 24] Inflammation of the prostatic epithelium is implicated in the carcinogenesis of PCa. Initial damage to prostate epithelium maybe due to:

- Infection ;
- Reactive oxygenative species (ROS);
- Reactive nitrogen species (RNS);
- Dietary carcinogens;
- Oxidative stress.

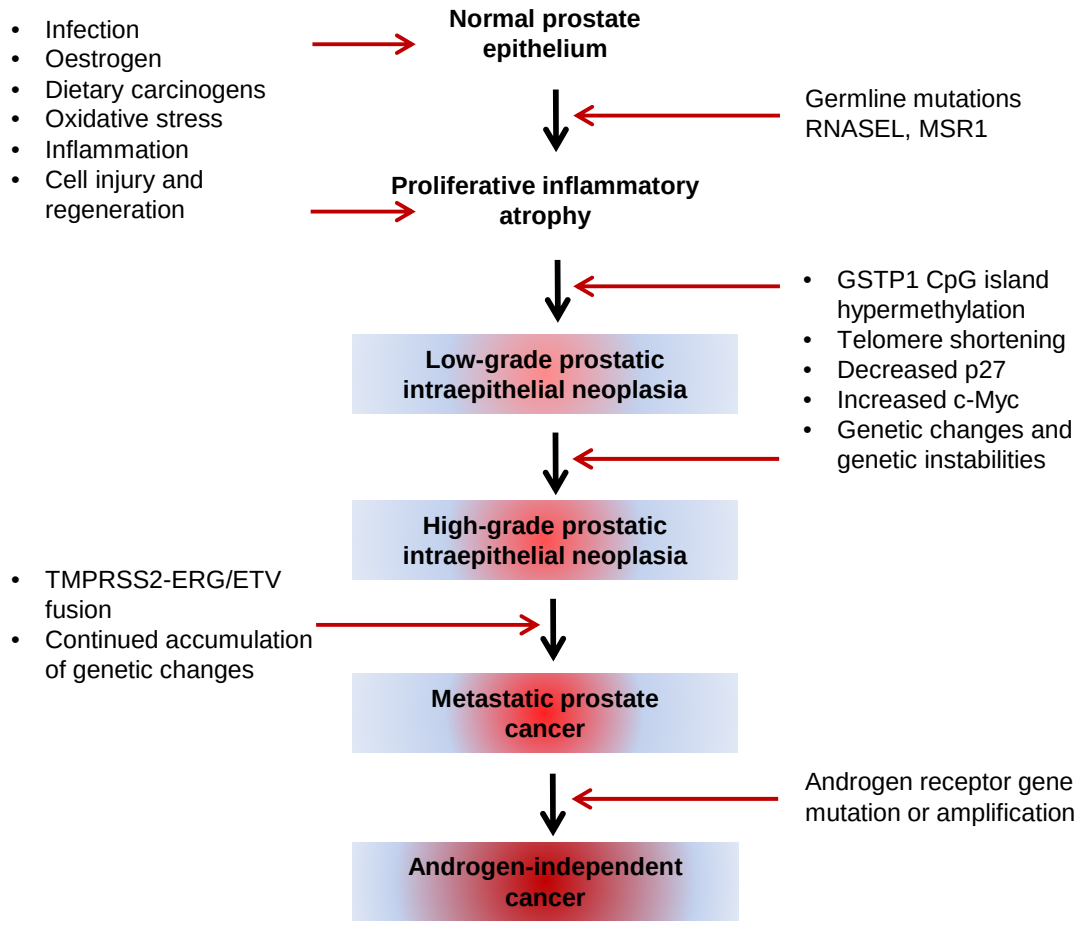


**Figure 2:** Pathogenesis of prostate cancer.[7, 24]

All these lead to genomic damage. The damage to the prostatic epithelium results in the appearance of lesions termed proliferative inflammatory atrophy (PIA), a precursor to prostatic intraepithelial neoplasia (PIN) and PCa. Epigenetic silencing (GSTP1), telomere shortening and activation of c-Myc gene expression trigger the pathogenic steps of PCa. Hypermethylation of a GSTP1 CpG island, an acquired gene defect that is present in nearly

all PCa cases, seems to occur at the very initiation of transformation between proliferative inflammatory atrophy and prostatic intraepithelial neoplasia or prostate cancer. GSTP1 is a glutathione S-transferase gene responsible for deactivating electrophilic carcinogens. Silencing of this gene by hypermethylation leaves cells with increased vunerability to carcinogens. Changes in DNA caused by epigenetic gene silencing may be the very earliest changes in the somatic genome.[7, 28, 29] Telomere is involved in stabilising chromosomes by preventing deleterious recombination and loss of DNA sequences. Telomere consists of repeated DNA sequence (5'-TTAGGG-3') bound to telomere-binding protein at the end of linear chromosomes. The DNA length of telomere can be shortened during cell division due to incomplete replication or as a result of oxidative damage. In normal cells, critically short telomeres trigger the initiation of apoptosis or an irreversible cell cycle arrest. This telomere length monitoring system is said to be inactivated in cancer cells leading to critically short telomeres. This give rise to genetic instabilities such as chromosomal fusion, breakage and rearrangement since telomere can no longer perform its function of stabilising chromosomes. PIN and PCa have been shown to display telomere shortening especially in the luminal epithelial cells.[7, 30-32] The overexpression of the oncogenic transcription factor, c-Myc protein, is observed in PIN lesions and prostatic adenocarcinomas.[33] Further epithelial damage occurs until an epigenetic gene mutation results in creating a transformed cell. Continual epigenetic and genetic instability leads to metastatic carcinoma. Formation of fusion transcripts between TMPRSS2 (an androgen-regulated differentiation gene) and oncogens such as ERG and ETV1 occur. This results in tumour cells opting out of androgen-regulated differentiation which normally suppress cell proliferation. Amplification and overexpression of androgen receptors increases the sensitivity of PCa cells to low levels of androgens thereby making them resistant to androgen deprivation.[24]

#### 1.4.3.6 Diagnosis

Procedures used in the diagnosis of PCa include:

- Digital rectal examination (DRE);
- PSA blood test;
- Trans-rectal ultrasound (TRUS);
- Needle biopsy.[34]

#### 1.4.3.6.1 Digital rectal examination

DRE involves the physical examination of the prostate gland to detect signs of tumour growth. When the volume of prostate tumour is about 0.2 mL or larger, it may be detected by DRE as most PCa are located in the peripheral zone of the prostate.[16] Tumours arising in the anterior to the midline of the prostate (up to 40%) is not detected by this diagnostic method. Only tumours located at the posterior and lateral part of the prostate can be detected by DRE. The chance of detection of tumours < 1.5 cm is only 41%.[2] The prostate gland is assessed for nodules, hardening and thickening of tissue. DRE alone can sometimes determine the need for further investigations.[25]

#### 1.4.3.6.2 PSA blood test

PSA is a kallikrein-like serine protease exclusively secreted by the epithelial cells of the prostate. PSA levels greater than the reference range (Table 1)[35] is indicative of prostate disease. The higher the level of PSA in serum, the greater the chance of being diagnosed with PCa.

**Table 1:** Age specific reference ranges for PSA

| Age (years) | Normal PSA range (ng $mL^{-1}$) | |
|---|---|---|
| | Black men | White men |
| 40-49 | 0-2.0 | 0-2.5 |
| 50-59 | 0-4.0 | 0-3.5 |
| 60-69 | 0-4.5 | 0-4.5 |
| 70-79 | 0-5.5 | 0-6.5 |

Increases in serum PSA levels do not occur exclusively in PCa. Other prostate conditions such as BPH and prostatitis can result in high PSA levels. Furthermore, some diagnosis of PCa has been made despite low levels of PSA. Serum PSA level is therefore not an absolute diagnostic tool for PCa.[16] For instance, if the usual cut of level of 4 ng $mL^{-1}$ PSA level is used to determine when further investigations are needed, the specificity of the PSA serum test is only 40%. This means if men with PSA level > 4 ng $mL^{-1}$ undergo biopsies, about 60% will not be diagnosed as PCa patients. Futhermore, only 30% of men with PSA range of 4-10 ng $mL^{-1}$ are diagnosed to have PCa. Patient with organ confined PCa tend to give a false negative PSA test results (< 4 ng $mL^{-1}$) and 15% of men with PSA levels < 4 ng $mL^{-1}$ will have PCa.[34, 35] Due to these limitations, several modifications of serum PSA value have been described with the aim of improving specificity of PSA in the early detection of PCa.[16] The age-adjusted PSA levels has been suggested to take into account the effect of age on PSA levels (Table 1). The free / total PSA (fPSA / tPSA) ratio is the modification most widely used in clinical practice to discriminate between BPH from PCa.[16] Men with PCa tend to have a relatively decreased fPSA / tPSA ratio as a

result of lower proportion of fPSA whilst in BPH, the total detectable PSA is lower and hence the fPSA / tPSA ratio higher.[35] The ratio is mainly used to assess the risk to PCa in men whose PSA levels lie between 4 and 10 ng $mL^{-1}$ with a negative DRE.[16]

#### 1.4.3.6.3 Trans-rectal ultrasound and needle biopsy

TRUS is used to obtain images of the prostate. Abnormal ultrasonic features include hypo-echoic areas, loss of differentiation of zones, asymmetry and capsular distortion.[27] TRUS is increasingly used to guide transrectal core biopsies which involve examination of the histopathological or cytological of specimens from the prostate gland.[17, 25]

#### 1.4.3.6.4 Grading and clinical staging

Grading and staging of PCa is used to ascertain the level of tumour development and to help decide on treatment choice. The Gleason grading system ($1 \rightarrow 5$) of prostate cancer is based on the extent of glandular differentiation. The sum of two of the most common patterns of tumour growth gives the Gleason score. This ranges from 2, being the least aggressive to 10, the most aggressive.[16, 18] The most frequently used method to describe the spread of prostate is the TNM (Tumour, Lymph Nodes and Metastasis) staging classification.[18] Table 2 gives the details of the two classification systems.[18, 35]

**Table 2:** Gleason grading and TNM staging of prostate cancer.[18, 35]

| Gleason grading | TNM staging |
|---|---|
| **Grade 1:** Well differentiated carcinoma with uniform gland pattern. | **T1:** Tumour not palpable nor visible by imaging |
| | (a) Incidental finding in < 5% of resected tissue |
| | (b) Incidental finding in > 5% of resected tissue |
| **Grade 2:** Well differentiated with glands varying in size and shape. | (c) Tumour identified by needle biopsy |
| | **T2:** Tumour confined to prostate |
| | (a) Involving half lobe or less |
| **Grade 3:** Moderately differentiated carcinoma with either (a) irregular acinae often widely separated or (b) well defined papillary / cribriform structures. | (b) Involving more than one half of one lobe |
| | (c) involving both lobes |
| | **T3:** Tumour extends through the prostatic capsule |
| | (a) Extracapsular extension |
| | (b) Tumour invades seminal vesicles |
| **Grade 4:** Poorly differentiated carcinoma with fused glands widely infiltrating the prostatic stroma. | **T4:** Tumour is fixed or invades adjacent structures other than seminal vesicles |
| | (a) Invades bladder neck and/or external sphincter and/or rectum |
| | (b) Invades levator muscles and/or is fixed to pelvic wall |
| **Grade 5:** Very poorly differentiated carcinoma with no or minimal gland formation. Tumour cell masses may have central necrosis. | **N1:** Metatases in regional lymph node(s) |
| | **M1:** Distant metastases |
| | (a) Non-regional lymph nodes |
| | (b) Bone |
| | (c) Other sites |

#### 1.4.3.7 Presentation

Initial stages of PCa are often asymptomatic and are increasingly diagnosed at routine PSA testing and DRE. Symptoms are experienced when about 80% of the tumour has locally advanced or metastasised. Lower urinary tract symptoms are the most common complaint. Renal failure at presentation can occur due to locally advanced tumour obstructing the ureters. Pain and pathological fracture can result from metastasis to the bone. Metastasis to the spinal cord can cause spinal cord compression which leads to symptoms such as urinary and faecal incontinence and limb weakness. Haematuria may occur secondary to infection or damage to

the prostate gland. Weight loss, cachexia, perineal pain and signs of lymphatic obstruction in the form of lymphaoedema can occur in advanced disease states.[18, 27]

#### 1.4.3.8 Management

The management of PCa is dependent on the stage of the disease. The slow progression of PCa means that majority of men can live with the disease without the need for treatment. A range of treatment regimens are available to treat patient with varying degree of disease progression.

##### 1.4.3.8.1 Localised prostate cancer

This refers to tumour confined within the prostate gland. A risk category based on PSA level, Gleason scores and clinical staging is assigned to men with localised PCa. This helps to determine the risk of recurrence and to decide which treatment options are recommended to patients.

###### 1.4.3.8.1.1 Watchful waiting and active surveillance

Watchful waiting and active surveillance involve no active treatment until progression of disease occurs. In watchful waiting, initiation of treatment is dependent on symptomatic progression (symptom-guided treatment), whilst in active surveillance (active monitoring), serial PSA monitoring and TRUS guided biopsy are carried out, allowing regular re-assessment of risk category to inform when treatment should be initiated.[16, 25, 34]

###### 1.4.3.8.1.2 Radical prostatectomy

This involves the surgical removal of the prostate, seminal vesicles and pelvic nodes if necessary. This treatment option is thought to be the best curative method for men with localised PCa. Radical prostatectomy is proven by a randomised controlled trial to reduce the development of metastases and reduce mortality. Side-effects include impotence (> 29%) and severe stress incontinence (0-15%).[16, 25, 27, 34]

#### 1.4.3.8.1.3 Radiotherapy

##### 1.4.3.8.1.3.1 External beam radiotherapy (EBRT)

This involves delivery of external radiation to the prostate tumour in daily fractions over 4-8 weeks. Intensity-modulated radiotherapy with / without image guiding is the gold standard of EBRT. It involves incremental delivery of radiation of upto 86 Gy to the tumour whilst reducing radiation risk to surrounding organs. Radiation toxicity to the bladder and bowel is common as these can fall within the field of radiation. Damage to the neurovascular system may result in erectile failure.[16, 25, 27, 34]

##### 1.4.3.8.1.3.2 Brachytherapy

This is a form of radiation therapy involving permanent implantation of radioactive seeds (low dose rate) or temporary implantation of radioactive wires (high dose rate) directly into the prostate under ultrasound control. Side-effects include impotence (50-60%), urinary incontinence (up to 30%) and bladder damage (10-20%).[25, 27, 34]

#### 1.4.3.8.1.4 Experimental local treatment

Heating the prostate gland using High-frequency ultrasound (HiFU) or freezing the prostate gland using cryotherapy are used to eradicate prostate cancer.[16, 34]

### 1.4.3.8.2 Metastatic prostate cancer

Metastatic prostate cancer has a poor outlook with 90% mortality within 5 years. Androgen withdrawal either surgically or medically can control the disease for several years.[27, 34]

#### 1.4.3.8.2.1 Hormonal therapy

About 20-30% of prostate tumours will not respond to this form of treatment. Androgen deprivation is achieved through orchidectomy or the use of luteinizing hormone-releasing hormone (LHRH) agonists to reduce testosterone levels to castration levels (< 50 ng $dL^{-1}$) (Figure 3). Anti-androgens acts at the receptor level in prostate cancer to counteract the effect of testosterone. The combination of androgen deprivation and the use of anti-androgens allows complete androgen blockade.[16, 27]

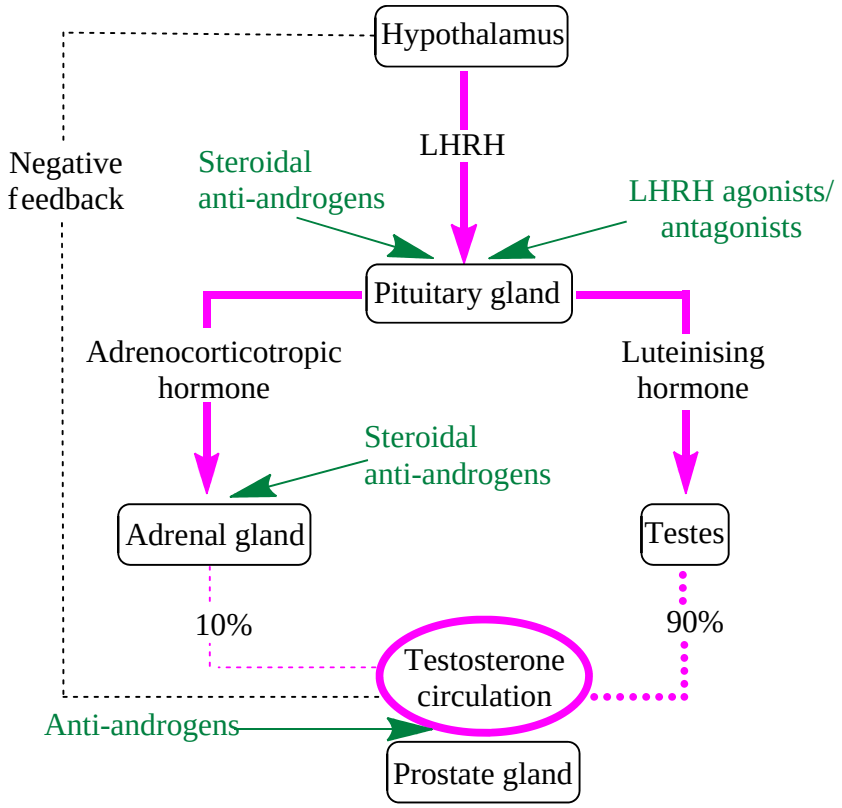


**Figure 3:** The effects of hormonal treatments on testosterone production.[36]

#### 1.4.3.8.2.2 Bilateral orchidectomy

Reduction of testosterone levels is achieved by removal of both testes. Common side-effects are hot flushes, loss of libido and impotence.[25]

#### 1.4.3.8.2.3 Luteinizing hormone-releasing hormone (LHRH) receptor agonists (*e.g.* busereline, gosereline)

These are used to reduce the level of testosterone by over-stimulating the LHRH receptors in the pituitary gland to stop release of luteinising hormone *via* a negative feedback mechanism (Figure 3). The long-term effect of these drugs is to down-regulate LHRH receptors.[36] This leads to the reduction of testosterone to castration levels within 2-4 weeks. However, about 10% of patients fail to achieve castration levels of testosterone. Reduction in tumour size occurs as well as slowing of the progression of tumour growth. These agents, however, do not eradicate the disease. The initial action of these drugs result in rapid increase in testosterone levels which can result in worsening of symptoms (*e.g.* increased bone pain, spinal cord compression). It is therefore recommended to start these drugs together with anti-androgens for two weeks to reduce the risk of symptom flare-ups. Side-effects of LHRH receptor

agonists include reduction in sex drive and impotence which are reversible on cessation of medication.[16, 25]

#### 1.4.3.8.2.4 LHRH antagonists (*e.g.* degarelix)

These agents competitively inhibit LHRH receptors in the pituitary gland to bring about reduction of LH and therefore testosterone. One advantage over LHRH agonists is that, these agents do not cause initial surge in testosterone levels and therefore need not to be given together with anti-androgens. Castration levels of testosterone is said to be achieved within ~3 d. Serious life-threatening side-effects have been associated with some of these agents.[16]

#### 1.4.3.8.2.5 Androgen receptor antagonists

Androgen receptor antagonists inhibit the effects of testosterone by blocking androgen receptors on the prostate gland (Figure 3). There are two classes of this group of agents namely, steroidal and non-steroidal anti-androgens.[25]

Steroidal anti-androgens (*e.g.* cyproterone acetate): This group of drugs are derivatives of hydroxyprogesterone and therefore have progestational properties. In addition to peripherally inhibiting androgen receptors, these drugs inhibit the release of LH and also suppress adrenal activity thereby reducing testosterone levels.[16]

Non-steroidal anti-androgens (*e.g.* bicalutamide): These drugs only inhibit androgen receptors without inhibiting the secretion of testosterone.[16]

Side-effects of these agents include breast enlargement, breast pain and hepatotoxicity. These agents also do not eradicate the disease but only serve to slow the progression.[16, 25]

### 1.4.3.8.3 Hormone-refractory prostate cancer

There is no known curative therapy for hormone-resistant PCa. Treatment is symptomatic and aims to improve quality of life and survival. A combination of docetaxel and prednisolone is licensed for treatment of this form of PCa. Docetaxel belongs to the taxane family and brings about apoptosis of cancer cells through inhibition of microtubule depolymerisation.[34, 37] This therapy also affects highly proliferating cells such as those of the bone marrow and intestinal epithelium as well as the tumour cells. This lack of selectivity results in immunosuppression

and gastrointestinal disorders. The side-effects are such that the use of docetaxel may not be possible if the cancer has progressed to a stage where it is causing significant symptoms. Those who cannot tolerate docetaxel are usually treated with the combination of mitoxantrone and prednisolone.[25, 34] Cabazitaxel is also licensed to be used with prednisolone / prednisone to treat hormone-refractory PCa. It is normally used in patients who have been on doctaxel containing regimen in the past. Hypersensitivity is a common side-effect with this new drug.[37]

The newly licensed drug, abiraterone (Figure 4) is a selective inhibitor of androgen biosynthesis which acts by irreversibly blocking CYP17A1 an enzyme involved in the synthesis of testosterone. It is licensed in the UK for use with prednisone / prednisolone for the treatment of metastatic castration-resistant PCa in men whose disease has progressed on or after a docetaxel-based chemotherapy regimen.[37, 38] Sipuleucel-T is a cellular vaccine designed to stimulate immune response against prostatatic acid phosphatase expressing prostate cancer cells.[37, 39] The radioisotope radium-223 and the anti-androgen, enzalutamide are also in use to manage hormone resistance PCa.[40]

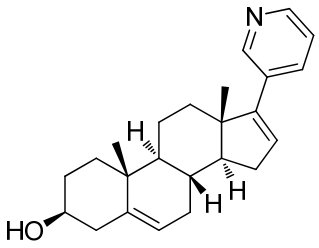

**Figure 4:** Structure of abiraterone

Ongoing trials are investigating different agents to treat PCa. These include inhibitors of intratumoural androgen synthesis (*e.g.* orteronel), inhibitors of angiogenesis (*e.g.* cabozantinib, tasquinimod) and immunomodulatory agents (*e.g.* ipilimumab).[37, 39] Second-line hormonal therapy with oestrogens or estramustin phosphate may give partial response but has not been shown to improve survival.[27]

#### 1.4.3.9 Novel therapeutic approaches

The lack of curative therapy for PCa and the many downsides with current therapies resulting from their non-selectivity has driven researchers to look into alternative therapies. The naturally occurring cyclopropapyrroloindole (CPI) anti-tumour antibiotics are represented by CC-1065 and duocarmycin SA. This family also includes duocarmycin A and yatakemycine, which are all derived from the fermentation cultures of *Streptomyces* sp.[41]

They are very potent cytotoxics with $IC_{50}$s against mammalian cell lines (*e.g.* leukaemia, pancreatic, renal and prostate tumour cell lines) in the picomolar range (Figure 5).[42, 43]Li *et al.*[43] have shown that in contact with L1210 cells for 3 d, the dose of CC-1065 required for

50% inhibition of growth ($ID_{50}$) is 0.017 ng $mL^{-1}$ (24.2 pM). These compounds contain a cyclopropapyrroloindole (CPI) DNA-alkylating pharmacophore (Figure 5) and derive their biological activity through selective alkylation in the minor groove of duplex DNA offering a new mode of cancer treatment.[41, 44, 45]

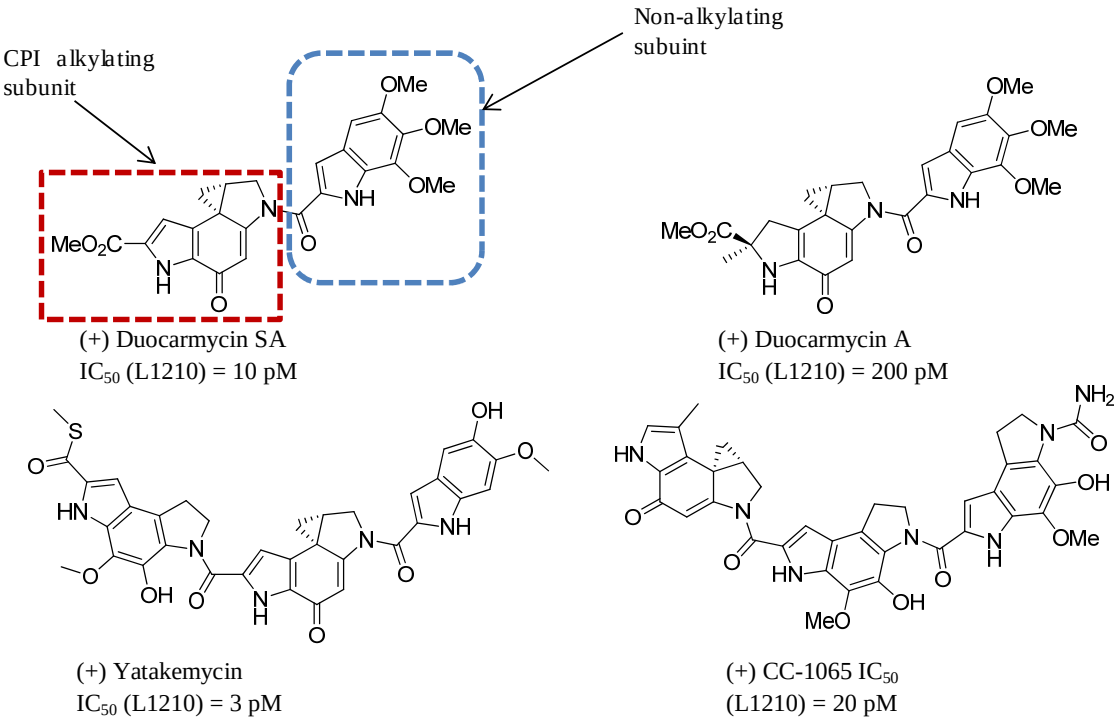


**Figure 5:** Structures of selected natural anti-tumour antibiotics.

These drugs, however, have proven to have too many toxic side-effects precluding them from clinical developments. For instance, admininistration of a single dose of CC-1065 to healthy mice resulted in delayed deaths (50-90 d) caused by hepatotoxicity.[46] The downsides of the natural products have led to the synthesis of many analogues (adozelesin, carzelesin, KW-2189, and bizelesin). Although these analogues show promising anticancer activities in animal model, all have failed in clinical trials in humans due to myelotoxicity.[47-49]

#### 1.4.3.9.1 Mechanism of the anti-tumour antibiotics

The pharmacophore of these compounds can be divided into the alkylating subunit and the DNA-binding non-alkylating subunit (Figure 5). The anti-tumour antibiotics effect a sequence selective alkylation of double-stranded DNA.

Binding to the DNA is aided by the non-alkylating subunit and occurs in the AT-rich regions of the minor DNA groove. Initial binding is *via* hydrophobic interactions and van der Waals forces. The binding causes a twist in the tumour antibiotic allowing alignment of adenine $N^3$ with the electrophilic strained cyclopropane ring. A reversible stereoelectronically-controlled covalent addition of adenine to the least substituted carbon of the cyclopropane ring occurs resulting in the formation of a drug-DNA adduct (Figure 6).

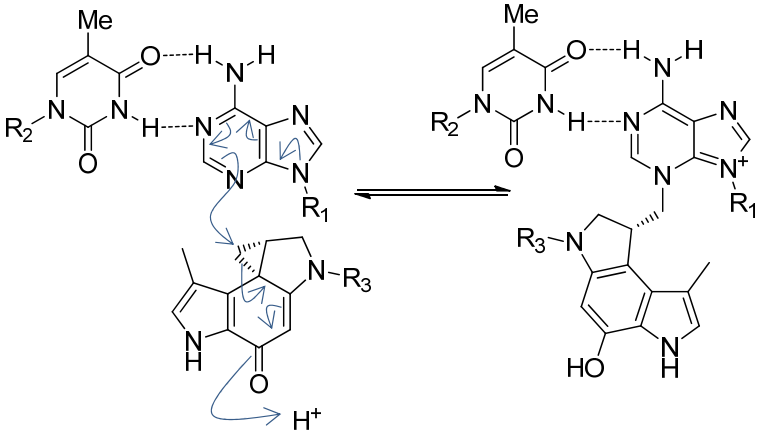


**Figure 6:** Alkylation of CC-1065 by adenine $N^3$.

The *seco* (non-cyclised) analogues generate the reactive cyclopropane ring *in situ via* Winstein-cyclisation before reacting with the DNA (Figure 7). Alkylation at adenine accounts for 86-92% (duocarmycin A), 90-100% (duocarmycin SA) and 80-90% (CC-1065) of DNA alkylation. Minor guanine-$N^3$ alkylation has been detected.[50-52]

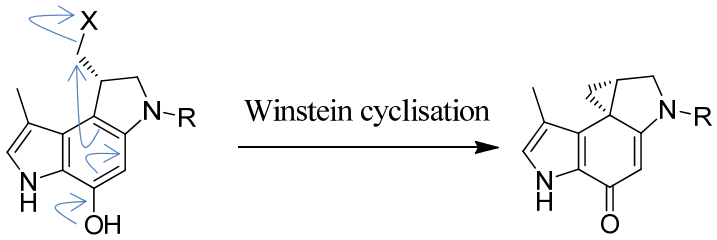


**Figure 7:** Proposed mechanism for *seco*-CPI.

### 1.4.3.9.2 Inhibition of macromolecular synthesis and enzymes

Li *et al.*[43] investigated the biological and biochemical effect of CC-1065 on L1210 leukaemia cells. It was found that CC-1065 inhibited DNA synthesis ten times more than RNA synthesis with protein synthesis being the least inhibited. A concentration of 5.7-8.5 nM was required to inhibit 50% of DNA synthesis whilst a concentration of 63.9-85.3 nM was needed to inhibit 50% of RNA synthesis.[43] A similar pattern was observed when the effect of CC-1065 was studied on the B16 cell line.[53] More than 90% of DNA inhibition in L1210 cells occurred at

CC-1065 concentration of 14.2 μM. The effect on enzymes directly or indirectly involved in DNA synthesis was also investigated. It was found that inhibition of dThd kinase was about 40% at drug concentration of 7.1 μM whilst inhibition of DNA polymerase α was 74% at 1.4 μM.[43] The thermal melting of calf thymus DNA ($\Delta T_m$) was increased by ≥ 31 deg. C at DNA-drug ratio of 6:9. It was shown that 80% of CC-1065 binds strongly to calf thymus DNA when the CC-1065:DNA ratio was 0.01. Further cytotoxicity studies on L1210 indicated that DNA-bound CC-1065 was far less cytotoxic than the free CC-1065. L1210 cells exposed to CC-1065 at a final concentration of 56.8 pM, experienced 85% growth inhibition. However, pre-mixing CC-1065 with as low as 0.02 μg $mL^{-1}$ calf thymus DNA, 10 min before adding to L1210 cells, resulted in significant reduction in growth inhibition. This effect was dependent on the concentration of calf thymus DNA used. At 0.5 μg $mL^{-1}$, the observed percentage growth inhibition markedly reduced to ~4%.[43]

#### 1.4.3.9.3 Apoptotic cell death

Cell death by the CPI anti-tumour antibiotics is thought to be through apoptosis. Wrasidlo *et al*.[42] microscopically examined Molt-4 leukaemia cells after exposure to duocarmycin and observed shrinkage and blebbing of the cells with no evidence of lysis. Exposure of Molt 4 and L1210 cells to duocarmycin (10 nM) also revealed characteristics typical of apoptotic cell death including chromatin condensation, fragmentation of nucleus and disintergration of affected cells (50-60%) into apoptotic bodies. Analysis of DNA isolated from Molt 4 cells showed intense endonuclease mediated internuclosomal DNA fragmentations.[42, 54] This has led to the proposal that sequence alkylation of DNA at internucleosomal sites is responsible for triggering a sequence of signalling pathways that eventually lead to apoptotic cell death.[42]

Propidium iodide stained flow cytometric analysis of cells treated with analogues of the anti-tumour antibiotics has also confiremed the likelihood of cytotoxicity through apoptosis. Flow cytometry is used to detect extensive DNA cleavage in cells which is characteristic of apoptotic cells. P815 mastocytoma cells incubated with a range of analogues of the anti-tumour antibiotics displayed a high level of DNA cleavage when analysed.[55-59]

#### 1.4.3.9.4 Structure-activity relationship

A range of studies using the natural CPI anti-tumour antibiotics as well as its analogues especially the CBI (1,2,9,9a-tetrahydrocyclopropa[*c*]benz[*e*]indole-4-one) analogues (Figure

8) have helped established the relationship between the pharmacophore of these agents and their acivitities.

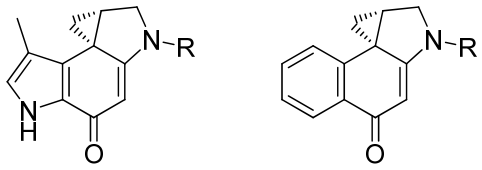


CPI CBI

**Figure 8:** Alkylating subunits for CPI and CBI analogues.

### 1.4.3.9.5 DNA-alkylation selectivity

Thermally induced depurination and strand cleavage of labelled DNA after exposure to agents have made it possible to identify sites of alkylation and the relative selectivity of the anti-tumour antibiotics. Sequence selectivity is controlled by the non-covalent binding in the minor groove of AT-rich regions of the DNA and the steric accessibility to the alkylation site which accompanies deep penetration into the AT-rich minor groove. The natural enantiomers (7b*R*, 8a*S*) bind to adenine in the 3' → 5' direction across adjacent bases. Each adenine $N^3$ alkylation site is flanked by two 5'-A or T bases. The (+)-duocarmycins and (+)-CC-1065 prefer the sequence 5'-AA<u>A</u> > 5'-TT<u>A</u> > 5'-TA<u>A</u> > 5'-AT<u>A</u>. The duocarmycins bind over 3.5 base pairs whilst CC-1065 binds over 5 base pairs. The fourth 5' base was more likely to be A or T rather than C or G.[60-62]

The unnatural enantiomers (−) of the duocarmycins and CC-1065 alkylates DNA in 5' → 3' direction. This reverse orientation is required for adenine alkylation of the least substituted cyclopropane carbon. (−)-Duocarmycin SA alkylates DNA at 10 × the concentration required for the natural enantiomer whilst (−)-CC-1065 has been shown to alkylate DNA at a rate and efficiency comparable to the natural enantiomer.[51, 61] Studies have shown that some simplified (−)-CPI analogues either failed to alkylate DNA or did so at a considerably higher concentrations. This effect is also correleated to *in vitro* cytotoxicity.[63, 64] The adenine alkylation site for the unnatural enantiomers is flanked by a 5' and 3' A or T bases. The sequence preference of (−)-duocarmycin SA is 5'-A<u>A</u>A > 5'-A<u>A</u>T > 5'-T<u>A</u>A > 5'-T<u>A</u>T and that of (−)-CC-1065 is 5'-A<u>A</u>A > 5'-T<u>A</u>A > 5'-A<u>A</u>T > 5'-T<u>A</u>T. The second 3' base from the alkylation site is preferred to be A or T.[51, 61] The sequence-selective alkylation is dependent on the minor groove shape and size chararacteristics of an AT-rich sequence which allows shape-selective and shape-dependent catalysis. Nucleosomal DNA has been reported to be accessible, recognised and selectively alkylated by these agents.[65] *Taq* DNA polymerase stop

assays have shown that analogues of these drugs stop activity of the enzyme at adenine rich sites confirming the alkylating site of these agents.[56, 58]

#### 1.4.3.9.6 Stereoelectronic control of ring opening of cyclopropane

Adenine-$N^3$ alkylation by the CPI anti-tumour antibiotics has been shown to occur almost exclusively at the least substituted secondary carbon of the cyclopropane ring. This regioselectivity was investigated by Boger *et al.*[66] using the CBI (1,2,9,9a-tetrahydrocyclopropa[*c*]benz[*e*]indole-4-one) analogues of the natural products. It was observed that the difference in alignment of the cyclopropane bond from the quaternary carbon to the secondary cyclopropane carbon and to the tertiary carbon was important in determining the site of reactivity (Figure 9).[66-68]

For N-Boc-CBI [(8b*R*,9a*S*)-*tert*-butyl 4-oxo-9,9a-dihydro-1*H*-benzo[*e*]cyclopropa[*c*]indole-2(4*H*)-carboxylate)], (Figure 9)[66] the molecular orbital of the secondary cyclopropane carbon (C8b-C9) is aligned perpendicularly to the plane of the cyclohexadienone and, consequently overlaps with the developing π-system of the phenol product. This is in contrast to the bond extending to the tertiary cyclopropane carbon (C8b-C9a) which is almost in plane (13°) with the cyclohexadienone and orthogonal to the developing π-system of the incipent phenol product. This effect is due to having a five-membered ring fused to the cyclopropane ring. The perpendicular alignment favours nucleophilic attack at the least substituted cyclopropane carbon. This selectivity is due to the stereoelectronic control, rather than the intrinsic electronic preference for ring expansion which would place a developing positive charge on a preferred tertiary carbon versus a secondary carbon. Besides, $S_N2$ reactions prefer addition to the least substituted carbon. Furthermore, breaking of the longer and therefore weaker C8b-C9 (1.532 Å) bond is favoured over breaking the C8b-C9a bond (1.508 Å).[67, 68]

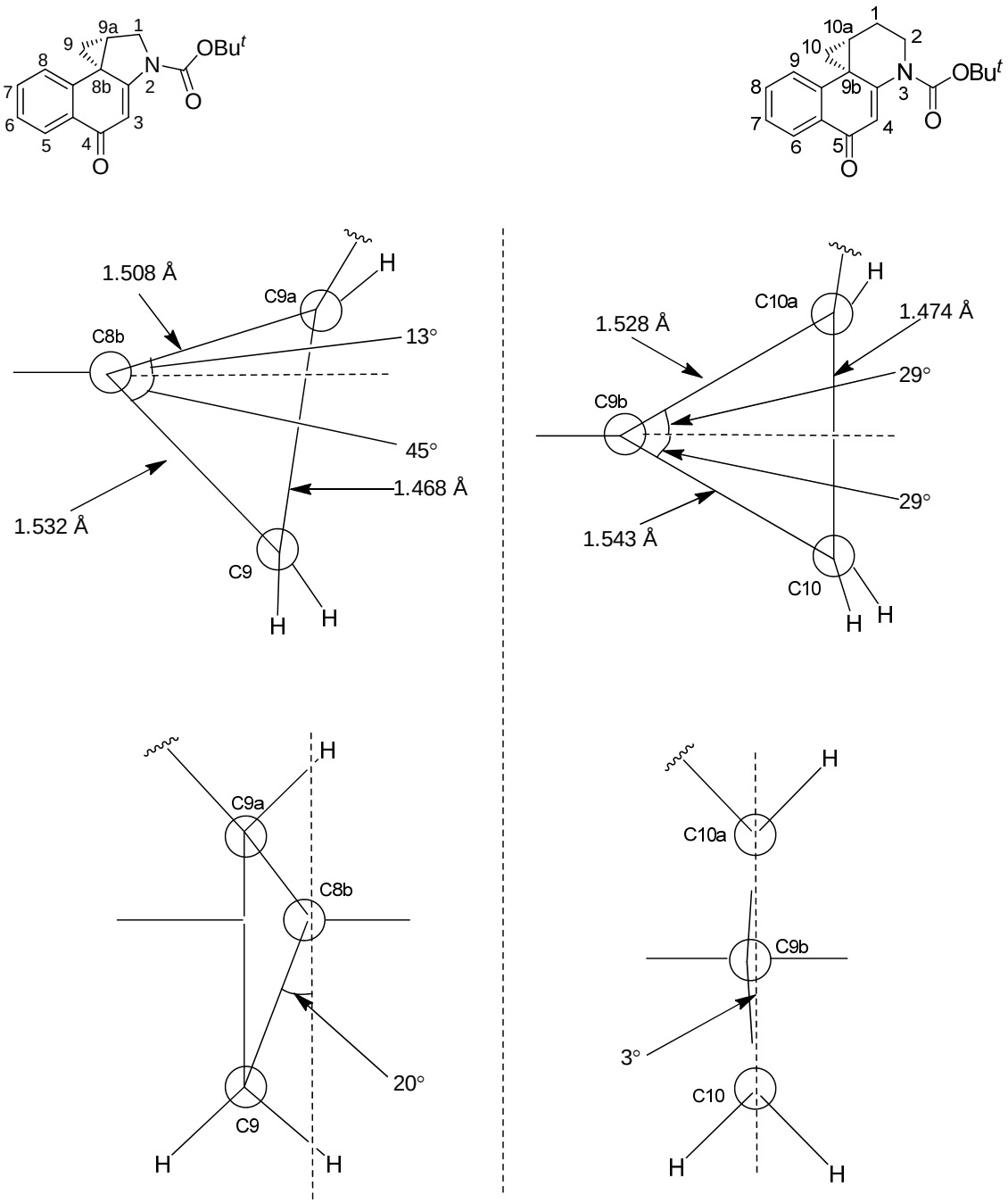


**Figure 9:** Side and 90° rotation view of cyclopropane ring of CBI and CBQ.[66]

With N-Boc-CBQ (9b*R*,10a*R*)-*tert*-butyl 5-oxo-1,2,10,10a-tetrahydrobenzo[*f*]cyclopropa[d]quinoline-3(5*H*)-carboxylate) (Figure 9), the plane of the cyclohexadienone equally bisects the cyclopropane ring with bonds to the secondary (C9b-10) and tertiary (C9b-C10a) carbons equally aligned (29°) with the π-system. Thus the available cyclopropane bonds are equally aligned for cleavage. Solvolysis of N-Boc-CBQ therefore occurs with nucleophilic addition to both C10 and C10a.[66]

Further evidence to support the role of the fused five-member ring is given by N-Boc-CNA (10b*R*,11a*S*)-*tert*-butyl 6-oxo-2,3,11,11a-tetrahydro-1*H*-cyclopropa[*c*]naphtho[2,1-b]azepine-4(6H)-carboxylate) (Figure 10) which has a seven-membered ring fused with the cyclopropane ring.

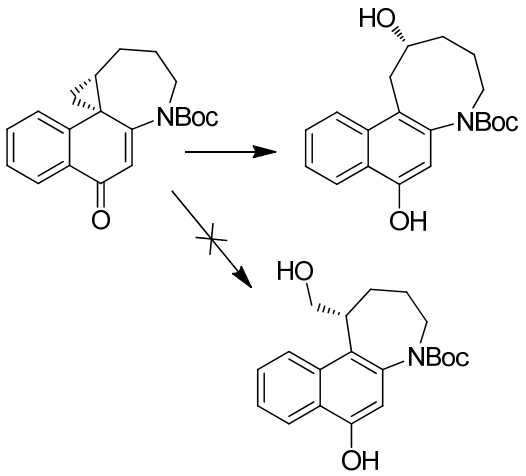


**Figure 10:** Acidic solvolysis of N-Boc-CNA using $CF_3CO_2H$ (0.12 eqv.) in $H_2O$/THF.[69]

The cyclopropane ring of this compound is nonideally conjugated with the π-system but in addition rises above the plane of the cyclohexadienone resulting in a better steroelctronic alignment of the more substituted carbon for nucleophilic attack. Acidic solvolysis of this compound (Figure 10) resulted in the formation of a single compound with a solvolytic half-life (pH 3) of 0.03 h, compared to 133 h for N-Boc-CBI. Further analysis of the product showed that nucleophilic addition to the cyclopropane ring occurred exclusively at the tertiary cyclopropane carbon rather than the least substituted carbon resulting in the ring expansion product.[68, 69]

#### 1.4.3.9.7 Functional reactivity and biological activity

The acid-catalysed activation of the anti-tumour antibiotics towards their alkylation of DNA led to suggestions that a linear relationship existed between reactivity and cytotoxicity. It was expected that increased electrophilicity of the cyclopropane ring would lead to increase cytotoxicity. Studies, however, reveal that the reverse is true. Agents with higher predicted stability show greater cytotoxicity. A direct relationship has also been established between stability towards solvolysis (pH 3) and biological potency. These observations are likely to be due to the requirement for sufficient stability for effective delivery of the agents to their

intracellular target balanced against the need for sufficient reactivity to alkylate DNA once they reach the target.[68, 70]

The high solvolytic stability and the consequent high cytotoxicity of the natural anti-tumour antibiotics have been attributed to the fused five-membered ring to the cyclopropane ring. X-ray structures of N-Boc-CBI and N-Boc-CBQ (Figure 9)[66, 68] show longer cyclopropane bond lengths in N-Boc-CBQ compared to N-Boc-CBI. This longer bond length of N-Boc-CBQ despite its cyclopropane ring being fused with the less strained six-membered ring is said to be due to the idealised conjugation of the ring with the cyclohexadienone π-system. The ideal alignment of the cyclopropane ring with the plane of cyclohexadienone, when viewed at 90° rotation, helps with this conjugation (Figure 9). When compared to N-Boc-CBI, the constraints by the fused five-membered ring pulls the cyclopropane ring down and to the side, placing the cyclopropane ring at 20° away from the plane of cyclohexadienone. This causes non-ideal alignment and non-ideal conjugation of the cyclopropane ring. This difference is the cause of the observed longer cyclopropane bond lengths, weaker bond strengths, higher solvolytic reactivity (63 ×) and therefore lower cytotoxicity (50 ×) of N-Boc-CBQ ($IC_{50}$ L1210 = 4 μM) compared to N-Boc-CBI ($IC_{50}$ L1210 = 0.08 μM).[61, 66, 68]

#### 1.4.3.9.8 Influence of the stability of vinylogous amide on reactivity

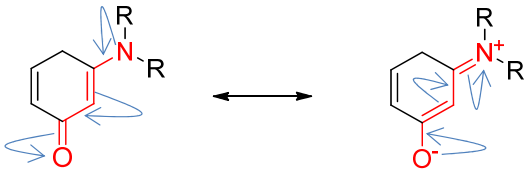


**Figure 11:** Vinylogous amide conjugation.

It has been established that the vinylogous amide (Figure 11) of the alkylation subunit contributes to the unusual stability of the anti-tumour antibiotics. Investigations to ascertain the effect of destabilising the conjugation of the vinylogous amide showed that the degree of conjugation of the cyclopropane and its reactivity is not only due to the geometrical alignment but also depends on the extent of the cross-conjugated vinylogous amide stabilisation (Figure 12).

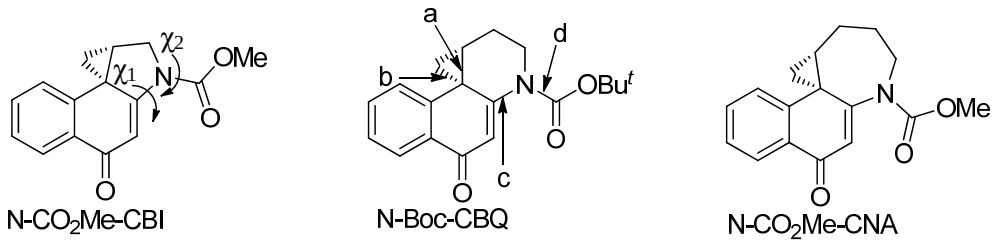


| X-ray bond lengths, Å | N-$CO_2$Me-CBI | N-Boc-CBQ | N-$CO_2$Me-CNA |
|---|---|---|---|
| a | 1.521 | 1.528 | 1.565 |
| b | 1.544 | 1.543 | 1.525 |
| c | 1.390 | 1.415 | 1.428 |
| d | 1.372 | 1.379 | 1.357 |
| X-ray dihedral angle ($\chi_1$) | 21.2° | 34.2° | 86.4° |
| Solvolysis reactivity $t_{1/2}$ (pH 3) | 133 h | 2.1 h | 0.028 h |

**Figure 12:** Effects of destabilising the vinylogous amide conjugation.

A typical C-N (c) bond length of a fully conjugated vinylogous amide is 1.312-1.337 Å. A reduction in vinylogous amide conjugation (*e.g.* increased dihedral angle $\chi_1$) results in an increased bond lengths of the cyclopropane ring (Figure 12). This diminished vinylogous amide conjugation also causes the cyclopropane bonds to be aligned at a more idealised conjugation with the π-system of the cyclohexadienone and, therefore, increases reactivity. *In vitro* cytotoxic studies confirmed the correlation between solvolysis reactivity and cytotoxic potency.[61, 68, 71]

Investigation of 1,2,9,9a-tetrahydro-1*H*-cyclopropa[*c*]benz[*e*]inden-4-one (CBIn) (Figure 13) which contains a five-membered carbocyclic skeleton lacking the vinylogous amide nitrogen further revealed the importance of this amide. CBIn proved to be 3200 × less stable than its nitrogen containing CBI counterpart at pH 3 and more reactive ($\times 10^3$-$10^4$-fold) at pH 7 where the nitrogen containing CBI is stable. Solvolysis studies revealed no dependency on acid concentration between pH 4-12, demonstrating that alkylation rate of these agents is independent on pH.[68]

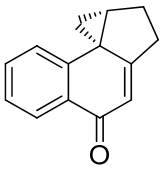


**Figure 13:** Structure of CBIn.

#### 1.4.3.9.9 Linking amide

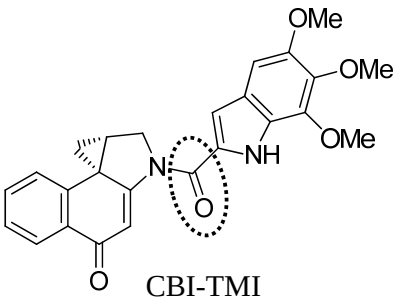


CBI-TMI

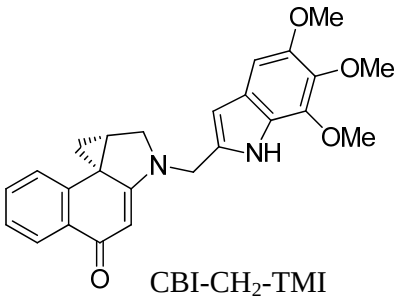


CBI-$CH_2$-TMI

| | |
|---|---|
| $IC_{50}$ (L1210) | 0.02 nM |
| $t_{1/2}$ (pH 3) | 230 h |
| | DNA alkylation easily detected at 25°C, $10^{-6}$ M, 24 h |

| | |
|---|---|
| $IC_{50}$ (L1210) | 14000 nM |
| $t_{1/2}$ (pH 3) | 31000 h (3.6 years) |
| | No DNA alkylation detected after 14 days, at 37°C, $10^{-4}$ M |

**Figure 14:** Effects of $N^2$ substitution.

The importance of a rigid $N^2$ substitution was demonstrated by comparing the above compounds (Figure 14).[68] Substituting the linking amide with a methylene group results in full vinylogous amide conjugation and an increased stability of the compound. The solvolysis half-life at pH 3 for CBI-$CH_2$-TMI is 3.6 y compared to 230 h for CBI-TMI. Despite this high stability towards solvolysis which is usually correlated to high cytotoxicity, the absence of the linking amide causes a decrease in DNA alkylation efficiency (> $10^6$-fold) and a decrease in potency ($10^4$-$10^5$-fold).[71, 72] Replacing the linking amide with the more electron-withdrawing thioamide also causes disruptions of the vinylogous amide leading to increased solvolysis reactivity ($t_{1/2}$ 160 h versus 230 h), reduced alkylation efficiency (× 10-100) and reduced cytotoxicity ($IC_{50}$ L1210 = 1.1 nM vs 0.02 nM) compared with CBI-TMI. This goes on to establish the linking amide as the optimum linkage unit. [71]

With the loss of the linking amide in CBI-$CH_2$-TMI, this should lead to a more basic C4 carbonyl and therefore, higher acid-catalysed reactivity. However, this was not the case, further suggesting that reactivity of these agents is pH independent. The results highlight an essential role for the linking amide in the mechanism of DNA alkylation and the need to have a balance between solvolytic reactivity and stability.[72]

### 1.4.3.9.10 Effect of relocating the C4-carbonyl group

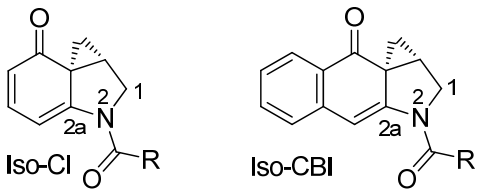

**Figure 15:** Structures o iso-CI and iso-CBI.

To investigate the proposal that the DNA alkylation selectivity of these agents is due to an acidic activation of the C4 carbonyl group by a strategically positioned phosphate group, Boger *et al.*[67] synthesised a series of iso-CIs and iso-CBIs (Figure 15) and analysed their structure-activity relationships. Structural studies of the DNA-agent adducts show that the C4 carbonyl of the natural anti-tumour antibiotics projects out of the minor groove and lies on the surface of the complex, making it accessible to the phosphate backbone. In contrast, the location of the C4 carbonyl in iso-CI and iso-CBI will lead to projection into the minor groove, where it is inaccessible to the phosphate backbone. Solvolysis studies showed that iso-CBI was less stable and 5 × more reactive than CBI. The increase in reactivity was attributed to the diminished vinylogous amide conjugation caused by relocation of the C4 carbonyl group. An X-ray structure showed an increase of the $N^2$-C2a bond length diagnostic of diminished vinylogous conjugation. Evaluation of the DNA alkylation properties of iso-CI and iso-CBI, however, showed that their reactivity was comparable to those of duocarmycin A and CC-1065. Nucleophilic addition to the cyclopropane ring of the iso-CBI also occurred with exclusive addition to the least-substituted carbon. The selectivity of alkylation of the iso-analogues was also similar to their natural analogues. These observations, therefore, do not support the idea that selectivity of alkylation is due to sequence-dependent protonation by the DNA phosphate backbone of the C4 carbonyl but supports the proposal that selectivity is determined by the non-covalent binding to the AT-rich region of the minor groove of the DNA and the steric accessibility to the adenine $N^3$ alkylation site.[52, 67]

### 1.4.3.9.11 Importance of the cyclopropane ring

Lajiness *et al.* synthesised an analogue of duocarmycin with modification to the cyclopropane ring. N-Boc-CbBI (Figure 16) was found to be very stable, being unreactive to solvolysis even at pH 1. This increased stability was due to increased vinylogous amide conjugation, confirmed by the diagnostic shortening of the $N^2$-$C^{2a}$ bond length. Reduction of ring strain energy and the non-ideal alignment of the cyclobutane with the cyclohexadienone compared to cyclopropane in N-Boc-CBI also contributed to this increased stability. A cytotoxicity assay, however, showed a $10^6$-fold reduction in cytotoxicity

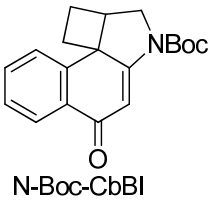

**Figure 16:** Structure of N-Boc-CbBI

compared to the natural products. This further confirmed the parabolic relationship between solvolysis and cytotoxicity.[70]

These observations in the analogues of the anti-tumour antibiotics has led to the proposal that DNA alkylation is facilitated by DNA-binding induced conformational change of the anti-tumour antibiotics, which disrupts the vinylogous amide stabilisation and, in turn, activates the cyclopropane ring for nucleophilic attack. When the agent is bound to DNA, it adopts a helical conformation which complements that of the minor groove of DNA. The result is a twisting of the $\chi_1$ bond which disrupts the vinylogous amide stabilisation effect and consequently enhances reactivity. $^1$H NMR spectra of DNA-bound duocarmycin SA show a 44 ± 2° twist between the alkylating subunit and the non-alkylating subunit. Most of this twist is due to the $\chi_1$ (20-35°) dihedral angle and is greatest within the narrow AT-rich minor groove. This explains the preferential selective alkylation of these agents in this region.[69, 72]

**1.4.3.9.12 Reversibility of alkylation**

A variety of experiments initially failed to show reversibility of DNA alkylation by CC-1065. The stability of the CC-1065-DNA adduct is considered to be essential to the extreme potency of this agent. Studies have, however, shown that CC-1065-DNA adduct is reversible in non-aqueous experimental conditions. The difficulty of not observing the akylation reversibility of some CPI agents in aqueous media is partly attributed to their insolubility. In aqueous media, eventhough reversal of alkylation might occur, the agent stays bound to the DNA. This encourages re-alkylation at the same site without dissociation.[73]

Warpehoski *et al.*[73] investigated the reversibility of alkylation of DNA by CPIs. CPI agents were treated with calf-thymus DNA to obtain the CPI-drug covalent adduct. The reversibility of this adduct was then studied in 0.25 M sodium phosphate buffer (SPB), pH 8.4. A slow recovery rate of CC-1065 from the drug-DNA adduct was observed. At higher temperature (55°C) in a mixture of butanol and 0.25 M SPB, pH 8.4, about 20% of CC-1065 was extracted into butanol after 20 h. At 80°C, CC-1065 was recovered efficiently by extraction into butanol. Studies on adozelesin (a CPI analogue)-DNA adduct at 37°C for 24 h gave a 40% recovery and at 55°C gave 30% recovery in 1 h.[73] Cytotoxicity studies with CPI-DNA adducts showed that adozelesin-drug adduct was quite potent (40 pM) compared to the free adozelesin (3 pM). This is consistent with the significant reversibility of the adozelesin-DNA adduct. The CC-1065-DNA adduct, however, showed no cytotoxicity at doses 60 times that of

CC-1065. This further proves that, although reversibility of CPI-DNA is possible, this adduct is irreversible under conditions used for cell growth.[73] The unnatural enantiomers form less stable adducts with DNA and therefore are more easily reversible.[52]

Lee *et al.*[74] have also shown that the interaction between bizelesin (a CPI analogue) and DNA is reversible. The reversibility was observed to increase with temperature (up to ~80°C), ionic strength and pH. It was also observed that single-stranded DNA-drug adducts undergo depurination in preference to reversal of alkylation. This suggests that conditions that result in instability of DNA (*e.g.* high temperatures) promote the depurination pathway.[74] Scheme 1 shows two decomposition pathways observed for a DNA-CPI adduct. Above 90°C, the depurination pathway-B which precedes DNA strand cleavage, predominates.[73]

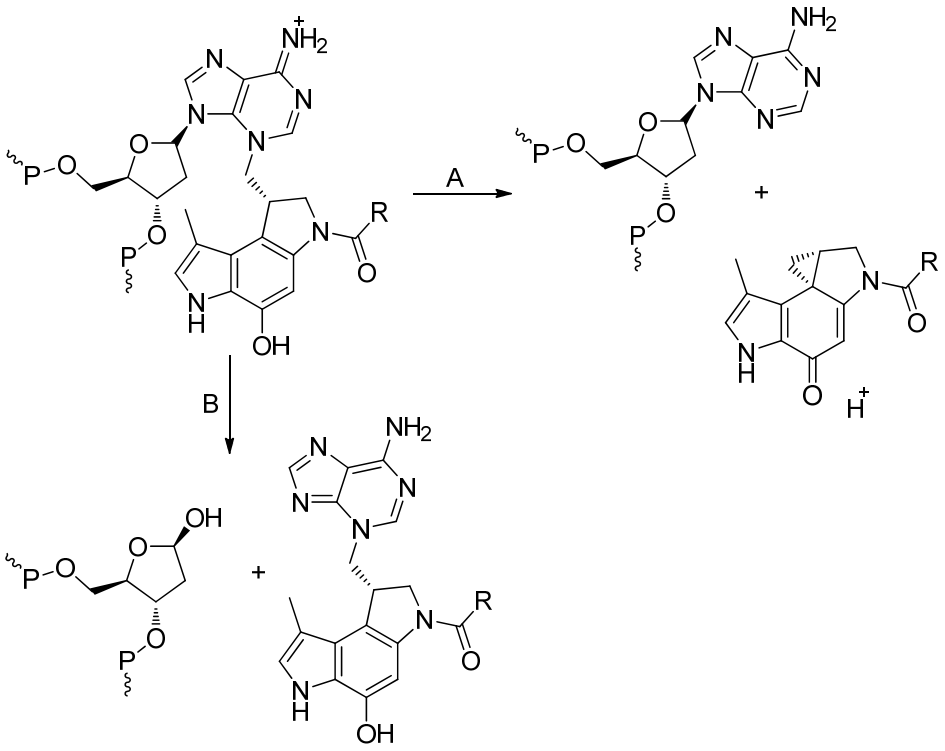


**Scheme 1:** Thermal decomposition of DNA-CPI adduct. A; reversal of alkylation, B; depurination.

### 1.4.3.9.13 Limitations of the natural anti-tumour antibiotics

The drawbacks to the natural anti-tumour antibiotics are two-fold; their extreme systemic toxicity and their structural complexity which makes them difficult to synthesise. McGovren *et al.*[75] showed that CC-1065 caused lethal delayed hepatotoxicity at therapeutic antineoplastic doses. It was observed that non-tumour-bearing mice died approximately 50 d after a single intravenous dose of 12.5 μg $Kg^{-1}$ and as much as 70 d after 10 μg $Kg^{-1}$ was

given intraperitoneally. Higher intravenous doses caused death within 12 d with hepatic necrosis, compared to changes in hepatic mitochondrial morphology when lower doses were given. A subtherapeutic dose of 9 pg $Kg^{-1}$ also caused delayed deaths (50-90 d) in healthy mice. This delayed lethality was mainly due to hepatotoxicity and peritonitis. Bone marrow depression was also observed. Changes in mitochondrial morphology and function probably due to binding of mitrochodrial DNA to CC-1065 have been implicated in the delayed toxicity. Doses of CC-1065 which did not cause delayed toxicity had little anti-tumour activity. Delayed toxicity at very low doses was also seen in rabbits suggesting that this effect is not limited to mice. Death in rabbits was associated with lesions in the liver and kidney.[46, 75] The use of agents (N-acetyl-L-cysteine) said to protect mice from lethal toxicities from DNA alkylating agents failed to have any effect on CC-1065 lethality.[75]

There has been great research into CC-1065 and its analogues in other to understand its structure and activity relationship. Analogues of CC-1065 with modification of the alkylating subunit also result in delayed death.[76] The delayed death effect was initially attributed to the presence of two ethylene moieties in the non-alkylating subunit of the molecule (Figure 17).[45]

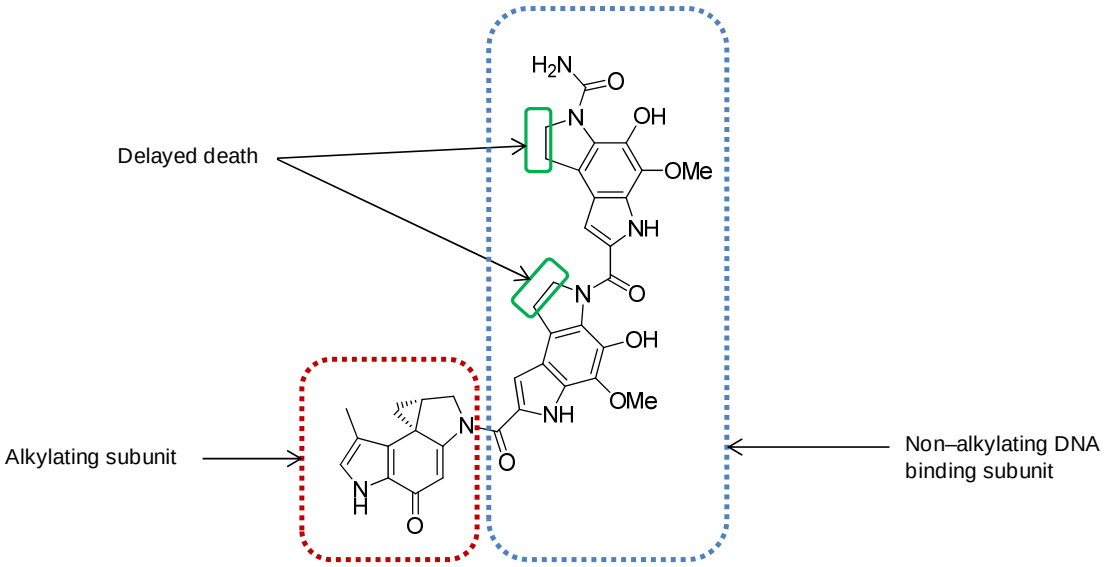


**Figure 17:** CC-1065 structure and activity relationships.

Wang *et al.*[49] found that analogues of CC-1065 without the ethylene groups but possessing a terminal amide moiety also caused delayed death in animals. Replacing the terminal amide group with fluorine resulted in a compound that did not cause delayed death.[49]

Duocarmycin SA is said to be the most stable and most potent member of the anti-tumour antibiotics lacking the fatal toxicity characteristic of CC-1065.[51] This has led to a drive

towards the total synthesis of this compound. Preliminary biological and physiological tests by Nagamura *et al.*,[47] however, discovered that duocarmycin SA exhibited an *in vivo* anti-tumour activity only at very narrow range of doses against murine sarcoma 180 and showed very poor water solubility. At a maximum tolerated dose of 0.10 mg $Kg^{-1}$, duocarmycin SA caused a reduction in tumour volume by 0.21, relative to the control. However, at half this dose, no anti-tumour activity was observed.[47]

The natural anti-tumour antibiotics are all associated with toxic side-effects mainly myelotoxicities. The toxicity of these natural anti-tumour antibiotics, their limited availability and their structure complexities have led to the synthesis of analogues with similar cytotoxicities but better *in vivo* profiles. Approaches to this include:

- Modification of the alkylating subunit;
- Simplification of non-alkylating DNA binding subunit;
- Design and synthesis of prodrugs.

#### 1.4.3.9.14 Modification of the CPI alkylating subunit

Modifications of the alkylation subunit of these agents have been extensively studied, primarily to establish the structure-activity relationships. Figure 18 shows a range of analogues of the original cyclopropapyrroloindole (CPI) alkylating subunit of the natural anti-tumour antibiotics. The presence of ring-A is essential, since, when absent as in N-Boc-CI, biological activity is reduced. This is likely to be due to the reduced conjugative stability provided by the fused aromatic system.[67] Cytotoxicity seems to be also dependent on the steric bulk at C6 comparing (+) N-Boc-CPI to (+) N-Boc-DSA. A range of studies have suggested that having ring C as a five-membered ring is the ideal ring size for cytotoxicity.[52, 61, 70]

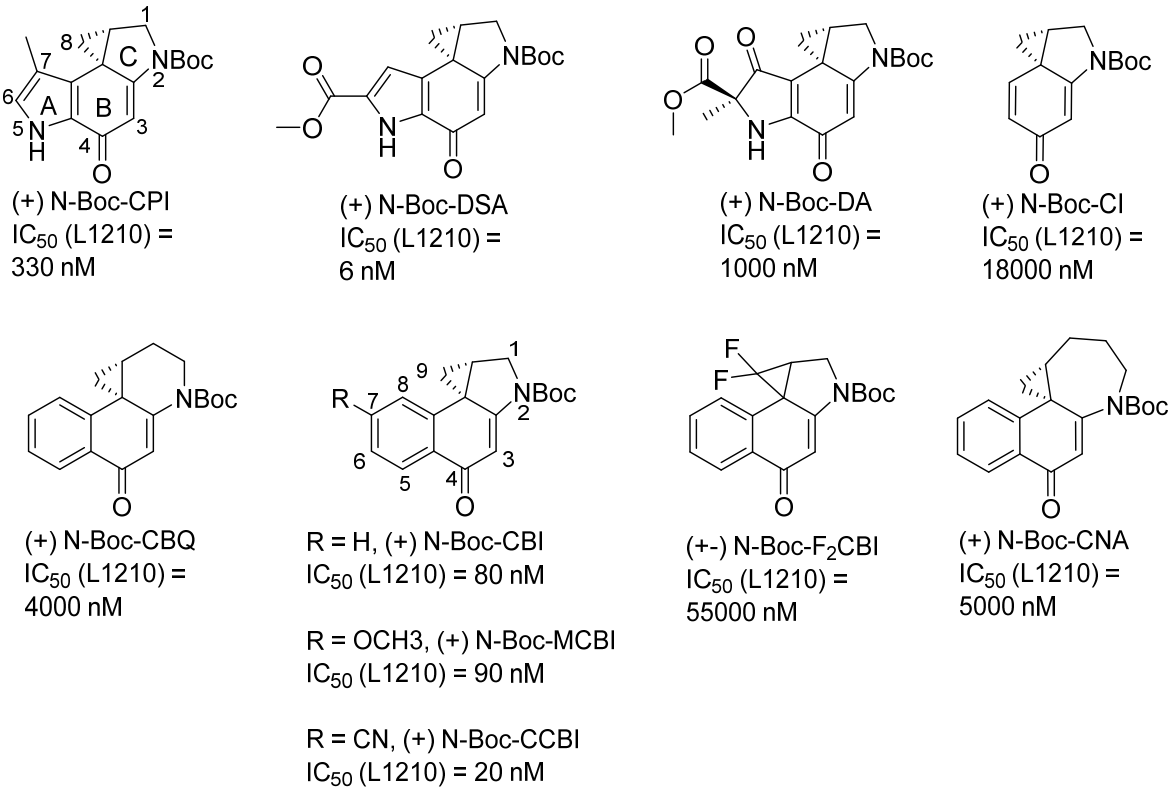


**Figure 18:** Analogues of the alkylating subunits of the anti-tumour antibiotics.

### 1.4.3.9.15 CBIs

1,2,9,9a-Tetrahydrocyclopropa[*c*]benz[*e*]indole-4-one (CBI)-based analogues of the anti-tumour antibiotics have been shown to be more stable (4 ×), biologically more potent (4 ×) and considerably more synthetically accessible than the corresponding agents incorporating the natural CPI alkylation subunit.[70, 77, 78] Boger *et al.* synthesised CBI-Indole$_2$ and compared its properties with the CPI analogue, CPI-Indole$_2$ (Figure 19). The CBI analogue proved to be 4 × more stable to acid-catalysed solvolysis and consequently 4 × more potent than CPI-Indole$_2$. The rate and intensity of DNA alkylation was also higher for the CBI analogue. Preliminary studies of *in vivo* anti-tumour activity revealed significant activity of CBI-Indole$_2$ at dosage levels for which there was little activity by CPI-indole$_2$. These observed differences are attributed to the enhanced availability of CBI-indole$_2$ due to its increased stability.[78] CBI-trimethoxyindole (CBI-TMI) ($IC_{50}$ = 20 pM) has also been shown to be as cytotoxic as duocarmycin SA ($IC_{50}$ = 10 pM) in L1210 leukaemia cells.[44]

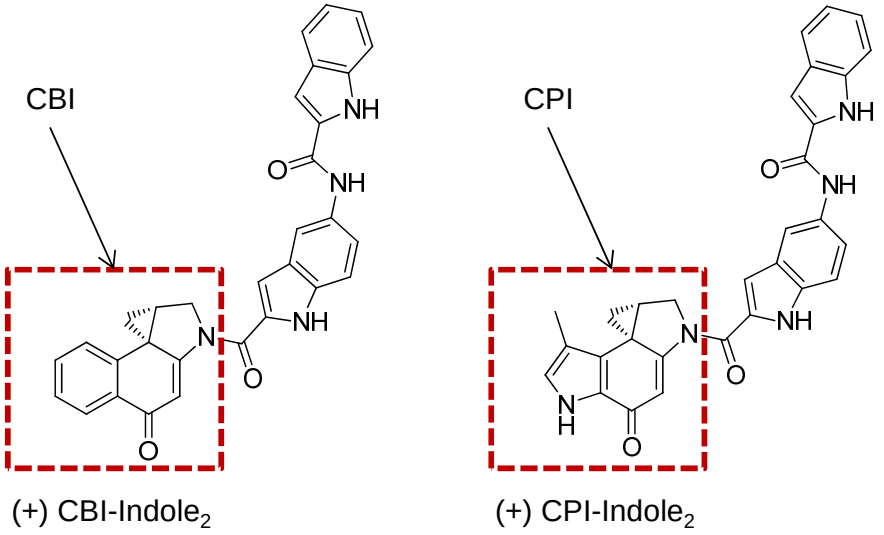


**Figure 19:** CBI and CPI alkylating subunits.

The 5-amino analogues of the CBI have gained popularity due to the ability to form more stable carbamate prodrugs (Figure 20). They have been shown to possess similar biological activity as their hydroxy counterparts. Carbamate prodrugs of the 5-hydroxy-CBIs have been reported (*e.g.* carzelesin) which are labile in plasma, releasing the corresponding phenol non-specifically. By providing more stable prodrug, 5-amino-CBI should persist in the plasma but allow specific release in the tumour tissue, ideally by a localised enzymatic activation step.[44]

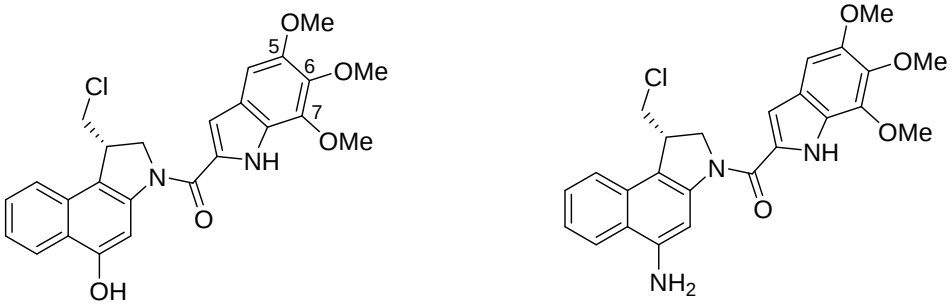


| Cell type | 5-Hydroxy-CBI-TMI | 5-Amino-CBI-TMI |
|---|---|---|
| AA8 | 0.21 ± 0.06 | 0.21 ± 0.03 |
| UV4 | 0.09 ± 0.004 | 0.14 ± 0.01 |
| EMT6 | 0.13 ± 0.01 | 0.13 ± 0.01 |

**Figure 20:** Cytotoxicity ($IC_{50s}$ in nM, 4 h exposure, ±SE) for nitrogen-substituted *seco*-CBI-TMI analogues. Average of two or more determinations.

Synthesis and evaluation of (+)-5-amino-CBI-TMI showed that it had almost an identical cytotoxicity when compared to its 5-hydroxy counterpart (Figure 20). The amino derivative was also shown to undergo exclusive alkylation at adenine.[44, 79]

#### 1.4.3.9.16 Modification of the non-alkylating subunit

The rate of alkylation of DNA and the cytotoxicities of the simplified analogues of the natural anti-tumour antibiotics lacking the non-alkylating subunit tend to be lower. This suggests an important role for the non-alkylating subunit in terms of enhancing the rate of alkylation and potency. Many modifications have been made on the non-alkylating subunit with the aim to understand the structre activity relationship and to obtain compounds with better solubility and lower toxicity.[52]

Increasing cytotocity is obsereved with increase in size and length of the non-alkylating subunit.[67] In saying this, (+)-CBI-indole$_2$ exhibits cytotoxic potency comparable to (+)-CC-1065.[77] Studies into the effect of the three methoxy groups of the 5,6,7-trimethoxindole (TMI) group of the duocarmycins, has shown that the substituent at C5 is more important than those at the other positions (Figure 20). C5 methoxy substituents alone provide fully active agents, with little or no input from the C6 and C7 methoxy group. NMR structures of DNA-bound duocarmycin and its analogue lacking the three methoxy groups showed that the presence of the methoxy group at C5 increases the twist in the DNA-bound agent.[52] Further studies into the effect of C5 substitution was made by Parrish *et al.*[50] It was observed that a variety of substituents in this postion had different effects on potency. For instance, when C5 had a hydroxy-substituent, there was a 4-fold reduction in potency but 5-fold increase in cytotoxicity was observed when the C5 substituent was an ethoxy group.[50, 67]

Investigations to find ways of improving the cytotoxicity and aqueous solubility of these agents led to Millbank *et al.*[80] synthesising a series of amino-*seco*-CI analogues with varying non-alkylating subunit. One of the non-alkylating subunit was dimethylaminoethoxyindol-2-carboxylic acid (DMAI) which retains a 5-alkoxy substituent for enhanced cytotoxicity and also contains a dimethylaminoethyl group to improve solubility. Biological and solubility assays showed that the analogue with the DMAI subunit was more potent across a range of cell lines compared to the analogue with C5 methoxy group. Solubility was also considerably increased in the DMAI analogue (Figure 21).[80, 81]

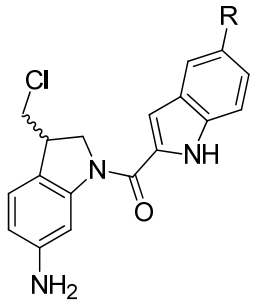


| R | Sol (μM)[a] | $IC_{50}$ (μM)[b] | | | |
|---|---|---|---|---|---|
| | | AA8 | UV4 | EMT6 | SKOV3 |
| 5-OMe | 23 | 0.31 ± 0.07 | 0.047 ± 0.001 | 0.23 ± 0.01 | 0.67 ±0.04 |
| 5-$O(CH_2)_2NMe_2$ | 700 | 0.16 ± 0.01 | 0.044 ± 0.001 | 0.12 ± 0.01 | 0.26 ± 0.04 |

**Figure 21:** Effects of DMAI non-alkylating subunit. *a* Solubility in 0.1 M phosphate buffer (pH 7.0) at room temperature. *b* $IC_{50}$; concentration of drug to reduce cell numbers to 50% of controls following a 4 h drug exposure. Average of 2-5 determinations ± SEM.

#### 1.4.3.9.17 Prodrugs

The anti-tumour antibiotics are unquestionably very potent. However, these agents lack intrinsic selectivity for tumour cells over normal cells. This undesired toxicity limits the efficacy of these agents. The design and synthesis of prodrugs to selectively deliver these agents to tumour cells is therefore very important.

#### 1.4.3.9.17.1 Tumour-activated produgs

Design of agents selectively activated within the target reduces toxicity and increases targeting. Tumour-activated prodrugs involve the design of non-toxic prodrugs where the therapeutic effect of the drug is masked until activated by unique phenotypic differences within the tumour environment. This activation can be enzymatic, chemical, spontaneous or a combination of these and allows the prodrug to undergo selective cellular metabolism.[82, 83] In general, tumour-activated prodrugs (TAPS) consists of a trigger, a linker and an effector (Figure 22).

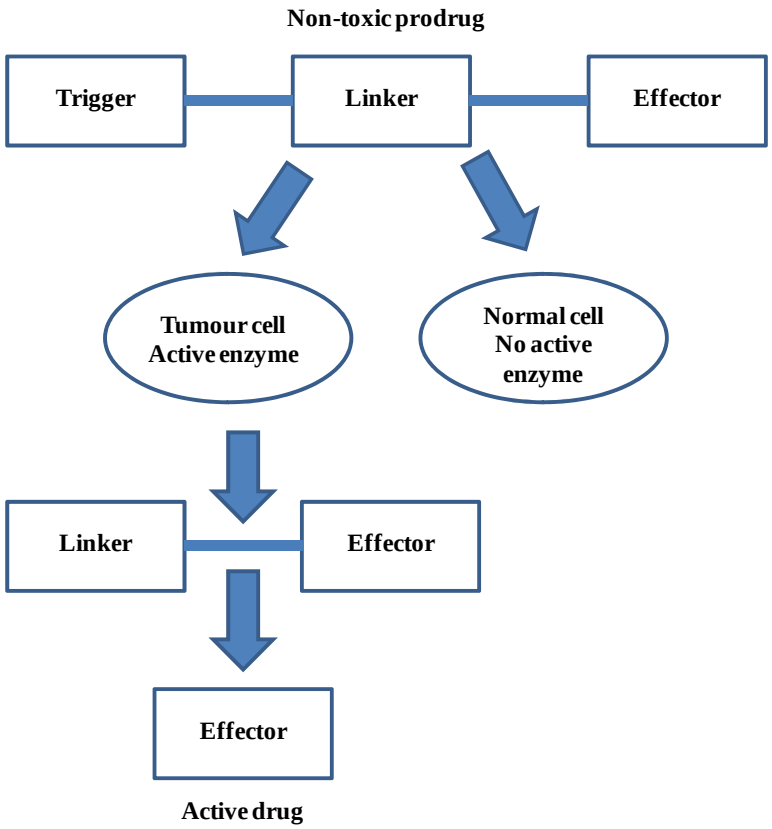


**Figure 22:** Model for tumour-activated prodrugs.[82,83]

The trigger controls selectivity and is joined to the effector which is the active agent through a linker.[82, 83] In order for this strategy to work, there are a number of requirements the prodrug has to meet:[84]

- Relatively stable *in vivo*;
- Less molar toxicity compared to active drug;
- High volume of distribution into tumour tissues;
- Efficient selective activation.

#### 1.4.3.9.17.2Enzyme-based activation of prodrugs

Enzyme based activation of prodrugs includes antibody-directed enzyme prodrug therapy (ADEPT), gene directed enzyme prodrug therapy (GDEPT) and prodrug monotherapy (PMT).[85]

#### 1.4.3.9.17.2.1 ADEPT

This concept introduced by Bagshawe in 1987[86] is a promising approach to selective delivery of drugs to cancer cells. It involves administration of an enzyme conjugated to a tumour

specific antibody which localises the enzyme at the tumour. A prodrug is then administered which acts as a substrate for the enzyme, resulting in the release of free drug at the tumour site thereby ensuring selective delivery of the drug.[52, 87]

Tietze *et al.*[81] developed a prodrug of a duocarmycin analogue, the activation of which depended on the ADEPT concept (Figure 23). The cytotoxic potency of the prodrug was very low ($IC_{50}$ = 3600 nM), compared to that of the prodrug in the presence of the activating enzyme β-galactosidase (β-Gal) ($IC_{50}$ = 0.75 nM).[81]

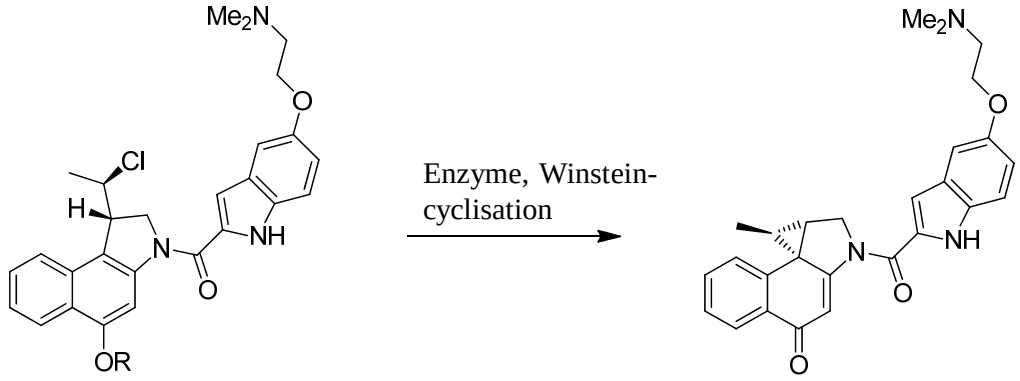


Prodrug
(+)-(1*S*, 10*R*), R = β-Gal, $IC_{50}$ = 3600 nM
R = H, $IC_{50}$ = 0.75 nM

(+)-Drug

**Figure 23:** Activation of a duocarmycin analogue *via* the ADEPT concept.[81]

This approach to selective delivery of drugs is, however, very complex as two separate agents and a time interval between their administration are required for their efficacy.[52] The ADEPT approach also tends to be expensive and the selected monoclonal antibody and enzyme must be able to cope with possible immune response.[88]

#### 1.4.3.9.17.2.2 GDEPT

This concept is similar to ADEPT, the difference being that the activating enzyme is introduced to the tumour through a gene delivered by a vector. Once expression of the enzyme occurs, a prodrug can be given, which is then selectively activated in the tumour. Ideally, the enzyme needs to be expressed exclusively at the tumour site compared to normal tissues or blood. The concentration and catalytic activity of the enzyme should also be sufficient to activate the prodrug under physiological conditions. A bystander effect is also desirable to kill neighbouring cells since not all tumour cells will express the enzyme. This requires that, after activation of the prodrug, the active drug kills both the tumour cells in

which activation occur as well as neighbouring tumour cells. The enzyme can be of non-mammalian origin or human origin where the enzyme is expressed at low concentration or is absent from the tumour cells. For enzymes of non-mammalian origin, the major drawback is their immunogenicity. With the human enzymes, their presence in normal tissues precludes selective activation unless modifications are made to the substrate requirements of the enzyme.[89]

#### 1.4.3.9.17.2.3 PMT

Prodrug monotherapy involves the exploitation of an intrinsic enzyme which is up-regulated in malignant tissues to selectively activate a prodrug.[85] Endoproteases are frequently up-regulated in tumour tissues as a consequence of tumour expansion or are sometimes a necessity for tumour expansion. One such enzyme is the prostate-specific antigen (PSA), which is exclusively expressed within the prostate and is able to cleave short peptide sequences, making it a good target for PMT. Peptide-conjugated prodrugs can therefore be designed to be activated by PSA to achieve selectivity.[82]

### 1.4.3.9.17.3 Prostate-specific antigen (PSA)

Prostate-specific antigen also known as human kallikrein 3 (hK3) is a serine protease with chymotrypsin-like specificity.[90, 91] PSA (Mw 33,000) is a single-chain glycoprotein.[92] The enzyme is secreted by normal and malignant cells of the prostate gland and leaks into circulation in higher proportion in prostate cancer. The level of PSA is elevated in prostate tumours and is more proteolytically active compared to normal prostate tissues which lack detectable PSA enzyme activity.[82] The majority of the enzyme molecules that leak into circulation are complexed with protease inhibitors present in serum which are at a $10^4$-$10^5$-fold molar excess. These inhibitors include α-1-antichymotrypsin (ACT), α-2-macroglobulin (A2M) and α-1-trypsin inhibitor (API).[35, 93, 94] The protease inhibitors bind in such a way as to cover the active site of the enzyme, thereby inhibiting enzymatic activity (Figure 24).[95] This means that PSA enzymatic activity is restricted to the prostate where it is secreted.

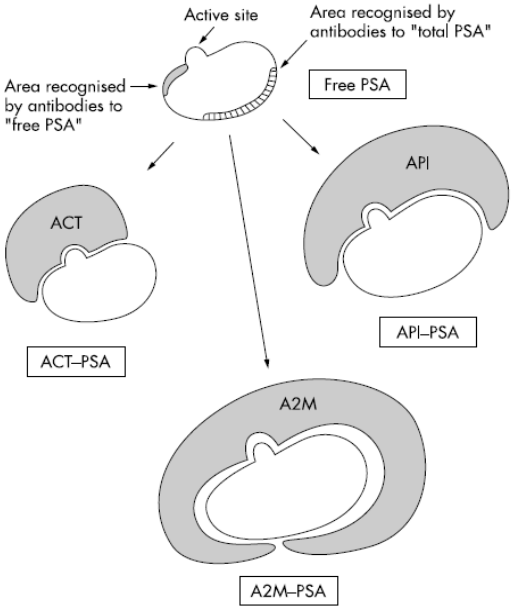


**Figure 24:** PSA protein binding.[95]

About 1-10% of the enzyme that leaks into circulation in prostate cancer patients is said to be, however, free and active.[93] The function of PSA is to dissolve the gel formed after ejaculation and thereby permit movement of sperm in the female genital tract.[35] The enzyme achieves this *via* selective cleavage of semenogelin at specific amino-acid sequences.[96] Isolation of the digestive fragments of seminogelin by PSA has made it possible to produce PSA cleavage maps for human semenogelin I. It was observed that the peptide bond between Gln and Ser at positions 349 and 350 in semenogelin I was the most readily cleaved bond. Modifications of the amino-acid residues surrounding this bond led to the synthesis of a heptapeptide (N-glutaryl-(4-hydroxyprolyl)-Ala-Ser-cyclohexylglycyl-Gln-Ser-Leu-OH) which is selectively cleaved by PSA.[97] Studies have shown that the peptide His-Ser-Ser-Lys-Leu-Gln-OH (HSSKLQ) is also a PSA-specific peptide substrate that is efficiently and selectively cleaved by the enzymatic activity of PSA.[98] With this knowledge, one can design a peptide prodrug that is activated by PSA within the prostate to achieve selective delivery of the drug to prostate tumour.

#### 1.4.3.9.17.3.1 PSA-cleavable prodrugs

Based on the PSA-cleavage map for semenogelin I and II, Denmeade *et al.*[99] synthesised a range of small peptides (≤ 7 amino-acids) and coupled their carboxyl terminus to 7-amino-4-methyl coumarin (AMC). This allowed monitoring of cleavage of the constructs by PSA, which results in increased fluorescence due to the release of the coumarin. The six-amino-acid

sequence HSSKLQ proved to be a good substrate with high degree of specificity for PSA over other peptidases. It also showed a good stability in sera even in men with elevated PSA levels and in human plasma, compared to other sequences especially those with tyrosine at the cleavage point which proved to be better substrates for other serine proteases, such as chymotrypsin and elastase. The only other enzyme with the ability to hydrolyse this peptide sequence significantly apart from PSA is cathepsin B, an intracellular lysosomal protease. This enzyme is, however, not significantly present in the extracellular fluid of normal cells but is substantially elevated around cancerous cells including prostate cancer cells. Hydrolysis by cathepsin B therefore provides another mode of selective cleavage of this peptide sequence within prostate tumours. The shorter amino-acid sequence SKLQ-AMC showed a higher $K_m$ but had the same $K_{cat}$:$K_m$ ratio and same serum stability when compared to HSSKLQ-AMC. SKLQ-AMC was also less soluble. The amino-acid sequence KLQ showed detectable cleavage whilst the two amino-acid sequence LQ-AMC showed no detectable cleavage at 5 mM concentration.[99]

Covalent linkage of the PSA cleavable peptide N-glutaryl-(4-hydroxyprolyl)-Ala-Ser-cyclohexylglycyl-Gln-Ser-Leu-OH) to doxorubicin led to the creation of a prodrug hydrolysed by PSA. In the presence of PSA-secreting prostate cells, the prodrug was hydrolysed to release leucyl-doxorubicin and, subsequently, doxorubicin, both of which are cytotoxic to tumour cells. Incubation of this prodrug with non-PSA-producing prostate cells resulted in less cytotoxicity compared to doxorubicin. The use of both the prodrug and doxorubicin at their maximally tolerated dose in nude mice showed that the prodrug was fifteen times more effective at inhibition of tumour growth than conventional doxorubicin. An eight-to-nine-fold molar equivalent dose of this prodrug could be administered *in vivo* without additional toxicity compared to doxorubicin.[82, 97] *In vitro* activity studies of the prodrug against human PSA-producing prostate cancer cells (LNCaP) proved that the concentration required to kill 50% of tumour cells was twenty-fold lower ($EC_{50}$ = 5 nM) than that required in non-PSA-producing prostate cancer cells such as DuPRO and PC3 ($EC_{50}$ = > 100 nM). This suggested that the activation of the prodrug was PSA-specific. The prodrug also reduced the weight of LNCaP tumours by 90% compared to doxorubicin which reduces tumours weight by just 6%. The concentration of doxorubicin in tumour from the prodrug was also higher than that from doxorubicin indicating the enhanced selective delivery of the drug to the target.[96, 97]

Denmeade *et al.*[100] also developed a PSA-activated thapsigargin prodrug, consisting of a primary amine-containing thapsigargin analogue coupled to PSA-specific peptide HSSKLQ. It was observed that not only was this prodrug effective against PSA-producing prostate cancer cells *in vitro* but also it had the ability to induce apoptosis in both lowly and highly proliferating cells.[100] Prostate cancer cell lines PC3 and DU145, however, have demonstrated the capacity to develop resistance to the cytotoxic effect of thapsigargin.[101] 5-Fluorodeoxyuridine has, in the same way been coupled to HSSKLQ and showed to have a remarkable inhibitory effect on tumour cells with little toxicity when given intravenously.[91]

Kumar *et al.*[94] developed paclitaxel prodrugs by coupling to PSA-cleavable peptides 2'-Mu-HSSKLQ or 2'-MuSSKYQ *via* an ethylenediamine (EDA) linker to give 2'-MuSSKLQ-EDA-paclitaxel or to 2'-MuSSKYQ-EDA-paclitaxel respectively (where Mu = morpholinocarbonyl protecting group). These compounds proved to be stable to degradation both in plasma and serum showing < 3% and < 2% degradation, respectively. The prodrug also showed improved solubilities (up to 70 mg $mL^{-1}$, ~38 mM) compared to paclitaxel (0.00025 mg $mL^{-1}$, ~0.29 µM). The half-life of the compounds in the presence of PSA was 10 h for 2'-MuSSKLQ-EDA-paclitaxel and 6 h for 2'-MuSSKYQ-EDA-paclitaxel. Incubation of 2'-MuSSKYQ-EDA-paclitaxel with a range of cell lines for 96 h showed a 3-5 fold increment in cytotoxicity ($IC_{50}$ ~1µM) in CWR22Rv1 PSA-producing prostate cell line than in the non-PSA-producing cell lines Du145 and TSU (Figure 25).[94]

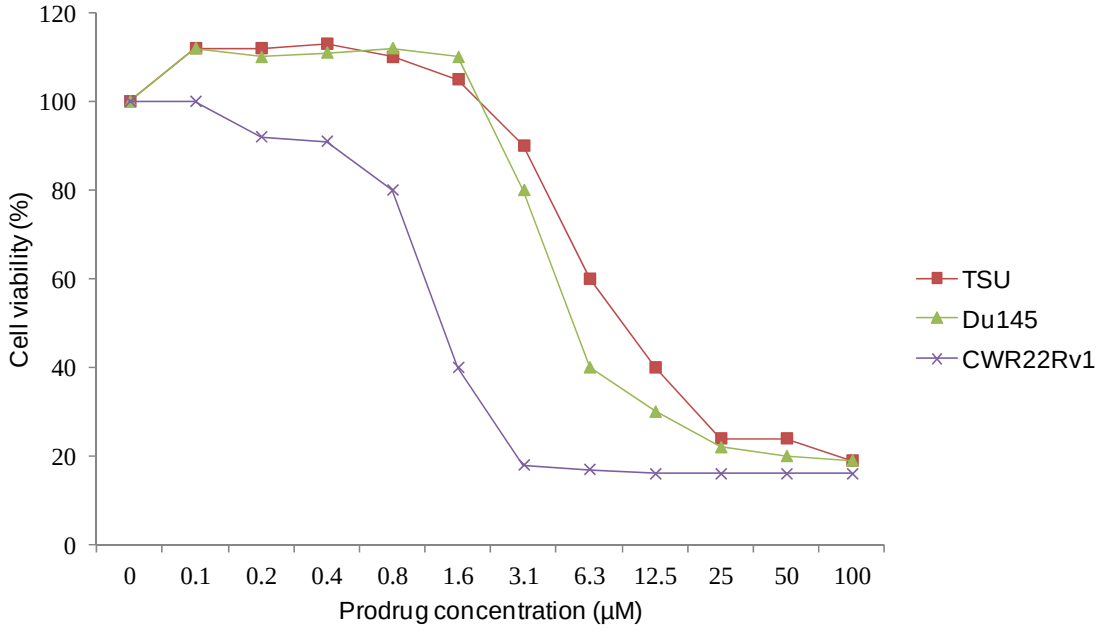


**Figure 25:** 2'-MuSSKYQ-EDA-paclitaxel effects on a range of cell lines.[94]

### 1.4.3.9.18 Self-immolative linkers

Insertion of a linker between the trigger and effector of a prodrug system is sometimes necessary. Directly linking the trigger to the effector (the parent drug molecule) in a prodrug system can reduced enzyme accessibility to the trigger due to steric hindrance caused by the bulky parent drug molecule resulting in lower rate of enzymatic hydrolysis.[102-104] After cleavage by the requisite enzyme, the linker-drug conjugate undergo self-immolation to release the drug. Elimination and intra-molecular cyclisation are among the most widely used self-immolation mechanisms (Figure 26). The rate of self immolation depends on:

- Nucleophilicity of the trigger group;
- The leaving ability of the drug;
- And the size of the ring formed.

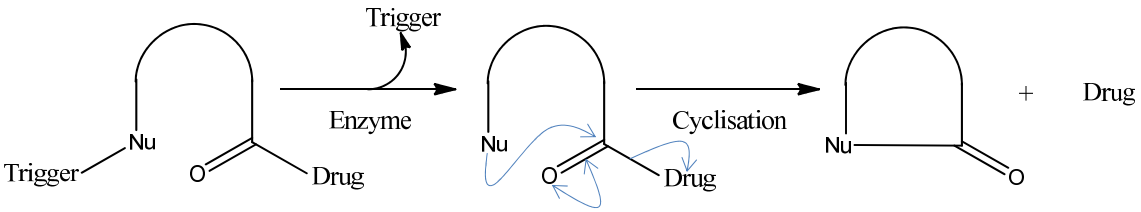


**Figure 26:** Mechanism for self-immolation of linkers.

The pKa of the masked nucleophile is essential to the rate of cyclisation. Aliphatic amines which are usually adopted as the trigger group, have a pKa of 9-11 and normally requires higher than physiological pH for optimal cyclisation. A study comparing hydroxylamine which has a lower conjugate acid pKa (~5.9) to aliphatic amine demonstrated that having a hydroxylamine as the trigger group resulted in a faster release of drug. This is explained by the fact that, at physiological pH, the majority of the aliphatic amine will be present in its protonated state, with reduced nucleophilicity compared to the hydroxylamine.[103]

#### 1.4.3.9.18.1 ADEPT based linkers

Using the ADEPT concept to investigate the effect of having a linker between the trigger and effector components in a prodrug system, Schuster *et al.* developed a β-D-galactosidase activatable prodrug of a duocarmycin analogue (Figure 27).[102]

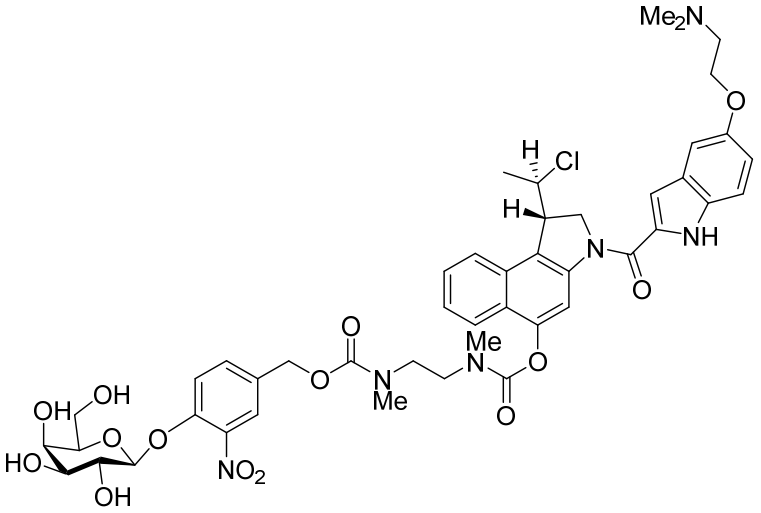


**Figure 27**: β-D-galactosidase activatable CBI prodrug.

The prodrug was shown to be stable over 24 h at pH 7.4 and 37°C with no cleavage of carbamate bonds and no generation of the free drug. The $IC_{50}$ of the prodrug was 29 nM whereas in the presence of β-D-galactosidase the $IC_{50}$ was 1.3 nM. The $IC_{50}$ of the prodrug in the presence of the enzyme is comparable to the $IC_{50}$ of the free drug (0.75 nM). This suggests that in the presence of the enzyme there is an efficient cleavage of the glycosidic bond and subsequent self-immolation to generate the free drug. DNA alkylation studies showed that the prodrug was not reactive towards DNA. Even at higher prodrug to DNA ratio of 3:1, the prodrug did not alkylate DNA.[102]

#### 1.4.3.9.18.2 PMT based linkers

The design of prodrugs to be activated by exopeptidases (especially carboxypeptidases) allows cleavage of peptide-based prodrugs directly from the C-terminal of short peptides. Endopeptidases on the other hand, cleave between amino-acids leaving pendant amino-acids attached to the drug.[105] The PSA-recognised sequence His-Ser-Ser-Lys-Leu-Gln↓Aaa is cleaved by PSA at the point shown ↓. PSA, being an endopeptidase, tends not to release drugs directly from the C-terminal of short peptides.[104, 105] This means that attachment of drug directly to the cleaving point of the amino-acid sequence can result in inefficient release of the drug since drug molecules are still attached to one or more amino-acid units which may or may not affect the desired pharmacological activity of the drug.[100, 105] For example, the doxorubicin prodrug developed by DiPaola *et al.*[96] was released as Ser-Leu-doxorubicin by the action of PSA. It was then left to aminopeptidases to produce the biologically active-forms Leu-doxorubicin and doxorubicin.[96] To address the problem whereby the presence of a

pendant amino-acid(s) attached to the released drug would diminish activity, self-immolative linkers can be interposed between the drug (effector) and the PSA-recognised peptide sequence (trigger). In this system, after the release of the linker-drug unit, the linker decomposed spontaneously to expel the drug.[106]

#### 1.4.3.9.18.3 Non-peptide linkers

Kumar *et al*.[94] synthesised a series of paclitaxel prodrugs linked to a PSA-cleavable peptide *via* the self-immolative linkers 4-aminobenzyl alcohol (PABA) and ethylenediamine (EDA). The half-life for hydrolysis by PSA of PAB-containing prodrugs ranged from 12-14 h releasing the PSA-cleavable peptide and free paclitaxel.

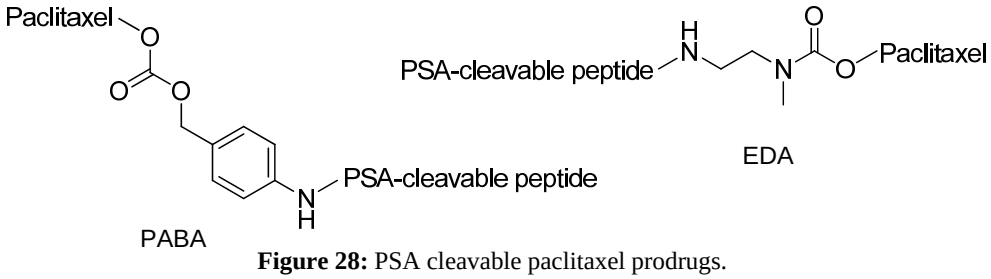


**Figure 28:** PSA cleavable paclitaxel prodrugs.

The cleavage product PABA-paclitaxel was not detected, demonstrating an instantaneous self-immolation of the linker to release the drug after PSA activation. The PABA linker was, however, unstable to non-specific hydrolysis in serum and plasma. This was attributed to the weak carbonate bond between PABA and paclitaxel. The EDA linker contains a carbamate bond with paclitaxel and proved to be stable in serum and plasma. The EDA containing prodrugs also showed improved PSA hydrolysis with a half-life 6-10 h.[94]

#### 1.4.3.9.18.4 Dipeptide-based linkers

Dipeptide-based linkers are cyclisation-based linkers that undergo intra-molecular cyclisation to release the drug. These linkers consist of a masked nucleophile that attacks the carbonyl of the –C(O)-X-Drug function after the action of the enzyme to cleave the trigger.[83]

##### 1.4.3.9.18.4.1 Proline-based dipeptide linkers

Investigations into antibody-drug conjugates led to the development of a novel linker by Manabe *et al.*[104] consisting of Gly-Pro dipeptide which forms a diketopiperazine when cyclised. The formed diketopiperazine is normally stable and non-toxic. This linker was incorporated into plasmin-cleavable paclitaxel prodrugs and biologically evaluated. Prodrugs

were found to be cleaved by plasmin within 24 h. A prodrug with a Gly-L-Pro linker released 39% of paclitaxel whilst only 15% of paclitaxel was released after 3 h when the linker was substituted with Gly-D-Pro. Plasmin-cleavable paclitaxel prodrug without the linker showed only 9% of drug release after 3 h.[104]

Brady *et al.*[107] also designed a vinblastine prodrug with the dipeptide, Ser-Pro, as the self-immolative linker. After the enzyme (PSA) cleavage, the linker undergoes intra-molecular cyclisation to form diketopiperazines (DKP), releasing the drug in the process (Scheme 2).[83]

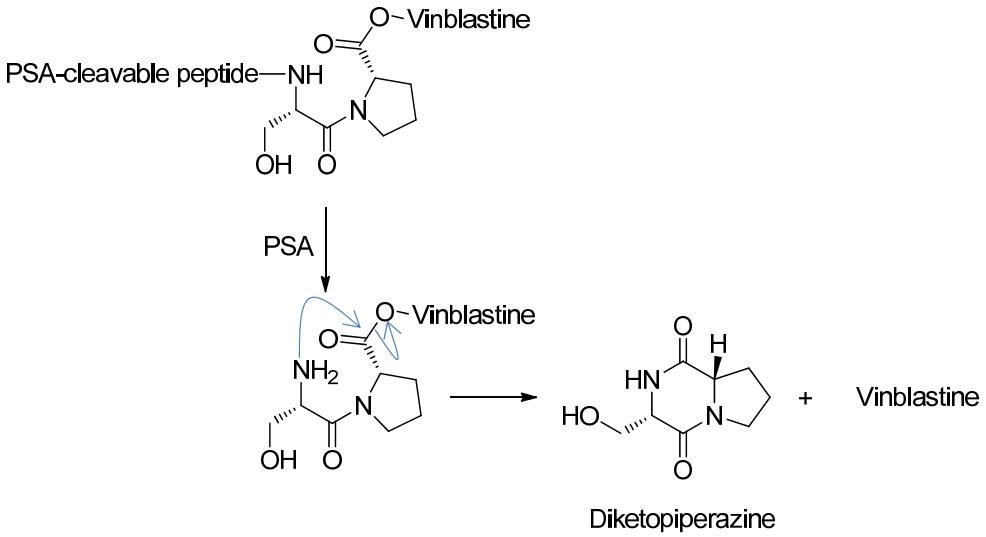


**Scheme 2:** Mechanism of drug release by cyclisation-based linkers.

The proportion of the dipeptide linker in the *cis*-amide conformation determines the rate of DKP formation (Figure 29). Most peptide sequences adopt the energetically favourable *trans* conformation; however proline is unique that as a tertiary amide, it can readily adopt a *cis*-amide conformation. The presence of proline increases the proportion of the dipeptide adopting the *cis*-amide conformation, thereby increasing the rate of DKP formation and therefore the release of the active drug.[83, 104]

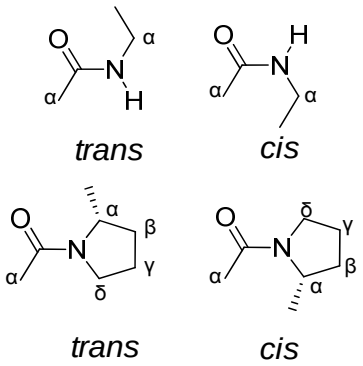


**Figure 29:** *Cis/trans* dipeptide configurations

The enhanced reactivity is due to the fact that the *cis*-amide conformation places the exposed nucleophile in close proximity to the electrophile unlike the *trans*-amide conformer.

#### 1.4.3.9.18.4.2 *Pseudo*proline based linkers

The *pseudo*prolines such as 5,5-dimethyl-4-thiaproline (Dmt) and 5,5-dimethyl-4-oxaproline (Dmo) (Figure 30) have been used in place of proline and found to force peptides into 100% *cis*-amide conformation.[106, 108] These peptides have mostly included *S*-Dmo or *R*-Dmt.[106, 108] It has been shown that Dmt dipeptides in the L,*S* diastereomeric series cyclise faster (*e.g.* L-Val-*S*-Dmt: $t_{1/2}$ pH 8.0 =15 min, pH 7.0 = 45 min) compared to those in the L,*R* series (*e.g.* L-Val-*R*-Dmt: $t_{1/2}$ pH 8.0 = 1600 min, pH 7.0 = > 2700 min).[105, 106] An attempt by Suaifan *et al.*[105] to incorporate Dmt in a peptide chain as the dipeptide, L-Val-*S*-Dmt, proved impossible since cyclisation into DKP was faster than coupling of L-Val-*S*-Dmt to other amino-acids. This effect was even observed when the amino group of L-Val was in the protonated form.[105] Furthermore, it has been shown that generation of Dmt within a growing peptide chain (*i.e.* Aaa-Cys → Aaa-Dmt) is not possible as reaction only occurs at the sulfur.[105]

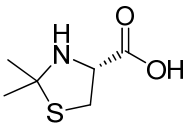

5,5-dimethyl-4-thiaproline

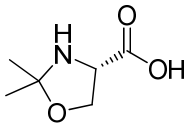

5,5-dimethyl-4-oxaproline

**Figure 30:** Structures of *R*-Dmt and *S*-Dmo.

Dmo has been frequently used as a masked form of serine to avoid solubility and aggregation problems that arise during peptide synthesis. It can be constructed within a peptide chain by treatment of Aaa-Ser or Aaa-Thr with 2,2-dimethoxypropane under acidic conditions.[109] This cyclic amino-acid causes peptides to adapt the *cis*-amide conformation and should encourage cyclisation and self-immolation after release from a prodrug system when used as a self-immolative linker.[105, 110, 111] With an appropriate selection of a self-immolative linker, drug release should be rapid at the tumour site and reduce the diffusion of the linker-drug intermediate outside the tumour site causing non-specific delivery of the drug.

### 1.4.3.10 Enhanced permeability and retention effect (EPR)

Differentiating between normal cells and tumour cells is one of the main challenges facing the development of selective chemotherapeutic drugs. EPR is one of the few tumour specific characteristic that allows selective delivery of macromolecules to tumour sites. The EPR effect has been showen to be universal for solid tumours. In an effort to increase nutrient and oxygen supply, tumours undergo extensive angiogenesis resulting in hypervasculature. The vascular system and the lymphatic drainage system become defective and impaired. There is an increase in permeability mediators such as bradykinin and nitric oxide as part of the

mechanism to increase nutrient and oxygen to tumour cells. The process results in tumour tissues being supplied with leaky blood vessels compared to normal cells (Figure 31).[112, 113]

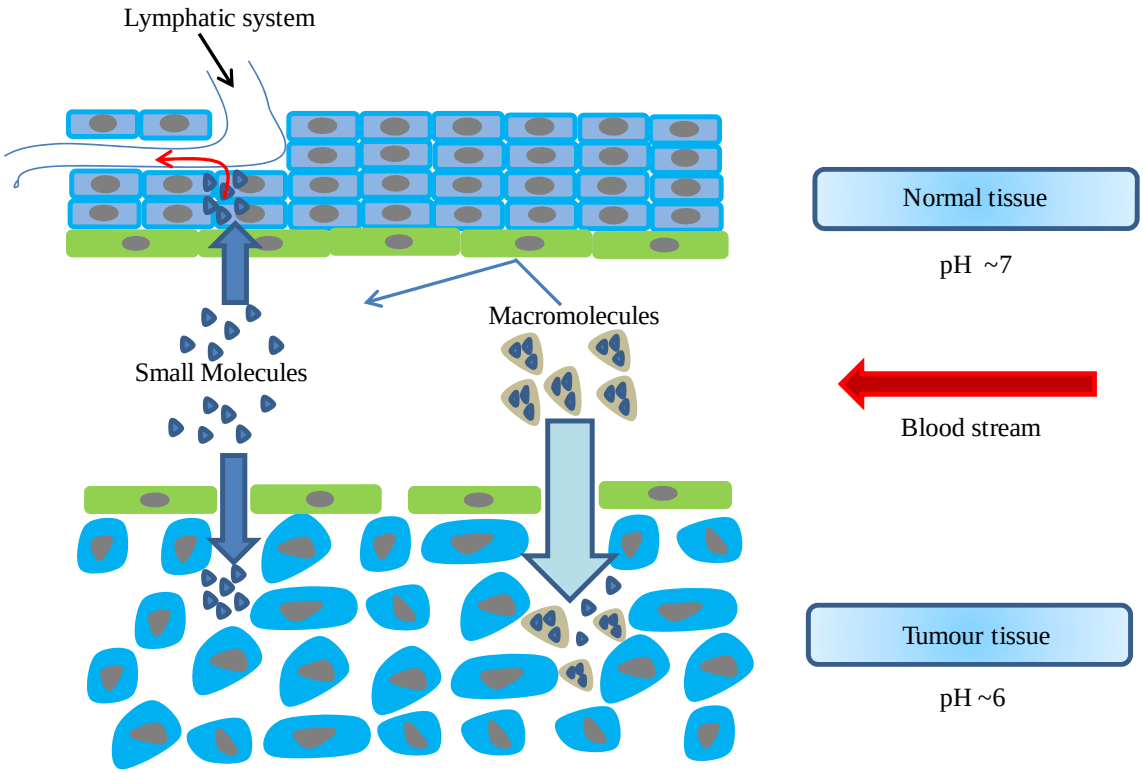


**Figure 31:** Anatomical differences between normal and tumour tissues.[114]

To enhance further the selective delivery of drug to tumour cells, the enhanced permeability and retention effect (EPR) can be exploited. Macromolecules are preferentially taken up by solid tumours due to the poor tissue drainage and increased tumour permeability of tumour tissue (Figure 31). Macromolecules delivered to the interstitial space of tumour tissues are cleared very slowly leading to accumulation at higher concentration of macromolecules over a prolonged period. Exploitation of these abnormalities of the tumour vasculature can deliver drugs selectively to tumours leading to enhanced therapeutic benefits as well as fewer systemic side-effects.[112, 114]

Most of the anticancer agents in use are of low molecular weight, exhibiting short plasma half-lives and high overall clearance. The small size of these molecules means they diffuse quickly into both normal tissues and tumour tissues. This result in relatively small amounts of drug reaching the tumour site calling for a higher dose to be administered which in turn results in increased side-effects.[115] Developing drugs linked to a macromolecule with molecular weight of ~20 KDa or above is expected to facilitate the EPR effect.[114]

#### 1.4.3.10.1 Drug-polymer conjugates

Conjugation of polymer to drugs with low molecular weight is one means of exploiting the EPR effect. Various polymers have been used as carriers of anti-cancer drugs, such as doxorubicin. An optimal polymeric drug carrier system would ideally be water-soluble, biocompatible and non-toxic. The use of polymeric carrier systems not only improves water solubility but also improves bio-distribution and plasma clearance of the drug.[115, 116]

Seymour *et al.*,[117] investigating the biodistribution of N-(2-hydroxypropyl)methacrylamide (HPMA) co-polymer-conjugated doxorubicin, observed that it showed a preferential localisation in tumour tissues 10-15 times more than that achieved using free doxorubicin administered at equal doses (5 mg of doxorubicin per Kg). The selective delivery of this polymer-conjugated doxorubicin meant that toxicity was low allowing elevated doses (18 mg of doxorubicin per Kg) to be administered which achieved levels of drug in the tumour, 45-fold higher than that resulting from the standard dose of free doxorubicin (5 mg $Kg^{-1}$). The polymeric doxorubicin also showed a lower volume of distribution and longer plasma half-life than free doxorubicin.[117]

Vasey *et al.*[118] undertook a phase 1 clinical and pharmacokinetic study on doxorubicin bound to N-(2-hydroxypropyl)methacrylamide (HPMA) copolymer through a lysosomally cleavable peptide linker. It was found that, despite the administration of higher doses, typical anthracycline-like toxicities were attenuated. For instance, with prophylactic $5HT_3$ antiemetic administration, nausea and vomiting was found not to pose any problem. Furthermore, only 8% of patients (3 of 36) experienced grade 2 alopecia and there were no incidences of congestive cardiac failure.[118]

To enhance the delivery and solubility of a PSA-cleavable peptide prodrug of a potent thapsigargin analogue-L12ADT, Chandran *et al.*[119] conjugated the peptidyl prodrug with HPMA copolymer (Figure 32).

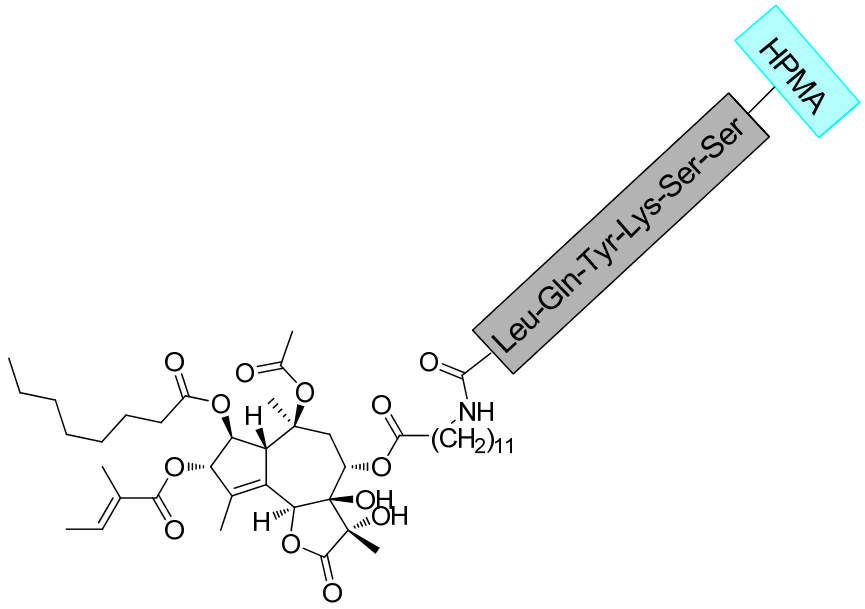


**Figure 32:** PSA-cleavable polymeric L12ADT prodrug- HPMA-SSKYQL-12ADT.

Stability studies which incubated the polymeric prodrug in human plasma did not show appreciable levels of L12ADT suggesting that the prodrug is stable to non-specific hydrolysis. PSA hydrolysis studies showed that the prodrug was cleaved by the enzyme to release the active drug. Cytotoxic assay was undertaken using the human prostate cancer cell line CWR22R. This cell line was shown to produce low percentage of enzymatically active PSA (≤ 5% active) *in vitro*. Therefore, in the absence of exogenous PSA, the polymeric prodrug did not show any cytotoxicity. Addition of exogenous active PSA (final concentration of 5 µg $mL^{-1}$), however, showed a concentration-dependent growth inhibition. *In vivo* studies to evaluate the uptake and release of active drug involved administering the polymeric prodrug to mice bearing the PSA-producing CWR22R-H xenografts. Intravenous doses of the polymeric prodrug were given either as a single injection or 4 × daily. After a single dose, a ~3-4 fold higher in concentration of L12ADT was detected in tumour tissues, compared with plasma or skeletal muscle. After four consecutive doses, the plasma concentration of the released drug was similar to the concentration observed when single dose was administered (Figure 33).[119]

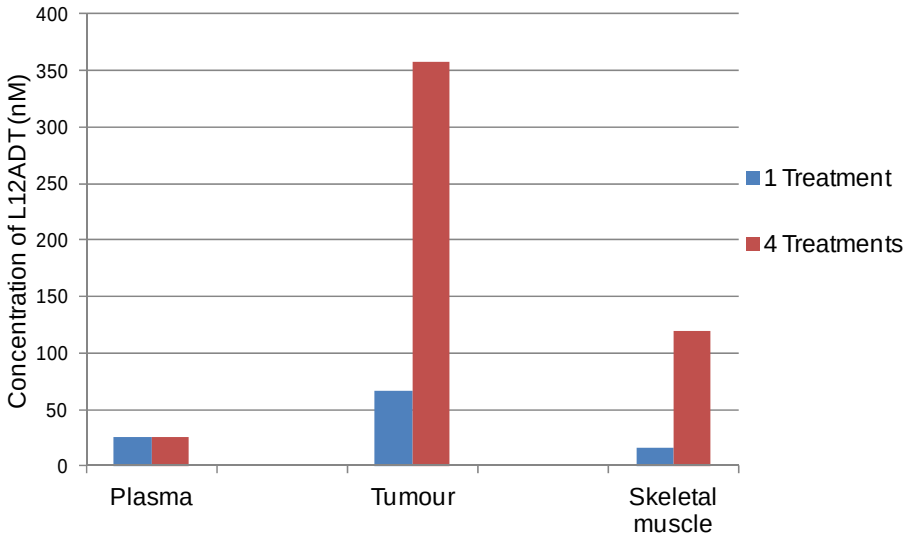


**Figure 33:** Levels of L12ADT at 24 h after i.v. injection of HPMA-SSKYQL-12ADT into nude mice bearing s.c. PSA-positive CWR22R-H xenografts.[119]

On the other hand, the concentration of drug in the tumour (~350 nM) was ~15-fold higher than in plasma and and 3.5-fold higher than the concentration in skeletal muscles. This confirmed the viability of the EPR effect by developing a small molecular weight drug into a macromolecule enabling increased tumour targetting.[119]

#### 1.4.3.10.2 PEGylated prodrugs

Polyethylene glycol (PEG) (Figure 34) is an amphiphilic molecule with its hydroxy end-groups easily derivatised. This allows easy coupling of PEG to other molecules. In aqueous environment such as the plasma, each ethylene oxide monomer within PEG is able to bind to 2-3 water molecules. This layer of water molecules formed around PEG is said to be responsible for its ability to keep away cells and proteins from its surface giving the polymer properties such as:

- Reduced immunogenicity;
- Reduced antigenicity;
- Resistance to enzyme degradation.

The degradation product of low molecular weight (MW) PEG (< 400 Da) is said to be toxic whilst no evidence of such toxic metabolites has been observed from higher MW PEG (> 1000 Da). Due to the good safety profile of high MW PEG, these have been used in food, pharmaceutical and cosmetic products. *In vivo* clearance of PEG is through urine and faeces (MW > 20 KDa) without structural change to the polymer.[120-122]

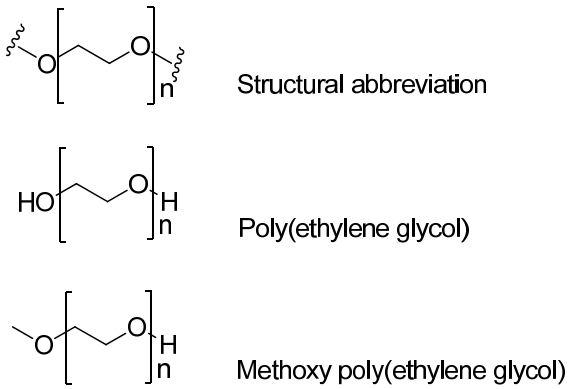


**Figure 34:** General structures for poly(ethylene glycol).

PEGylated proteins possess better clinical features compared to unmodified proteins. These include resistance to proteolysis, increased solubility, improved chemical / thermal stability and being shielded from the immune system. PEGylation also prolongs the circulation of these agents, a feature attributed to the reduced clearance of these agents from the circulation system by kidney filtration. PEGylation often results in marked reduction in potency of drugs and can therefore be exploited in the development of a prodrug if PEG is released as part of the activation process.[116, 120, 121] For instance water soluble PEGylated paclitaxel-7-carbamates showed $10^3$ less activity than the free paclitaxel *in vitro* and were non-toxic in mice.[122]

PEG has also been used to develop prodrugs of small cytotoxic molecules in other to exploit the EPR system for selective delivery. These drugs include taxol, campothecin and doxorubicin. PEGylation results in the properties of PEG being transferred to the conjugated drugs leading to improved properties such as increased solubility and improved pharmacokinetics.[121] A PEG-peptide-doxorubicin prodrug (Figure 35) designed to be activated by lysosomal thiol-dependent protease (triosomes) was synthesised by Veronese *et al*.[123] PEG of molecular weight of 5-20 kDa was used. *In vitro* assay showed that the PEG-peptide-doxorubicin was 10-100 fold less toxic ($IC_{50}$ = > 2µg $mL^{-1}$) than free doxorubicin ($IC_{50}$ = 0.24 µg $mL^{-1}$) against B16F10 cells. Conjugates with higher MW PEG had a longer circulation in the blood after intravenous injection due to reduced renal clearance compared to free doxorubicin. This led to increased tumour targeting leading to higher tumour doxorubicin concentration. All PEG conjugates had a longer plasma half-life.

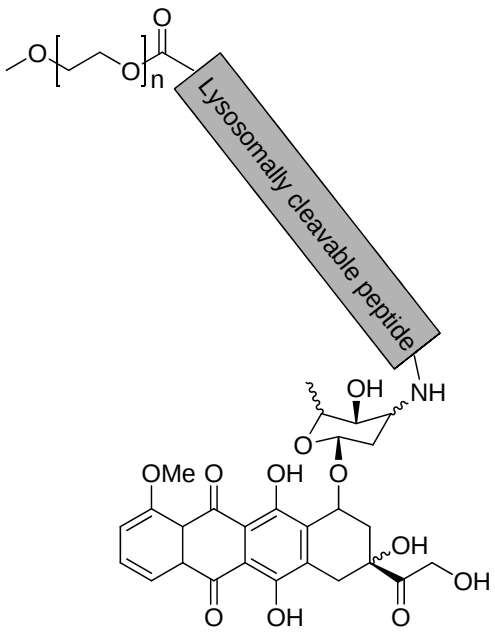


**Figure 35:** Lysosomally cleavable polymeric prodrug.

Despite the highest MW PEG conjugate showing greater tumour levels, the $PEG_{5KDa}$ had the most favourable tumour to heart ratio which is important in the case of doxorubicin since cardiotoxicity is a known dose-limiting toxicity. It was also observed that release of the drug by lysosomal enzymes was dependent on the peptide linker and had little dependency on the PEG carrier. *In vivo* studies using mice bearing subcutaneous B16F10 murine melanoma, showed that PEGylated peptidyl doxorubicin was more active than free doxorubicin which showed no significant anti-tumour activity.[123]

The use of a polymeric-peptide-prodrug system to achieve selective delivery to prostate tumour allows dual targeting based on EPR effect and protease activation. The EPR effect ensures that macropolymeric prodrug selectively accumulates in tumour tissues. Activation of the prodrug by PSA occurs in the extracellular fluid surrounding tumour cells. Prodrugs are therefore not required to penetrate tumour cells before being activated. The presence of active drug within the extracellular fluid will allow a bystander cytotoxic effect on both PSA-positive and negative cancer cells since not every cell in the tumour will be required to produce PSA before coming into contact with the active drug. This has a potential to reduce the chances of resistance developing.[119]

# 2 Aims and objectives

## 2.1 Aims

The project aims to develop a polymeric prodrug system, which will deliver highly potent drugs selectively to prostate tumours. The Enhanced Permeability and Retention effect (EPR) ensures that water-soluble polymers, such as PEG, accumulate in solid tumours (*e.g.* prostate cancer).[112, 114] Prostate-Specific Antigen (PSA) has been shown to be catalytically active only in the prostate.[35, 93, 94] Conjugating a drug to a polymer *via* a PSA-cleavable peptide will create a polymeric prodrug system with two modes of selectivity. The polymeric prodrug system that this project aims to develop will consist of a CBI anti-tumour antibiotic analogue precursor (*seco*-CBI) **3** attached to PEG through a PSA-cleavable peptide (SSKLQ) with or without a molecular clip (Leu-*R*-Dmo) to form the polymeric prodrugs **1** or **2** (Figure 36).

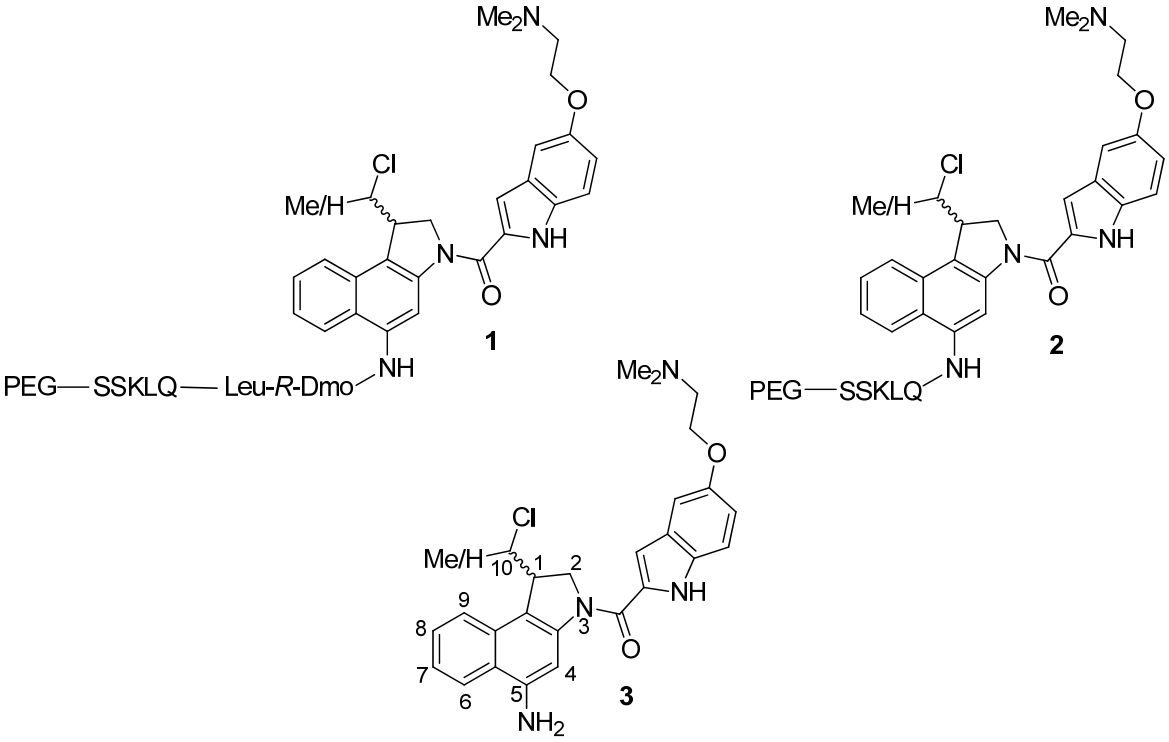


**Figure 36:** Proposed *seco*-CBI and the corresponding polymeric prodrugs.

## 2.2 Objectives

The project will proceed in three stages:

- Chemical synthesis and cytotoxic evaluation of the proposed CBI drug to be delivered selectively;
- Synthesis and evaluation of an advanced model to test PSA-triggered release of the CBI drug;

- Assembly and *in vitro* preliminary evaluations of the polymeric prodrug for PSA-triggered delivery of the CBI drug.

The proposed CBI drug comprises of a CBI alkylating subunit and 5-(2-dimethylaminoethoxy)indole-2-carboxylic acid (DMAI) as the non-alkylating DNA-binding subunit. DMAI is involved in extra non-covalent binding to the minor groove of DNA. CBIs have been extensively studied and have shown to be more stable, more potent and more synthetically accessible than the corresponding CPIs.[70, 77, 78] The proposed CBI drug is a modification of a 5-hydroxy-CBI drug synthesised by Tietze *et al.*[124] to allow linkage to the peptide delivery system through an exocyclic nitrogen rather than oxygen. This will allow an amide to be formed with the PSA-cleavable peptide, which will be more stable than would the corresponding ester. Substituting the 5-OH with an amine has been shown not to be deleterious to the activity of the CBI drug.[44, 79] The DMAI non-alkylating subunit **127** is chosen for ease of synthesis (Scheme 3). The tertiary amine also has the advantage of enhancing water solubility as the corresponding salt.[52, 81] The indole core of **127** will be synthesised using a Fisher-like indole synthesis. An alkoxy substituent will then be introduced at the C5 position of the indole.

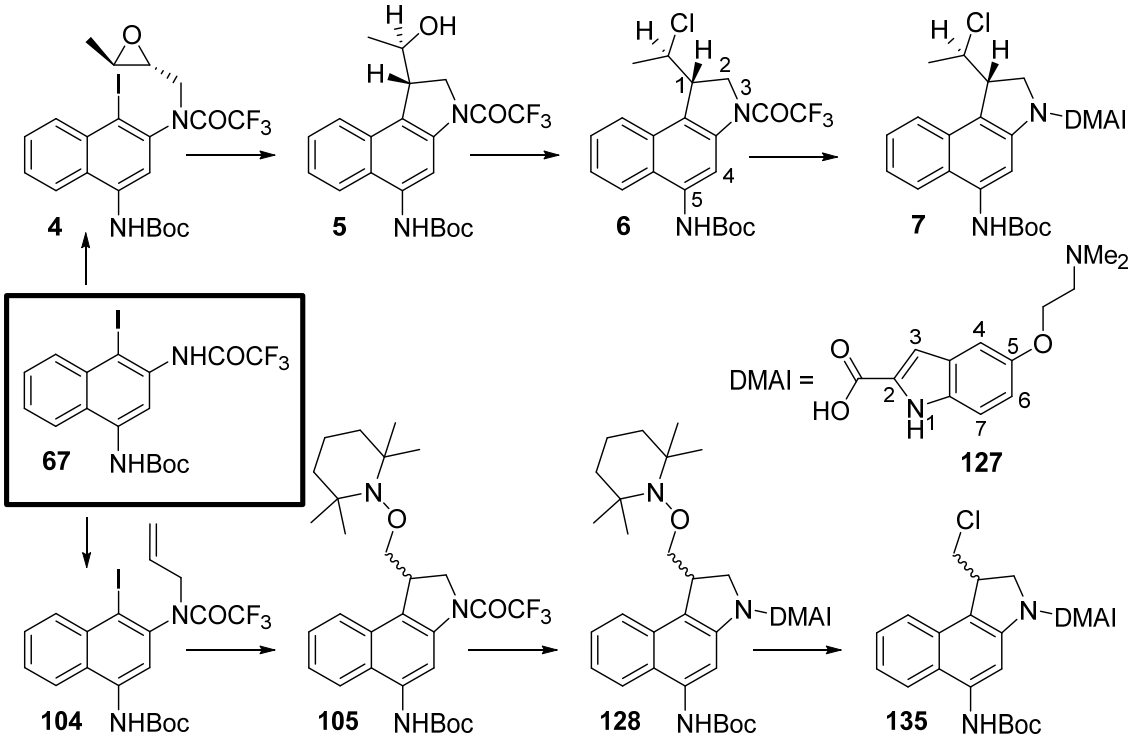


**Scheme 3:** Synthesis of the alkylating subunit of proposed *seco*-CBI drug.

Synthesis of the CBI drug will be achieved *via* the key naphthalene intermediate **67** which will be accessed through nitrated naphthalene derivatives. Reduction of the nitro groups

followed by orthogonal protection of the amino groups and substitution of the 1-position with iodine will give **67**. The ideal protection at the *ortho*-amino group of **67** will be small and more electronegative than the protection at the *para*-amino group. This will enable selective alkylation at the *ortho*-amino group with either *2R*,3*S*-3-methyl-2-(4-nosyloxymethyl)oxirane or allyl bromide to give **4** or **104**, respectively. The homochiral nosylate reagent will be synthesised using Sharpless epoxidation to give the epoxy alcohol, followed by functionalisation of the hydroxy group into the nosylate. A metal-mediated cyclisation of **4** will form the pyrrolidine ring of **5**. Efforts will be made to introduce an extra methyl group at position-10 of the CBI drug **3** using this synthetic route (Figure 36). This methyl group through steric hinderance will be expected to reduce reactivity of the *seco*-CBI by preventing direct alkylation at C10. This will contribute to the expected reduction in the cytotoxicity of the prodrug compared to the spirocyclised active drug.[125] The hydroxy group of **5** will then be converted to the chloride using a Mitsunobu-like reaction with retention of configuration. Deprotection of the $N^3$ protecting group will then allow coupling to the DMAI non-alkylating subunit to give **7**. With **104**, free-radical cyclisation with TEMPO trap will be explored to synthesise the pyrrolidine ring. The 2,2,6,6-tetramethylpiperidine will then conveniently act as a protecting group of the hydroxy group of **105**. Removal of the $N^3$ protecting group and coupling to the non-alkylating subunit will be followed by reductive removal of the 2,2,6,6-tetramethylpiperidine group to unmask the hydroxy group. Substitution of the hydroxy with chloride will give the protected *seco*-CBI **135**. Removal of the remaining protection on the C5 amino group of **7** and **135** will give the final *seco*-CBI.

DNA alkylation studies will be carried out on the synthesised *seco*-CBI to ascertain the effect on the melting temperature on calf-thymus DNA. This will inform the extent of DNA alkylation and also the effect of the drug upon DNA alkylation. The degree of shift in the DNA-melting temperature of calf-thymus DNA will show the potency of the *seco*-CBI. An MTS cytotoxicity assay will also be carried out on prostate cancer cell lines using **3** as well as the protected precursors **7** and/or **135**. Cytotoxicity tests on **7** and/or **135** will help predict the effect of conjugating the *seco*-CBI drug **3** to the peptide to form a prodrug.

An advanced model to test PSA-triggered release of the synthesised CBI will firstly involve synthesis of a non-cytotoxic model drug with an aromatic amine group and coupling to the peptide, Ser-Ser-Lys-Leu-Gln, which contains the amino-acid sequence Ser-Lys-Leu-Gln, claimed to be the minimal sequence required for recognition and cleavage by PSA.[99] The peptide-model drug conjugate will be incubated with PSA and the mixture examined by

HPLC to measure the rate of release of the model drug. This will give an insight into whether PSA can cleave the aromatic amine model-drug directly from the peptide as reported.[99] If the release is poor, the molecular clip, Leu-Dmo (2,2-dimethyl-1,3-oxazolidine-4-carboxy, analogue of proline) will be inserted between the peptide and model drug. This will allow PSA (an endopeptidase) to cleave between Gln and Leu-Dmo and release the Leu-Dmo-model-drug. The molecular clip is designed to then detach spontaneously, releasing the free drug.

Following on from this, the peptide-model drug complex will be linked to poly(ethylene glycol) at the N-terminal of the peptide. This polymer has extensive use in prodrug development due to its non-toxicity, non-immunogenicity and excellent pharmaceutical properties.[120-122] The polymer comes in a variety of molecular weights but for the purposes of exploiting the EPR effect, molecular weight of 20,000 Da will be used.[114] Preliminary trials to couple the peptide-model drug to the polymer will, however, involve PEG of 5,000 Da molecular weight. The polymer comes as the diol, with both ends having a hydroxy group and in a version where one of the ends is capped with a methyl group. This will give the possibility of attaching the peptide–model-drug to one or both ends of the polymer after functionalising the hydroxy group(s) into a nosylate. The polymeric-peptide-model-drug conjugate will then again be subjected to enzymatic assay for release of the model drug.

Once the polymeric prodrug concept has been proven, coupling of the synthesised CBI drug to the PSA-cleavable peptide will take place followed by assessment of cytotoxicity of the peptide-CBI drug complex against a range of prostate tumour cell lines. Cytotoxicity assay in non-PSA-producing cell lines such as Du145 and TSU will inform on the toxicity of the CBI prodrug whilst cytotoxicity assay in PSA-producing cell lines such as LNCaP and CWR22Rv1 will inform on the PSA-mediated release of the CBI drug.[94] The peptide-CBI prodrug will further be linked to PEG (20,000 Da) and subjected to further *in vitro* evaluations.

# 3 Results and discussion

The limited range of chemotherapeutic treatments for prostate cancer and the lack of intrinsic selectivity of most of these drugs has created a need to develop more selective novel agents to target prostate tumour. The anti-tumour antibiotics CC-1065 and the duocarmycins belong to a class of agents with high cytotoxicity to various tumours including prostate tumour cell lines.[42] These agents have been, however, precluded from clinical use due to toxic effects such as myelosuppression and delayed death in the case of CC-1065.[45, 47-49, 75] These compounds are also not easily synthetically accessible.

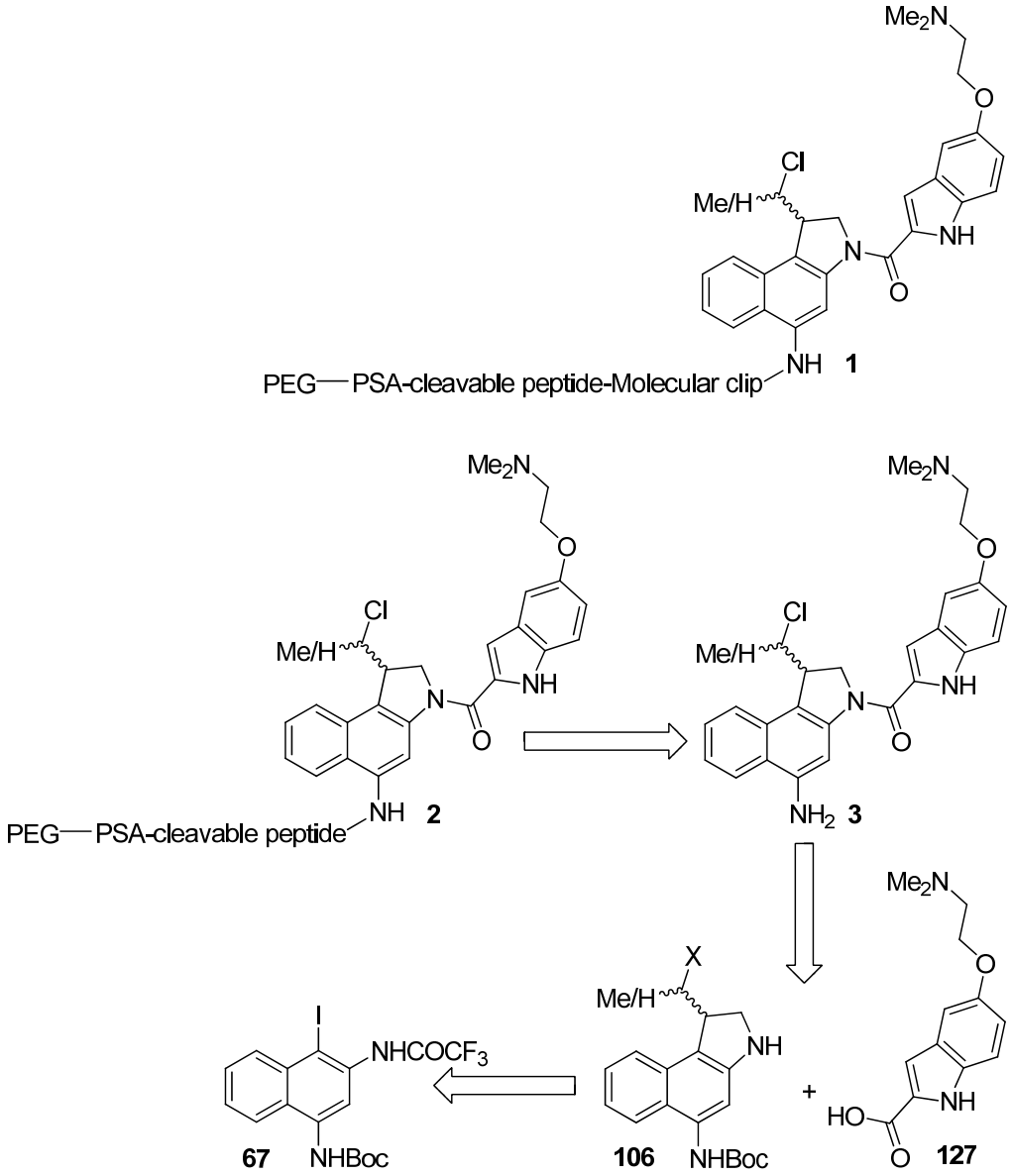


**Scheme 4:** Retrosynthesis of proposed polymeric prodrug system.

1,2,9,9a-Tetrahydrocyclopropa[*c*]benz[*e*]indole-4-one (CBI)-based analogues of the anti-tumour antibiotics have been shown to be more stable (4 ×), biologically more potent (4 ×) and considerably more synthetically accessible than the corresponding agents incorporating the natural cyclopropapyrroloindole (CPI) alkylation subunit.[70, 77, 78] Synthesis of the CBI-analogue will be followed by developing of a polymeric prodrug system for selective delivery to prostate tumours. The proposed polymeric prodrug **1** or **2** (Scheme 4) consists of a *seco*-CBI drug attached to one or both ends of the water-soluble polymer, PEG, *via* a peptide linker designed to be cleaved selectively by PSA. PSA has been shown to be able to cleave aromatic amines (*e.g.* 7-amino-4-methylcoumarin) directly from PSA-cleavable peptides.[99] Direct attachment of drug to the PSA-cleavable peptide **2** will therefore be investigated. However, direct attachment of drug to the cleavage point of the peptide linker sometimes results in inefficient release of the drug. For instance, a peptide prodrug of doxorubicin was released as leucyl-doxorubicin.[82, 97] To avoid situations where pendant amino-acid(s) attached to drugs can be deleterious to the activity of the drug, insertion of a self-immolative molecular clip between the PSA-cleavable peptide and the drug **1** will be investigated. In this way, enzymatic cleavage is followed by self-immolation of the pendant molecular clip to release the active drug. The synthesis of the polymeric prodrug system began with the synthesis of the proposed CBI drug followed by biological assay to investigate the potency of the drug and finally the synthesis of the prodrug.

## 3.1 Synthetic approaches to the CBI "warhead"

There are various approaches to the synthesis of the CBI analogues of the natural anti-tumour antibiotics. The synthesis of CBI is divided into two parts namely; the synthesis of the alkylating subunit ("warhead") and the synthesis of the non-alkylating subunit. Access to the alkylating subunit has proven much more challenging than the non-alkylating subunit. Most of the difficulties have centred on efforts to functionalise the pyrrolidine ring of the benz[*e*]indole core to introduce a hydroxymethyl group. The hydroxy group can be subsequently substituted to a better leaving group such as chlorine, which is necessary for spirocyclisation to form the highly reactive cyclopropane ring. The majority of the investigations into the synthesis of CBI alkylating subunit have involved the 5-hydroxy analogues. Below is a review of some of the synthetic approaches adopted in the synthesis of the CBI "warhead".

### 3.1.1 Synthesis of the key intermediate of the 5-hydroxy-CBI derivatives

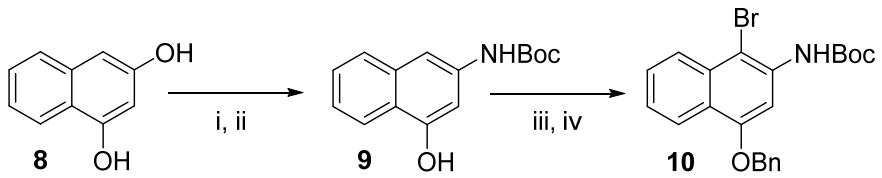


**Scheme 5**: Synthesis of *tert*-butyl (4-(benzyloxy)-1-bromonaphthalen-2-yl)carbamate **10**. *Reagents and conditions:* i. liquid $NH_3$, −78°C → 130°C, 1100 psi, 16 h; ii. $Boc_2O$, dioxane, 100°C, 4 h, iii. BnBr, $K_2CO_3$, n-$Bu_4NI$, dry DMF, $N_2$, 23°C, 8 h; iv. NBS, conc. $H_2SO_4$, THF, $N_2$, −60°C, 5 h.

Boger *et al.*[126] developed a synthetic route to access the 5-hydroxy analogue of the CBI alkylating subunit (Scheme 5). Starting from the commercially available 1,3-dihydroxynaphthalene **8**, reacting with ammonia gave 1-hydroxy-3-naphthylamine, followed by Boc-protection of the amine to give **9**. Orthogonal benzyl protection at the hydroxyl group followed by electrophilic bromination with N-bromosuccinimide gave the key intermediate **10**.[126] Introduction of a range of alkylating groups at the $N^2$ position allows the synthesis of the pyrrolidine ring of the CBI alkylating subunit.

### 3.1.2 Post- and pre-cyclisation functionalisation of the CBI pyrrolidine ring

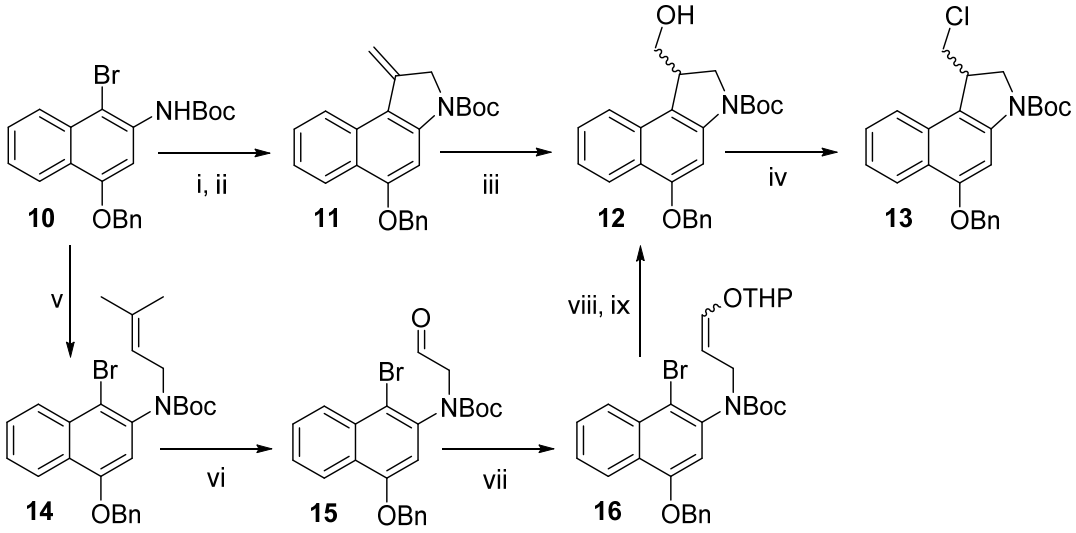


**Scheme 6:** Pre- and post-functionalisation of CBI pyrrolidine ring. *Reagents and conditions:* i. NaH, $HC{\equiv}CCH_2Br$, THF / DMF, $N_2$, 24°C, 3 h; ii. $Bu_3SnH$, AIBN, benzene, $N_2$, 80°C, 1 h; iii. $BH_3.SMe_2$, THF, Ar, 0-24°C, 3 h then $H_2O_2$, NaOH, 0 → 45°C, ~1 h; iv. $Ph_3P$, $CCl_4$, $CH_2Cl_2$, Ar, 24°C, 10 h; v. $BrCH_2CH{=}CMe_2$, NaH, DMF, Ar, 0 → 24°C, 8 h; vi. 3% $O_3/O_2$, $Me_2S$, $CH_2Cl_2$ / MeOH, −78 → 24°C, 3 h; vii. $Ph_3PClCH_2OTHP$, THF/HMPA, −78°C → 24°C, n-BuLi, 24 h; viii. $Bu_3SnH$, AIBN, benzene, Ar, reflux, 1 h, ix. MeOH, Amberlyst 15, 45°C, 6 h.

Initial efforts to synthesise the hydroxymethylindoline **12** involved post-cyclisation functionalisation of the pyrrolidine ring to introduce the hydroxymethyl group (Scheme 6). Treatment of the sodium salt of **10** with 3-bromopropyne followed by a 5-*exo*-dig aryl

radical–alkyne cyclisation when treated with tri-butyltin hydride and azobisisobutyronitrile (AIBN) gave the unstable 1-methylenebenzindoline **11**. Hydroboration-oxidation of **11** gave the hydroxymethylindoline **12** and chlorination was effected with triphenylphosphine and carbon tetrachloride to give **13**. Challenges faced with this synthetic route include partial / complete isomerisation of methylenebenzindoline to 1-methylbenz[*e*]indole on chromatographic purification. Besides, the cyclisation reaction proved very reliant on reaction time and the concentration of tri-butyltin hydride used and therefore stringent adhesion to reaction conditions was required.[127]

Another way of accessing the hydroxymethylindoline involves pre-functionalisation of the alkylating group before cyclisation (Scheme 6). This method has the advantage of avoiding the challenges faced with post-cyclisation functionalisation.[126] Boger *et al.*[128] alkylated **10** with 1-bromo-3-methyl but-2-ene to give **14**. Ozonolysis with subsequent reductive workup gave **15**. Treatment of **15** with [(2-tetrahydropyranyloxy)-methylene]triphenylphosphorane introduced a vinyl ether group to give **16**. Free-radical cyclisation was effected with tri-butyltin hydride and AIBN. Removal of the tetrahydropyranyloxy protecting group afforded the hydroxymethylindoline **12**. Substitution of the hydroxy group of **12** with chlorine gives **13** as the alkylating subunit to be coupled to the non-alkylating subunit. This synthetic route, however, has the constraint of having to incorporate the hydroxy functionalisation into the acceptor alkene before cyclisation and also requires carefully defined reaction conditions (ozonolysis) and subsequent Wittig reaction with a functionalised methylenetriphenylphosphorane. An easier and simpler synthetic route to **12**, will be to incorporate functionality during cyclisation.[128]

### 3.1.3 *In situ* functionalisation of the CBI pyrrolidine ring

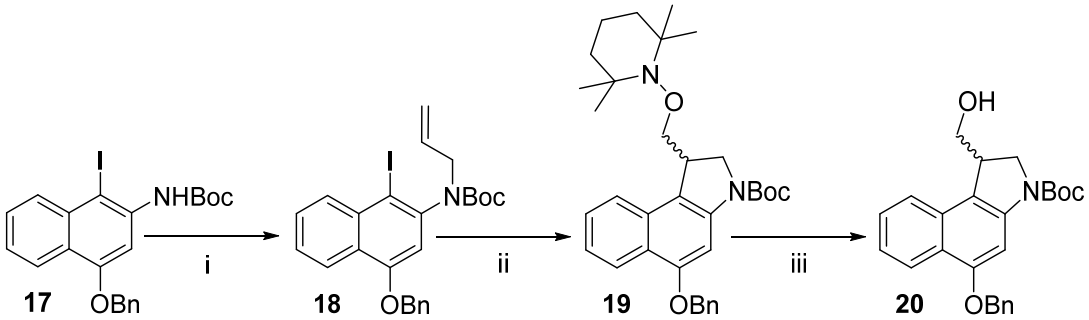


**Scheme 7:** Synthesis of CBI pyrrolidine ring with TEMPO trap. *Reagents and conditions:* i. NaH, $BrCH_2CHCH_2$, DMF, 0 → 25°C, 3 h; ii. $Bu_3SnH$, TEMPO, benzene, $N_2$, 70°C, 105 min; iii. Zn, AcOH / THF / $H_2O$ (3:1:1), 70°C, 2 h.

The functionalisation of the pyrolidine ring during cyclisation works better with iodine at C1 in contrast to bromine at this position.[128] O-Benzyl protection and electrophilic iodination of **9** gave **17** (Scheme 7). Alkylation of **17** with 1-bromoprop-2-ene gives **18**. Treatment of **18** with tri-butyltin hydride and TEMPO gives **19** with the incorporated protected hydroxy functionality. Reduction of the tetramethylpiperidine by reductive cleavage of the N-O bond exposes the hydroxy group, which can be subsequently substituted with chlorine to give **13**. This method avoids the need of pre- or post-cyclisation functionalisation to introduce the hydroxy group, since the TEMPO trap incorporates this functionality during cyclisation.[128]

### 3.1.4 Metal-mediated cyclisation

Tietze *et al.*[81] synthesised the CBI alkylating subunit **23** in their investigation into the design of a prodrug based on the ADEPT concept (Scheme 8). Alkylation at the $N^2$ position of **17** with (2*R*,3*S*)-2,3-epoxy-1-nitrobenzenesulfonyloxybutane) afforded **21** followed by a metal-mediated cyclisation to give **22** with the hydroxy functionality revealed during the reaction. Using the Appel reaction, the hydroxy group of **22** was replaced with chlorine to give **23**. Removal of the Boc group of **23** allowed coupling to a range of non-alkylating subunits.

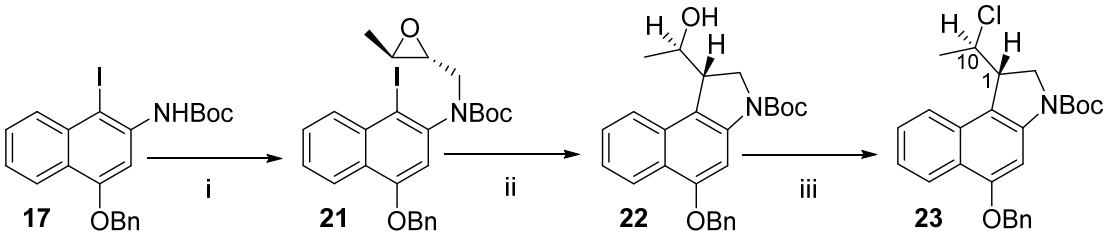


**Scheme 8:** Synthesis of CBI pyrrolidine ring *via* metal-mediated cyclisation. *Reagents and conditions*: i. NaH, (2*R*,3*S*)-2,3-epoxy-1-nitrobenzenesulfonyloxybutane, DMF, 25°C, 1.5 h; ii. MeLi, CuCN, −78 → 25°C, ~2.25 h; iii. $PPh_3$, $CCl_4$, $CH_3CN$, −18 → 0°C, 3 h.

This synthetic route offers the prospect of enantiopure synthesis. The methyl group at position-10 of **23** was introduced in order to reduce the chance of direct reaction of the *seco*-compound with the DNA which would be detrimental to the design of prodrugs. The design of prodrugs with these agents relies on the reduced reactivity of the *seco*-analogue compared to the spirocyclised CBI. By introducing the methyl group at position-10, the primary alkyl chloride was transformed into a secondary, sterically hindered chloride, discouraging inter-molecular reaction.[125] The introduction of the extra methyl groups results in a new stereogenic centre absent in the natural products. It has been observed that, when the two stereogenic centres of CBI drugs incorporating the alkylating subunit **23**, are *syn* (1*S*/10*S* or 1*R*/10*R*) the *seco*-CBI drug possesses a low toxicity and is not suitable for development as a prodrug, whilst the *anti*-orientation (1*S*/10*R* or 1*R*/10*S*) leads to the appropriate properties.[124]

Furthermore, a CBI incorporating the (+) (1*S*,10*R*) diastereoisomer of **23** has been found to be more active ($IC_{50}$ = 0.75 nM) compared to the (−) (1*R*,10*S*) diasteroisomer (550 nM) against human bronchial carcinoma cells (A549).[81, 124, 129]

### 3.1.5 Synthesis of the 5-amino CBI derivatives

A CBI prodrug incorporating the alkylating subunit **13** (Scheme 6) with the 5-hydroxy group functionalised as O-galactoside prodrug showed an unexpected high cytotoxicity [($IC_{50}$ = 4.8 nM (A549)] in the absence of the activating enzyme (β-D-galactosidase) compared to the activated analogue ($IC_{50}$ = 0.15 nM (A549)]. This observation was partly attributed to non-enzymatic cleavage of the galactoside and highlights the need for a more stable prodrug.[125] Carzelesin, a 5-hydroxy-CPI carbamate prodrug, is labile in plasma, rapidly releasing the active drug. Preparation of a more stable prodrug that persists in the plasma but allows specific release within the tumour by localised enzyme(s) is desirable.[44] The 5-amino-CBI derivatives are said to possess the same biological properties as the hydroxy-CBI. One advantage of the amino-CBI is their ability to form more stable amide prodrugs.[79] The synthesis of the amino-*seco*-CBIs are, however, very challenging. The synthesis of such an amino-CBI was carried out by Yang *et al.*[79] Starting with 2,4-dinitronaphthalen-1-ol, they undertook a sequence of synthesis [triflation, $S_NAr$ displacement with iodide, reduction (with loss of iodine), protection with $Boc_2O$ and restoration of the iodine)] to access **25** (Scheme 9).

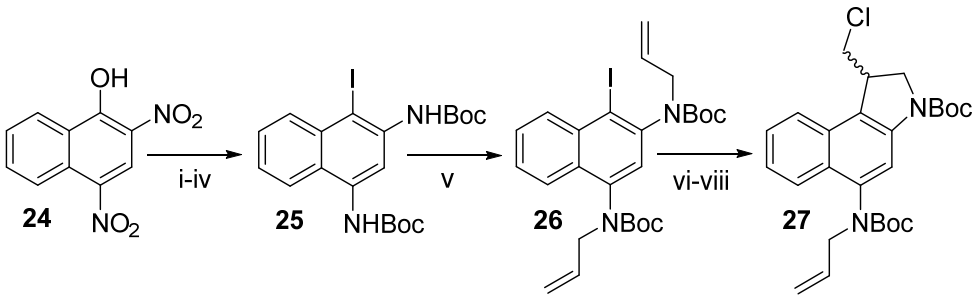


**Scheme 9:** Synthesis of 5-amino CBI derivative. *Reagents and conditions:* i. $(CF_3SO_2)_2O$, $Et_3N$, $CH_2Cl_2$, 0°C then rt, 2 h; ii. NaI, EtOAc, reflux, 2 h; iii. $SnCl_2$, EtOAc, reflux, 30 min, basic workup then $Boc_2O$, THF, reflux, 5 h; (iv) NIS, TsOH, 1:1 THF/MeOH, −78°C then rt over 4 h; v. NaH, then $CH_2$=$CHCH_2Cl$; vi. TEMPO, $Bu_3SnH$, benzene, 60°C, 130 min; vii. Zn powder, THF/AcOH/$H_2O$, 70°C, 10 h; viii. $Ph_3P$, $CCl_4$, $CH_2Cl_2$, rt, 2 h.

Discriminating between the two nitrogens of **25**, however, proved difficult. Non-selective allylation of **25** was therefore undertaken followed by free-radical cyclisation with TEMPO entrapment. Removal of the TEMPO group followed by substitution of the hydroxy group with chlorine gave **27**. The final steps in the synthesis of the amino-CBI involved removal of the $N^3$-Boc protecting group and coupling of the alkylating subunit to the non-alkylating subunit followed by removal of the 5-allyl group, a step which proved challenging.[79] A

synthetic route which allows easier discrimination between the nitrogens is, therefore, highly desirable. Efforts will be made in the present study to distinguish between the $N^2$ and $N^4$ amines of **25** to afford a more selective alkylation at the $N^2$ amine which will enhance the efficiency in the synthesis of the proposed CBI drug.

## 3.2 Synthesis of the alkylating subunit of the proposed CBI drug

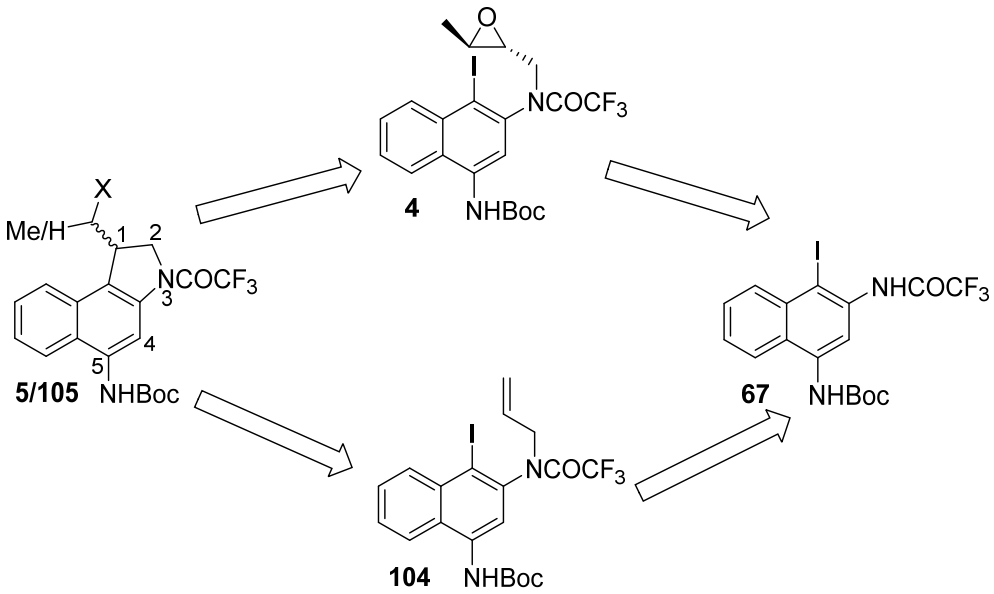


**Scheme 10:** Retrosynthesis of the alkylating subunit of the proposed CBI drug.

The synthesis of the proposed CBI drug has two parts, namely, synthesis of the alkylating subunit and synthesis of the non-alkylating subunit. The synthesis of the alkylating subunit proceeds *via* a naphthalene derivative **67** with an iodo-substituent at position-1 and orthogonally masked amines at positions-2 and -4 (Scheme 10). Selective alkylation at the $N^2$ of **67** with the appropriate group will allow a cyclisation reaction to be performed to generate the five-membered pyrrolidine ring. There will be two approaches to this. Firstly, enantiopure synthesis will be attempted by alkylating $N^2$ with an enantiopure epoxide followed by metal-mediated cyclisation to give **5** (Scheme 3). The second approach will be based on racemic synthesis by adopting free-radical cyclisation to give **105** (Scheme 3) after introducing an allyl group at $N^2$ of **67**. Deprotection at the $N^2$ of **5/105** will then allow coupling to the non-alkylating subunit to give the proposed CBI drug**.** The masked amine at position-5, once deprotected will be coupled to a poly(ethylene glycol) *via* a PSA-cleavable peptide linker to form the polymeric prodrug.

### 3.2.1 Mono-nitration of naphthalen-1-ol

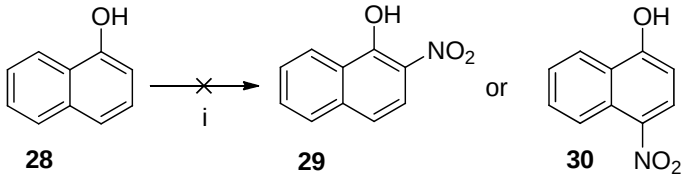


**Scheme 11:** Attempted mononitration of naphthalene-1-ol. *Reagents and conditions:* i. $H_2SO_4$, $HNO_3$, 0°C → r.t., 10 min.

An initial attempt was made to synthesise 2-nitronaphthalen-1-ol **29** (or 4-nitronaphthalen-1-ol **30**) by mononitration of naphthalene-1-ol **28** (Scheme 11). The expected nitration at the 2- or 4-positions of naphthalen-1-ol was based on the *ortho/para*-directing effect of the mesomerically electron-donating hydroxy group. Furthermore, since nitro groups are mesomerically electron-withdrawing and deactivating, it was expected that dinitration should proceed slowly if at all. The rationale was to introduce a nitro group at one of these positions of naphthalen-1-ol **28** and then to reduce to the amine and protect this group. A second nitro group would then be introduced, reduced and protected with a different (orthogonal) protecting group. This will help to avoid the issue of selectivity which arises when using a dinitro-naphthalen-1-ol. This approach, however, was unsuccessful as multiple nitration occurred with formation of many products, which were impossible to separate. A new approach was adopted to access naphthalen-1-ol derivatives with orthogonally protected amino groups at the 2- and 4-positions.

### 3.2.2 Selective nitration of 4-aminonaphthalen-1-ol

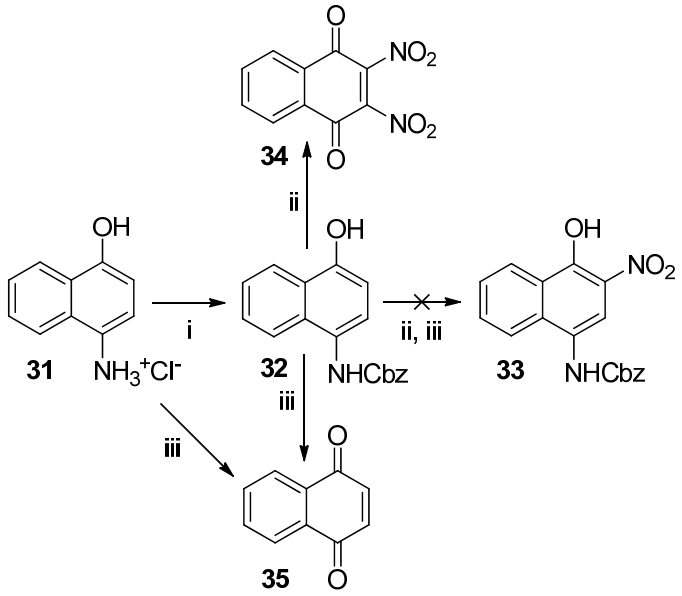


**Scheme 12:** Nitration of 4-amino-naphthalen-1-ol. *Reagents and conditions*: i. KOBu$^t$, benzyl chloroformate, −70°C to r.t., $N_2$, 16 h; ii. $HNO_3$, 0°C to r.t., 3 h; iii. $CF_3CO_2H$, $KNO_3$, −20°C, 30 min.

4-Aminonaphthalen-1-ol hydrochloride **31** presents a molecule with an amino group already present at position-4 (Scheme 12). Introduction of a second amino group at position-2 after protection of the 4-amino group will give an intermediate with orthogonal amino groups. Benzyloxycarbonyl (Cbz) protection of the amino group of 4-amino-naphthalen-1ol **31** was undertaken using benzyl chloroformate in the presence of a base to give **32**. Selective protection of the amino group over the phenolic group is based on the superior nucleophilicity of the amino group under mildly basic conditions and also due to the stable carbamate product formed. The presence of an amide-like protection at the 4-amino group also had a secondary purpose. Both the hydroxy and amino group of **31** are *ortho/para* directing. Protection of the amino group therefore serves to deactivate somewhat the directing effect of the amino group, thereby allowing selective nitration at the position *ortho* to the phenolic group. Selective nitration at the position *ortho* to the hydroxy group of **32**, however, proved difficult. The rationale was that once nitrated, the nitro group could then be reduced and the resulting amine protected with an orthogonal protecting group after substituting the hydroxy group with iodine to give the key intermediate **67**. Attempts to nitrate benzyl N-(4-hydroxynaphthalen-1-yl)-carbamate **32** using nitric acid as a mild nitrating agent resulted in a product mixture that included **34**. This suggested that dinitration as well as oxidative deamination had occured. The use of one equivalent of potassium nitrate, together with trifluoroacetic acid, as a source of the nitronium ion was investigated. Nitration of **32** with this reagent, however, resulted in oxidative deamination as well, but without nitration at the desired position to give **35**. Direct

nitration of the starting material 4-aminonaphthalen-1-ol hydrochloride **31** was undertaken with the rationale that, once in acidic medium, the amino group will stay protonated, deactivating nitration at the position *ortho* to the amino group and thereby allowing selective nitration at position-2. This effort also resulted in the oxidised product **35** without the desired nitration. Scheme 13 shows the proposed mechanism for the oxidative deamination.

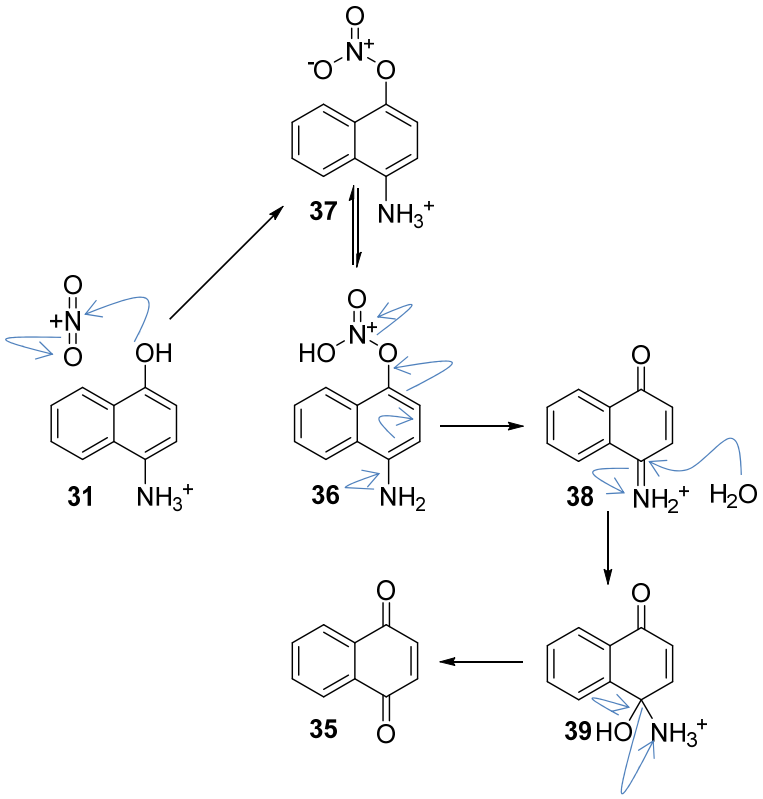


**Scheme 13:** Proposed mechanism of oxidative deamination of **31.**

Nucleophilic attack on the generated nitronium ion by the phenolic group of **31** results in nitration at the phenolic oxygen to give **36**. Delocalisation of electrons from the amino group results in an elimination process which releases nitrous acid / nitrite ion. Hydrolysis of the iminonaphthalenone salt **38** with loss of ammonia produces naphthoquinone **35**. In the case of using excess nitric acid as the nitrating agent, the reaction proceeds further with the naphthalene ring undergoing an electrophilic substitution with the nitronium ion to give **34**. The fact that **35** was obtained when one equivalent of the nitronium species was used ($KNO_3$), suggests that nitration at the phenolic group and the subsequent oxidative deamination precedes nitration of the naphthalene ring. These challenges faced with this synthetic route led to investigation into other ways of accessing the key intermediate **67** in the synthesis of the proposed CBI drug.

### 3.2.3 Attempted nucleophilic displacement of triflate group with iodide in 4-(tert-butoxycarbonyl)amino-2-nitronaphthalen-1-yl trifluoromethanesulfonate (38)

With the commercial availability of 2,4-dinitronaphthalen-1-ol **24** as the dye Martius Yellow, the question was asked if selective reduction of one of the nitro groups could be achieved. If possible, then protection of this amino group followed by substituting the hydroxy group with iodine and then subsequent reduction / protection of the remaining nitro group will give access to the key intermediate **67**. An extensive literature search suggested that selective reduction of the 4-nitro group was possible.[130]

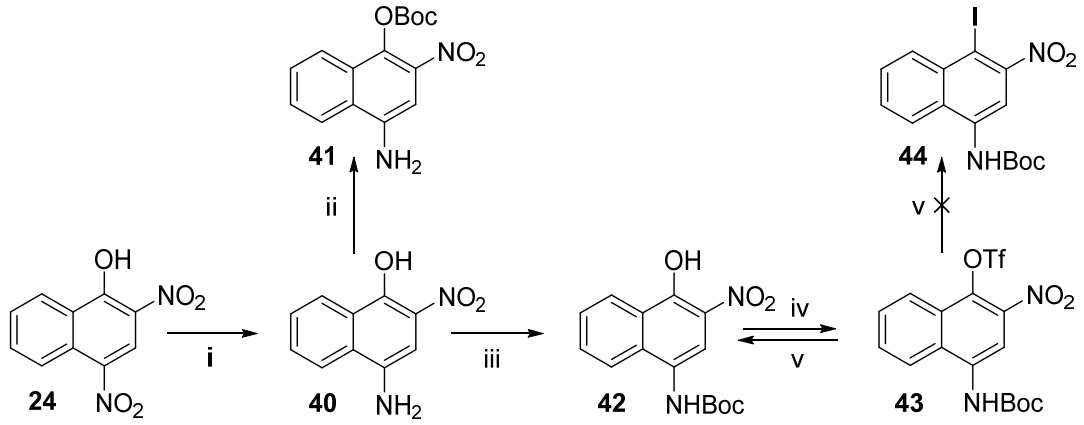


**Scheme 14:** Attempted substitution of triflate group with iodide. *Reagents and conditions*: i. $SnCl_2.2H_2O$, EtOH, conc. aq. HCl, < 30°C, 17 h; ii. $Boc_2O$, DMAP, $N_2$, $CH_2Cl_2$, r.t., 30 min; iii. $Boc_2O$, THF, $N_2$, 16 h; iv. $(CF_3SO_2)_2O$, pyridine, $N_2$, 0°C to r.t., 1 h; v. NaI, DMF, 80°C, 2 h.

The nitro group at position-4 of 2,4-dinitronaphthalen-1-ol **24** was selectively reduced under ethanolic acidic conditions with tin(II) chloride (3 equivalents) to give **40** (Scheme 14). The temperature of the reaction had to be controlled to less than 30°C in order to avoid over reduction. The phenolic group appears to be involved in the protection of the *ortho*-nitro group from reduction. Similar reduction of 1-methoxy-2,4-dinitronaphthalene led to a product mixture of nitro-amines.[130] A stabilising effect by coordination or hydrogen-bonding between the phenolic group and the 2-nitro group [(precluding simultaneous co-ordination of Sn(II)] may be responsible for the non-reduction of the *ortho*-nitro group of **24**. 4-Amino-2-nitronaphthalen-1-ol **40** was treated with di-*tert*-butyl dicarbonate and a catalytic amount of 4-dimethylaminopyridine (DMAP) at room temperature. This surprisingly resulted in the acylation of the phenolic group rather than of the amino group to give **41** in a yield of 17%. The 4-dimethylaminopyridine acts to activate di-*tert*-butyl dicarbonate as a better electrophile. In this instance, it seems also to have acted as a base to deprotonate the acidic phenolic group which was made more acidic by the adjacent electron-withdrawing nitro group. This meant that the phenoxide generated was more nucleophilic than the amino group and, at room

temperature, reaction of the phenolic group is favoured over the amino group. The low yield of **41** is partly due to the unstable nature of the carbonate group formed by acylation of the phenol. The reaction was repeated without 4-dimethylaminopyridine (DMAP). Using di-*tert*-butyl dicarbonate and heating under reflux gave the desired product **42**. Treatment of **42** with trifluoromethanesulfonic anhydride in the presence of pyridine as a solvent and base converted the phenolic group into a triflate **43**. The use of excess base in this reaction was essential since trifluoromethanesulfonic acid is generated in the reaction and might deprotect the acid-labile BocNH. The triflate group serves as a better leaving group to aid the next step of the synthesis which was to undertake a nucleophilic substitution of the triflate with iodine. It was also hoped that the presence of the nitro group will activate the molecule to nucleophilic substitution. This nucleophilic aromatic substitution ($S_NAr$) takes place *via* the addition and elimination mechanism and not by direct substitution. It is essential to have an electron withdrawing group *ortho* and/or *para* to the leaving group in order to accommodate and stabilise the negative charge from the nucleophile through inductive effect or conjugation. The importance of this requirement is best shown by comparing the $^{13}C$ NMR of the carbocation and carbanion intermediates of benzene[131] (Figure 37).

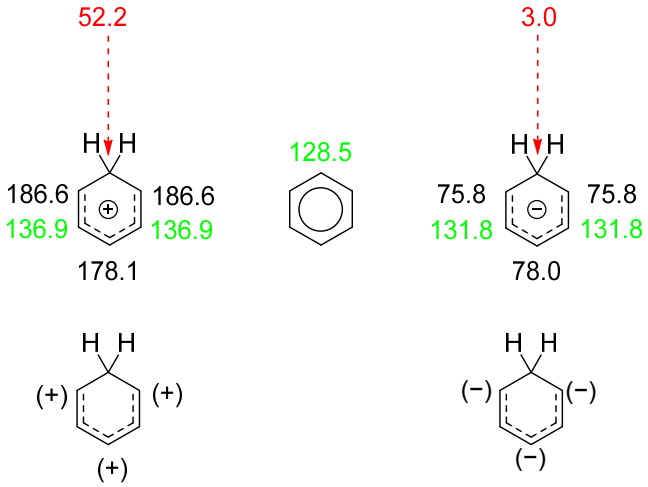


**Figure 37:** Carbocation and carbanion intermediates of benzene and their $^{13}C$ NMR shifts (ppm).

As can be observed from Figure 37, the chemical shift for the *meta*-carbon of both ions differs only slightly from the chemical shifts corresponding to the benzene carbons. However, there is a significant downfield shift for the *ortho*- and *para*-carbons of the benzene cation and a significant upfield shift for the *ortho*- and *para*-carbons of the benzene anion. It is very clear from these results that the ionic charges are delocalised mainly on the *ortho*- and *para*-carbons. This means that, in nucleophilic aromatic substitution, the electron-withdrawing activating group, such as the nitro group of **43**, must be on the *ortho*- or *para*-carbons to have

any stabilising effect on the generated anion.[131] Several attempts using a range of reaction conditions, however, failed to give the iodinated product **44**. Sodium iodide and potassium iodide were used as sources of the iodide, different dry solvents were investigated (ethyl acetate, dimethylformamide, dimethylsulfoxide) and a range of temperatures (≤ 90°C) were tested. In all these circumstances the phenolic product **42** was obtained. Scheme 15 shows the proposed mechanism for this reaction and also the mechanism of the desired $S_NAr$ reaction.

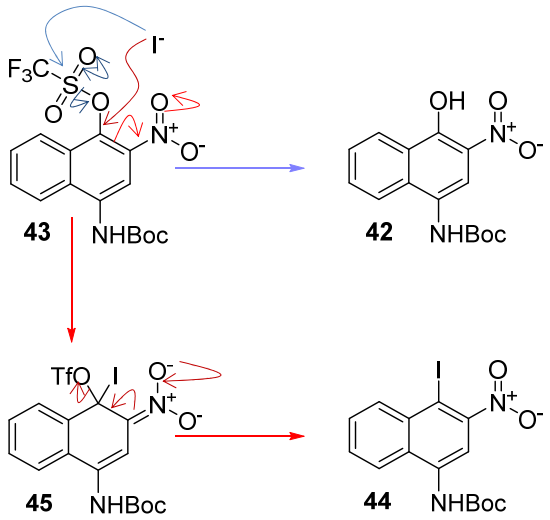


**Scheme 15:** Proposed mechanisms of iodination of **43** and regeneration of **42**.

It appears that the single nitro electron-withdrawing group does not make the 1-position sufficiently electrophilic for nucleophilic attack by the iodide ion. The lack of sufficient electron-withdrawing groups on the aromatic ring of **43** allows an alternative reaction. The iodide attacks the best remaining electrophile in the molecule, which is the triflate sulfur.

### 3.2.4 Reduction of the aryl triflate

Following the failure to substitute the triflate group of **43** with iodine, attempts to remove this group reductively to form **46** were investigated (Scheme 16). Iodine could then be introduced through electrophilic substitution with N-iodosuccinimide. Deoxygenation of phenolic hydroxy groups is challenging due to their stability. The triflate group increases the leaving ability of the aryl oxygen of **43**.[132] Mori *et al.*[132] have shown that dissolving magnesium in methanol, in the presence of palladium on charcoal as the catalyst, can reduce aryl triflates to generate the corresponding arenes. The source of hydrogen in this reduction is the acidic hydrogen atom of the methanol. Methanol was chosen due to the enhanced reactivity of magnesium with this solvent. Other protic solvents (*e.g.* ethanol, propan-2-ol) capable of being hydrogen donors failed to produce a reaction.[132] Mori *et al.*[132] have proposed that the reaction proceeds *via* an initial single-electron transfer from $Pd^0$ to the aromatic ring of the

aryltriflate to give a radical anion. Elimination of trifluoromethanesulfonate (OTf) anion gives rise to an aryl radical. A second single electron transfer from $Pd^{I}$ to the aromatic ring takes place to give an aryl anion followed by protonation from methanol to give the deoxygenated product together with $Pd^{II}$ which is reduced back to $Pd^{0}$ by the magnesium.[132] This synthetic method was adopted in the efforts to reduce the triflate group of **43** (Scheme 16).

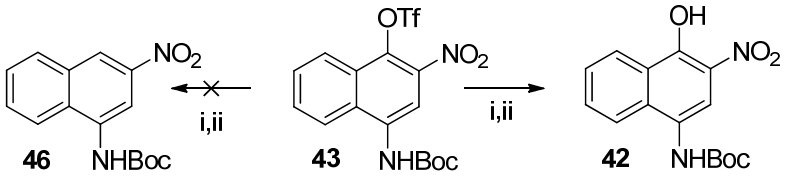


**Scheme 16:** Attempted reduction of the triflate group of **43**. *Reagents and conditions:* i. Mg, Pd/C(10%), MeOH, r.t., Ar, 16 h; ii. $PPh_3$, $Pd(OAc)_2$, $Et_3N$, formic acid, DMF, 65°C, 1 h.

Compound **43** in methanol was treated with palladium on charcoal and magnesium and stirred at room temperature overnight. The isolated product from this reaction was, however, the regenerated phenolic compound **42**. This again suggested a nucleophilic attack at the sulfur atom as observed with the attempted iodination of **43** (Scheme 14), where the iodide ion attacked the sulfur atom to give **42**. This problem was encountered by Mori *et al.*[132] in their investigations. It was reported that the use of excess reagents and the addition of ammonium acetate helped overcome this problem as well as accelerating the reaction.[132] Ammonium acetate dissociates into acetic acid and ammonia *in situ*. The acetic acid facilitates the dissolution of magnesium in methanol which in turn enhances the reduction of $Pd^{II}$ to $Pd^{0}$ by magnesium. Coordination of ammonia to the $Pd^{0}$ accelerates the single-electron transfer process to the aryl triflate.[132] Adopting this method for **43**, however, failed to give the desired product.

The use of triethylammonium formate as a reducing agent to cleave the C-O bond of aryl triflates has been reported by Peterson *et al.*[133] This method was shown to be efficient with aryl triflates with electron-withdrawing groups as well as with electron-donating groups.[133] The hydrogen donor in this reaction is the formate. Triphenylphosphine reduces palladium(II) acetate *in situ* to generate bis(triphenylphosphine)palladium(0). Insertion of palladium(0) between the aryl-triflate bond occurs through oxidative addition. Triflate is then displaced by formate ion followed by loss of carbon dioxide generating aryl-palladium(II) hydride. Reductive elimination results in the deoxygenated aryl product and regeneration of the catalytically active palladium species [(palladium(0)].[134] Compound **43** was treated with triethylamine, formic acid, palladium(II) acetate and triphenylphosphine. Isolation and

purification of product again showed that the phenol **42** was regenerated. The idea of substituting the triflate of **42** with iodide in two steps was, therefore, abandoned.

### 3.2.5 Reduction of the nitro group of 4-(*tert*-butoxycarbonylamino-2-nitronaphthalen-1-yl trifluoromethanesulfonate (43)

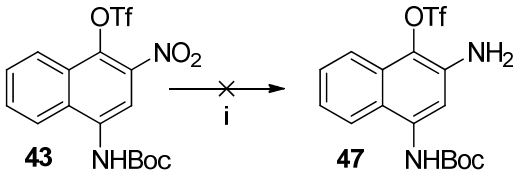


**43** **47**

**Scheme 17:** Attempted reduction of the nitro group of **43**. *Reagents and conditions:* Pd/C (10%), MeOH, $H_2$, 1.5 h.

The purpose of having the iodine at position-1 of the key intermediate **67** is to exploit the reactivity of iodine towards a cyclisation reaction to form the five-membered pyrrolidine ring of the CBI drug. The question was, therefore, asked as to whether triflate can take up this role. If that was the case, then reduction of the nitro group of **43**, followed by protection, will give an intermediate compound capable of undertaking the role of the desired key intermediate **67**. Efforts to reduce the nitro group of **43** included hydrogenation with palladium on charcoal catalyst and the use of sodium dithionite as the reducing agent (Scheme 17). These, however, gave complex product mixtures which could not be separated. Reduction of the nitro group may have well occurred but the presence of the triflate group in such a close proximity to the exposed amine can lead to transfer of the triflate group to the amine giving a range of possible products. One way of avoiding the transfer of triflate to the amino group will be to carry out the reaction in acidic medium so as to trap the amino group as the protonated form and thereby reduce its nucleophilicity. This method runs the risk of causing the deprotection of the acid-labile Boc group. The use of tin(II) chloride to reduce the nitro group of **43** was tried but this led to a product mixture that included the loss of the Boc-group due to the acidic reaction conditions.

### 3.2.6 Masking of the phenol group

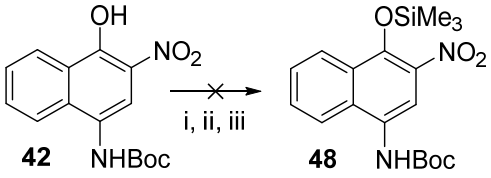


**Scheme 18:** Attempted silylation of **42.** *Reagents and conditions*: i. $ClSiMe_3$, $Pr^i_2NEt$, $CH_2Cl_2$, $N_2$, 40°C, 16 h; ii. hexamethyldisilazane, DMF, $N_2$, 80°C, 48 h; iii. $ClSiMe_3$, imidazole, THF, Ar, r.t., 24 h.

Protection of the phenolic group of **42** before reduction of the nitro group followed by orthogonal protection of the formed amino group, was another idea investigated (Scheme 18). The protecting group of the phenol will then be removed and the exposed hydroxy group converted to a triflate group. This compound can then be investigated for cyclisation to form the pyrolidine ring of the proposed CBI drug after alkylation at the $N^2$-position with appropriate alkylating group. Treatment of compound **42** with silylating agents, such as chlorotrimethylsilane and hexamethyldisilazane, in different reaction conditions, however, failed to give **48** but instead resulted in recovered starting material (Scheme 18).

### 3.2.7 Unexpected formation of a quinone imine on reduction of *tert*-butyl N-(4-hydroxy-3-nitronaphthalen-1-yl)carbamate (42)

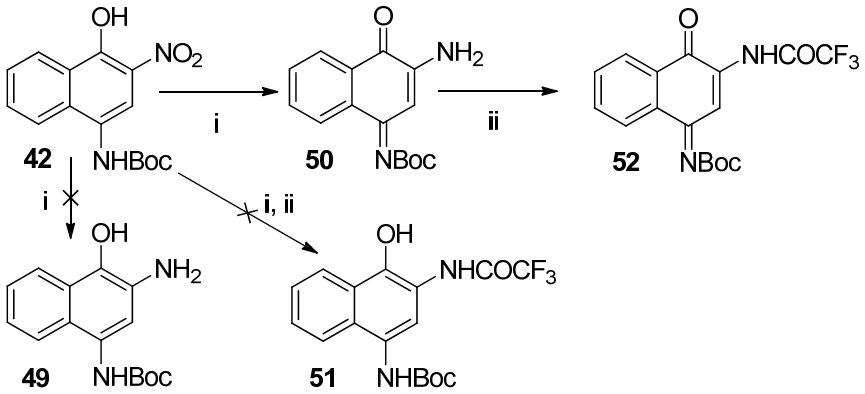


**Scheme 19:** Formation of quinone imine. *Reagents and conditions*: i. $Na_2S_2O_4$, $K_2CO_3$, $CH_2Cl_2/H_2O$, $N_2$, 35°C, 16 h; ii. $(CF_3CO)_2O$, $Pr^i_2NEt$, $CH_2Cl_2$, 0°C to r.t., 16 h.

The challenges faced resulted in another strategy being investigated. This involved reduction of the nitro group of **42** followed by selective protection of the amino group and then triflation of the phenolic group. Reducing agents such as catalytic hydrogenation and sodium dithionite were used in reducing **42** (Scheme 19). This resulted in the reduction of the nitro group but also oxidation of the product to give the quinone imine **50** as the *E*-isomer. This was confirmed by the observation of a correlation between the Boc-protons and the C3 proton of **50** on a NOESY spectrum. It was suspected that exposure of the reduced product to air was

responsible for this oxidation. Reduction of the nitro group of **42** and protection of the intermediate amine in the absence of air was attempted. This involved reduction of **42** using sodium dithionite in a biphasic dichloromethane / water system under nitrogen. Once reduction was complete, the organic phase, which should contain the product, was syringed out and placed under nitrogen. Treatment of the mixture with trifluoroacetic anhydride under basic conditions should then give **51**. This, however, resulted in the oxidised product **52**. A literature search to ascertain the possibility of reducing **50/52** to regenerate the phenolic group was undertaken. Although no specific method was found for the reduction of a quinone imine, it was observed that quinones could be reduced to the hydroquinones using a range of reducing agents including sodium dithionite[135, 136] and Raney nickel.[137] However, since the reduction of **42** had been effected by sodium dithionite but still resulted in the oxidised product **50** and also the failure to synthesise **51** led to the thinking that, even if reduction of **50** or **52** were possible, this would revert back to its oxidised form on exposure to air and therefore this idea was abandoned.

### 3.2.8 Attempted reduction of the nitro group(s) of 1-iodo-2,4-dinitronaphthalene (54) and the synthesis of N,N'-bis(*tert*-butoxycarbonyl)-1-iodonaphthalene-2,4-diamine (25)

Due to the challenges faced, efforts were made to introduce the iodine onto the naphthalene ring of **24** to give **54** before reduction of the nitro groups (Scheme 20). This will allow attempted selective reduction of the *para*-nitro group with the aid of the bulky iodine shielding the *ortho*-nitro group from reduction. Protection of the *para*-amino group will be followed by reduction of the *ortho*-nitro group using more vigorous reductive conditions. This will allow orthogonal protection of the *ortho*-amino group to give the key intermediate **67.** Alternatively, reduction of both nitro groups of **54** will still present the possibility of selectively protecting one of the amino groups followed by orthogonal protection of the other. Synthesis of **25** will be pursued if the above strategies fail. This will allow the exploration of selective deprotection / re-protection of **25** to access the orthogonally protected 1-iodo-naphthalene-2,4-diamine key intermediate. Investigation into these possibilities was undertaken (Scheme 20).

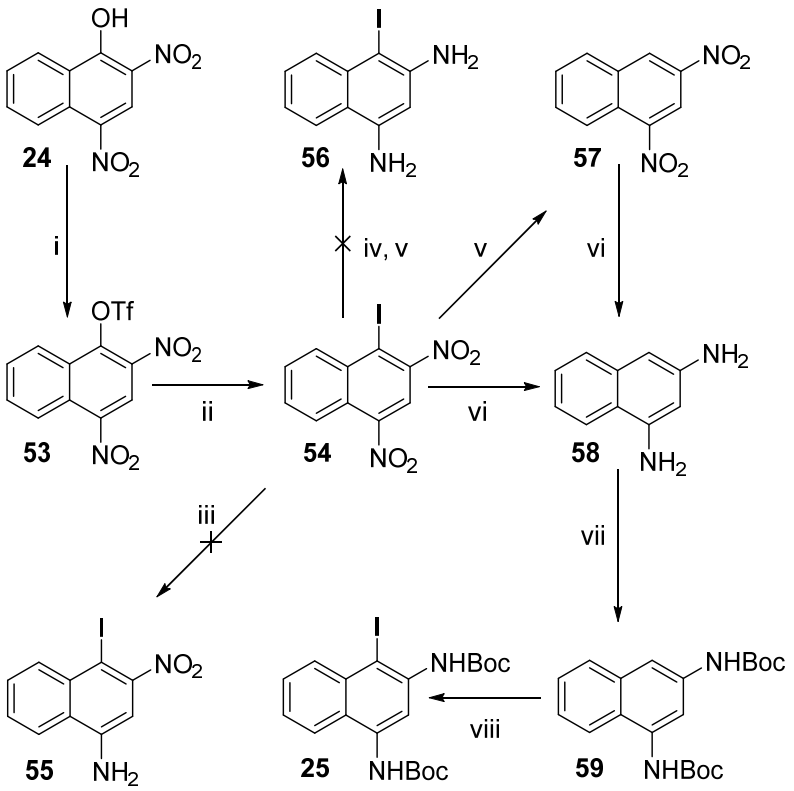


**Scheme 20:** Attempted reduction of the nitro group(s) of **54** and the synthesis of **25**. *Reagents and conditions:* $(F_3CSO_2)_2O$, $Et_3N$, $CH_2Cl_2$, 0°C to r.t., 2 h; ii. NaI, EtOAc, reflux, 2 h; iii. $SnCl_2.2H_2O$, conc. aq. HCl, EtOH, r.t., 16 h; iv. Pt/C(1%), $H_2$, THF, 20 h; v. Pd/C(10%), $NaBH_4$, MeOH, THF, 0°C, 4 h; vi. $SnCl_2.2H_2O$, EtOAc, reflux, 1 h; vii. $Boc_2O$, THF, reflux, 16 h; viii. NIS, $pTsOH.H_2O$, THF/MeOH, −78°C to r.t., 4h.

### 3.2.8.1 Synthesis of 1-iodo-2,4-dinitronaphthalene (54)

The synthesis of **54** was achieved in two steps, the first being triflation at oxygen to give **53** (Scheme 20). Nucleophilic aromatic substitution was then undertaken with iodide to give **54**. Unlike the failed $S_NAr$ reaction of compound **43** (Scheme 14), compound **53** has two activating nitro groups at the *ortho*- and *para*-positions to the triflate. The enhanced activation increases the electrophilicity of the C1 to nucleophilic attack rather than the sulfur atom of the triflate group. The reaction was studied in ethyl acetate and in acetone, with acetone giving a higher yield (74%) than in ethyl acetate (66%). This might be due to the greater solubility of sodium iodide in acetone.

### 3.2.8.2 Attempted reduction of the 4-nitro group of 1-iodo-2,4-dinitronaphthlene (54)

Compound **54** was exposed to the same reaction conditions that allowed selective reduction of the 4-nitro group of **24** (Scheme 14). It was hoped that selective reduction of one of the nitro groups could be achieved. Efforts to reduce selectively the 4-nitro group of **54** using tin(II) chloride in acidic ethanol resulted in a mixture of products which included the de-iodinated

diamine **58** (Scheme 20). Prolonged reaction time was needed for progression of the reaction, probably due to poor solubility of **54**, and the product mixture formed was difficult to separate. The inability to reduce selectively the 4-nitro group of **54** supports the role of the hydroxy group at the C1 position of **24** in the selective reduction of the nitro group (Scheme 14).

#### 3.2.8.3 Reductive de-iodination

Reduction of both nitro groups without loss of iodine was also attempted. Various reagents were considered for the reduction of **54**. This difficult reduction can also result in de-iodination.[138] Hydrogenation in the presence of palladium-on-charcoal in a range of solvents (methanol, tetrahydrofuran, acetic acid) gave the de-iodinated diamine **58** (Scheme 20). It was hoped that the use of acetic acid as a solvent will make the mixture more acidic and reduce the possibility of dehalogenation which proceeds more effectively under basic conditions.[139] This was, however, not the case as de-iodination still occurred. Sodium borohydride was used as a source of a fixed number of equivalents of hydrogen. Sodium borohydride degrades to generate hydrogen which gets adsorbed onto palladium on carbon to reduce the nitro groups. This is a form of hydrogenation but with the ability to control the amount of hydrogen present. The use of sodium borohydride (2 eq.), however, remarkably resulted in selective de-iodination to give **57** without reduction of the nitro groups. Platinum is said to be better at preserving halogens during hydrogenation combined with a fast rate of nitro group reduction.[138, 140] Platinum-on-carbon (5% and 1%) together with hydrogen or sodium borohydride were used but either resulted in de-iodination together with reduction of the nitro groups (5% Pt/C) or was unreactive (1% Pt/C).

#### 3.2.8.4 The synthesis of N,N'-bis(*tert*-butoxycarbonyl)-1-iodonaphthalene-2,4- diamine (25)

The difficulty encountered with efforts to reduce the nitro groups selectively meant that a new strategy was needed to circumvent these challenges. Synthesis of the key intermediate **67** without orthogonal protection of the amino groups was pursued (Scheme 20). Once synthesised, efforts will then be made to ascertain the possibility of selective deprotection / re-protection. Reduction of the nitro groups of **54** with concomitant de-iodination was carried out using tin(II) chloride. Protection of the amines with di-*tert*-butyl dicarbonate gave **59**, which was readily isolated. Regioselective acid-catalysed electrophilic iodination of **59** with N-iodosuccinimide gave the aryl iodide **25** in a yield of 71%.[79]

### 3.2.9 Acidic de-iodination of N,N'-bis(*tert*-butoxycarbonyl)-1-iodonaphthalene-2,4-diamine (25)

Selective removal of one of the Boc-protection groups was attempted by treating **25** with dilute trifluoroacetic acid (0.85% v/v) in dichloromethane at room temperature (Scheme 21).

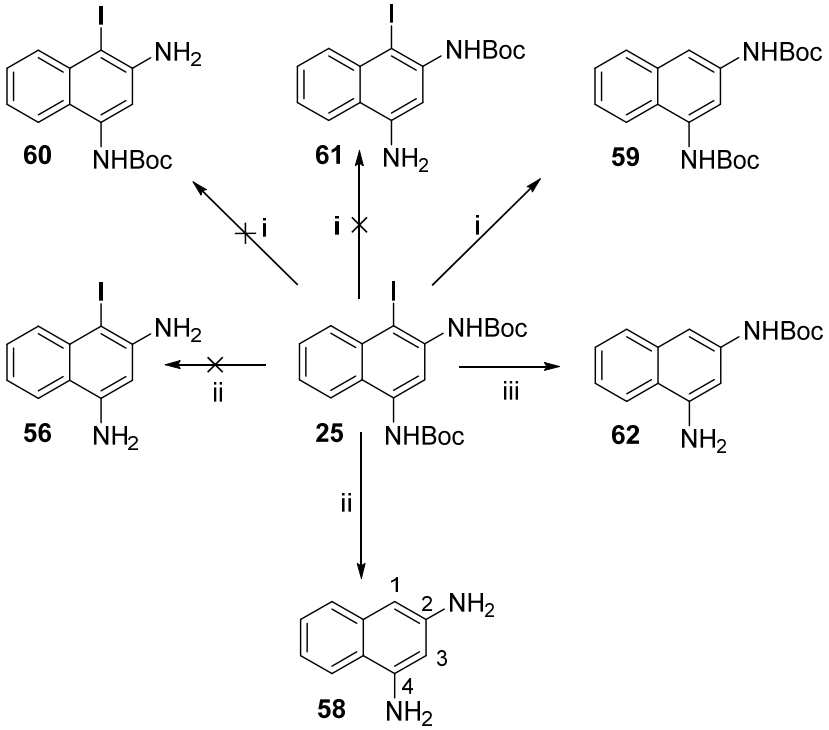


**Scheme 21**: Acidic de-iodination. *Reagents and conditions:* i. $CF_3CO_2H$ (upto 4 equiv), $CH_2Cl_2$, r.t., 7 d; ii. $CF_3CO_2H$, 0°C, 1.5 h; iii. (a). HCl / dioxane (4 M), r.t. 45 min, (b). $Boc_2O$, $Pr^i_2NEt$, THF, $N_2$, r.t, 10 d.

An overall amount of 4 equivalent of the trifluoroacetic acid solution was added over 7 d. Isolation and purification of the product showed that de-iodination had occurred without deprotection to form **59** [experiment conducted by Wenyi Wang].[141] Efforts were then made to remove both Boc groups and then exploit the steric hindrance provided by the iodine to re-protect the 4-amino group selectively. Initial attempts to remove both Boc groups involved the use of trifluoroacetic acid at 0°C. This, however, gave the de-iodinated diamine product **58**. Hydrogen chloride in dioxane (4.0 M) was then used with the view that the product formed after deprotection will precipitate as an hydrochloride salt and perhaps stop the de-iodination step. This product would then be quickly treated with di-*tert*-butyl dicarbonate to protect the 4-amino group selectively. This procedure resulted in a de-iodinated monoprotected product product **62** in a low yield (6%).

Assuming that deprotection with hydrogen chloride in dioxane had gone to completion, along with de-iodination, this observation suggested that selective protection of the $N^2$-amine of **58**

was possible. It also meant that the $N^2$-amine in absence of the iodine was more reactive since it is more sterically accessible. Protection of the $N^4$-amine of **62** with a bulkier protecting group (*e.g.* benzyloxycarbonyl group), followed by electrophilic iodination at C1 will provide an intermediate with the potential of selective alkylation at $N^2$. This could then be used as the key intermediate in the synthesis of the proposed CBI. Having a smaller and more electronegative protecting group at $N^2$ and a bulkier and less electronegative group at $N^4$ is, however, much more desirable.

### 3.2.10 Synthesis of the naphthalene key intermediate (67)

The observation of the ability to protect 1,3-naphthalenediamine **58** selectively gave a new direction to the synthesis of the key intermediate **67**. This selective protection has also been achieved by the treatment of **58** with 2-(*tert*-butoxycarbonyloxyimino)-2-phenylacetonitrile to give **62** at a yield of 8%.[142] The $N^2$-amine of **58** will be protected by a smaller and more electronegative protecting group compared to the orthogonal protection at the $N^4$-amino group. Having a smaller protecting group at the $N^2$-amine will give greater accessibility to the alkylating agent and also with a more electronegative protecting group, the remaining proton at $N^2$ will be more acidic allowing easier deprotonation and selective alkylation. The chosen protecting group at $N^2$ was trifluoroacetyl and the orthogonal protection for the 4-amino group will be *tert*-butylcarbonyl.

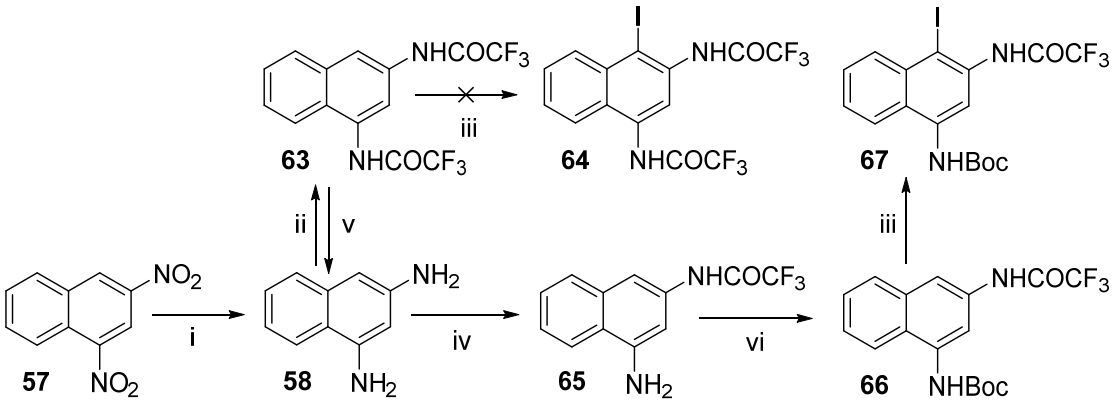


**Scheme 22:** Synthesis of the key intermediate **67**. *Reagents and conditions:* i. 10% Pd-C, $H_2$, THF, r.t., 16 h; ii. $(CF_3CO)_2O$, $Pr^i_2NEt$, dry THF, $N_2$, 0°C → 20°C, 16 h; iii. NIS, pTsOH.$H_2O$, dry THF, $N_2$, −78°C → 20°C, 20 h; iv. dilute $(CF_3CO)_2O$ in dry THF (1.1% v/v), $Pr^i_2NEt$, dry THF, $N_2$, 0°C → 20°C, 16 h; v. aq. NaOH (5 M), THF, r.t., 105 min. vi. $Boc_2O$, dry THF, reflux, 16 h.

The synthesis of the key intermediate **67** began by reduction of commercially available 1,3-dinitronaphthalene **57** to the diamine **58**, which was treated with one equivalent of trifluoroacetic anhydride in the presence of diisopropylethylamine at 0°C in dry tetrahydrofuran (Scheme 22). This unfortunately gave the di-protected compound **63** in 26%

yield and recovered starting material. Repeating the reaction in pyridine led to isolation of the same product **63** and unreacted starting material. Electrophilic iodination of **63** to form **64** will give a product that can be explored for selective deprotection in basic conditions with the hope of de-iodination not occurring. An attempt to undertake an electrophilic iodination of **63** to give **64**, however, failed. The presence of the electron-withdrawing trifluoroacetamide protection rather than Boc protection as in **59** may be responsible for the lack of progress of this electrophilic iodination. The absence of a monoprotected product in the attempted selective protection of **58** using trifluoroacetic anhydride was an interesting observation. This was despite the use of one equivalent of anhydride. One would expect statistically that there should be at least some mono-protected compound(s). Trifluoroacetic anhydride is a very reactive electrophile and even weaker nucleophiles react with it. Ethyl trifluoroacetate was therefore used as a milder electrophile with the hope of promoting monoprotection.

Compound **58** in tetrahydrofuran was treated with ethyl trifluoroacetate in basic conditions. This reagent, however, proved very unreactive even when used in excess at room temperature. The use of trifluoroacetic anhydride was revisited. It was thought that part of the reason for exclusive di-protected product was due to adding the anhydride as a neat liquid which created a local high concentration leading to the di-protected compound **63**. Compound **58** was therefore treated with dilute trifluoroacetic anhydride in tetrahydrofuran (~1.1% v/v), added dropwise over 2 h at 0°C. This interestingly led to isolation of the desired product **65** in a yield of 15% together with the di-protected compound **63** and recovered starting material **58**. Several attempts were made to optimise this process including the use of different solvents (*e.g.* dimethylformamide, dichloromethane), different temperatures (*e.g.* −30°C, −70°C) and different concentrations of trifluoroacetic anhydride in tetrahydrofuran. These resulted in di-protection or gave a similar percentage yield of the mono-protected product. Temperatures lower than 0°C did not have a significant effect on the yield of the desired product and the use of DMF resulted in the di-protected product **64** only.

Despite the modest yield of **65**, the di-protected compound could be deprotected with a nucleophilic base (*e.g.* NaOH, $NH_3$) and recycled to give the starting material **58**. Deprotection of **63** to **58** was initially done using aqueous ammonia (35%) and methanol as the solvent. Solubility issues as well as the volatile nature of ammonia meant that this reaction took a long time to give the desired product, even after heating (50°C). Besides, one by-product of this reaction is trifluoroacetamide which necessitates purification of the product.

Due to these reasons, aq. sodium hydroxide was used to deprotect **63**. This method results in trifluoroacetate ion as the by-product which is easily extracted into the aqueous layer during work-up. Protection of the $N^4$-amine of **65** was achieved with the bulkier and less electronegative *tert*-butoxycarbonyl protecting group to give **66**. Electrophilic iodination with N-iodosuccinimide gave **67**, the key intermediate in the synthesis of the alkylating unit of the CBI drug.

### 3.2.11 NMR investigation into the de-iodination of iodonaphthalenediamines in acidic media

One of the major unexpected result in the synthesis of the key intermediate **67** was the de-iodination of 1-iodonaphthalene-2,4-diamine under acidic conditions. For instance, the use of dilute trifluoroacetic acid in dichloromethane (0.85% v/v, one equivalent) in an attempt to deprotect **25** regioselectively resulted in de-iodination without removal of the Boc groups (Scheme 21). The rationale for this experiment had been to remove only one of the Boc groups. Regardless of which Boc group was removed, an appropriate orthogonal protection could be carried out on the exposed amine to obtain a compound that could fulfil the role of the key intermediate **67**. Furthermore, when the concentration of the acid (trifluoroacetic acid or hydrogen chloride) was increased in an attempt to cleave the Boc-protection groups of **25**, this also resulted in de-iodination, in addition to loss of the Boc groups. These fascinating observations where de-iodination occurred in acidic media led to the design of a series of NMR studies to ascertain the cause of de-iodination and to elicit the mechanism of this process.[141]

### 3.2.11.1 Wheland-like intermediates in the de-iodination of N,N'-bis(*tert*-butoxycarbonyl)-1-iodonaphthalene-2,4-diamine (25) in acidic media

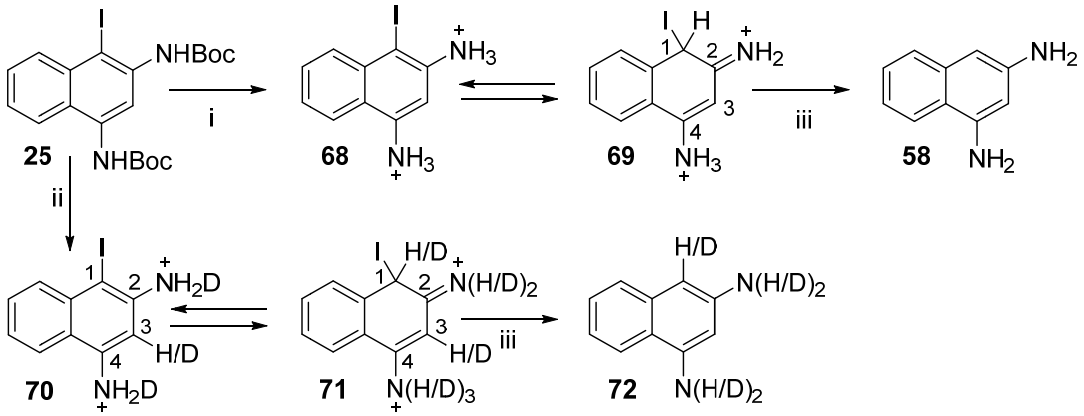


**Scheme 23:** Reactions of **25** with $CF_3CO_2H$ and with $CF_3CO_2D$ in $CDCl_3$, showing Wheland-like intermediates. *Reagents*: i. $CF_3CO_2H$ / $CDCl_3$ (3:1); ii. $CF_3CO_2D$ / $CDCl_3$ (3:1); iii. aq. work-up.

Compound **25** was added to a mixture of $CF_3CO_2H$ / $CDCl_3$ (3:1) at 0°C. Once dissolved, the solution was transferred into an NMR tube and placed into a pre-cooled (0°C) spectrometer probe. A series of NMR spectra was taken over time at 0°C and at 20°C (Figure 38).

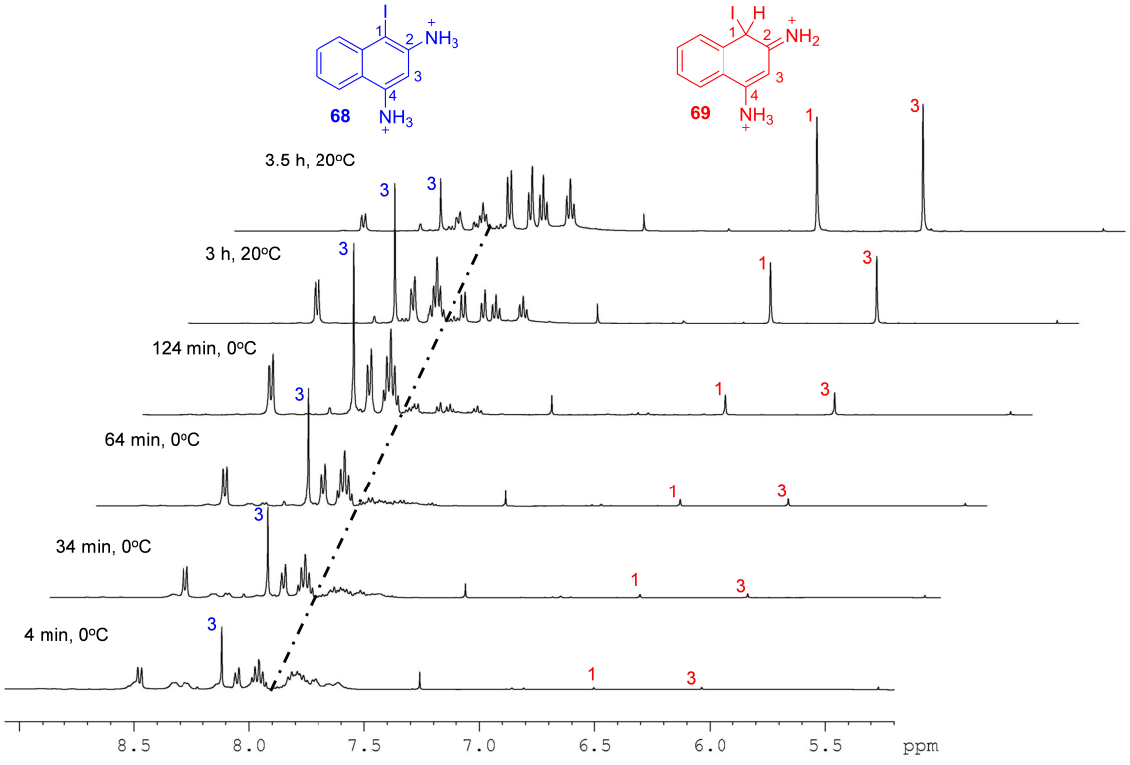


**Figure 38:** Time-course of $^1$H NMR spectra of reaction of **25** with $CF_3CO_2H$ / $CDCl_3$ (3:1).

The first major identifiable compound was the deprotected compound **68** with the iodine still intact (Scheme 23). This compound was fairly stable after 2 h at 0°C giving a yield of ~90% by NMR. The NMR showed the existence of a minor product in addition to **68** at this temperature. Raising the temperature of the spectrometer probe to 20°C resulted in the emergence of a new compound which was identified as the Wheland-like intermediate **69**. This compound became the dominant product after 2 h at 20°C, giving a yield of ~> 90% with the remaining ~10% being compound **68**. This suggested that an equilibrium existed between **68** and **69**, favouring **69** at this temperature. A new peak corresponding to the proton at position-1 of **69** was observed at δ 6.51 in the proton NMR spectrum (Figure 38). This peak correlated by HSQC with a $sp^3$ carbon peak at δ 9.76 in $^{13}C$ NMR spectrum in contrast to the $sp^2$ $^{13}C$ NMR peak of δ 101.74 corrresponding to C1 of **68**. The upfield shifts observed for **69** are due to:

- Loss of aromaticity by formation of the Wheland-like intermediate;
- The shielding effect of the iodine;
- The stabilisation of the positive charge.

There was a significant change in chemical shift of the proton at position-3 from δ 8.11 in **68** to δ 6.05 in **69** (Figure 38) and a corresponding change in $^{13}C$ chemical shifts of δ 116.88 in **68** to δ 91.48 in **69**. Compound **69** was quite stable in this solution at 20°C even after 7 d. However, all attempts to isolate **69** gave **58** through collapse of the Wheland intermediate with loss of an equivalent of $I^+$. To enhance our understanding of this de-iodination process, the above experiment was repeated with **25** using $CF_3CO_2D$ / $CDCl_3$. Again, the first compound formed was the deprotected product **70** followed by formation of the tetrahedral cationic species **71** on warming to 20°C (Scheme 23). Figure 39 shows a series of $^1H$ NMR spectra of a mixture of the two compounds.

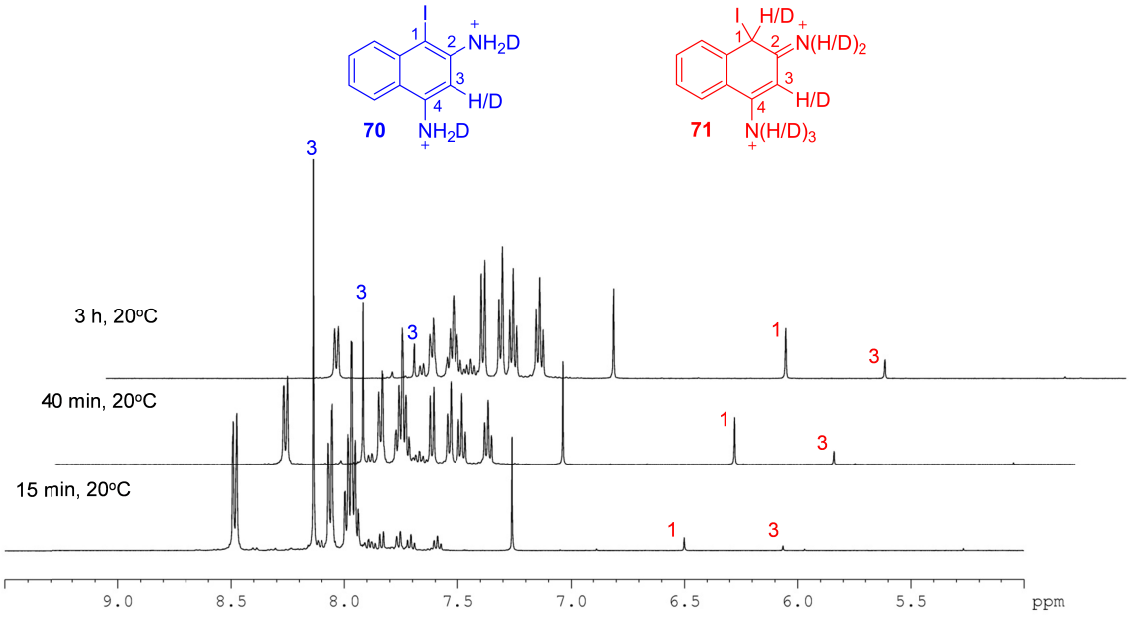


**Figure 39:** Time-course of $^{1}$H NMR spectra of reaction of **25** with $CF_3CO_2D$ / $CDCl_3$ (3:1).

Compound **70** was very stable at 0°C even after 4 h and showed no signs of incorporation of deuterium at this temperature. Once the mixture was warmed to 20°C, a mixture of the two compounds **70** and **71** could be identified in equilibrium by NMR. Both of these compounds underwent extensive incorporation of deuterium over time. At 15 min, there was no evidence of deuterium exchange at position-3 of **70**, which was the dominant species at this stage. As time went on, the proton peak at δ 8.11, corresponding to the proton at position-3 of **70**, reduced in intensity to 0.3 H (Figure 39). Thus at 3 h, this position had been 70% deuterated. The proportion of **70** in equilibrium to **71** also reduced from 10:1 at 15 min to 3:5 at 3 h. Incorporation of deuterium also occurred at positions-1 and -3 of compound **71**. Incorporation of deuterium at position-1 of **71** was 76% initially and increased over time to ~80% after 3 h at 20°C. The incorporation of deuterium observed at position-3 of **71**, however, remained fairly constant at ~93% which reflects the overall ratio of exchangeable D to H in solution. Attempts to isolate **71** gave **72** with multiple deuterium incorporation which was confirmed by mass spectrometry. The higher initial percentage of protium (24%) at position-1 of **71** compared to the overall ratio in solution suggest that the source of this new proton may have intra-molecular origin. If there were no intra-molecular contribution then the initial percentage deuteration should reflect the overall ratio of exchangeable D to H in solution. It follows then that, even though initial addition of deuterium to $N^2$ occurs rapidly, H to D exchange is quite slow, allowing intra-molecular transfer of proton from $N^2$ to position-1. This intra-molecular proton then undergoes deuterium exchange with solution.

### 3.2.11.2 Wheland-like intermediates from naphthalene-1,3-diamine in acidic media

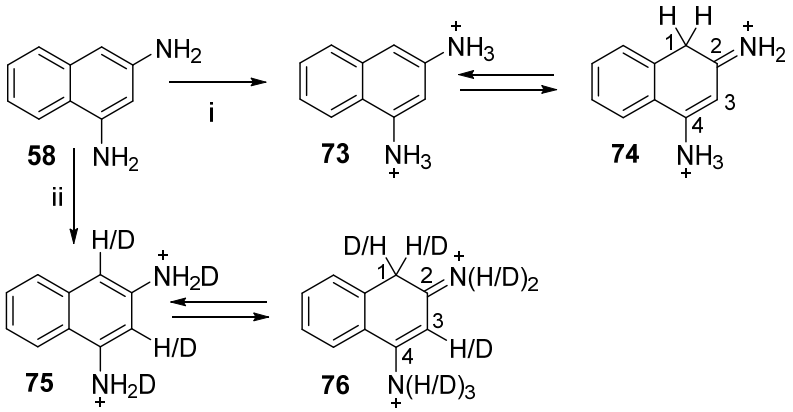


**Scheme 24:** Reactions of **58** with $CF_3CO_2H$ and with $CF_3CO_2D$ in $CDCl_3$, showing Wieland-like intermediates. *Reagents*: i. $CF_3CO_2H$ / $CDCl_3$ (3:1); ii. $CF_3CO_2D$ / $CDCl_3$ (3:1); iii. aq. work-up.

In order to ascertain if the observed Wheland intermediates were due to the presence of iodine at position-1, compound **58** was subjected to the same reaction conditions as above at 20°C. Exposure of **58** to $CF_3CO_2H$ / $CDCl_3$ gave **73** and **74** in an equilibrium ratio of 4:1 which stayed constant even after 7 d (Scheme 24). Of particular interest in **74** was the observation of a $CH_2$ peak at δ 4.13 in the proton NMR spectrum, which correlated with a peak at δ 33.28 in the $^{13}C$ NMR spectrum. This was confirmed with a phase-sensitive HSQC and DEPT analysis (Figure 40).

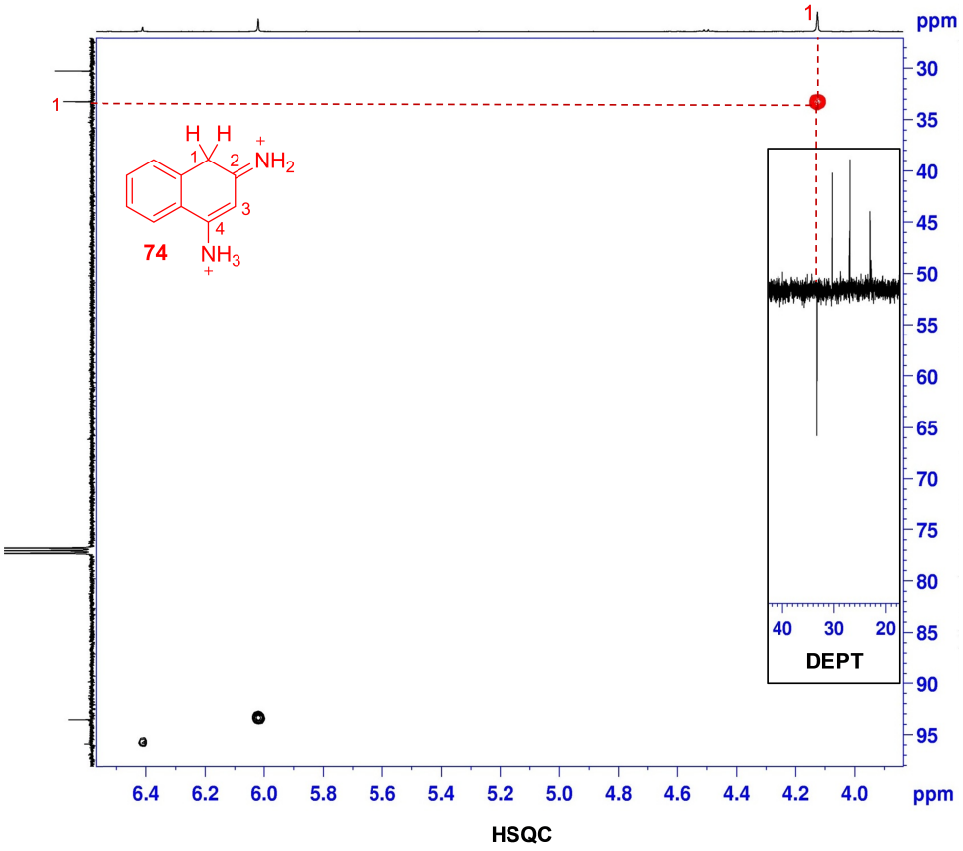


**Figure 40:** HSQC and ADEPT spectra of **74**.

This upfield chemical shift of the aromatic protons of **74** is in line with the observation made for **71**. Exposure of **58** to $CF_3CO_2D$ / $CDCl_3$ led to **75** and **76** in equilibrium ratio of ~5:1 (Scheme 24). Incorporation of deuterium occurred at position-1 and -3 of **75**. Incorporation of deuterium into position-1 of **75** was slower than position-3 (Figure 41). No incorporation of deuterium was observed at position-1 up to 1 h at 20°C. Incorporation of deuterium was observed after 6 d at 72%. This was in contrast to deuterium exchange at position-3 of **75**. Incorporation of deuterium into position-3 of **75** varied from 0% at 5 min to 49% at 40 min and finally 75% on day six (Figure 41).

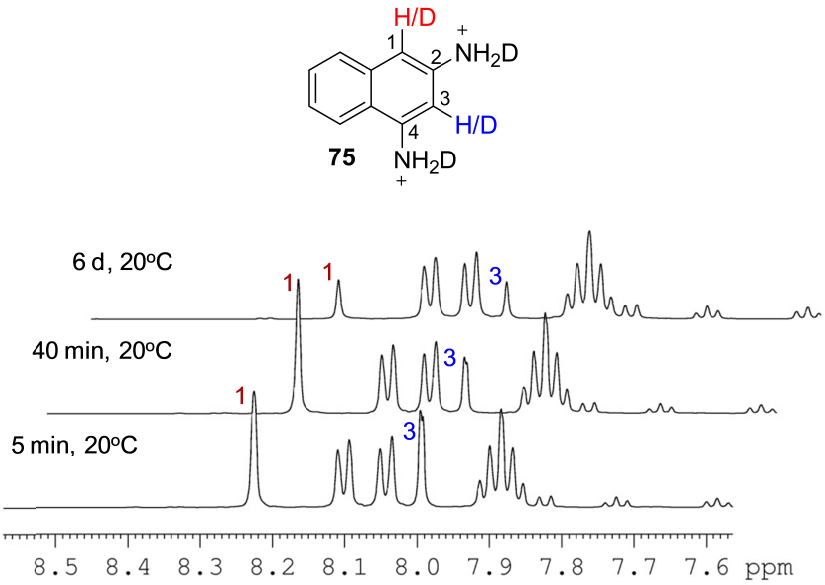


**Figure 41:** Time course $^{1}$H NMR showing increasing deuteration at C1 and C3.

The faster deuterium exchange at position-3 compared to position-1 is expected since the proton at position-3 is surrounded by the two amino electron-donating groups compared, to the position-1 proton which is adjacent to only one amino group. In regards to the observed Wheland intermediate **76**, there was a general upfield chemical shift of the protons due to reasons discussed above. Separate peaks corresponding to CHD and $CH_2$ protons at position-1 of **76** were identified in the proton NMR spectrum at δ 4.11 and δ 4.13 owing to isotope shifts (Figure 42).

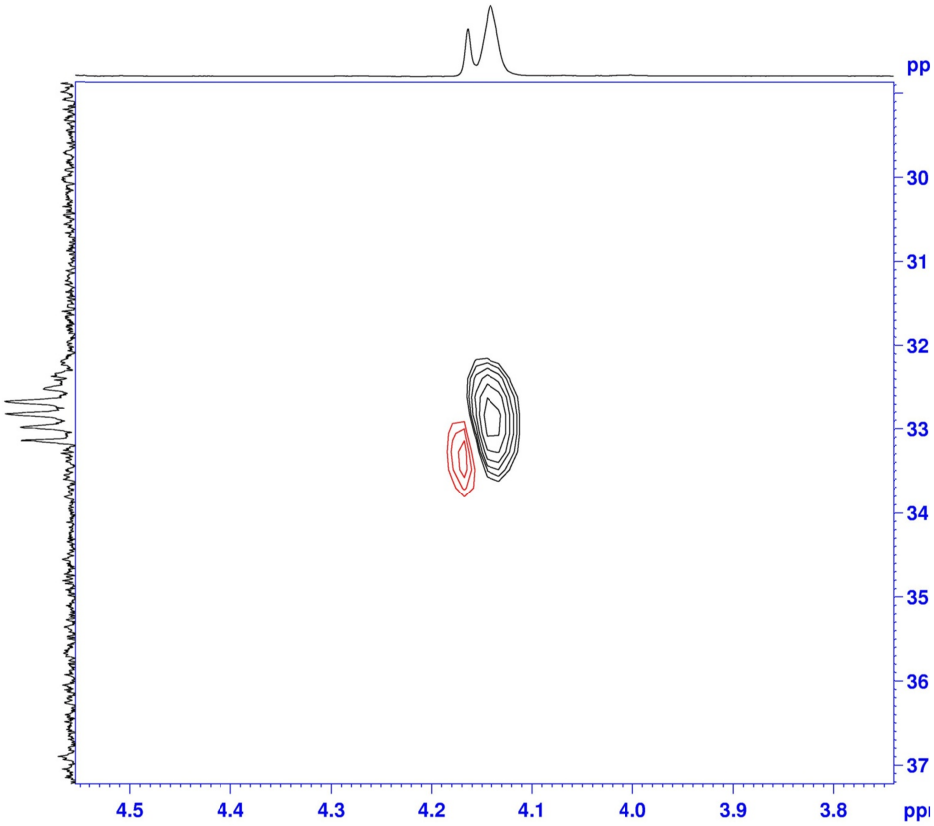


**Figure 42:** HSQC spectrum of **76** showing the CHD and $CH_2$ signals and corresponding $^{13}C$ signals.

Initially, a singlet integrating for two protons was present at δ 4.13 in the $^{1}H$ NMR spectrum. This corresponded to the $CH_2$ at position-1 of **76**. Over time, this peak diminished with the appearance of another peak upfield at δ 4.11 corresponding to CHD. The initial observation of a $CH_2$ peak corresponding to protons at position-1 again highlights the role of intra-molecular transfer of hydrogen to this position from the adjacent amino group. If the source of proton were from the solution (inter-molecular), then one would expect some deuteration right from the start. It can therefore be said that intra-molecular transfer of protons from $N^2$ to position-1 occurs before H → D exchange. It was also noticed that the incorporation of deuterium at position-3 was faster than at position-1 and stayed constant (~80%) throughout the experiment. However, deuteration at position-1 of **76** ranged from 0% at 5 min to 95% on day six. Deuterium incorporation at position-1 and -3 of **76** was confirmed by $^{13}C$ NMR which showed $^{13}C$-D coupling ($J$ = 20 Hz for C1 and 24.5 Hz for C3).

### 3.2.11.3 De-iodination of *tert*-butyl N-(4-iodo-3-trifluoroacetamidonaphthalen-1-yl)carbamate (67) in acidic media

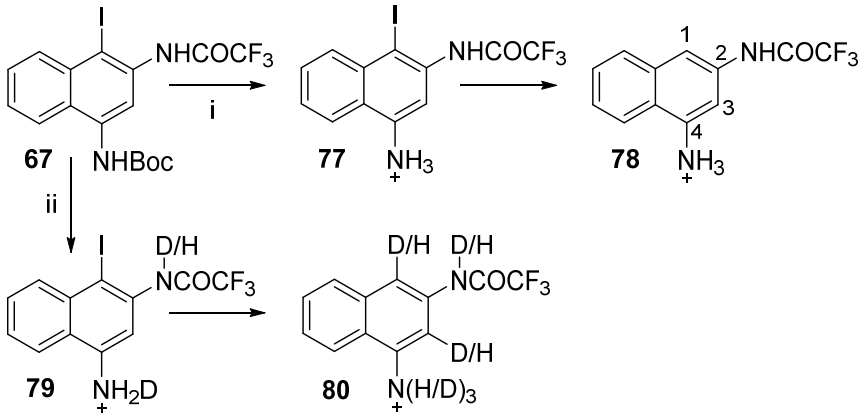


**Scheme 25:** Reactions of **67** with $CF_3CO_2H$ and with $CF_3CO_2D$ in $CDCl_3$, showing Wheland-like intermediates. *Reagents:* i. $CF_3CO_2H$ / $CDCl_3$ (3:1); ii. $CF_3CO_2D$ / $CDCl_3$ (3:1); iii. aq. work-up.

To investigate the influence of a non-acid-labile electron-withdrawing group at $N^2$, compound **67** was added to a mixture of $CF_3CO_2H$ / $CDCl_3$ (3:1) at 0°C for 2 h to give the Boc-deprotected **77**. This after warming to 20°C for 48 h gave the deiodianated compound **78** without observation of a Wheland-like intermediate. A transient Wheland-like intermediate might be involved but the equilibrium concentration in this case is too low for it to be observed. This compound was confirmed by the existence of an extra $^1H$ peak at δ 8.29 corresponding to the new proton at position-1 of **78**.

The experiment was repeated with $CF_3CO_2D$ / $CDCl_3$ to give **79** initially and then **80** on warming to 20°C. Compound **79** did not show any significant incorporation of deuterium at position-3 at 0°C, with this signal integrating to almost one proton in the spectra. Initial $^1H$ NMR spectra after ~15 min of warming to 20°C showed the presence of both **79** and **80**. The spectra showed that a significant amount of deuterium (72%) was incorporated at position-3 of **79**. Significant incorporation of deuterium also occurred at position-1 (80%) and position-3 (69%) of **80** at 15 min. Keeping the reaction mixture at 20°C for 48 h led to the complete conversion of **79** to **80**. Increased incorporation of deuterium also occurred at position-1 (86%) and position-3 (82%) of **80**. The $N^2$-amide proton of **79** and **80** was extensively exchanged with deuterium (95-100%) owing to its acidic nature. In regards to the proposal of intra-molecular transfer of protium / deuterium from $N^2$ to the position-1 carbon, the observation of a very high level of deuteration at position-1 of **80** after just 15 min of warming re-affirms this claim. With the $N^2$-amide proton extensively exchanged with deuterium, one will expect that if the intra-molecular theory was true then there should be a

higher deuterium at position-1 of **80** right from the beginning as observed. The faster incorporation of deuterium at position-1 (80%) than position-3 (69%) at 15 min is partly due to the enhanced acidic nature of the $N^2$-amide deuterium and the fact that intra-molecular deuterium exchange seems to favour the C1 position over the C3 position. Incorporation of deuterium was further confirmed by observation of $^{13}C \rightarrow D$ coupling in the $^{13}C$ NMR.

### 3.2.11.4 Incorporation of deuterium into 2-methyl propene

In each case where deprotection of Boc occurred (**25** and **67**), $^{13}C$ NMR spectroscopy showed that the *tert*-butyl group was trapped by the acid to give *tert*-butyl trifluoroacetate **81** (Figure 43).

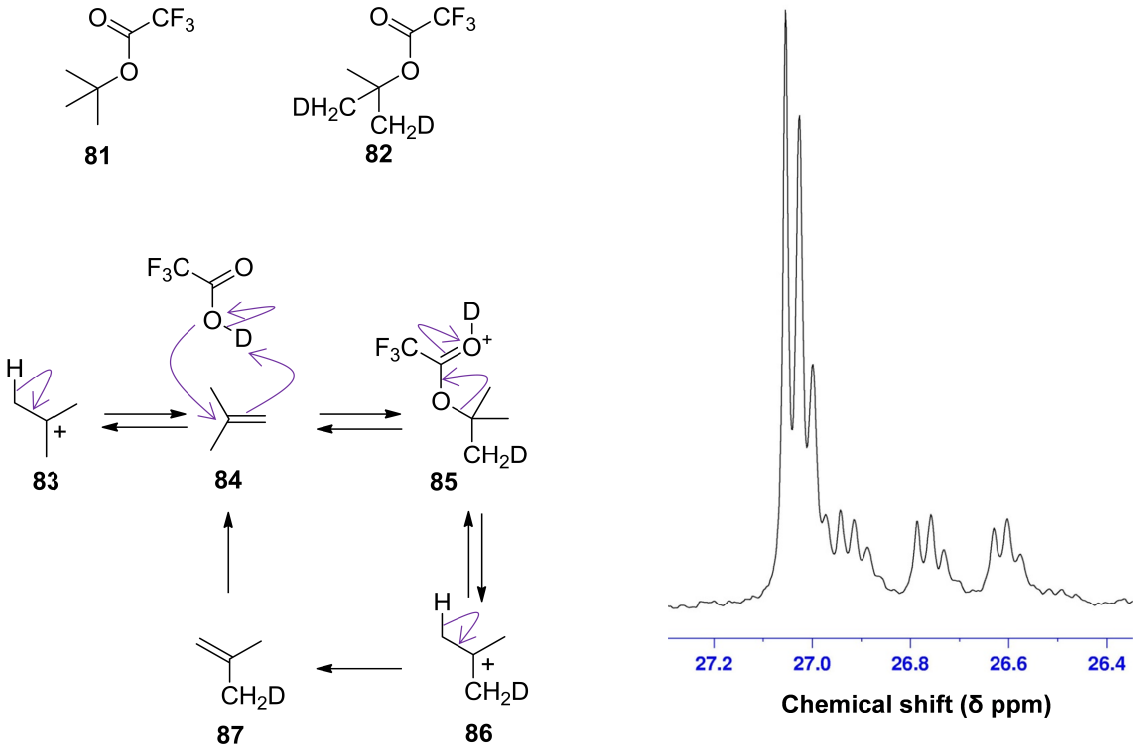


**Figure 43:** Mechanism of incorporation of deuterium in Bu$^t$ trifluoroacetate and $^{13}$ CNMR showing C → D coupling as a result of incorporation of deuterium into Bu$^t$.

When $CF_3CO_2D$ / $CDCl_3$ was used, it was observed that incorporation of deuterium into the *tert*-butyl groups occurred to give **82**. Evidence of incorporation of multiple deuteriums was seen in the $^{13}C$ NMR spectrum (Figure 43). The intermediate *tert*-butyl cation formed during the deprotection of Boc undergoes β-elimination to form 2-methylpropene. The *tert*-butyl cation and the 2-methylpropene exist in equilibrium until trapped by a nucleophile. Nucleophilic attack of 2-methylpropene by trifluoroacetic acid leads to the first opportunity of deuterium incorporation into the formed *tert*-butyl trifluoroacetate **85** (Figure 43). The *tert*-

butyl protected trifluoroacetic acid **85** is subjected to further deprotection in the acidic media and and subsequent β-elimination giving further opportunities for deuterium incorporation. The end result is multiple deuterium incorporation which leads to multiple splitting in the $^{13}C$ NMR corresponding to the *tert*-butyl primary carbons (Figure 43). *Tert*-butyl was therefore a potential source of inter-molecular protons contributing to the new proton observed in the Wheland intermediates.

### 3.2.11.5 Proposed mechanism for de-iodination of 1-iodonaphthalen-2,4-diamine (68) *via* Wheland intermediate

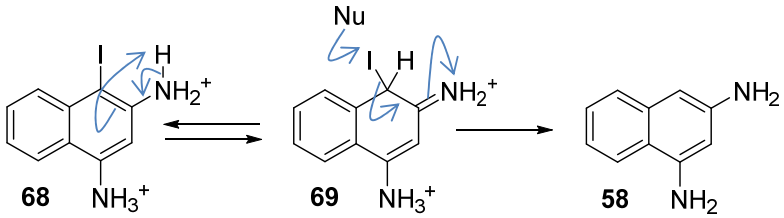


**Scheme 26:** Proposed mechanism of de-iodination of 1-iodonaphthalen-2,4-diamine.

Scheme 26 shows the proposed mechanism for the de-iodination of 1-iodonaphthalene-2-diamine **68**. Proton transfer from $N^2$ to C1 of **68**, causes loss of aromaticity leading to the Wheland-like intermediate **69**. The source of the new proton in the Wheland intermediate, has an intra-molecular origin. Nucleophilic abstraction of the iodine and restoration of aromaticity leads to the de-iodinated product **58**. The nucleophile responsible for trapping the iodine as $I^+$-equivalent is likely to be the trifluoroacetate ion. However, when the solutions were left for prolonged days (~7 d) the colour turned dark red, suggesting the presence of $I_2$. The loss of iodine is accelerated by the presence of electron-withdrawing group on the ring, such as trifluoroacetamido as in **77** → **78**. Electron-withdrawing groups make the iodine more electrophilic pushing the reaction towards the de-iodinated product. This means the Wheland intermediate becomes less stable as seen in **77** → **78** (**79** → **80**) where this intermediate was not observed by NMR.

Electrophilic aromatic substitution proceeds *via* a π-complex, which eventually converts to a "σ-complex" also known as Wheland intermediate. Charge transfer UV/vis absorption of several π-complexes has been used in their identification as well as crystallography.[143] The majority of these intermediates are transient and unstable due to their rapid deprotonation making it difficult to observe them by NMR. The Wheland intermediates tend to be observed only by femtosecond time-resolved laser absorption spectroscopy. Few compounds such as

1,3,5-trimethylbenzene and hexamethylbenzene reacts with $NO_2^+BF_3^-$ at -70°C under super-acidic conditions to give Wheland intermediates that are observable by NMR. These intermediates are unstable at higher temperatures and therefore decompose on warming.[144, 145] Wheland intermediates with carboranyl counter ions have also been isolated and observed by NMR.[146-148] Furthermore, molecules with both Wheland-like cations and Meisenheimer-like anions have been isolated.[149] Efforts to understand why de-iodination of Boc-protected naphthlenediamines occurs during the synthesis of the key intermediate **67** of the alkylating subunit of the proposed CBI drugs, have led to the observation of the first Wheland-like intermediates derived from amino-naphthalenes. These cations are very stable, even at room temperature and decompose on isolation. The Wheland intermediates are stabilised by delocalisation of the positive charge involving both nitrogens. In addition, the Wheland intermediate with iodine **71** is further stabilised by the transformation of the $sp^2$ hybridised C1 to $sp^3$ hybridised carbon which help to relieve the steric compression between the bulky iodine and the *peri* 8-H. These experiments have provided an insight into why de-iodination is a major challenge in the acidic deprotection of Boc-protected iodo-naphthalenediamines.

### 3.2.12 Sharpless epoxidation

With the synthesis of **67**, the next step was to alkylate the $N^2$ of **67** with an alkylating unit that could participate in a cyclisation step to form the pyrrolidine ring of the proposed CBI drug **3**. The first of such groups to be introduced was an epoxide. Sharpless epoxidation[150] was employed in the enantioselective synthesis of the epoxy alcohol **90** (Scheme 29). This method provides 2,3-epoxy alcohols with high enantioselectivity. Depending on the tartrate enantiomer used, selective synthesis of a particular enantiomer of the epoxy alcohol can be attained. When the alkene unit is in plane of drawing with the hydroxymethyl substituent at the lower right corner, as shown in Scheme 27, the delivery of the epoxide oxygen occurs either from the top (D-(−)-diethyl tartrate), or from underneath the plane (L-(+)-diethyl tartrate) regardless of the substituent pattern.[150] This method allows the selective synthesis of highly enantiopuric epoxy alcohols.

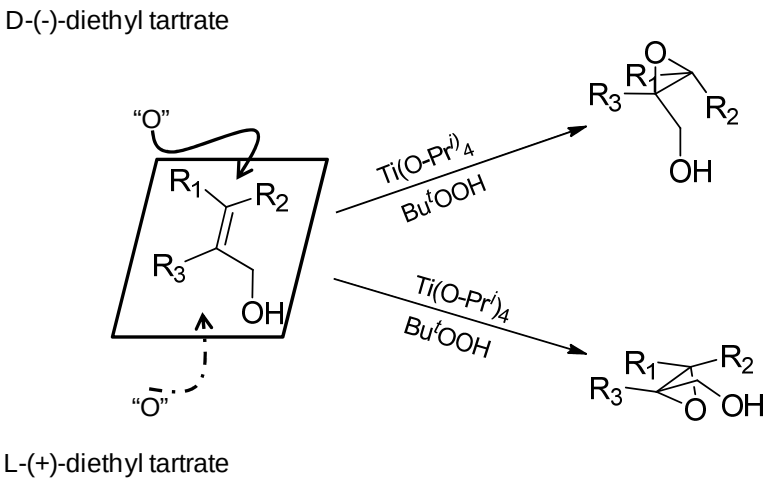


**Scheme 27:** Delivery of the epoxide oxygen to the double bond in Sharpless epoxidation.

For instance, epoxidation of (*E*)-buten-2-ol with D-(−)-diethyl tartrate gives the 2*R*,3*R* enantiomer, whilst the use of L-(+)-diethyl tartrate gives the 2*S*,3*S* enantiomer.[151] The 2*R*,3*R* epoxy alcohol was selected since this configuration eventually leads to a CBI drug with a configuration (1*S*,10*R*), which has been shown to have superior cytotoxicity.[81] The use of the methylepoxy alcohol **90** in the synthesis of the alkylating subunit of the proposed CBI drug will lead to the introduction of an extra stereogenic centre (10*R*), which is absent in the natural products. The extra methyl group is introduced in order to reduce the chance of direct alkylation by the *seco*-CBI of DNA, which would be detrimental to the design of prodrugs.[125] Analogues incorporating the (+) (1*S*,10*R*) diasteroisomer of the alkylating subunit has been found to be more active compared to the (−) (1*R*,10*S*) diasteroisomer.[81] It has also been observed that, when the two sterogenic centres are *syn* (1*S*/10*S* or 1*R*/10*R*) the *seco*-CBI drug possess a low toxicity and not suitable for development as a prodrug.[124]

Alkylation of the $N^2$ of **67** with 2*R*,3*S*-3-methyl-2-(4-nosyloxymethyl)oxirane will be followed by opening of the epoxide in a metal-mediated cyclisation. This is proposed to go *via* the lithium coordinated transition state **88** (Scheme 28). Attack of the epoxide carbon occurs in an anti-fashion causing inversion of configuration at the stereogenic centre involved in the cyclisation to give (1*S*,10*R*)-**5** (Scheme 28).[81]

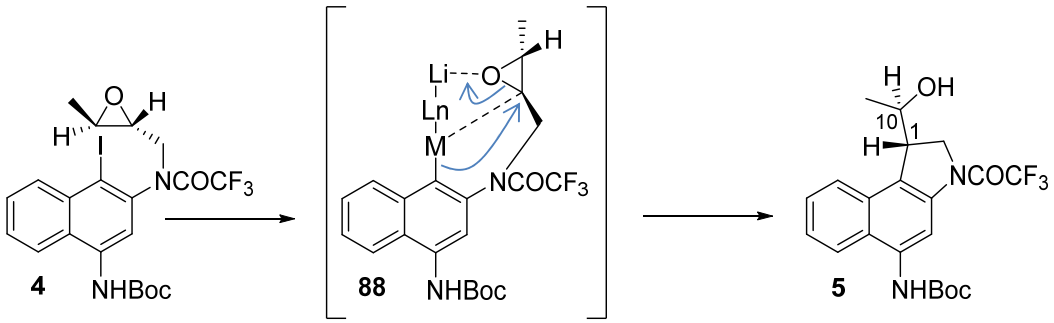


**Scheme 28:** Metal mediated cyclisation with lithium coordinated transition state.

Commercially available buten-2-ol **89** (*E*/*Z* mixture 19:1), was added to a mixture of titanium tetraisopropoxide and D-(−)-diethyl tartrate, followed by *tert*-butyl hydroperoxide (TBHP) (Scheme 29). The titanium tetraisopropoxide and D-(−)-diethyl tartrate react together to form a catalyst complex which helps deliver the oxygen from TBHP to the double bond.

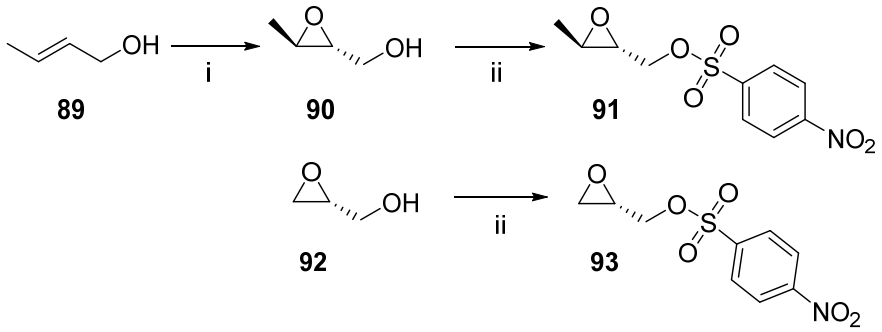


**Scheme 29:** Sharpless epoxidation. *Reagents and conditions:* i. Ti(O-Pr$^{i}$)$_4$, D-(−)-diethyl tartrate, dry *tert*-butyl hydroperoxide, dry $CH_2Cl_2$, $N_2$, −23°C, 20 h; ii. 4-Nitrobenzene sulfonyl chloride, $Et_3N$, toluene, 0°C → 20°C, 30 min.

The original procedure for the Sharpless epoxidation, which included an alkaline hydrolysis step, is said to be difficult when the produced epoxy alcohol is water-soluble and/or volatile, as in **90**. In such situations, very poor yields are observed since it is difficult to extract the epoxy alcohol into organic phases.[150, 152] A modified work-up without an alkaline hydrolysis step, designed for water-soluble epoxides, was used but this still led to majority of the product being lost, resulting in very low yields.[152] Precipitation of excess reagents with $Et_2O$ followed by filtration and chromatographic purification gave **90** in a yield of 50%.[153] Compound **90** was then nosylated to give **91**. Repeated recrystallisation to raise the enantiomeric purity gave the enantiopure **91** in an overall yield of 11% (68% ee in reference to literature value[81]). The challenges met during the synthesis of **91** and the low yield attained led to the synthesis of **93** which could be easily accessed from the commercially available homochiral epoxy alcohol **92**. In this way, **93** could be used to establish the feasibility of the chemistry in the synthesis

of the pyrrolidine ring of the proposed CBI drug before committing the precious supply of **91**. *R*-Glycidol **92** was nosylated under basic conditions to give **93** (> 99% ee in reference to literature value[154]). The importance of having the nosylate leaving group is that it makes the exocyclic $CH_2$ of the epoxide a more powerful electrophile than the $CH_2$ of the oxirane. In this way, attack of nucleophiles will take place exclusively at the exocyclic $CH_2$, with clean $S_N2$ displacement of the nosylate retaining the stereochemical configuration at the oxirane. With weaker leaving groups, such as chloride, initial attack of a nucleophile will be at the oxirane $CH_2$, opening the oxirane; the alkoxide formed will attack the exocyclic $CH_2$, leading to introduction of a $CH_2$-oxirane unit but with inversion of configuration. Intermediate-strength leaving groups, such as tosylate, proceed by both mechanisms, leading to loss of stereochemical integrity.[41] Synthesising the nosylates of the epoxides also produces a solid that can be purified by repeated recrystallisation to raise the enantiopurity. Tietze *et al*.[81] have reported that the chloride, mesylate, triflate and the nonaflate are difficult to purify compared to the nosylate.

### 3.2.13 Selective $N^2$-alkylation of *tert*-butyl N-(1-iodo-2-(trifluoroacetamidonaphthalen-4-yl)carbamate (67)

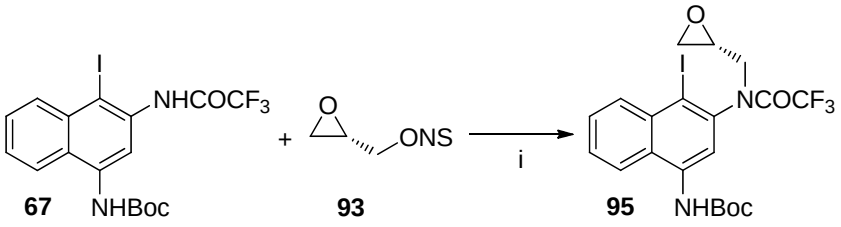


**Scheme 30:** Selective $N^2$-alkylation of **67**. *Reagents and conditions:* i. $K_2CO_3$, acetone, $N_2$, 50°C, 72 h.

One of the reasons for having orthogonal protections on the amino groups of **67** was to allow a selective alkylation to take place at $N^2$. The proton on the trifluoroacetamide group is more acidic, due to the electron-withdrawing trifluoroacetamide group, compared to the Boc protected $N^4$-amine. Therefore, by careful selection of a suitable base, selective deprotonation of $N^2$ with subsequent alkylation with **93** can be achieved. In addition, the bulky nature of the Boc-group in comparison to the trifluoroacetamide protecting group should allow selective alkylation of the nitrogen of the trifluoroacetamide of **67**. Selective $N^2$-alkylation of **67** was investigated to give **95** (Scheme 30). The base used initially for deprotonation of the $N^2$ proton was potassium *t*-butoxide. Several attempts using this base in different reaction conditions (*e.g.* r.t., 50 → 70°C, 2 h → 72 h), however, did not give the desired product **95**. Even the use of excess reagents did not give the product but instead the starting material was recovered in all cases. Monitoring by thin layer chromatography suggested that the epoxide

**93** was being consumed in the reaction. There is therefore a possible chance of a nucleophilic attack by potassium *t*-butoxide on **93**, consuming it and resulting in no alkylation of **67**. This was despite a sequential addition of potassium *t*-butoxide to **67** before addition of the epoxide **93**. The base was changed to potassium carbonate. The pKa of the conjugate acid of the carbonate anion lies between the pKa of $NHCOCF_3$ and NHBoc and therefore selective deprotection of the former is always likely to take place. Besides, the bulky nosylate group of **93** will aid in the selective $N^2$-alkylation. The low solubility of $K_2CO_3$ in acetone also means that a two-phase reaction takes place reducing the chance of nucleophilic attack of the oxirane nosylate by the carbonate anion. The reaction of **67** with **93** gave two compounds. The initial interpretation was that these could be due to regioselective alkylation. Mass spectrometry confirmed that these compounds were isomers and each contained only one oxiranylmethyl group. Furthermore, 2D NMR spectroscopy (HMBC, NOESY) confirmed that, in both compounds, the oxiranylmethyl group was located at the $N^2$-amide group and not the Boc-amide group. In the $^1H$ NMR spectrum of one isomer, there was evidence of the existence of two rotameric forms about the $F_3COC—N^2$ amide bond in a ratio 1.3:1. This dispelled the idea that the two separated compounds could be rotamers about this bond. It was concluded that the two compounds were diasteroisomers of **95**. The diastereoisomers **95a** and **95b** (Figure 44) were obtained in yields of 34% and 39%, respectively (*i.e.* 73% overall yield).

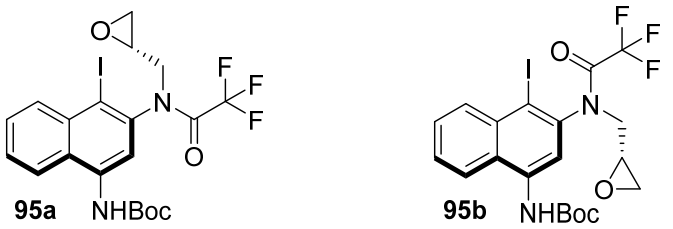


**Figure 44:** Atropisomerism arising from restricted rotation about the N-aryl bond caused by the bulky iodine.

Despite the existence of only one overt chiral centre in **95**, the bulky iodine at position-1 restricts rotation around the C2—$N^2$ single bond giving two atropisomers. The naphthyl ring adopts an orientation perpendicular to the plane of the trifluoroacetamide creating a virtual chiral centre at the middle of the N-aryl bond (Figure 44).[81, 155] The atropisomers did not interconvert, meaning there existed two separable diastereoisomers both containing the same configuration at the oxirane. Unfortunately, it was not possible to identify the configurations at the virtual chiral centres of the two diastereoisomers. Observation of such atropisomerism in related compounds has been made by Tietze *et al.*[155] where they showed that removal of the iodine resulted in a single isomer and also cyclising the two atropisomers resulted in a single product with same configuration. Selective alkylation of the $N^2$-amide was therefore achieved

in good yield despite the use of excess potassium carbonate (4 eq.) which was needed for completion of reaction.

### 3.2.14 Metal-mediated cyclisation

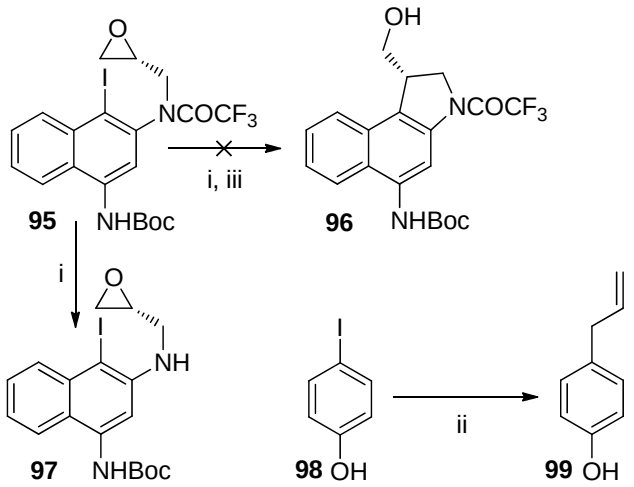


**Scheme 31:** Attempted metal mediated cyclisation. *Reagents and conditions*: i. MeLi, CuCN, dry THF, −78°C → 25°C, 72 h; ii. $ZnCl_2$, Bu$^t$Li, 3-bromopropene, $N_2$, −78°C → 40°C, 72 h; iii. $ZnCl_2$, Bu$^t$Li, $N_2$, −78°C → 40°C, 72 h.

The next step was to undertake a metal-mediated cyclisation of **95a** and **95b** to give **96** (Scheme 31). A study by Tietze *et al.*[81] showed that higher-order cuprate $Li_2Cu(CN)Me_2$ and the zinc organyl $Li_2Zn(SCN)Me_3$ were the best reagents for metallation in a similar cyclisation reaction. Lithium reagents were chosen due to the ability of lithium to coordinate with the oxygen of the epoxide to form a sterically fixed transiton state **88** (Scheme 28). There are two possible site of attack on the epoxide to form either 5-*exo*-trig **96** and/or the 6-*endo*-trig products **100** (Scheme 32). However, Teitze *et al.* observed that in their cyclisation reactions, only the 5-*exo*-trig products were formed.[81] Formation of the 6-*endo*-product is not detrimental, since substituting the hydroxy group with a better leaving group followed by Boc-deprotection will trigger spirocyclisation to generate the essential pyrrolidine ring and the electrophilic cyclopropane ring **102** (Scheme 32).[41, 156]

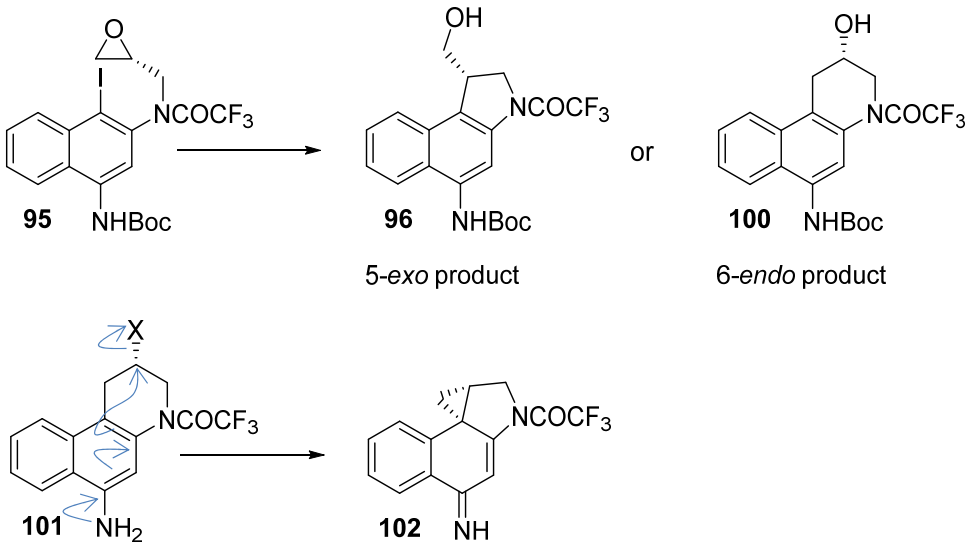


**Scheme 32:** Possible 5-*exo*-trig and 6-*endo*-trig cyclisation products and spirocyclisation of the *endo*-product to generate the pyrrolidine ring and the electrophilic cyclopropane ring.

$Li_2Cu(CN)Me_2$ was prepared *in situ* by addition of MeLi to CuCN. This was treated with compound **95a** or **95b** with the aim of replacing the iodine with copper and allowing the aryl-copper to attack the oxirane to give **96**. However, the sole product was **97**, the result of loss of the trifluoroacetyl group (Scheme 31). This was attributed to the highly nucleophilic cyanide / methyl ion. The NMR of **97** showed the existence of conformers. This is likely to be due to slow rotation around the carbamate N-C(O) bond and the $N^2$-epoxide bond. The use of dilithium tetra-*tert*-butylzincate ($Bu^t_4ZnLi_2$) was investigated. First of all, this reagent was tested for its ability to substitute an iodine on 4-iodophenol **98** with a propenyl group (Scheme 31). Dilithium tetra-*tert*-butylzincate was prepared *in situ* by adding *tert*-butyllithium to zinc chloride. 4-Iodophenol **98** was then added to allow iodine → zinc exchange followed by addition of 3-bromopropene. The first attempt using 1.1 equivalent of dilithium tetra-*tert*-butylzincate resulted in recovered starting material as the acidic phenolic proton was deprotonated rather than the desired halogen → zinc exchange. The procedure was repeated with two equivalents of dilithium tetra-*tert*-butylzincate to compensate for the presence of the acidic phenolic proton of **98**. This modification led to the synthesis of **99** and suggested that this method could work with **95**.[157] Compound **95a** and **95b** were exposed to the same conditions with excess dilithium tetra-*tert*-butylzincate to compensate for the acidic Boc-carbamate proton. This, however, resulted in a complex product mixture that could not be separated. It is possible that removal of the N-H of **95a** / **95b** results in an unstable product leading to decomposition of the compound. It has also been reported that the electron-rich naphthalene ring tend to slow down metal-halogen exchange even in the case of naphthyl iodide and thus proton abstraction from the Boc-amide is favoured.[41]

### 3.2.15 Free-radical cyclisation

A new approach to the synthesis of the pyrrolidine ring of the alkylating subunit of the proposed CBI drug was needed. The route of trying to synthesis an enantiopure CBI drug had to be suspended. A racemic synthesis of the pyrrolidine ring was pursued. This involved selective alkylation of the $N^2$-amide with 3-bromopropene followed by free-radical cyclisation.

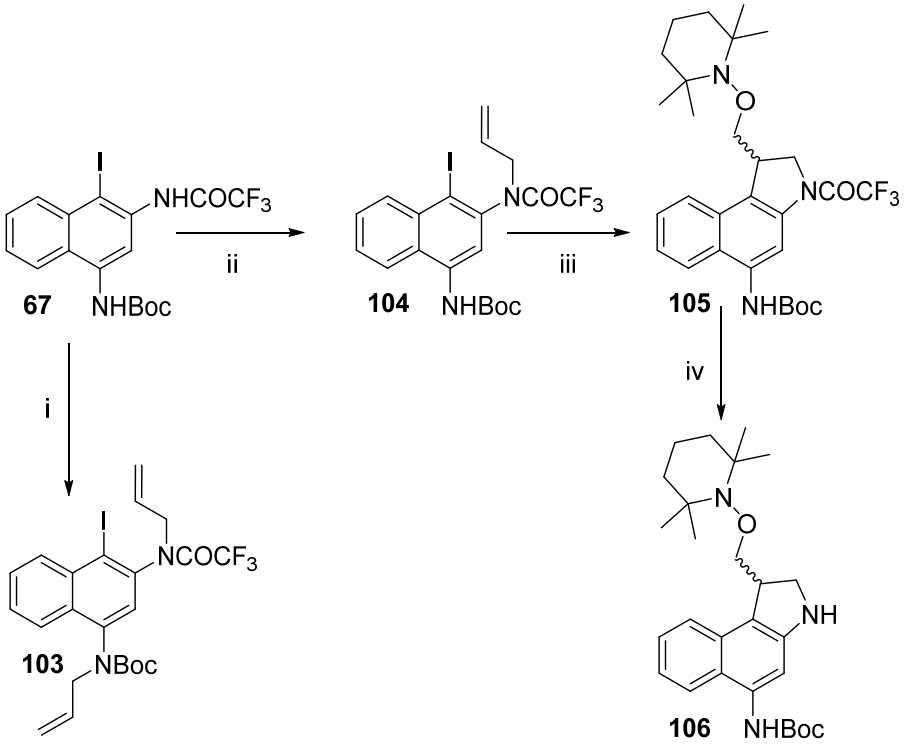


**Scheme 33:** Free radical cyclisation with TEMPO trap. *Reagents and conditions:* i. $K_2CO_3$, 3-bromopropene, acetone, $N_2$, 50°C, 16 h; ii. KOBu$^t$, 3-bromopropene, THF, $N_2$, 20°C → 50°C, 16 h; iii. TEMPO, $Bu_3SnH$, 60°C, 135 min; iv. aq. NaOH (5.0 M), THF, r.t., 105 min.

An initial attempt to synthesise **104** using similar conditions as used in the synthesis of **95** (four equivalents of potassium carbonate, allyl bromide) gave the di-alkylated product **103**. This suggests that steric hindrance between the Boc group of **67** and the bulky nosylated epoxide **93** contributed to the selective synthesis of **95** (Scheme 30). Compared to **94**, 3-bromopropene is small enough to gain access to the Boc-amide nitrogen as well as the $N^2$-amide nitrogen. The NMR of **103** showed the presence of two diastereoisomers, probably due to the slow rotation about the C-NBoc and C-$NCOCF_3$ bond (Figure 45).

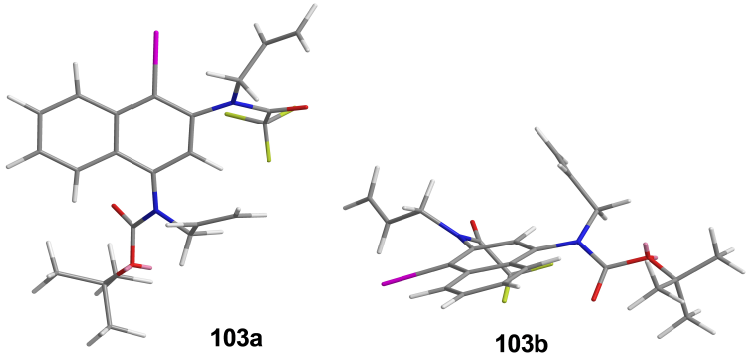


**Figure 45:** Structure of **103** derived from energy-minimising MM2 calculations.

The slow rotation about the C-NBoc and C-NCOCF$_3$ is due to the bulkiness of the groups on N$^2$ and N$^4$ as well as a possible steric clash with the bulky iodine and the *peri*-5 hydrogen during rotation around the C—N bond. This means that the allyl groups can either be on the same side or the opposite side of the naphthalene ring, resulting in the observed diastereoisomers. Potassium *tert*-butoxide (one equivalent) was used to remove selectively the N$^2$-amide proton of **67**, followed by allylation to give **104**. The N$^2$-allyl compound **104** was treated with tri-butyltinhydride ($Bu_3SnH$) and 2,2,6,6-tetramethyl-piperidine-1-oxyl (TEMPO), which promoted a 5-*exo*-trig free radical cyclisation with *in situ* TEMPO trap of the intermediate cyclisation product radical to give racemic **105**. The TEMPO radical also acts as the free radical initiator to generate tri-butyltin radical. Abstraction of iodine by the *tri*-butyltin radical generates an aryl radical which then attacks the allyl double bond to generate the free radical cyclisation product. Entrapment by TEMPO generates the final product **105**. This reaction does not go to completion unless excess reagents are used. This is likely to be due to the competing reaction between TEMPO and the generated tri-butyltin radical. This is especially true since the rate constant ($k = \sim 8 \times 10^8$ $M^{-1}s^{-1}$ at 80°C) of tri-butyltin radical abstracting the iodine is similar to the rate constant ($k = \sim 7.6 \times 10^8$ $M^{-1}s^{-1}$ at 25°C) for reaction between the TEMPO and tri-butyltin radical. Aryl bromides have been shown to give lower conversions to product compared to the aryl iodides highlighting the essential role of having the iodide in the key intermediate **67**.[128] The 2,2,6,6-tetramethylpiperidine also conveniently acts as a protecting group for the next step of acylation at N$^2$. Selective base-catalysed hydrolysis of the trifluoroacetamide group of **105** with sodium hydroxide gave **106**, ready to be coupled to the non-alkylating subunit.

## 3.3 Synthesis of the non-alkylating subunit of proposed CBI drug.

The non-alkylating subunit of the ant-tumour antibiotics is essential for their biological activity. The initial non-covalent binding of the anti-tumour antibiotics to double-stranded DNA is mediated by the non-alkylating subunit. The extent of binding by this subunit determines the potency and toxic effects of these agents. For instance, the ability of CC-1065 to cause delayed death and also its high potency have been attributed to its non-alkylating subunit.[49, 75] The non-alkylating subunit chosen for the proposed CBI drug was 5-(2-dimethylaminoethoxy)indole-2-carboxylic acid *(*DMAI). This subunit is devoid of the delayed death effect of CC-1065 which has been attributed to the presence of the two ethylene moieties and the terminal amide moiety present in the non-alkylating subunit.[45, 49] It is also simpler to synthesise and its ability to form salts enhances aqueous solubility of the synthesised compound.[80, 81] Total synthesis of this subunit was undertaken by adopting a Fisher-like indole synthesis.

### 3.3.1 Fisher-like indole synthesis

The Fisher synthesis of indoles involves the condensation of an arylhydrazine with a ketone, whilst an aryldiazonium salt replaces the arylhydrazine in the modified Fisher-like indole synthesis. Furthermore, the nucleophile in this Fisher-like indole synthesis is the enol tautomer of the ketone whilst in Fisher indole synthesis the nucleophile is the arylhydrazine. Compound **110** was prepared by Fisher-like indole synthesis from the substituted aniline **109** (Scheme 34).

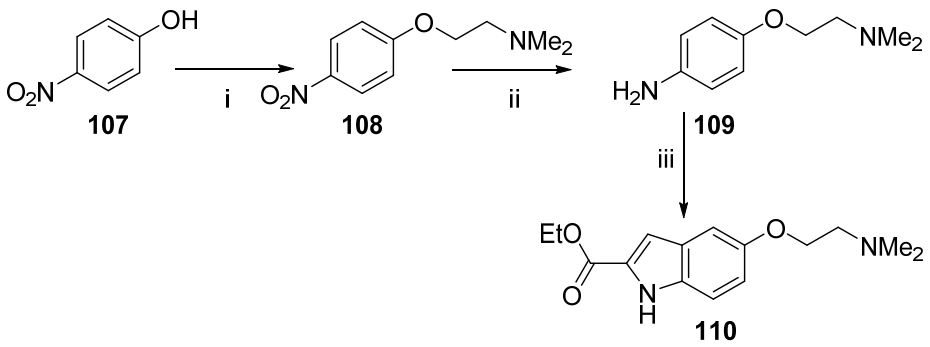


**Scheme 34:** Synthesis of ethyl 5-(2-dimethylaminoethoxy)-1*H*-indole-2-carboxylate **110**. *Reagents and conditions:* i. (a). KOH, EtOH, r.t. (b). $Me_2NCH_2CH_2Cl$, toluene, reflux, 17 h; ii. $SnCl_2$, HCl, 0°C → r.t., 19 h; iii. $NaNO_2$/HCl, -20°C then ethyl 2-methyl-3-oxobutanoate/NaOAc, 20°C, 16 h, then HCl/EtOH/reflux, 30 min.

A Williamson ether synthesis was used to generate the nitrophenyl ether **108**. The highly acidic phenolic proton of 4-nitrophenol **107** was removed by potassium hydroxide. This base will also liberate 2-chloro-N,N-dimethylethylamine from its hydrochloride salt; this amine has a mustard structure and will be in equilibrium with the 1,1-dimethylaziridinium ion. This

powerful electrophile reacts readily with the phenoxide to give **108**. Reduction of the nitro group of **108** using tin(II) chloride in acid medium gave the aniline **109** at a yield of 88%. Compound **109** was diazotised with sodium nitrite in the presence of an acid catalyst. The acid initially reacts with the sodium nitrite to give the reactive nitroso species ($NO^+$). This then attacks the lone pair on the primary amine of **109**, followed by dehydration to yield the diazonium salt. Scheme 35 shows the proposed mechanism for the formation of the indole ring of **110**.

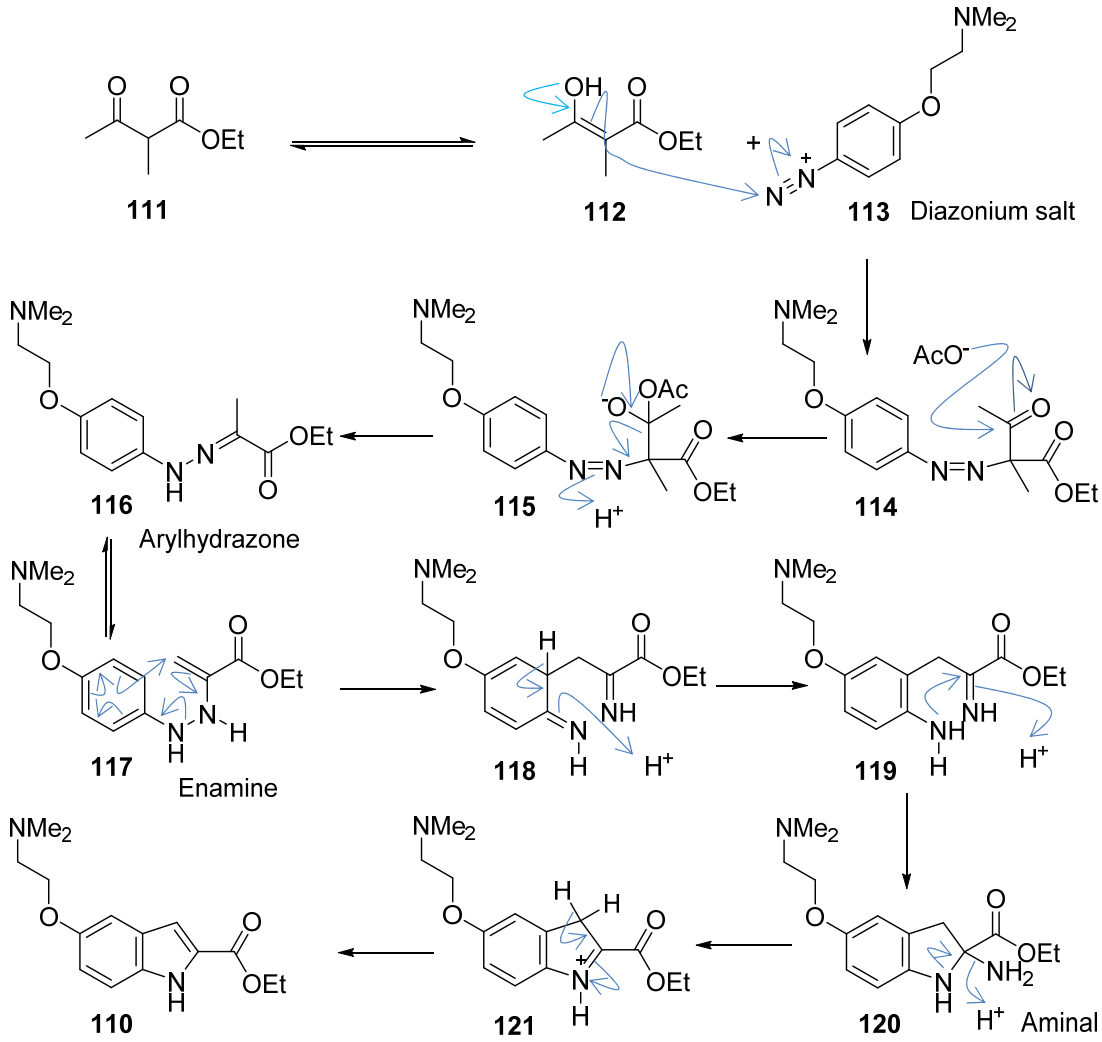


**Scheme 35:** Proposed mechanism of the synthesis of **110** *via* a diazonium intermediate rather than the usual hydrazine intermediate of Fisher indole synthesis.

Treatment of the diazonium salt **113** with ethyl 2-methyl-3-oxobutanoate **112** in the presence of the weak base sodium acetate gives a hydrazone **116**. The arylhydrazone tautomerises to the enamine **117** which then undergoes [3,3]-sigmatropic rearrangement and re-aromatisation of the benzene ring to give an aminal **120**. Acid-catalysed decomposition of the aminal with the release of ammonia allows the loss of a proton and the formation of the aromatic indole

**110** at the modest yield of 15%. This synthesis of the indole **110** proved very challenging. The initial conditions for this reaction were diazotisation at 0°C, followed by treatment with ethyl 2-methyl-3-oxobutanoate for 1 h. This, however, did not give the desired product, even after increasing reaction time to 2 h. Finally, diazotisation was carried out at −20°C, which provided the desired product but at a low yield. Attempted optimisation by using excess reagents ($NaNO_2$ / HCl) or using a stronger acid ($H_2SO_4$) at the diazotisation step did not have any significant effect on the yield. As part of the work-up, the product had to be extracted with hot hexane in the presence of decolourising charcoal. Adsorption on the charcoal is one of the ways by which aromatic products may be lost. Furthermore, the last step of the synthesis involved heating the mixture with ethanolic HCl. The presence of water in this step will inevitably lead to hydrolysis of the ethyl ester group to produce the indole acid. This will then be easily lost in the water layer during basic work-up. The challenges faced with the Fisher-like synthesis meant that a different approach was needed in the efficient synthesis of **110**.

### 3.3.2 Synthesis of 5-(2-dimethylaminoethoxy)indole-2-carboxylic acid (DMAI) (127)

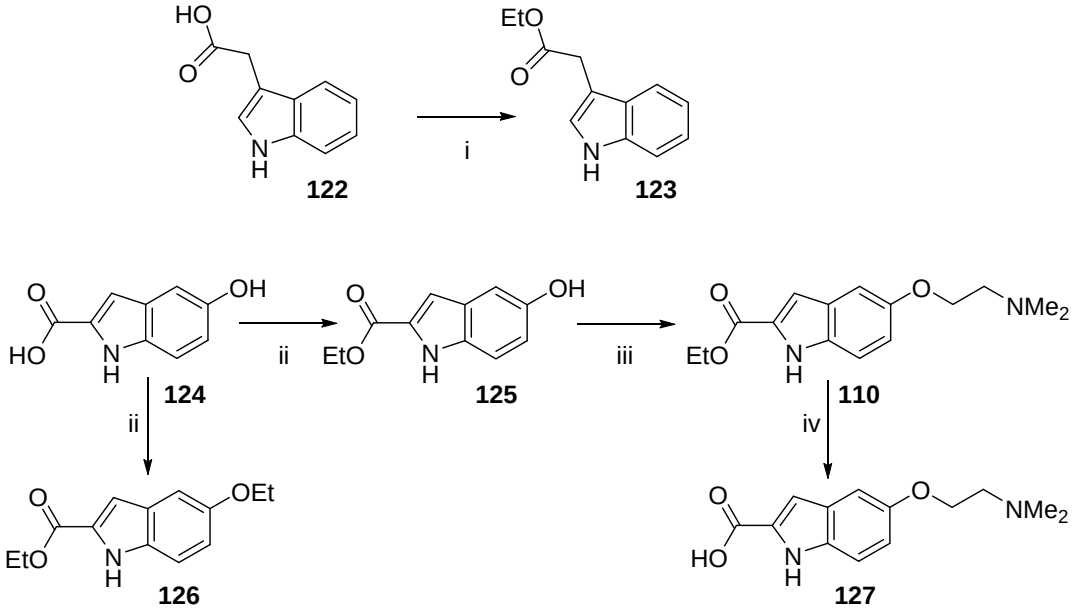


**Scheme 36:** Synthesis of DMAI. *Reagents and conditions:* i. sat. Ethanolic HCl, $N_2$, reflux, 1 h; ii. (a) $SOCl_2$, EtOH, 80°C, 1 h; (b) sat. ethanolic HCl, reflux, 4-16 h; iii. 2-chloro-N,N-dimethylamine hydrochloride, $K_2CO_3$, $CHCl_3$, $H_2O$, 65 → 81°C, 16 h; iv. $CsCO_3$, MeOH/$H_2O$ (2:1), reflux, 2 h.

When the indole-2-carboxylic acid **124** became commercially available, a new and shorter approach to the synthesis of **110** was adopted (Scheme 36). This involved esterification of **124**, followed by Williamson ether synthesis to alkylate the phenolic hydroxyl group to introduce the O-(2-dimethylamino)ethyl unit. Hydrolysis of the ester should then give the

desired indole carboxylic acid **127** to couple to **106**. Esterification of the carboxylic group of **124** was initially attempted using *para*-toluenesulfonic acid to activate the carboxylic group to nuleophilic attack by ethanol. Analysis of the crude products formed suggested the presence of some desired product **125**, starting material **124** and a possible dimer of **124**. Compound **124** in ethanol was treated with thionyl chloride under reflux conditions. Thionyl chloride reacts with ethanol to generate hydrochloric acid which then catalyses the esterification. This procedure, however, resulted in a poor yield of **125** (3%) and a range of side products. The use of ethanolic-hydrogen chloride for the esterification was investigated by boiling 2-(indol-3-yl)acetic acid **122** in saturated ethanolic hydrogen chloride to give **123** at 82% yield. Extension of this procedure to compound **124** gave **125** at a yield of 92%. In one instance of the synthesis of **125** using ethanolic-hydrochloric acid, the reaction was allowed to run overnight (16 h). This resulted in the formation of the side product **126** (~10%) as well as the desired product **125** (Scheme 36). Ethanol is protonated by hydrochloric acid to form an electrophilic ethyloxonium ion. Nucleophilic attack at this ion by the phenolic hydroxy group gives **126** with the loss of water. Compound **125** was then alkylated with 2-chloro-N,N-dimethylethylamine to give **110** in 80% yield. Basic ester hydrolysis of **110** gave the required indole acid **127** for coupling to the alkylating subunit **106.**

## 3.4 Coupling of the alkylating and non-alkylating subunits

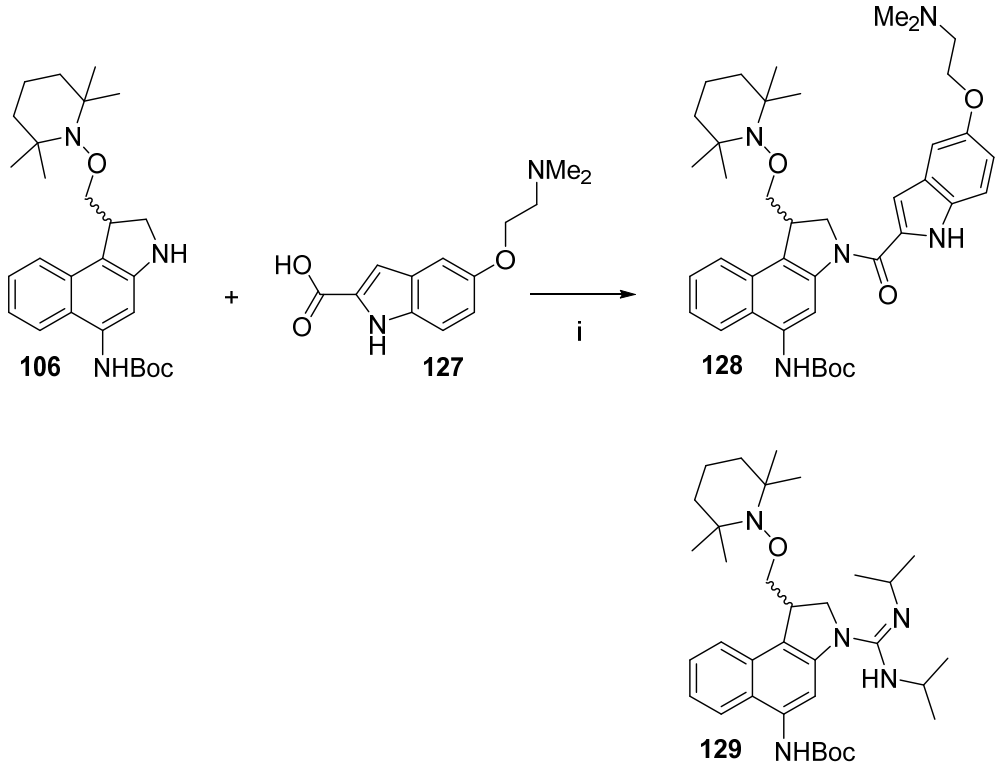


**Scheme 37:** Coupling of the alkylating subunit **106** and the DMAI subunit **127**. *Reagents and conditions:* i. N,N-diisopropylcarbodiimide, HOBt, DMF, $N_2$, 0°C → 40°C, 18 h.

With the synthesis of the alkylating subunit **106** and the non-alkylating subunit **127** of the proposed CBI drug having been achieved, the next step in the synthetic process was to couple the two together. Initial efforts to synthesise **128** *via* the acid chloride of **127** failed, resulting with recovery of starting material, despite the use of 4-dimethylaminopyridine as a catalyst (Scheme 37). The use of the coupling agent, N-(3-dimethylaminopropyl)-N'-ethylcarbodiimide hydrochloride (EDC.HCl) was tried but this attempt also failed even after extending the reaction time. The preactivation of carbodiimide coupling agents relies on protonation of the carbodiimide by the carboxylic acid.[158] The unhindered basic amino group present in **106** is likely to interfere with this preactivation step by being preferentially protonated. Thus initial preactivation before addition of **106** is desirable. Carpino *et al.*[158] have also observed that the neutral diisopropylcarbodiimide (DIC) is more effective compared to other carbodiimide coupling agents with protonated / quartenised tertiary amino groups (*e.g.* EDC.HCl). Coupling using diisopropylcarbodiimide and 1-hydroxybenzotriazole to preactivate **127** before addition of **106** was therefore investigated. The indolecarboxylic acid **127** was pre-treated with diisopropylcarbodiimide and 1-hydroxybenzotriazole to allow formation of the active benzotriazolyl ester. Compound **106** was then coupled to the

benzotriazolyl ester to give **128** at a satisfactory yield of 64%. Despite the precautions taken by sequential addition of compounds / reagents, mass spectrometry suggested that a small amount of the alkylating subunit **106** had reacted with the carbodiimide to give the guanidine **129** [MS ($ES^+$) *m/z* 580.4250 (M + 1) ($C_{34}H_{54}N_5O_3$ requires 580.4227)]. [159]

## 3.5 Reductive removal of the 2,2,6,6-tetramethylpiperidine protecting group

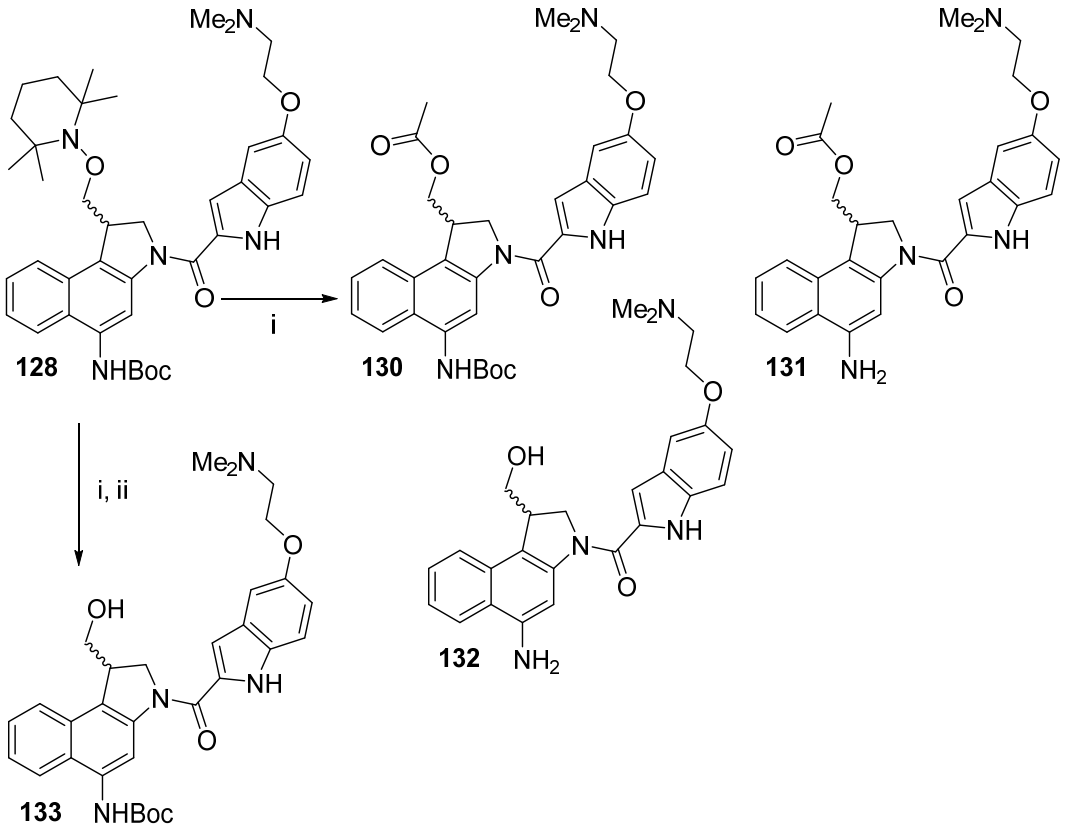


**Scheme 38:** i. Reduction of 2,2,6,6-tetramethylpiperidine. *Reagents and conditions*: i. THF/AcOH/$H_2O$ 1:3:1, activated Zn dust, 70°C, 23 h; ii. THF/AcOH/$H_2O$ 3:1:1, activated Zn dust, 70°C, 16 h.

The next step in the synthesis of the proposed CBI drug was to remove the masking 2,2,6,6-tetramethylpiperidinyl group by reductive cleavage of the N-O bond. This involved the use of zinc dust as the reducing agent in acidic conditions. Several attempts in tetrahydrofuran / acetic acid / water or ammonium chloride / methanol with excess zinc dust did not result in significant reaction. Activation of the zinc by stirring in aqueous hydrogen chloride (10%) was therefore undertaken; the activated dust was added to **128** in a solvent mixture of tetrahydrofuran / acetic acid / water at a ratio of 1:3:1. This procedure led to the complete reductive removal of the tetramethylpiperidinyl group. However, side products **130**, **131** and **132** as well as the desired product **133** were formed (Scheme 38). The side products could be

converted back to the desired product by either protecting the amino group and/or hydrolysing the acetyl group. The use of a high proportion of acetic acid and the sequence of addition of reagents was thought to be responsible for the problems encountered. The Boc group is acid-labile and thus may be prone to destruction by acetic acid. The acetylation of the hydroxy group is facilitated by $Zn^{2+}$ ions formed, which act as Lewis acids catalysing the esterification. As a result of these problems, the reaction was repeated with smaller proportion of acetic acid (*i.e.* tetrahydrofuran / acetic acid / water 3:1:1) and sequential addition of reagents with acetic acid being the last to be added. This gave **133** at a yield of 71% without side products.

## 3.6 Activation of the proposed *seco*-CBI drug

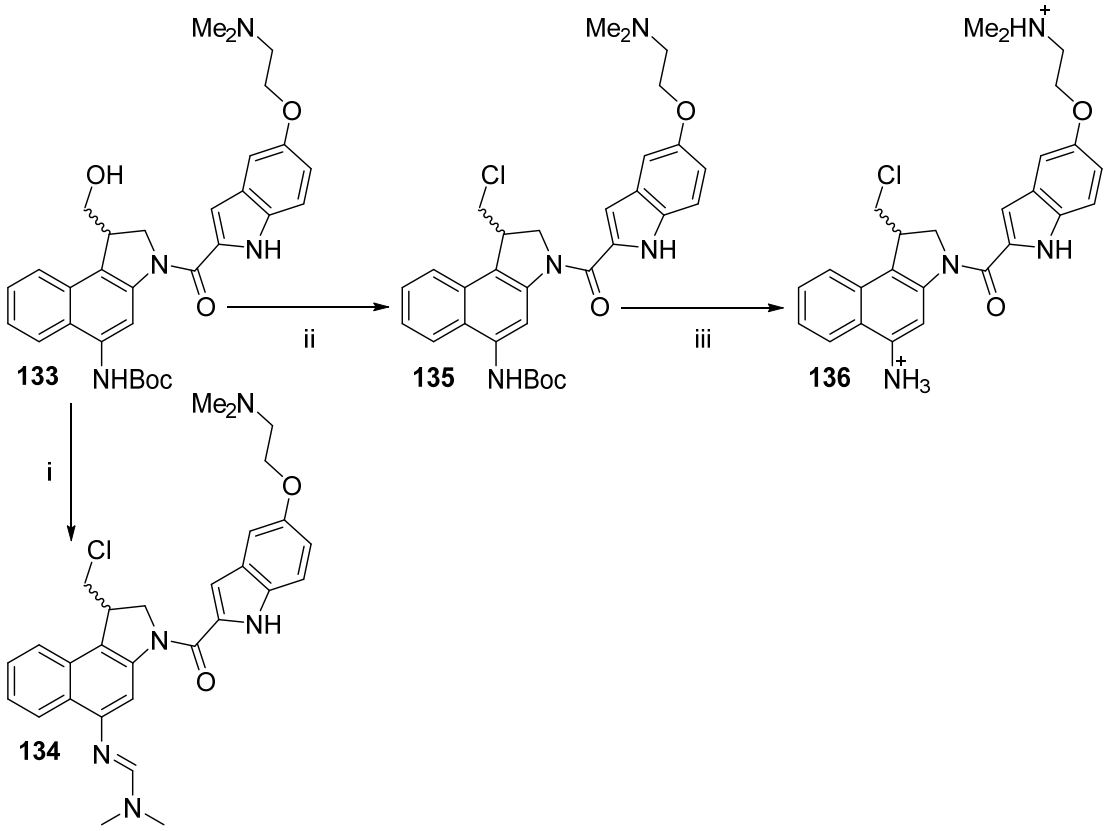


**Scheme 39:** Activation of *seco*-CBI drug. *Reagents and conditions:* i. MsCl, $Et_3N$, DMF, $N_2$, 0°C, 1 h then LiCl, 20°C, 3 d; ii. MsCl, pyridine, $N_2$, 0°C, 1 h then LiCl, 20°C, 7 d; iii. HCl in dioxane (4.0 M), 20°C, 2 h.

Substitution of the pendant hydroxy group of **133** with a better leaving group is required to aid Winstein cyclisation of the *seco*-drug to form the reactive cyclopropane ring needed for potency. Substitution of the hydroxy group of **133** with chlorine to form **135** was initially

attempted under Appel reaction conditions[81] using triphenylphosphine and tetrachloromethane in dry dimethylformamide (Scheme 39). Scheme 40 shows the proposed reaction mechanism.

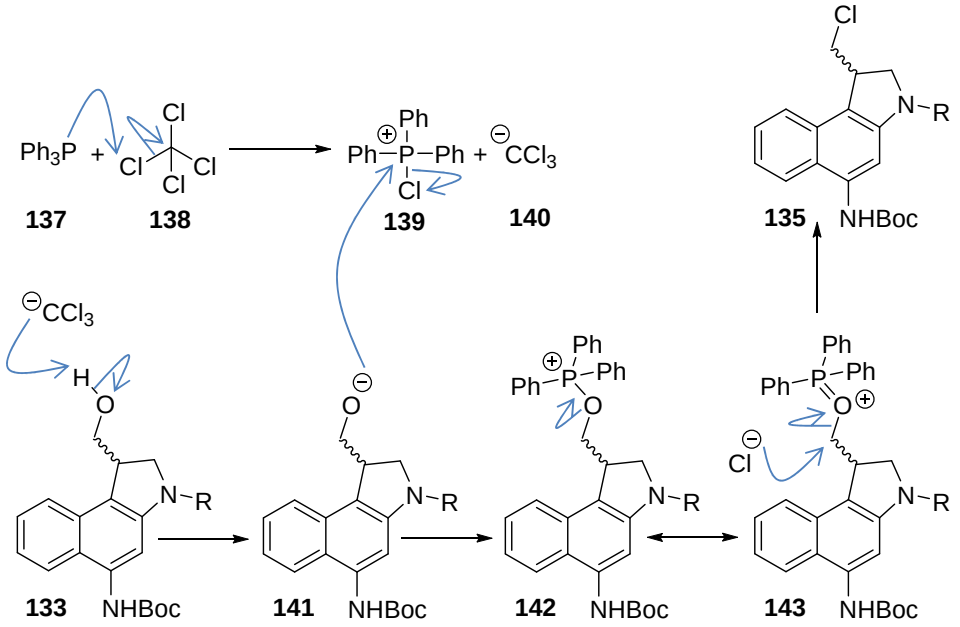


**Scheme 40:** Proposed mechanism of attempted Appel reaction.

The source of the chlorine in the Appel reaction is the tetrachloromethane. Triphenylphosphine **137** initially reacts with tetrachloromethane **138** forming the intermediate phosphonium salt **139** and trichloromethane anion **140**. The trichloromethane anion deprotonates the hydroxy group of **133**, yielding the alkoxide **141** and forming chloroform as the side product. Nucleophilic attack of the phosphonium salt **139** by the alkoxide **141** gives the oxyphosphonium intermediate **142**. The oxygen is converted into a leaving group followed by $S_N2$ displacement by the *in situ* generated chloride ion to form the desired product **135**. The reaction also releases triphenylphosphine oxide as a co-product. This reaction was, however, unsuccessful with **133** (Scheme 39). Mass spectrometry showed the presence of triphenylphosphine oxide and suggested that there was another source of oxygen reacting with the reagent. This led to pre-drying the solvent with molecular sieves to remove any trace of water and carrying the reaction under $N_2$ atmosphere. A large excess of triphenylphosphine was also used with the aim of compensating for any additional source of oxygen present. However, the reaction did not proceed even after raising the temperature. The limited solubility of compound **133** in organic solvents meant that this method of chlorination could not be pursued with other solvents.

Thionyl chloride was then investigated as a method to convert the $–CH_2OH$ into $–CH_2Cl$. The use of this acidic reagent meant that steps had to be taken to protect the Boc group of **133**. Compound **133** in dry dimethylformamide was treated with triethylamine and thionyl chloride. The basic triethylamine should serve to shield the Boc group from acidic deprotection. This method also failed to yield **135** giving rise to a complex product mixture in which the components could not be identified.

The next trial was to treat **133** with methanesulfonyl chloride in the presence of triethylamine. The idea was that, once the alkyl mesylate had formed, the chloride ions from the triethylamonium salt will then displace the mesylate group to yield **135**. Monitoring by mass spectrometry showed that the mesylation step was successful whilst the substitution with chloride failed. Tetra-butyl ammonium chloride was then added to the mixture to increase the concentration of chloride ions. This, however, also failed to yield the chloro product **135**. The reaction was repeated and lithium chloride was used as the source of excess chloride ions. Purification and characterisation of the product formed, however, surprisingly showed that, in addition to the desired formation of the $–CH_2Cl$ group, the Boc-protection had been lost and the exocyclic nitrogen had condensed with a derivative of N,N-dimethylformamide to give the dimethylformamidine **134**. Scheme 41 shows a proposed mechanism for this observation.

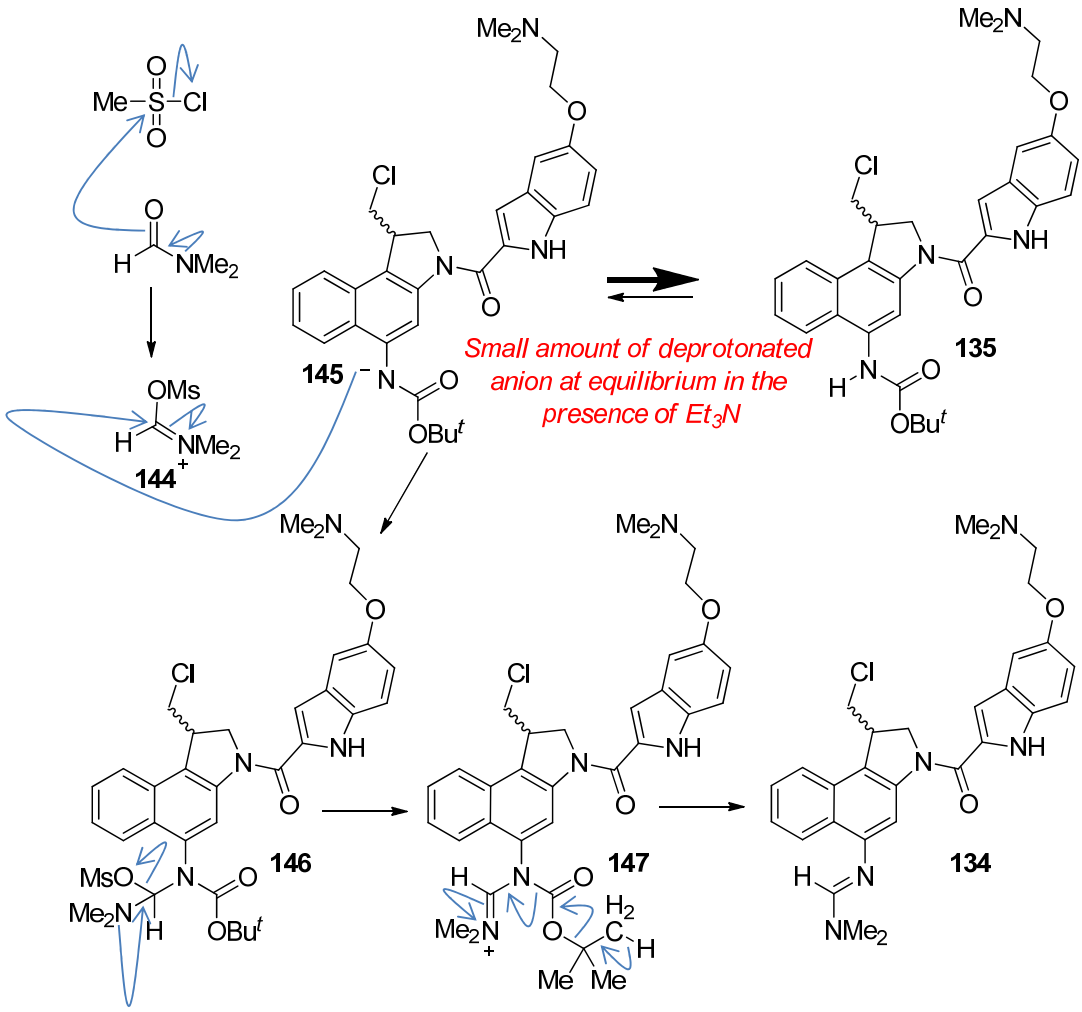


**Scheme 41:** Proposed mechanism for condensation of the exocyclic nitrogen of **135** with a derivative of dimethylformamide.

Dimethylformamide reacts with the excess mesyl chloride to give the imidate anhydride **144**. Nucleophilic attack at **144** by the Boc-amine anion **145** gives the intermediate **146**. Loss of methanesulfonate gives **147**. The Boc-protecting group is then lost to give the dimethylformimidamide **134**, driven by quench of the iminium cation. The reaction was repeated with pyridine as the solvent. Mesylation followed by substitution of the mesylate with chlorine afforded **135** at a good yield of 66%. Treatment of **135** with hydrogen chloride in dioxane removed the Boc-protecting group to give the final *seco*-CBI drug as the dihydrochloride salt **136**. Biological evaluations were undertaken on **136** to assess its DNA-binding ability and its cytotoxicity.

## 3.7 Calf-thymus DNA melting assay

The temperature at which double stranded DNA unwinds and unzips (denatures) is a useful tool to assess the binding of drugs to DNA. DNA absorbs light in the UV region due to the presence of the aromatic bases adenine, thymine, guanine and cytosine. Stacking interactions, hydrogen bonding and hydrophobic effects between the bases are responsible for the helical and compact nature of DNA. The compact nature of duplex DNA limits the resonance of the aromatic rings in the UV region and thus the DNA absorbs at a lower intensity. As denaturation of DNA occurs (*e.g.* by heating), the duplex structure unwinds and unzips to form single-stranded DNA (Scheme 42).

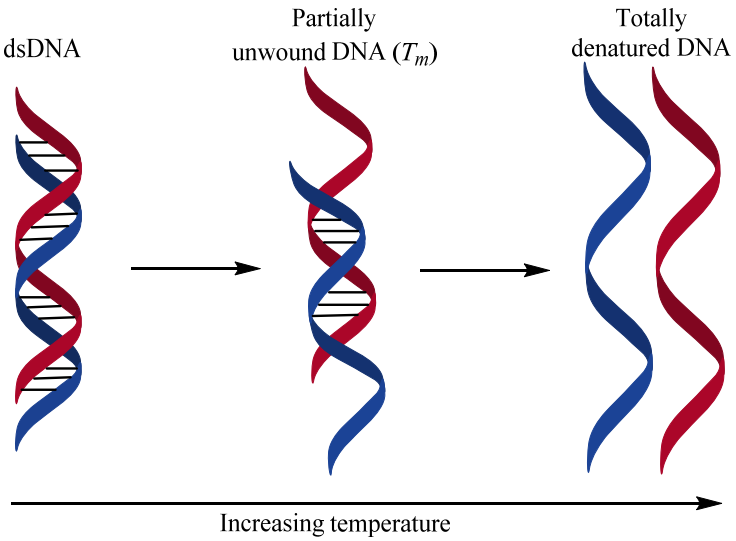


**Scheme 42:** The melting of double stranded DNA by increasing temperature.

The bases become unstacked in the process, as hydrogen bonds are broken allowing higher intensity of absorbance. When denaturation of DNA is effected by increase in temperature, this is also referred to as melting. The temperature at which the absorbance is 50% of the maximum is referred to as the transition-melting temperature ($T_m$).[160] At this temperature, 50% of the DNA is denatured. Modification of the DNA structure by binding to molecules causes a change in the $T_m$ value. For instance, agents that bind to and stabilise the DNA double helix (*e.g.* doxorubicin) increase the $T_m$, whilst agents that destabilise DNA (*e.g.* benzoacronycine derivatives) reduces the $T_m$.[161] The extent of increase / decrease of $T_m$ is correlated to the strength of interaction between the agent and DNA.

Melting temperature measurements using calf-thymus DNA were undertaken to investigate the effect of the proposed CBI drug **136** on dsDNA. Calf-thymus DNA was treated with a

range of concentrations of **136** and allowed to incubate for 1 h. The amount of drug needed per molar equivalent to dsDNA ($9.06 \times 10^{-5}$ M) was calculated using the equation below:

*Volume of sample = Molar concentration of diluted DNA × Volume of diluted DNA × MW of drug sample × Molar equivalent required (0.01 → 0.6)*

The mixtures were slowly heated up to 95°C to denature the DNA with continuous monitoring of UV absorption at 256 nm. An initial investigation to determine the appropriate time of incubation of the drug with DNA involved incubating **136** at 0.1 molar equivalents (MEq) for 1 h and 24 h with calf-thymus DNA. The results obtained showed that there was no significant difference between the data at the two incubation times and that binding to DNA and subsequent alkylation by **136** was a relatively fast process. This highlights the rapid nature of the Winstein cyclisation of **136** at near neutral pH to form the highly reactive cyclopropane ring leading to subsequent alkylation. Based on this result, subsequent tests were carried out with a 1 h incubation time. Figure 46 shows a graph for the normalised absorbance against temperature for the different concentrations of **136**.

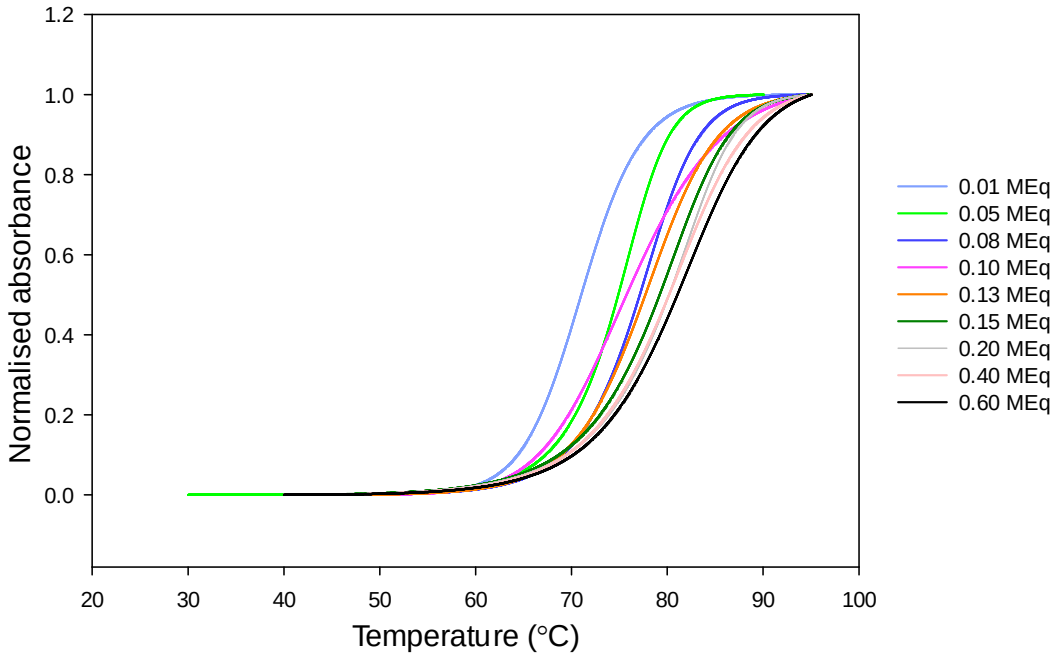


**Figure 46:** Normalised melting curve for **136** at different molar equivalents (MEq).

The normalised absorbance is calculated by subtracting the control absorbance (Buffer + DMSO + dsDNA) from the test absorbance (buffer + DMSO + dsDNA + **136**). Plotting this against temperature gives a sigmoid curve. The rightward shift of the sigmoid curve on increasing the concentration of **136** shows an increasing $T_m$. This confirms that **136** binds to

double-stranded DNA and that the effect of this binding is to stabilise the dsDNA. Destabilising agents should cause a reduction in $T_m$ upon increasing the concentration. As the temperature is increased, the absorbance initially rises very slowly. At this point, the majority of the DNA is in the duplex form, tightly held together by hydrogen bonds. At a characteristic temperature, there is a sudden rise in absorbance. This reflects the melting of dsDNA into single strands. As all the dsDNA are melted, the absorbance becomes constant causing the curve to plateau. At this point, the bases constituting DNA are fully unstacked and at maximum resonance and thus have maximum UV absorbance. The mid-point of the sigmoid curve is the $T_m$ but this is best visualised by plotting the first derivative curves of the normalised absorbance curves (Figure 47).

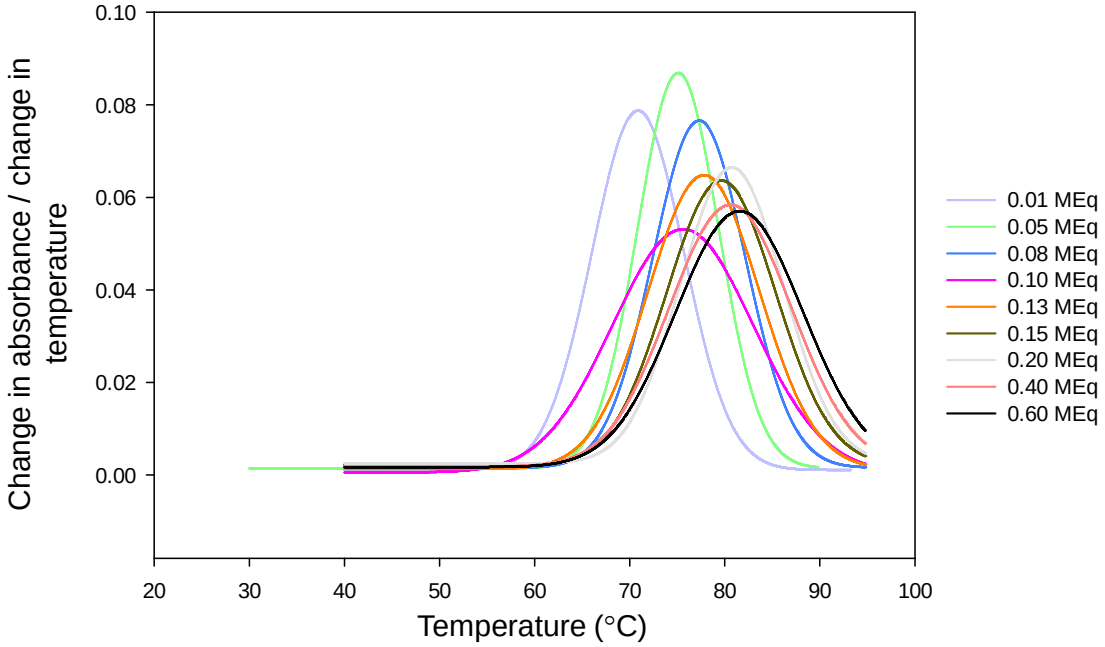


**Figure 47:** First derivative melting curve for **136** at varying molar equivalents (MEq).

The first derivative of the melting curves (Figure 47) is obtained by plotting the change in absorbance / change in temperature against temperature. This gives a bell-shaped curve, the peak (midpoint) of it being the $T_m$ for the particular concentration of drug. There is a general increase (rightward shift) of the peak of the curves which corresponds to an increase in $T_m$ with concentration. The measured melting temperature of calf-thymus DNA in absence of **136** (control) was 68.4°C. The effect of increased concentration of **136** on the change in melting temperature is shown in Figure 48.

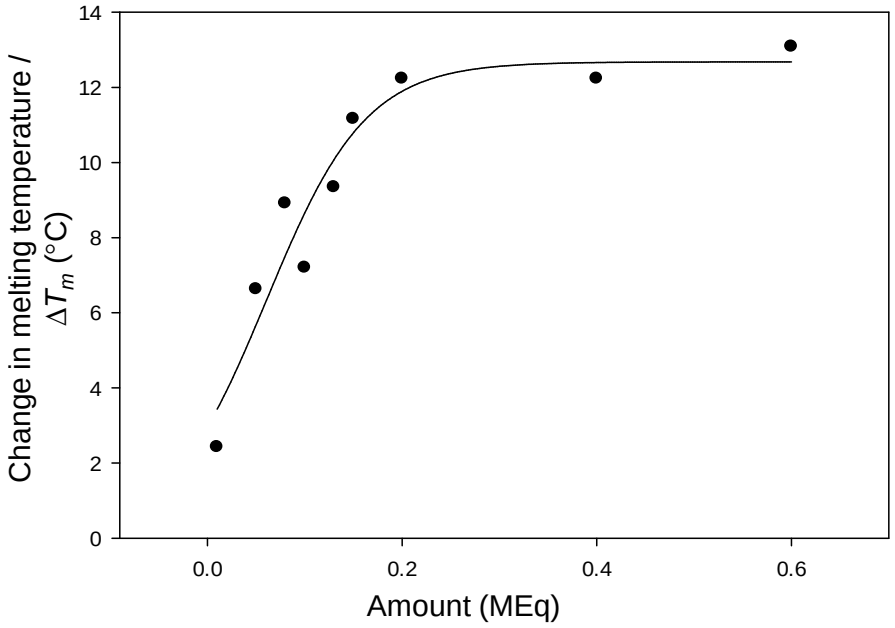


**Figure 48:** $T_m$ shift against molar equivalent (MEq) of proposed CBI drug **136**.

As the concentration of **136** increases per given concentration of DNA ($9.06 \times 10^{-5}$ M), there is a rise in melting temperature until saturation of the DNA binding sites occurs. The results above from the DNA-binding assay show that the proposed CBI drug is capable of binding to DNA. The effect of the drug is brought about by its ability to stabilise the double-stranded DNA. This should interfere with cellular processes such as transcription and translation of DNA, leading to cell death. $\Delta T_m$ can be used to assess how strongly an agent binds to DNA. For instance CC-1065 has been predicted to have a maximum $\Delta T_m$ value of > 31.5 deg. C at a DNA : drug ratio of 6.9 (0.14 MEq).[43] This high $\Delta T_m$ suggests that CC-1065 binds very strongly to DNA. This is in agreement with the observation that CC-1065 binds irreversibly with DNA under aqueous physiological conditions.[73] This irreversible DNA binding has been linked to the high cytotoxicity caused by CC-1065 and also its ability to cause delayed death. The maximum near-saturation $\Delta T_m$ observed for the proposed CBI drug **136** is approximately 13.0 deg. C at a DNA : drug ratio of 1.6 (0.6 MEq) which is similar to the clinically used cytotoxic agent, doxorubicin ($\Delta T_m$ = 18 deg. C).[43] The unnatural enantiomers of the anti-tumour antibiotics have been shown to possess a lower DNA alkylation efficiency compared to the natural enantiomers. For instance (−)-duocarmycin SA alkylates DNA at a concentration ten times lower than that required by (+)-duocarmycin SA.[61] The significant evlevation of the $T_m$ of calf-thymus DNA by **136** despite being the racemate suggests that this compound is highly efficient at DNA alkylation.

## 3.8 Cell viability assay

In order to test the cytotoxicity of the synthesised drug **136**, an MTS assay was carried out. This is a chromogenic assay to test cell viability. Mitochondrial reductase enzymes in viable cells are able to convert the MTS tetrazolium reagent into the coloured aqueous soluble formazan product (Scheme 43).[162]

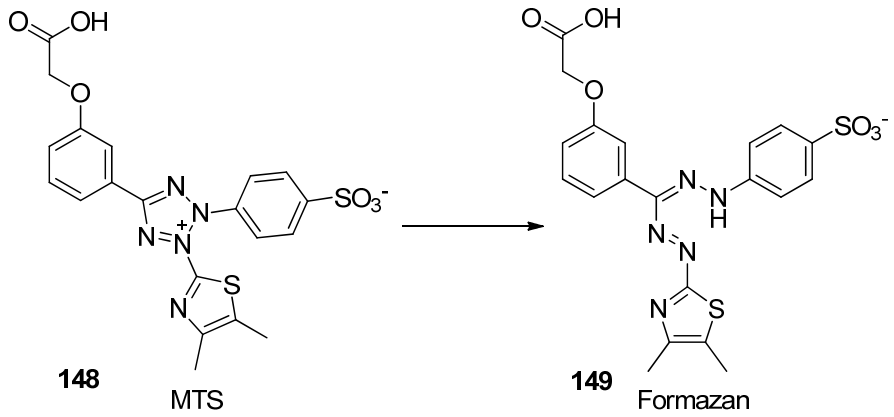


**Scheme 43:** Structures of MTS tetrazolium and its formazan product.

The amount of formazan produced (colour intensity) is proportional to the number of viable cells and can be measured at 490 nm.[162, 163] This assay requires fewer steps compared to its precursor, the MTT (3-(4,5-dimethylthiazol-2-yl)-2,5-diphenyltetrazolium bromide) assay. The MTT assay produces a crystalline fomazan dye which needs an extra step to dissolve before recording of the absorbance at 590 nm.[164] Cytotoxic agents cause reduction in the number of viable cells and therefore a diminution in formazan levels. This effect should be proportional to the concentration of the cytotoxic agent.

The inhibitory effect of **136** on prostate cancer cell lines was investigated using LNCaP cells. LNCaP cells are a PSA-producing human prostate cancer cell line which is also androgen sensitive.[165] A range of concentrations of **136** (1 nM → 1 µM) was added to LNCaP cells in a 96-well plate. Incubation at 37°C in a humidified atmosphere containing 5% $CO_2$ (v/v) was carried out for 3 d. The number of viable cells was quantified using the MTS reagent and measuring the absorbance of the produced formazan at 490 nm. In reference to the control cell number, the results were expressed as percentage inhibition against the concentration of **136** (Figure 49).

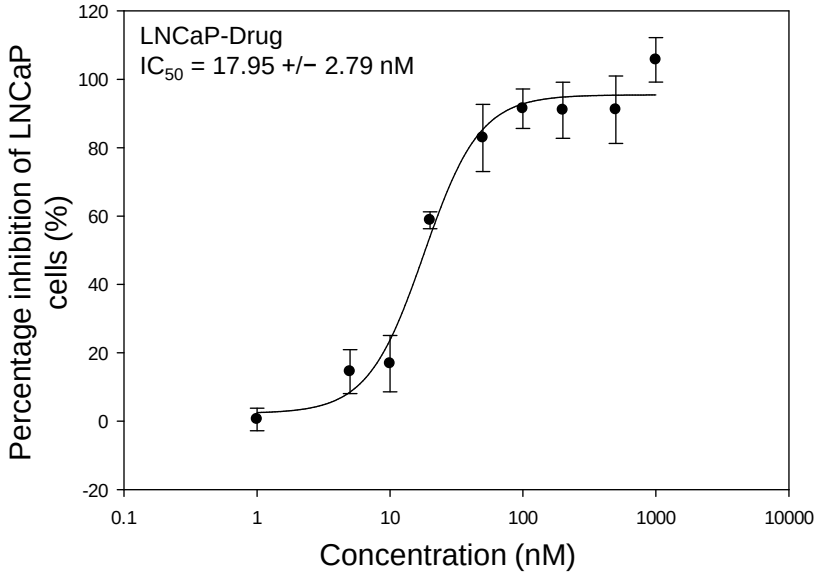


**Figure 49:** Inhibitory effect of **136** on LNCaP cells ±SD.

The inhibitory effect of the racemate of **136** on LNCaP cells was observed even at a very low concentration (1 nM). Approximately 60% inhibition occurred at 20 nM of drug concentration. The preliminary $IC_{50}$ for this compound as a racemate was 18.0 nM highlighting the extreme potency of **136**. This correlates well with the ability of **136** to alkylate DNA and inhibit cellular processes. The natural *S*-enantiomer of **136** is expected to have an even higher cytotoxicity. *In vitro* studies have shown that the natural *S*-enantiomer of the analogues of the anti-tumour antibiotics have superior potency compared to the *R*-enantiomers.[166] Furthermore, *in vivo* studies of hypoxia-selective nitro analogues of the anti-tumour antibiotics indicated that the *R*-enantiomer was inactive whilst the *S*-enantiomer showed significant cytotoxicity greater than the racemate as expected.[166] The reduced cytotoxicity of the *R*-enantiomer has been linked to the different steric interactions with double-stranded DNA.[167] Future enantiomeric purification of **136** to isolate the required stereoisomer should therefore give a molecule with extreme potency.

In order to estimate the cytotoxic effect of the proposed prodrug, the Boc-protected compound **135** was subjected to the MTS assay. LNCaP cells were treated with a range of concentrations of **135** (100 nM → 100 μM) and incubated under the same conditions as described above. The results were presented as percentage inhibition of LNCaP cell viability against the concentration of **135** (Figure 50).

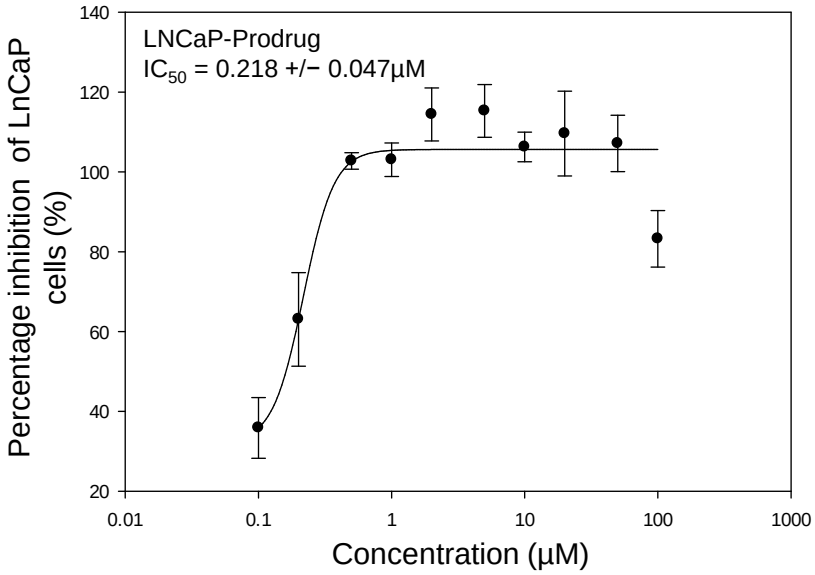


**Figure 50:** Inhibitory effect of **135** on LNCaP cells ±SD.

Overall, a given concentration of **135** resulted in lower percentage inhibition compared to **136** at the same concentration. For instance at a concentration of 100 nM, **136** resulted in 91% inhibition whilst **135** caused 36% inhibition. The preliminary $IC_{50}$ recorded for this compound was 218 nM which is approximately 10-fold lower than the $IC_{50}$ of **136**. This highlights the importance of the *seco* precursor **136** being able to undergo Winstein cyclisation to form the highly electrophilic cyclopropane ring (Figure 51).

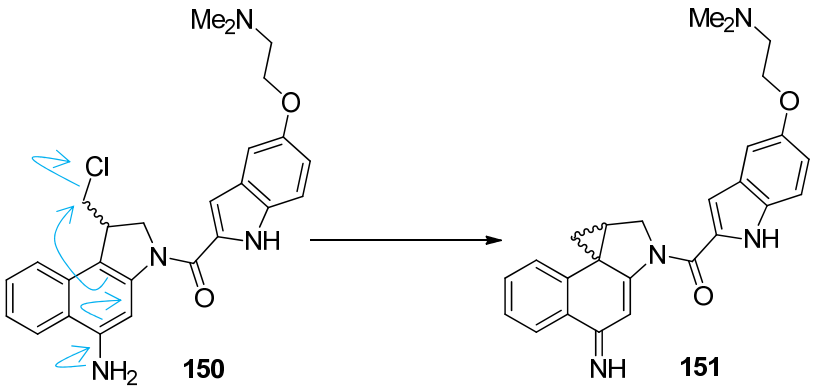


**Figure 51:** Winstein cyclisation by the *proposed seco*-CBI.

With the Boc-protection, the electron density of the 5-amino group is reduced and thus the Winstein cyclisation is slowed or prevented from happening, leading to reduced activity. It has been suggested that the ideal ratio of cytotoxicity between a prodrug and the corresponding drug ($QIC_{50}$) [$QIC_{50}$ = $IC_{50}$ (prodrug) / $IC_{50}$ (prodrug + activating enzyme)] should exceed 1000.[87] The lower observed ratio (~10) between **135** and **136** can be attributed to the fact that the measured cytotoxicities are only preliminary results and therefore further

tests would be required to verify the potency of these drugs. Besides, the higher than expected cytotoxicity of **135**, could be due to the Boc-protecting group being cleaved allowing spirocyclisation to form the more reactive cyclopropane ring. Slow cyclisation of the Boc-protected compound **135** may also be responsible. Alternatively, direct alkylation of the DNA by the Boc protected *seco* compound **135** without formation of the cyclopropane ring may account for the higher than expected cytotoxicity. The type of a prodrug is also very important. For instance, when a β-D-galactoside prodrug was subjected to *in vitro* cytotoxicity assay against human bronchial carcinoma cells of line A549, it was observed to have a lower cytotoxicity than the active drug by a factor of just 80 whilst a benzyl analogue of the same drug showed a lower cytotoxicity by a factor of 1600 compared to the active drug.[125] Compound **135** as a carbamate prodrug is not as stable as the proposed amide prodrug that would be synthesised by coupling of **136** to a PSA-cleavable peptide. Non-enzymatic cleavage of the carbamate group occurs easier than an amide bond. Having an amide prodrug as well as coupling of the drug to the bulky peptide and polymer will further reduce the cytotoxicity of the prodrug and give a higher $QIC_{50}$ value.

## 3.9 Peptide synthesis

With the synthesis of the active drug **136**, the next step involved the synthesis of the PSA-cleavable peptide intended to be used in the development of the prodrug. The amino-acid sequence Ser-Lys-Leu-Gln is claimed to be the minimal sequence required for recognition and cleavage by PSA.[99] The protected sequence Fmoc-Ser(Bn)-Ser(Bn)-Lys(Cbz)-Leu-Gln-OH containing the minimum required sequence was synthesised as a substrate for PSA. An attempt was made to use solution-phase peptide synthesis to make the peptide. Difficulties mainly due to the presence of the primary amide side-chain of Gln, often affect solution phase synthesis of Gln-containing peptides.[168] These include limited solubility of the Gln reagent and the produced peptide which leads to purification problems. Unwanted side-reactions, such as dehydration at the γ-carboxamide of Gln to produce the corresponding nitrile or cyclisation of carboxy-activated $N^{\alpha}$-protected Gln to $N^{\alpha}$-protected α-aminoglutarimides, can occur during the synthesis in peptides incorporating Gln (Scheme 44).

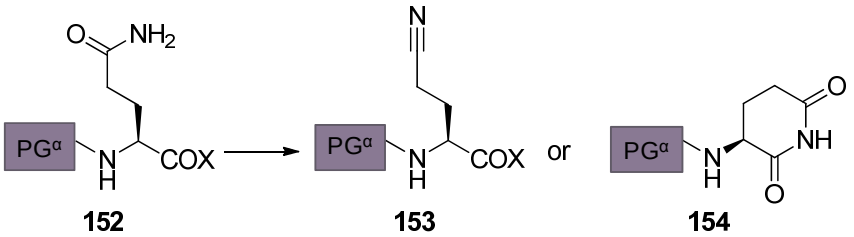


**Scheme 44:** Dehydration of Gln to form the nitriles **153** or the glutarimides **154**.

In order to avoid unwanted side-chain reactions of Gln and enhance solubility of Gln containing peptides, a range of sterically bulky protecting groups of the Gln side-chain have been used. These include 4-methoxybenzyl[169] 2,4-dimethoxybenzyl[169, 170] 2,4,6-trimethoxybenzyl[171] tetralin-1-yl,[172] monomethoxybenzhydryl,[173] trityl[174, 175] and monomethyltrityl.[176] 2-Nitrobenzyl has also been used as a photo-cleavable protection.[177] All of these protecting groups have the disadvantage of being atom-inefficient, with the bulky protecting groups containing many atoms and producing involatile side-products upon removal. In order to avoid the solubility issues and undesired reactions presented by Gln during solution-phase peptide synthesis, efforts were made to mask the primary amide side-chain of Gln as the nitrile. Compatibility of the nitrile protection strategy with other protecting groups was also studied.[178] These studies will then inform on the use of nitrile-Gln in the solution-phase synthesis of the proposed PSA-cleavable peptide.

### 3.9.1 Formation of Fmoc-aminoglutarimide

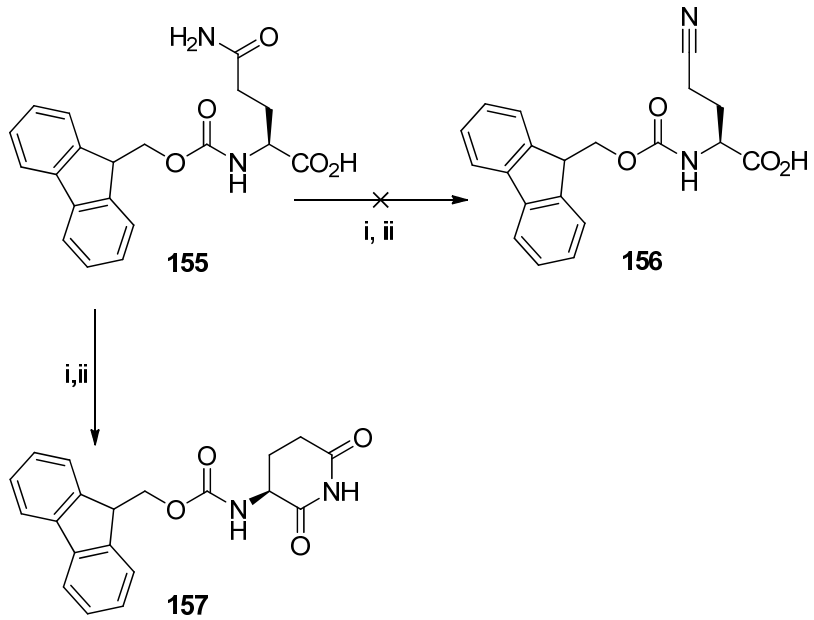


**Scheme 45:** Formation of Fmoc-aminoglutarimide. *Reagents and conditions:* i. DCC, dry pyridine, $N_2$, r.t., 3 h; ii. $(CF_3CO)_2O$, dry pyridine, THF, $N_2$, 0°C 6 h.

Dehydration of the Gln primary amide side-chain was attempted using Fmoc-Gln-OH **155** as a model substrate. Fmoc-Gln-OH **155** in pyridine was treated with the dehydrating agent, dicyclohexylcarbodiimide (DCC) at room temperature.[179] This led to the cyclised dehydrated product, the imide **157**, at 48% yield, rather than the desired product of dehydration of primary amide **156** (Scheme 45). Treatment of **155** with pyridine and trifluoroacetic anhydride[180] also resulted in **157** at 59% yield. Scheme 46 provides mechanisms for these cyclisation reactions.

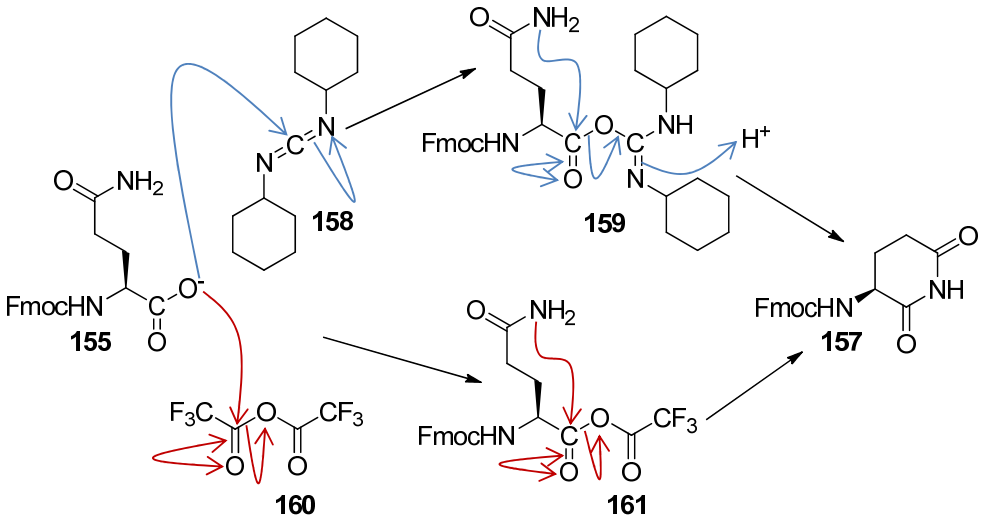


**Scheme 46:** Mechanism for formation of Fmoc-glutarimide with DCC and with trifluoroacetic anhydride.

Pyridine deprotonates the carboxylic acid group of **155** to form the carboxylate anion. This reacts with DCC to form the acyl isourea. Intra-molecular attack at the activated carbonyl of the acylisourea by the weakly nucleophilic nitrogen of the primary amide results in the cyclised imide, with dicyclohexylurea as the powerful leaving group.

### 3.9.2 The use of β-cyanomethyl-L-Ala as a masked form of L-glutamine

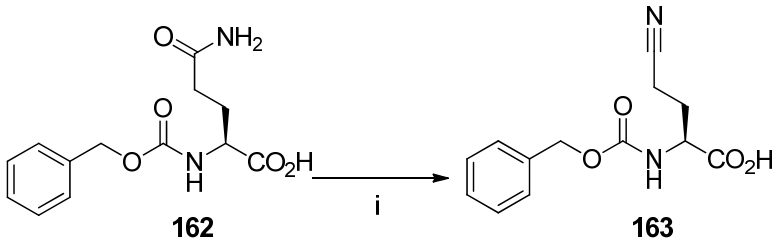


**Scheme 47:** Dehydration of the side-chain amide of Gln to give the nitrile. *Reagents and conditions:* i. DCC, dry pyridine, $N_2$, r.t., 16 h.

With the difficulties encountered with Fmoc-Gln-OH **155**, a different $N^{\alpha}$-protected Gln was used to test if the presence of the Fmoc-protecting group had any influence in the formation of the glutarimide **157**. Interestingly, treatment of Cbz-Gln-OH **162** with DCC in pyridine gave the nitrile **163** at 82% yield (Scheme 47). This result suggested that, the Fmoc protecting group favours the cyclisation reaction whilst the Cbz protecting group favours the formation of the nitrile. Scheme 48 shows a proposed mechanism in the synthesis of **163**.

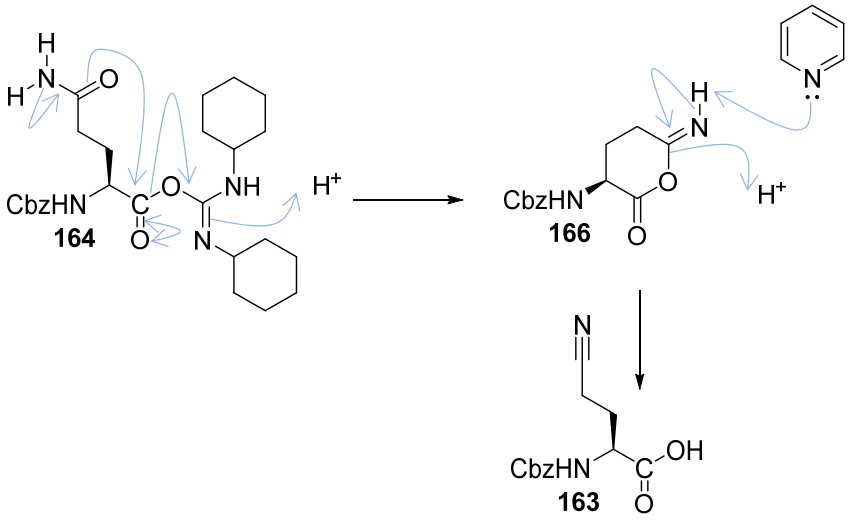


**Scheme 48:** Proposed mechanism for the dehydration of the γ-carboxamide side-chain of glutamine to form the nitrile.

After the formation of the isourea "mixed anhydride" **164**, removal of a proton from the side-chain amide leads to the formation of the imidate. Cyclisation to form the pyranone ring **166**, followed by base-catalysed elimination then gives the nitrile **163**.

Beauchard *et al*.[178] invstigated the ability to incorporate Gln(CN) into peptide chains and also its compatibility with other protecting groups (Scheme 49) [experiments conducted by Anne Beauchard].

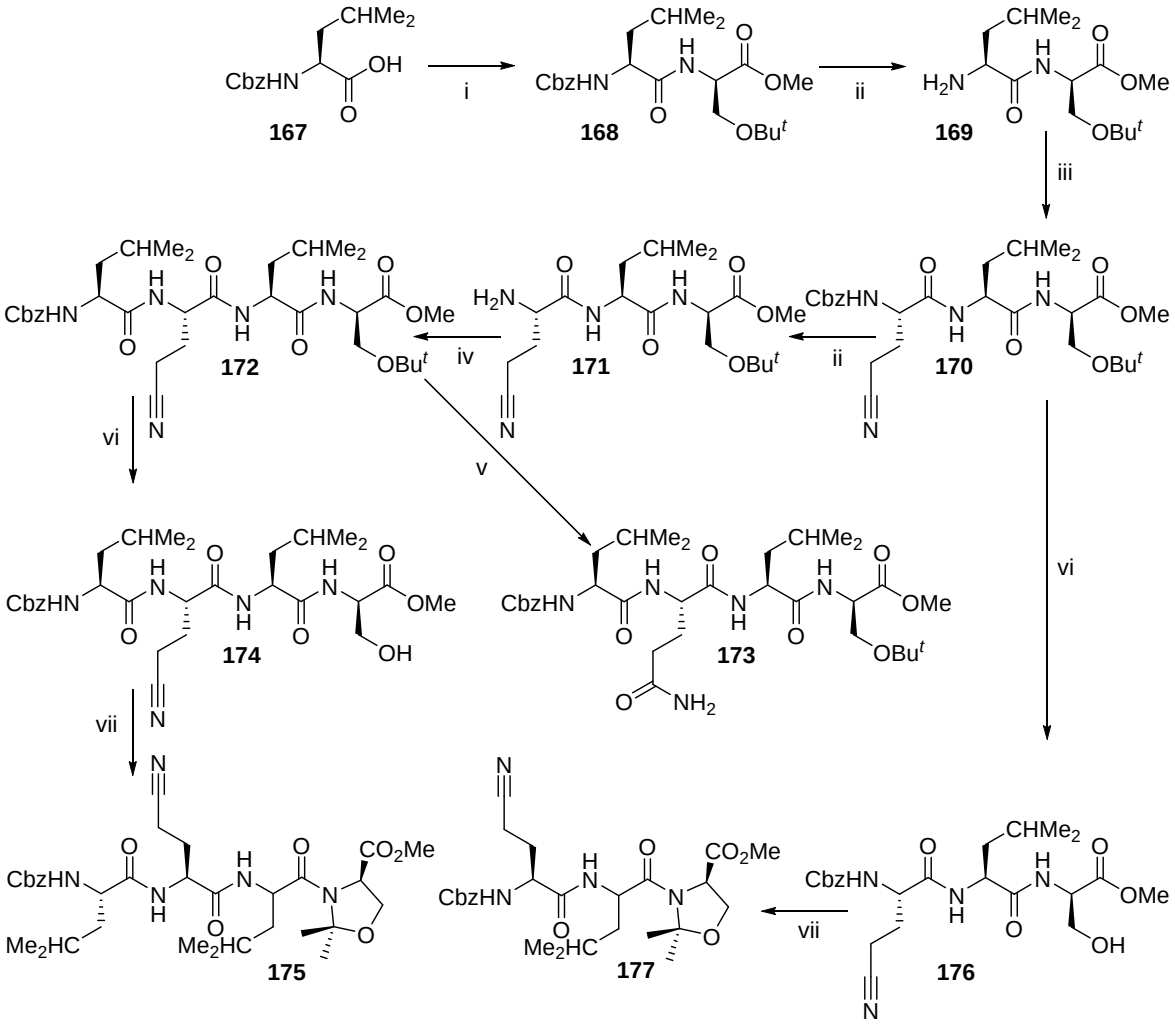

**Scheme 49:** Incorporation Gln(CN) into a growing peptide chain and its compatibility with other protecting groups. *Reagents and conditions:* i. D-Ser(OBu$^t$)-OMe, PyBOP, $Et_3N$, $CH_2Cl_2$, r.t 24 h (ii) $H_2$, Pd/C, MeOH, r.t. 16 h; iii. **163**, HATU, $Pr^i_2NEt$, $CH_2Cl_2$, r.t. 20 h; iv. **167**, PyBOP, $Et_3N$, $CH_2Cl_2$, r.t. 2 d; v. aq. $H_2O_2$, NaOH, r.t. 1 h; vi. $CF_3CO_2H$, $CH_2Cl_2$, r.t. 1h, vii. $Me_2C(OMe)_2$, TsOH, $CH_2Cl_2$, $N_2$, reflux, 19 h.

To test the ability to couple Gln(CN) to a growing peptide chain, the dipeptide L-Leu-D-Ser(OBu$^t$)-OMe **169** was synthesised. Cbz-L-Leu-OH **167** was coupled with D-Ser(OB$^t$)OMe using benzotriazol-1-yl-oxytripyrrolidinophosphonium hexafluorophosphate (PyBOP) as the coupling agent. Initial nucleophilic attack of the positively charged phosphorus atom of PyBOP by the carboxylate anion of **167** forms the phosphonium ester, eliminating benzotriazolate anion in the process. This anion subsequently substitutes the phosphonium ester to give the more reactive benzotriazole ester, which then reacts with D-Ser(OBu$^t$)-OMe to give **168** in an excellent yield of 95%. Hydrogenolysis of **168** removed the Cbz group to give the dipeptide **169** L-Leu-D-Ser(OBu$^t$)-OMe. This was then coupled with N-Cbz-β-cyanomethyl-L-Ala **163** using O-(7-azabenzotriazol-1-yl)-N,N,N′,N′-tetramethyluronium hexafluorophosphate (HATU) to test compatibility of this coupling method with the nitrile

group. This afforded the protected tripeptide **170** at a yield of 77% demonstrating that Gln(CN) can be added easily to growing peptide chain. Removal of the Cbz protecting group was effected with hydrogen and palladium-on-carbon catalyst to give **171** without any sign of competing reduction of the nitrile group. Coupling of **171** with Cbz-L-Leu-OH **167** led to the protected peptide **172** showing that peptide coupling at the N-terminus of Gln(CN) are efficient. Regeneration of Gln was achieved *via* mild hydration with hydroperoxide under basic conditions to give **173** without hydrolysis to the acid (Glu) or hydrolysis of the methyl ester. To test the stability / compatibility of the nitrile in acidic conditions, removal of the *tert*-butyl protection of **172** was undertaken using trifluoroacetic acid to give **174**. Condensation of **174** with 2,2-dimethoxypropane under acid catalysis gave **175** which contains both the C-terminal D-Dmo residue (which can be considered as a masked D-Ser, a *pseudo*proline) and the β-cyanomethyl-L-Ala (masked Gln). The *tert*-butyl group of Cbz-Gln(CN)-Leu-D-Ser(OBu$^t$)-OMe **170** was also removed under acidic conditions, followed by condensation with 2,2-dimethoxypropane to give **177**. Scheme 50 gives a further demonstration of the compatibility of Gln(CN) in solution-phase peptide synthesis.

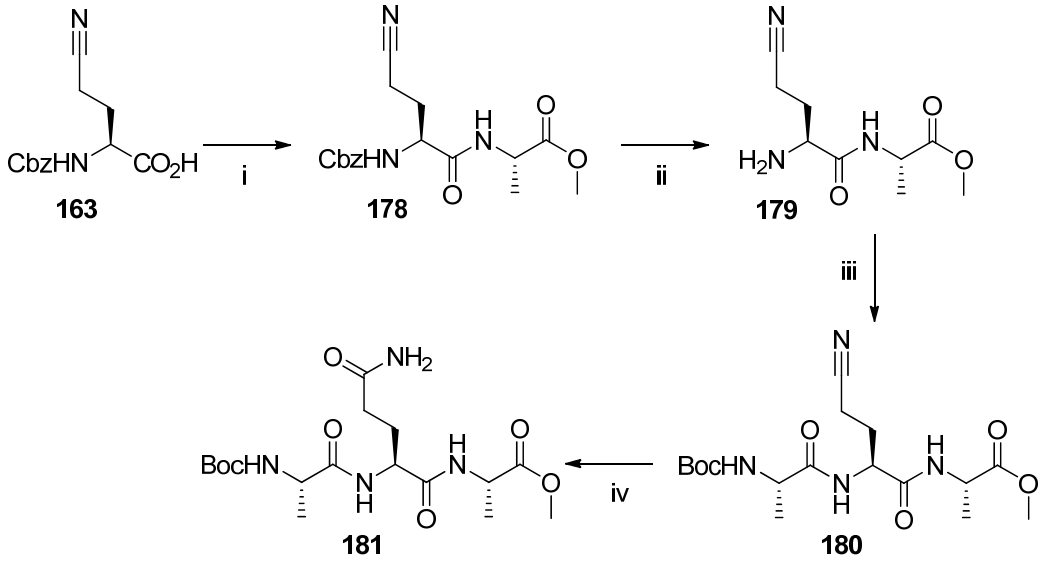


**Scheme 50:** Compatibility of Gln(CN) with Cbz and Boc protecting groups. *Reagents and conditions:* i. L-Ala-OMe.HCl, Pr$^i_2$NEt, PyBOP, r.t., 3 d; ii. 10% Pd-C, $H_2$, MeOH, r.t., 2 h iii. Boc-L-Ala-OH, Pr$^i_2$NEt, HATU, DMF, r.t., 2 h; iv. aq. 35% $H_2O_2$, aq. 1 M NaOH, MeOH, 0°C, 6 h.

The protected dipeptide Cbz-Gln(CN)-Ala-OMe **178** was prepared by coupling L-Ala-OMe with Cbz-Gln(CN)-OH **163** using PyBOP. Hydrogenolysis of the N-terminal Cbz-protecting group of **178** afforded **179** (Scheme 50). Careful monitoring of the hydrogenolysis was needed since prolonged reaction time resulted in reduction of the nitrile group to form **182** followed by a possible cyclisation to form **183** (Figure 52). Reducing the reaction time from 16 h to 2 h allowed the synthesis of **179** without reduction of the nitrile. When this compound

was left at room temperature overnight, NMR spectra suggested that some of the compound had cyclised to give the diketopiperazine **184** (Figure 52).

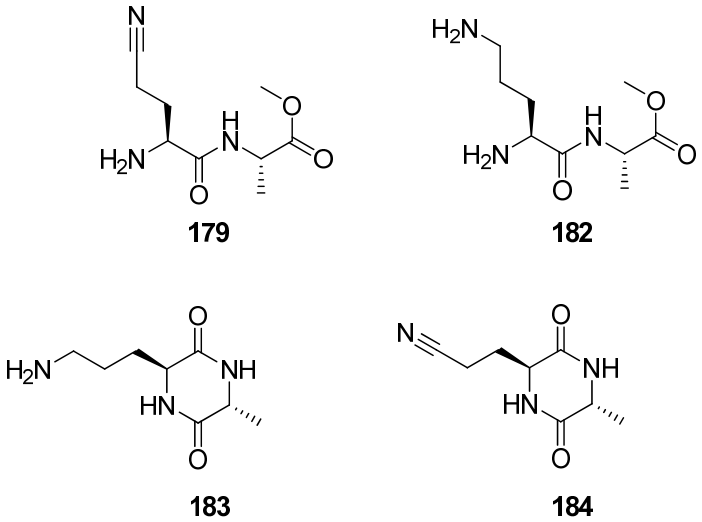


**Figure 52:** Possible products from prolonged hydrogenolysis of Cbz-Gln(CN)-Ala-OMe.

Synthesis of Boc-Ala-Gln(CN)-Ala-OMe **180** was achieved by immediate coupling of **179** to Boc-L-Ala-OH using HATU as the coupling agent (Scheme 50). Hydration of the nitrile group of **180** with the hydro-peroxide anion had to be carried out carefully to avoid side reactions. Carrying out the reaction at room temperature using hydrogen peroxide / sodium hydroxide resulted in hydrolysis of the methyl ester group as well as hydration of the nitrile. The reaction was repeated with the hindered base potassium *tert*-butoxide and urea hydrogen peroxide in methanol. At room temperature, no progression of the reaction occurred highlighting the reduced reactivity of the reagents. Heating the reaction at 40°C resulted in hydration of the nitrile but also hydrolysis of the methyl ester. The use of diisopropylethylamine as a base with aqueous hydrogen peroxide or urea hydrogen peroxide resulted in a mixture of products. The reaction had to be carried out at 0°C with sequential addition of aqueous hydrogen peroxide and sodium hydroxide and the mixture carefully neutralised at this temperature before bringing to room temperature to avoid hydrolysis of the ester. Neutralisation with aqueous hydrogen chloride proved problematic due to the risk of losing the Boc-protecting group. Sodium thiosulfate was therefore used to quench the reaction. Careful hydration of the nitrile **180** without disruption of the N-Boc protection and the methyl ester was achieved using 35% w/w aqueous hydrogen peroxide and 1 M aqueous sodium hydroxide in methanol to afford **181** at a modest yield of 23%. This low yield was mainly due to slow progression of the reaction since the majority of the starting material was recovered. Longer reaction time or the use of excess reagents should improve the yield.

### 3.9.3 Hydration of terminal Gln nitrile group

After proving the concept of masking the side-chain amide of Gln as a nitrile, within the peptide chain, the possibility of regenerating the amide side-chain was investigated when Gln(CN) is the C-terminal amino-acid. This is important because, in the proposed PSA-cleavable pentapeptide to be synthesised, Gln is the C-terminal amino-acid. Attempted hydration of Cbz-Gln(CN)-OH **163** using aqueous hydrogen peroxide and sodium hydroxide resulted in hydrolysis of the nitrile group completely to the carboxylate (Scheme 51).

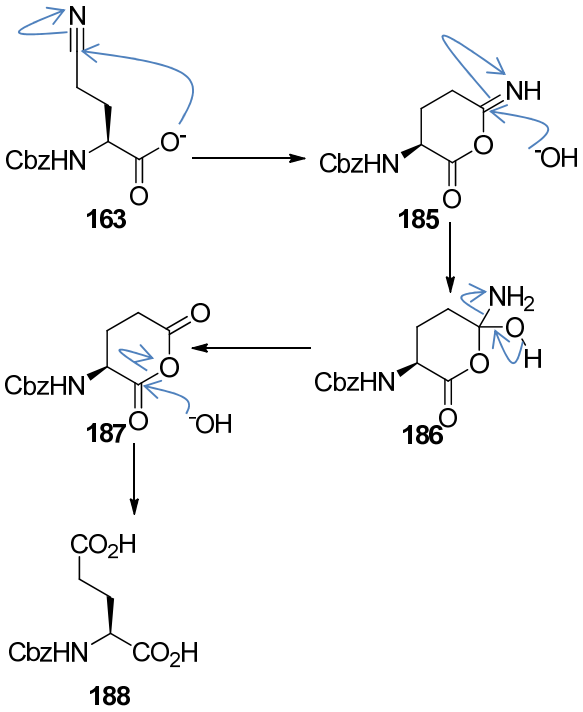


**Scheme 51:** Proposed mechanism for hydrolysis of **163** to **188**. *Reagent and conditions*: aq. $H_2O_2$, NaOH, r.t., 30 min.

The proposed mechanism (Scheme 51) suggests an intra-molecular nucleophilic attack by the α-carboxylate of **163** to form imino-oxotetrahydropyran **185**. This seems to out-compete the inter-molecular attack of the nitrile group by hydroperoxide ion. Nucleophilic attack by hydroxide ion on the imidate **185** results in a tetrahedral intermediate **186** from which ammonia leaves to yield the cyclic anhydride **187**. Further nucleophilic attack by hydroxide ion yields Cbz-Glu-OH **188**. This result suggested that the strategy of hydrating Gln(CN) at the C-terminus of the proposed PSA-cleavable peptide, Ser-Ser-Lys-Leu-Gln, will not be useful. A decision was therefore made to use solid-phase peptide synthesis to circumvent the difficulties presented by Gln when used in solution phase peptide synthesis.

### 3.9.4 Solid-phase peptide synthesis

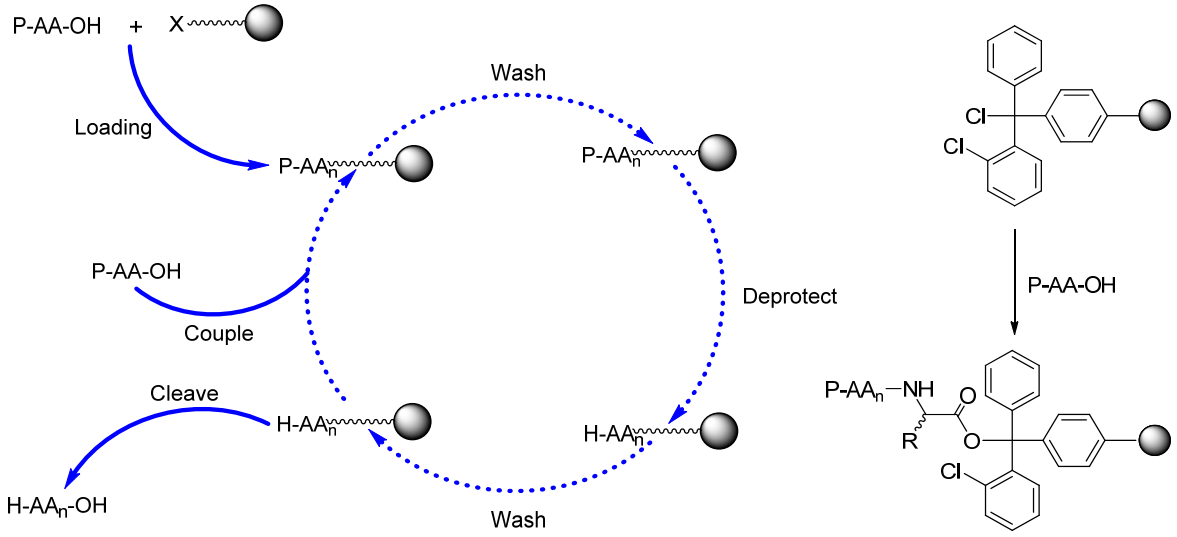


**Scheme 52:** Solid phase peptide synthesis cycle and coupling of amino-acids to 2-chlorotrityl chloride resin.

Solid-phase peptide synthesis allows sequential coupling of α-protected-amino and side-chain-protected amino-acids onto an insoluble polymeric support (Scheme 52). Removal of the protection from the α-amine allows subsequent amino-acids to be added using a coupling agent or pre-activated amino-acid derivative. The synthesised peptide is attached to the polymer *via* a linker through the C-terminus of the peptide. Cleavage of the peptide from the resin and followed by removal of the protecting groups gives the desired peptide. One advantage of solid-phase synthesis over solution phase peptide synthesis is that it allows excess reagents to be washed out of the reaction at each coupling stage, obviating the need for purification at each step of the synthesis. Besides, the use of dimethylformamide means that masking the side-chain primary amide group of Gln is not necessary as Gln is soluble in dimethylformamide. Peptides was synthesised using standard Fmoc solid-phase peptide synthesis [benzotriazol-1-yloxy-trispyrrolidino-phosphonium hexafluorophosphate (PyBOP) / N,N-diisopropylethylamine ($Pr^i_2NEt$) couplings]. 2-Chlorotrityl chloride polystyrene resin was used to enable mild acidolytic cleavage of the peptide from the 2-chlorotrityl linker without removal of the N-terminal Fmoc protecting group or the side-chain protecting groups. This resin also avoids epimerisation making it ideal for synthesis of sensitive residues. The bulk of the trityl linker also helps to prevent formation of diketopiperazines from dipeptide intermediates.[181] Furthermore, other side-reactions such as reattachment of residues during acidic cleavage and side-chain deprotection, are minimised.[182]

### 3.9.4.1 Synthesis of Fmoc-Ser(Bn)-Ser(Bn)-Lys(Cbz)-Leu-Gln-OH (189)

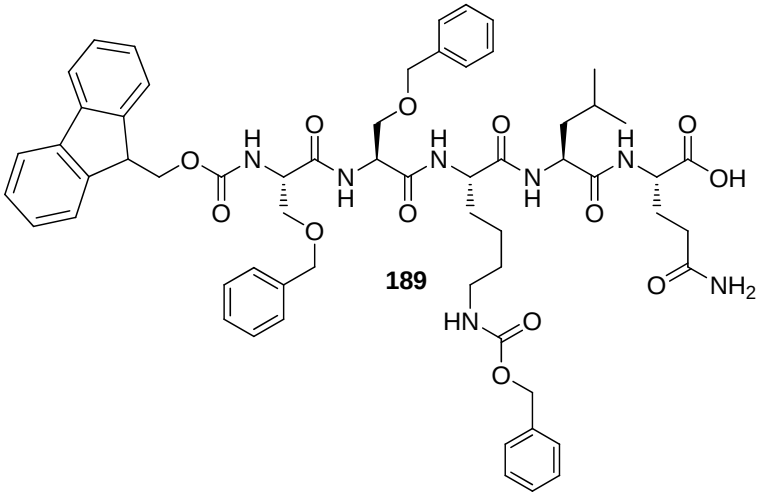


**Figure 53:** Structure of Fmoc-Ser(Bn)-Ser(Bn)-Lys(Cbz)-Leu-Gln-OH.

The synthesis of **189** began by loading Fmoc-Gln-OH onto 2-chlorotrityl chloride polystyrene under anhydrous conditions, using excess $Pr^{i}_{2}NEt$, a non-nucleophilic tertiary amine base to generate the more nucleophilic carboxylate. The nucleophilic carboxylate group attacks the aliphatic carbon of 2-chlorotrityl chloride to substitute the chlorine atom with an ester group. The remaining trityl chloride units of the resin were capped by treatment with methoxide to substitute the chlorine with a methoxy group. This prevents reaction of subsequent amino-acids directly with the resin. The loading attained was 73%. In each cycle, the Fmoc-protection was removed by treatment of the resin with piperidine (20% v/v in DMF) and the remaining amino-acids (Fmoc-Leu-OH, Fmoc-Lys(Cbz), Fmoc-Ser(OBn) (× 2), respectively were added stepwise using PyBOP as the coupling reagent to activate the carboxy component of the $N^{\alpha}$-protected amino-acid. The side-chain protections of Fmoc-Ser(OBn) and Fmoc-Lys(Cbz) was chosen to ensure orthogonality with the cleavage of the N-terminal Fmoc-protecting group and also the C-terminal chlorotrityl group. The benzyl and carboxybenzyl protections can be removed under the same conditions which will reduce the number of different deprotection reactions required. These cycles yielded the resin-bound Fmoc-protected pentapeptide, which was cleaved from the resin with 1% v/v trifluoroacetic acid in dichloromethane to give the required protected pentapeptide **189** in 93% yield. Trifluoroacetic acid serves as a source of protons to protonate the carbonyl group at the C-terminal of the resin-bound peptide. This results in the cleavage of the trityl O-bond and release of the peptide. The process also results in generation of the highly stabilised chloro trityl carbocation, which can be trapped with scavengers (*e.g.* triisopropylsilane). The use of scavengers is only important when highly nucleophilic groups are present in the peptide

residue (*e.g.* Trp, Met, Tyr, Cys). If these nucleophilic groups are absent / protected, then the use of scavengers becomes unnecessary.[181]

### 3.10 Synthesis of 1-benzyloxyisoquinolin-5-amine (193) as a model drug

To test the proposed polymeric prodrug system for release of an aromatic amine such as the *seco*-CBI **136**, a model drug was synthesised. This will enable the assessment of the ease of coupling aromatic amine directly to the peptide **189** and also whether PSA can selectively cleave the peptide-drug conjugate at the planned site. The model drug **193** was chosen due to its structural similarities to the proposed CBI drug. Besides, the model drug is non-toxic unlike α-naphthylamine which is the obvious choice as a model drug but is implicated in bladder cancer.[183] Furthermore, once coupled to the pentapeptide **189**, the benzyl group of the model drug together with Bn and Cbz group of the pentapeptide **189** would be cleaved in one step affording the delivery of 5-aminoisoquinolin-1-one, a well-known PARP-1 inhibitor.[184-187]

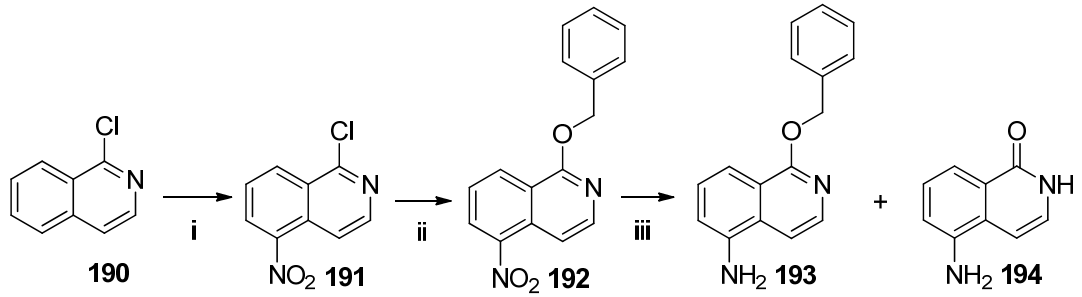


**Scheme 53:** Synthesis of 5-AIQ-model drug. *Reagents and conditions:* i. $H_2SO_4$ / $HNO_3$, 0°C for 2 h then r.t. for 10 min; ii. benzyl alcohol, NaH, dry DMF, r.t. for 15 min then 100°C for 2 h; iii. MeOH, Pd/C, $NaBH_4$ r.t. for 30 min then HCl.

The model drug **193** was made by firstly nitrating 1-chloroisoquinoline **190** to give **191** at a yield of 66%. It was important to protonate and deactivate fully **190** before addition of the nitrating reagents to ensure selective nitration at the C5 position.[184] The next step was a $S_NAr$ nucleophilic substitution (addition / elimination reaction) of the 1-chlorine with a benzyloxy group. This was effected by reaction of **191** with sodium benzyloxide under anhydrous conditions to give **192**. Selective reduction of the nitro group without loss of the OBn was tried with different reagents, including tin(II) chloride, palladium on carbon / sodium borohydride and palladium on carbon / ammonium formate. The reaction was tried at 0°C, room temperature and under reflux to determine the optimum conditions. All the conditions, however, resulted in reductive removal of the benzyl group to give 5-aminoisoquinolin-1-one (5-AIQ) **194** as well as the desired product **193**. Palladium on carbon / sodium borohydride

were selected to reduce the nitro group of **192** due to the ability to control the number of hydrogen equivalents added in order to limit the reduction of the benzyl group. This allowed the synthesis of **193** at a yield of 33%.

## 3.11 Coupling of model drug to peptide

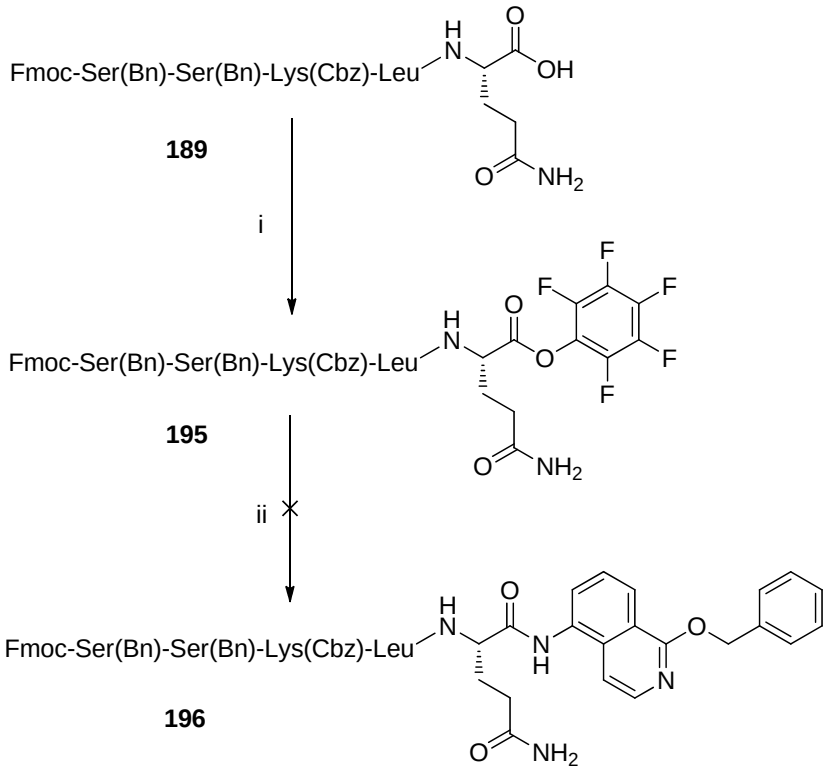


**Scheme 54:** Coupling of proposed PSA-cleavable peptide **189** to 5-AIQ derivative **193**. *Reagents and conditions*: DCC, pentafluorophenol, DMF, $N_2$, 0°C, 4 h; ii. **193**, $Et_3N$, DMAP, DMF, r.t., 16 h.

An attempt was made to couple the synthesised model drug **193** with the peptide **189**. The pentafluorophenyl active ester **195** was synthesised using pentafluorophenol with dicyclohexylcarbodiimide (DCC) as the coupling reagent. DCC served to activate the carboxylate group of **189** to nucleophilic attack by the *in situ* generated pentafluorophenoxide. Mass spectrometry confirmed that the pentafluorophenyl ester **195** was formed [*m/z*: 1264.5141 (M + H)]. Owing to purification difficulties as well as instability of the pentafluorophenyl ester, an attempt was made to couple the model drug **193** directly to the crude pentafluorophenyl ester to give **196**. This, however, failed and also caused loss of the Fmoc group in some cases. PyBOP-activated **189** was also investigated to couple the model drug but this failed too.

## 3.12 Synthesis of 4-methoxynaphthalen-1-amine (200) as a model drug

The challenges faced with coupling of **193** to the peptide led to the synthesis of a new model drug. 4-Aminonaphthalen-1-ol hydrochloride **31** was considered as a candidate to convert into a model drug. Silyl protection is known to be selective for hydroxy groups over amines due to the stability of the silicon-oxygen bond. Silyl protection of the phenolic group of **31** with chlorotrimethylsilane to give **197**, however, failed.

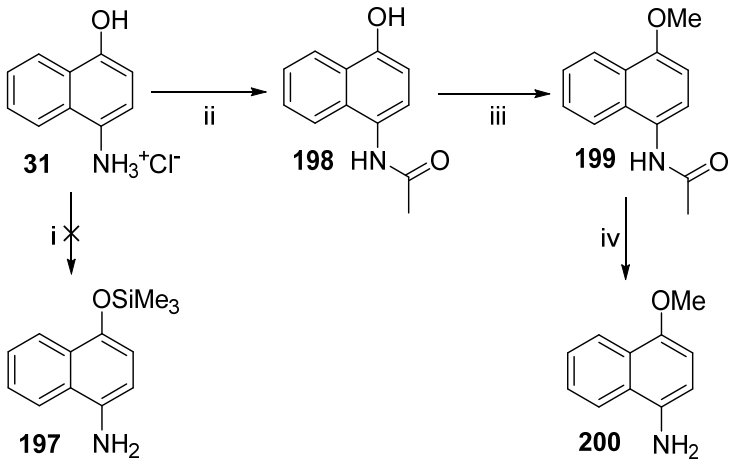


**Scheme 55:** Synthesis of naphthalene-based model drug. *Reagents and conditions:* i. (a) Chlorotrimethyl silane, imidazole, THF, Ar, r.t., 24 h; (b) Chlorotrimethyl silane, $Et_3N$, dry DMF, $N_2$, 72 h; ii. (a) Acetyl chloride, $Et_3N$, THF, $N_2$, r.t., 30 min; (b) $Ac_2O$, $Et_3N$, MeOH, 50°C, 1 h; iii. MeI, $K_2CO_3$, acetone, reflux, 16 h; iv. aq. HCl (3.0 M), MeOH, 90°C, 4 h.

The next idea was to acetylate the amino group of **31** followed by protection of the phenolic group and then deacetylation to yield the model drug **200**. Due to risk of O-acetylation in the presence of excess base, as observed with 2-nitro-4-aminonaphthalen-1-ol **40** (Scheme 14), only one equivalent of triethylamine was used to free the amino group of **31**. Even if non-selective acetylation should occur, the O-acetyl group, being an ester, should be easier to hydrolyse without cleavage of the N-acetyl group. Acetylation of the amino group of **31** with acetyl chloride gave a mixture of several products. Purification resulted in the isolation of **198** at a very low yield (~2%). It was thought that the acetyl chloride might have been too reactive resulting in formation of several products. Acetylation of **31** was therefore effected with acetic anhydride to give **198** at a yield of 93%.[188] Methylation of the phenolic group of **198** was carried out using methyl iodide with potassium carbonate as the base, giving rise to **199**. Acidic hydrolysis of the N-acetyl group **199** gave 4-methoxynaphthalen-1-amine **200** as the new model drug. The next step was to couple this model drug to the proposed PSA-cleavable peptide **189**.

## 3.13 Coupling of 4-methoxynaphthalen-1-amine to proposed PSA-cleavable peptide

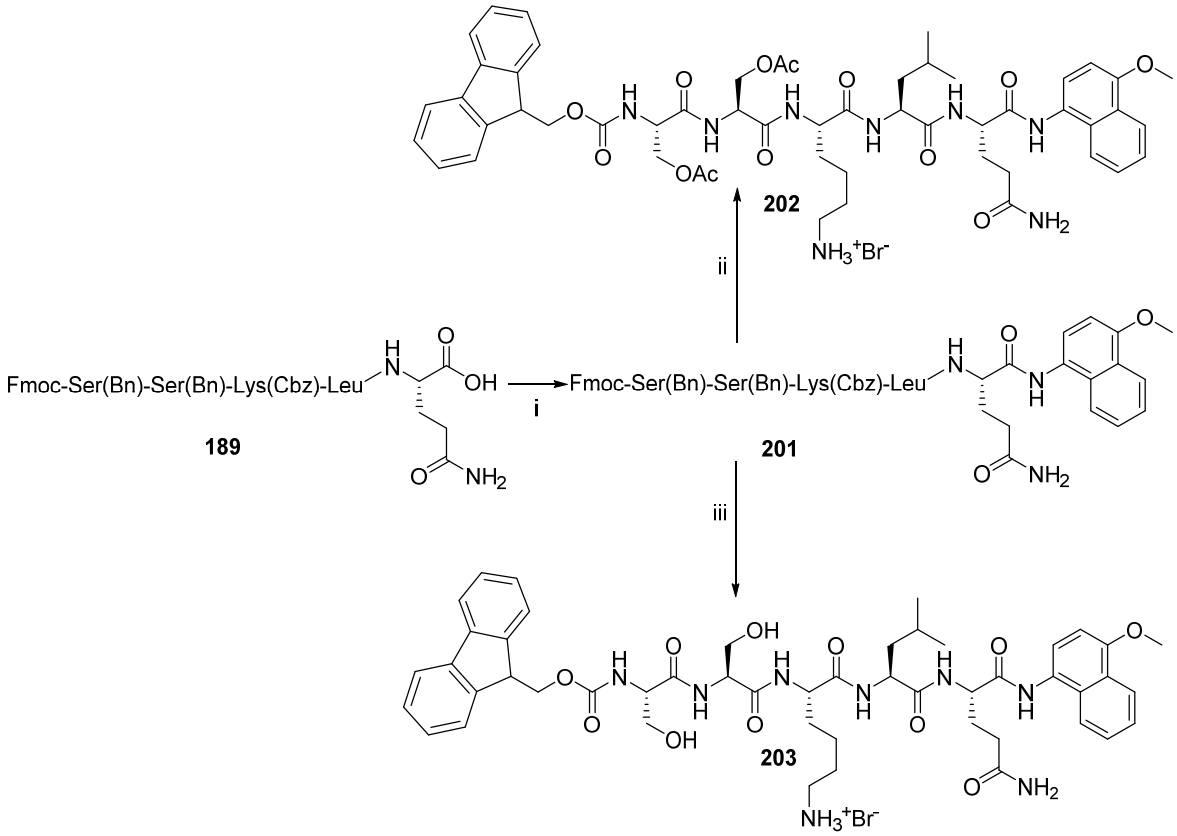


**Scheme 56:** Synthesis of Fmoc-peptide-model drug conjugate. *Reagents and conditions:* i. 4-Methoxynaphthalen-1-amine **200**, EDC.HCl, HOBt, DMF, $N_2$, 0°C → 20°C, 2 d; ii. HBr in AcOH (33%), 20°C, 2 h then $Et_2O$; iii. HBr in AcOH (33%), 20°C, 2 h then MeOH.

Coupling of 4-methoxynaphthalen-1-amine **200**, was initially attempted with pentafluorophenol and DCC or 1-ethyl-3-(3-dimethylaminopropyl)carbodiimide hydrochloride (EDC.HCl). This procedure, however, did not yield the desired results. Activation with EDC.HCl / hydroxybenzotriazole was then employed. The carboxyl group of **189** reacts with the EDC.HCl to form the O-acylurea which can react with 4-amethoxynaphthalen-1-amine to yield the product. The use of carbodiimide coupling agents in peptide synthesis tends to be associated with oxazolone formation leading to epimerisation. Hydroxybenzotriazole acts to reduce epimerisation by reacting with the O-acylurea to give the benzotriazole active ester which enhances reactivity by encouraging / stabilising the approaching amine *via* hydrogen bonding.[159] Nucleophilic substitution of the benzotriazolyl ester by **200** gave the crude peptide-model drug **201 (**Scheme 56**)**. As mentioned before, the unprotected primary amide side-chain of Gln results in solubility issues during solution-phase peptide synthesis. Purification of **201** therefore proved very challenging. The peptide-model

drug conjugate did not have appreciable solubility in either organic or aqueous solvents. Extraction and chromatography could therefore not be used to purify **201**. The insolubility of the peptide was, however, exploited in its purification by repeated trituration with $Et_2O$ and hot methanol affording **201** at a yield of 78%. Deprotection of acid-labile Cbz and benzyl protecting groups of **201** was effected with hydrogen bromide in acetic acid. Precipitation of the deprotected peptide (now a hydrobromide salt at the Lys side-chain) interestingly gave a product with a mass of eighty-four units higher than the expected mass. NMR investigation into this showed that both the serine β-hydroxy groups had been acetylated. Clearly, the hydrogen bromide was a strong enough acid to catalyse the esterification with solvent acetic acid under these conditions to give **202**. The deprotection of **201** was repeated using the same reagents, hydrogen bromide in acetic acid. After completion of the reaction, methanol was added to methanolyse the acetate esters to give **203**. Compound **203** was then subjected to enzyme assay to assess the ability of PSA to cleave the model drug.

## 3.14 Study on the PSA-catalysed cleavage of Fmoc-Ser-Ser-Lys-Leu-Gln-4-methoxynaphthalenamide

The ability of PSA to cleave the peptide and release the model drug was investigated. Compound **203** (~2 mM) was incubated with PSA (10 mM) at 37°C. The reaction was carried out in 50 mM Tris-HCl and 140 mM NaCl buffer at pH 7.4. These conditions were chosen in an attempt to mimic physiological conditions. A control experiment was also set up without the enzyme to make sure that cleavage is due to the action of PSA. Samples were taken at different time intervals and added to a solution of $ZnCl_2$ (20 mM) to precipitate the enzyme. Centrifugation followed by HPLC analysis of the supernatant, however, did not detect any product or starting material. The absence of product or starting material in the supernatant led to the conclusion that the starting materials / product do not have sufficient aqueous solubility. This was supported by the observation that precipitates formed in the reaction mixture about 2 h into the experiment. The collected precipitates after centrifugation were suspended in methanol to dissolve the peptide. Analysis of the supernatant, however, showed that cleavage by the enzyme had not occurred, as only starting material **203** was detected. The lack of cleavage was attributed to the precipitation of the starting material during the experiment. The insolubility of the peptide-model drug conjugate **203** was attributed to the Fmoc-protecting group. The synthesis of peptide-model drug conjugate without the Fmoc-protecting group was pursued.

### 3.15 Synthesis of Ser-Ser-Lys-Leu-Gln-(4-methoxynaphthalen-1-yl)amide

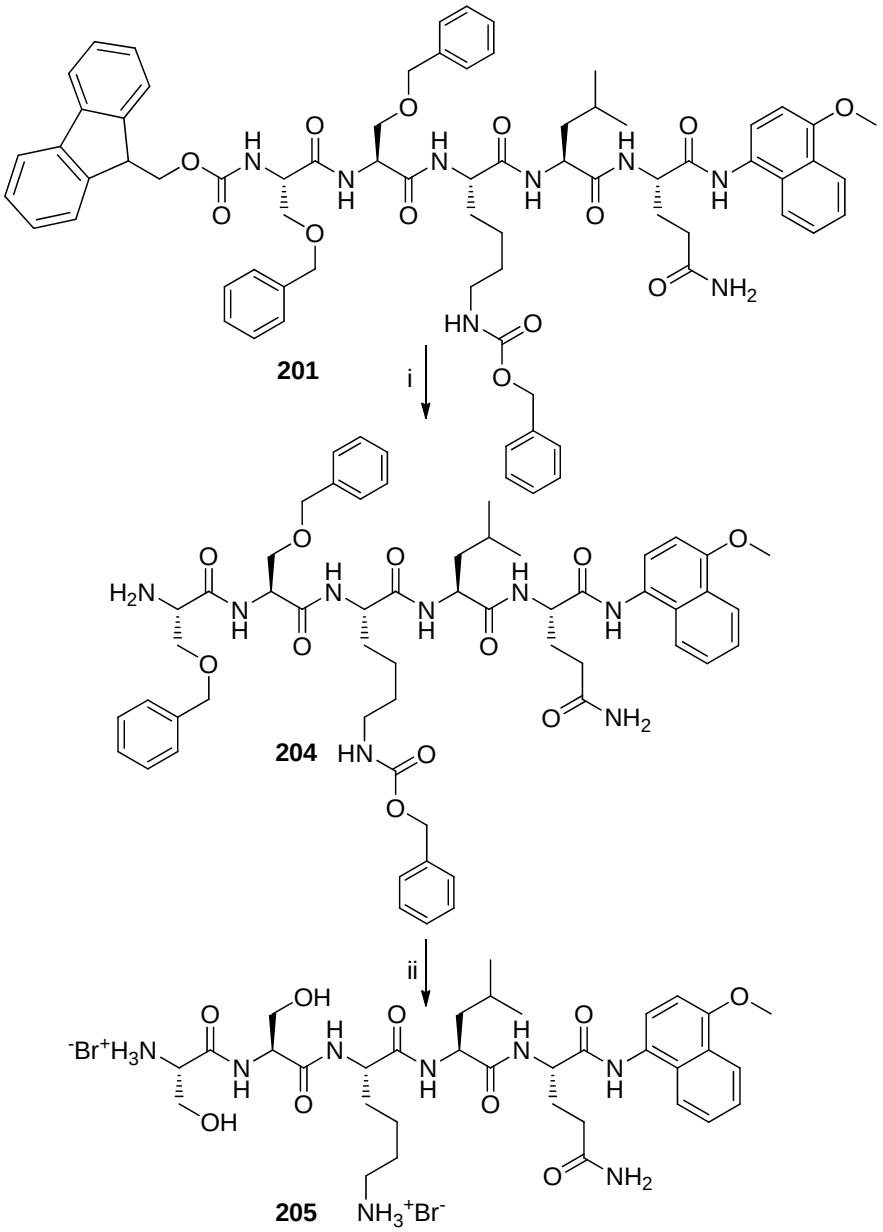


**Scheme 57:** Synthesis of peptide-model drug conjugate **205**. *Reagents and conditions:* i. Piperidine / DMF 1:5, 20°C, 45 min; HBr in AcOH, 20°C, 2 h then MeOH.

Treatment of **201** with piperidine removed the Fmoc-protection to give **204**. The benzyl-type protecting groups in the side-chains were then removed with hydrogen bromide / acetic acid, to give **205** (63%). This peptide-model drug conjugate was then subjected to enzyme assay to ascertain if PSA could release the model drug directly from the peptide.

## 3.16 Study on PSA-cleavage of Ser-Ser-Lys-Leu-Gln-(4-methoxynaphthalen-1-yl)amide

Compound **205** (~2 mM) was incubated with PSA (10 mM) at 37°C. The reaction was carried out in 50 mM Tris-HCl and 140 mM NaCl buffer at pH 7.4. A control experiment was also set up to make sure that cleavage was due to the action of PSA. Samples were taken at different time intervals and added to a solution of $ZnCl_2$ (20 mM) in other to precipitate the enzyme. The mixture stayed clear throughout the experiment, indicating the enhanced water solubility of **205** compared to **203**. HPLC analysis at 280 nM and 220 nM of the supernatant over 7 d, however, showed the presence of only starting material. This observation could be due to a number of reasons. Firstly, the activity of the enzyme was not ascertained before the experiments. Very low activity of the enzyme will require higher amounts to be used in order to observe cleavage. Carrying out an activity test of PSA using the commercially available PSA substrate, Mu-His-Ser-Ser-Lys-Leu-Gln-AMC, would help clarify this. Furthermore, it is possible that the proposed peptide is not a substrate for PSA. However, this reason is unlikely since from literature it has been established that the HSSKLQ is cleavable by PSA.[99] Denmeade *et al.* also showed that shorter amino-acid sequences SKLQ and KLQ were both cleavable by PSA.[99] Synthesis of the polymeric prodrug system was pursued further with coupling of the peptide-model drug to poly(ethylene glycol). This together with **205** can then be tested against a new batch of active PSA.

## 3.17 The synthesis of polymeric peptide-model drug

Polymeric prodrugs enable the exploitation of the EPR effect when used to treat solid tumours like prostate cancer. The polymer serves to increase the molecular weight of the prodrug and thus restricts its diffusion across blood vessels of healthy tissues whilst allowing easy diffusion across the leaky blood vessels of cancer tissues. The size of the polymer means there is reduced renal excretion. This together with the fact that solid tumours have poor lymphatic drainage systems, promotes selective accumulation of drugs at tumour sites, thereby reducing unwanted side-effects.[112, 114] The proposed prodrug system for the delivery of potent anti-tumour agents consists of a polymer, the linking peptide and the active drug. With the synthesis of the peptide-model drug conjugate, the next step in the synthesis is to couple the peptide-model drug conjugate to a polymer (Scheme 58).

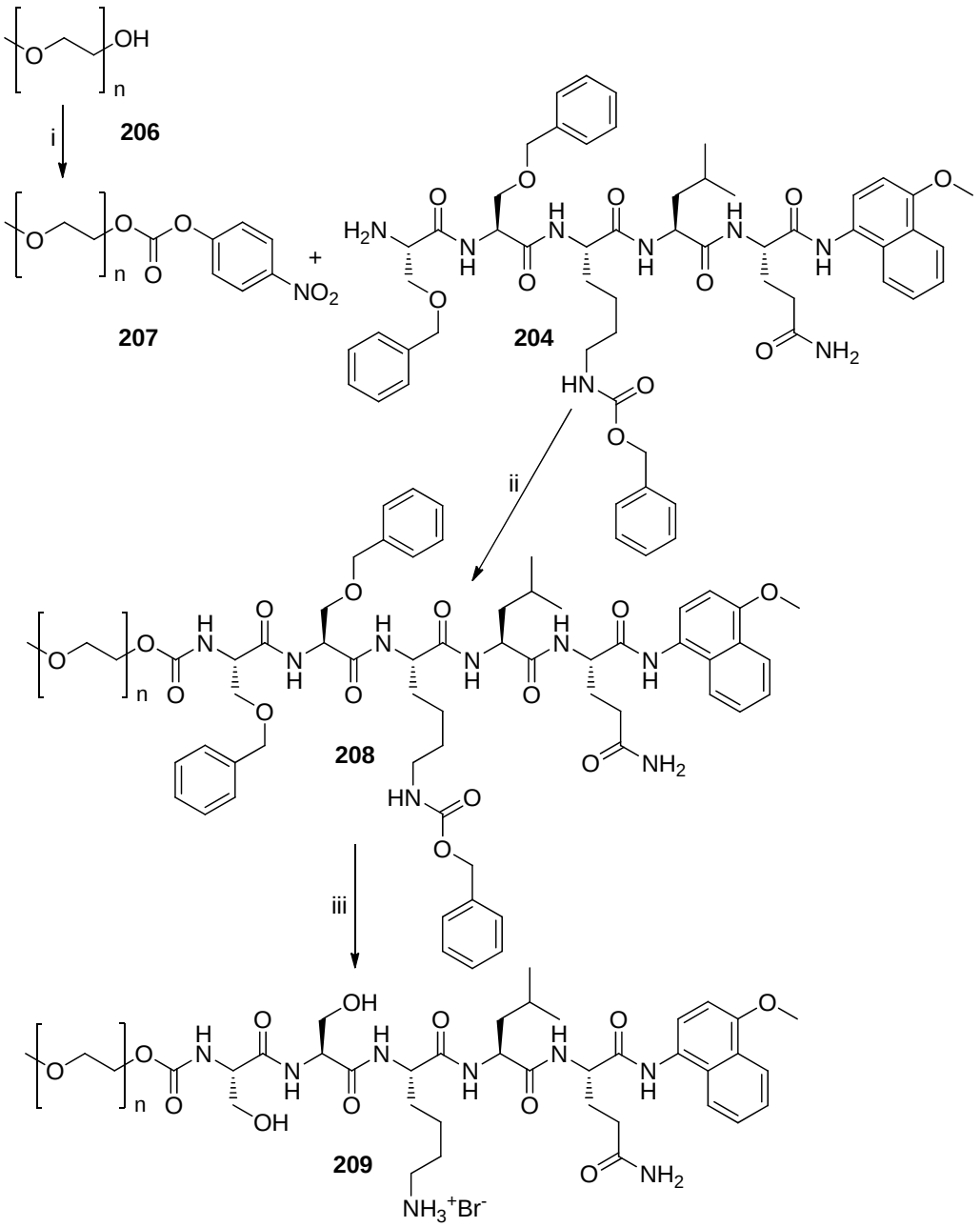


**Scheme 58:** Synthesis of polymeric peptide prodrug. *Reagents and conditions:* i. 4-Nitrophenyl chloroformate, $Et_3N$, 1,2-dichloroethane, 20°C, 16 h; ii. $Et_3N$, dry DMF, $N_2$, 20°C, 8 d; iii. HBr in acetic acid, 20°C, 2 h then MeOH.

The polymer chosen is this instance is poly(ethylene glycol) (PEG). This polymer is widely used in pharmaceuticals due to its non-toxicity, non-immunogenicity and its ability to improve the water solubility of drugs.[120-122] The proposed ideal molecular weight needed for the exploitation of EPR effect is said to be ~20 KDa.[114] Linear PEG (~5 KDa) was chosen to establish the chemistry with the aim of eventually using PEG (~20 KDa). Furthermore, coupling was made to only one end of the linear PEG. The hydroxy group of the commercially available monomethoxy poly(ethylene glycol) (mPEG, MW ~5000 g $mol^{-1}$) had

to be functionalised so it could be coupled to the peptide-drug conjugate **204** (Scheme 58). The polymer comes with high moisture content which interferes with the functionalisation of the hydroxy group. It therefore had to be pre-dried through azeotropic distillation with toluene. The hydroxy group of monomethoxy poly(ethylene glycol) (MW ~5000 g $mol^{-1}$) **206** was converted into the electrophilic nitrophenyl carbonate **207** using 4-nitrophenyl chloroformate. The nitrophenyl carbonate **207** was coupled with **204** to give **208**. This was confirmed by mass spectrometry. Removal of the protection group of **208** will then give the polymeric peptide prodrug **209** which can be tested to ascertain if prostate specific antigen can cleave the peptide to release the model drug. Figure 55 and Figure 54 shows the mass spectra for **207** and **208** respectively.

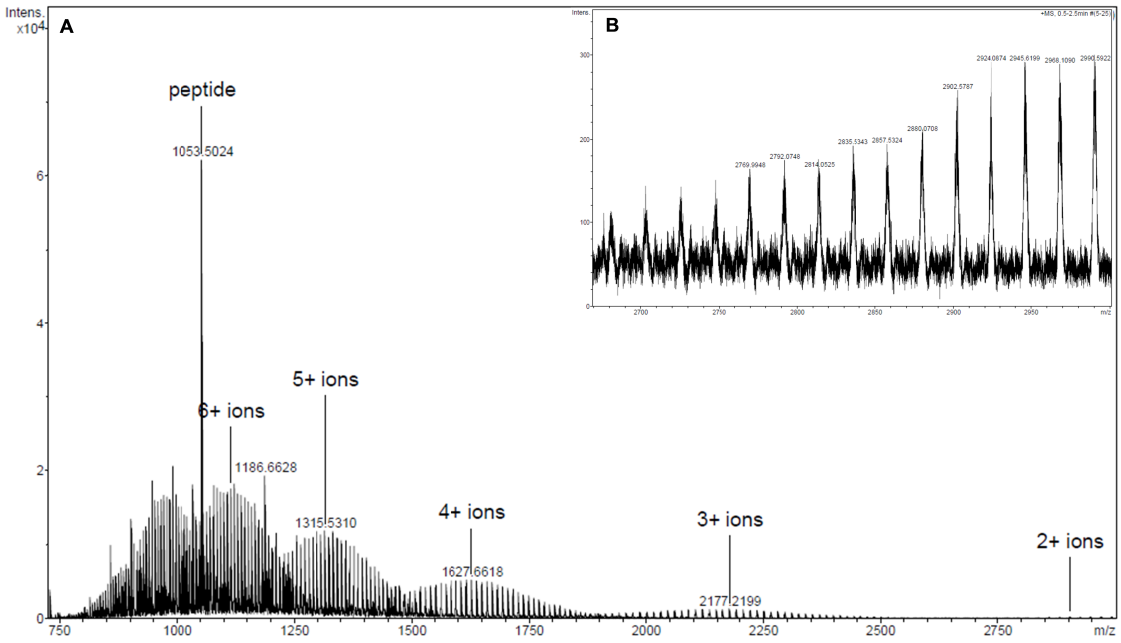


**Figure 54:** Mass spectra for **208** showing multiply cationised species.

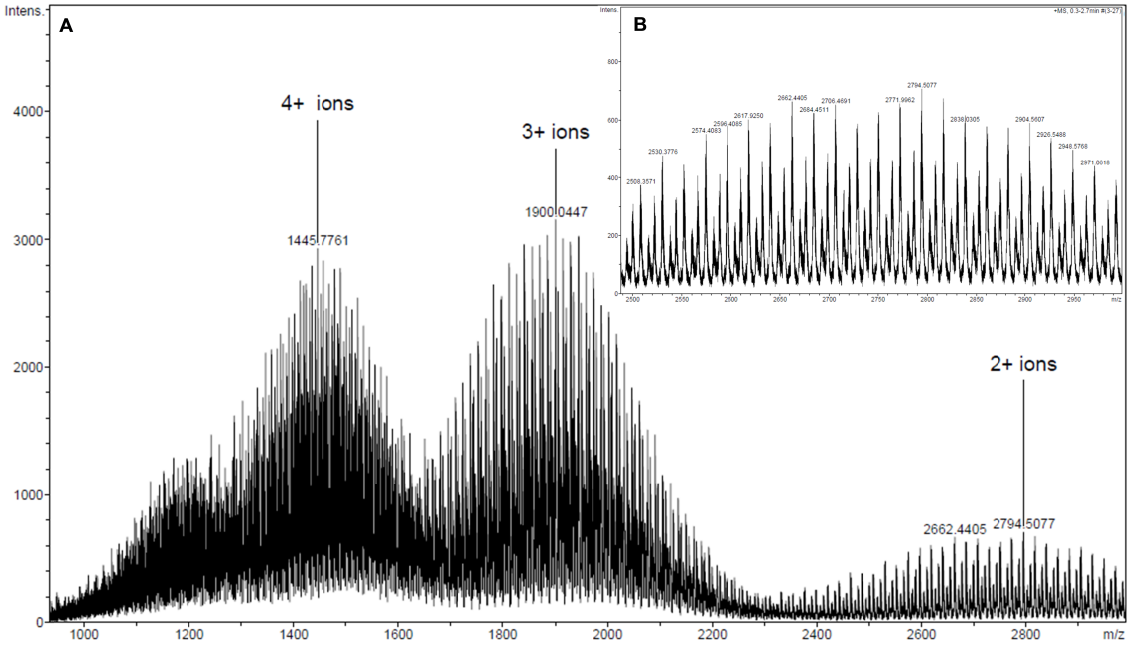


**Figure 55:** Mass spectra for **207** showing multiply cationised species.

The samples were prepared in an acidic media in order to reduce the chances of getting the $Na^+$-cationised polymers. Due to the size of the polymer, detected ions are usually multiply charged. Most polymers have a degree of polydispersity which gives a bell-shaped distribution in the spectra. The distribution pattern of the peaks in each bell-shaped distribution helps identify the kind of polymer and the number of charges on the polymer. The molecular weight of the repeating unit of PEG is forty-four and, therefore, for a mono-charged species, one will observe peaks separated by forty-four units. This also means that for doubly charged species, a separation of twenty-two units should be observed between peaks. Expansion of the region in spectrum-A, corresponding to species with double charge shows a distribution twenty-two units apart (spectrum-B), confirming the nature of polymer and charge. A comparison between the mass spectra for **207** and **208** shows an average increase in molecular weight per given charge distribution. For instance the average MW of the quadruply charged species of **207** (Figure 55) is 1445.78. An average molecular weight of ~1668.65 will be expected for the quadruply charged species of **208** (Figure 54). The average molecular weight observed for the quadruply charged species is ~1627.66 which is close enough to the predicted value to suggest that coupling of the peptide to the polymer occurred. The difficulty in finding a peak that corresponds exactly to the predicted value is mainly due to the extended polydispersity of the polymer. Also for multiply charged polymers, there will be both $Na^+$ and $H^+$-cationised polymers which complicates efforts to identify an exact *m/z*. The $^1H$ NMR spectrum of **208** showed a downfield chemical shift for the α-H of the N-

terminal serine (~3.62 → 4.12) when compared to the uncoupled peptide **204**. This confirmed that this N-terminal amino-acid had been acylated.

## 3.18 Investigation into the use of molecular clip

PSA, as an endopeptidase, tend to cleave peptide bonds between amino-acids. A study by Denmeade *et al.*, however, showed that PSA was able to cleave 7-amino-4-methyl coumarin directly from a PSA-cleavable peptide.[99] This led to the synthesis of the pentapeptide **189** and the subsequent coupling to a model drug and enzyme assay of this prodrug system. In order to deal with a situation whereby an active PSA fails to cleave a drug directly from the pentapeptide, a heptapeptide [Fmoc-Ser(Bn)-Ser(Bn)-Lys(Cbz)-Leu-Gln-Leu-D-Ser-OH] was synthesised with the intention of inserting a dipeptide molecular clip (Leu-Dmo) between the PSA-cleavable peptide (SSKLQ) and the attached drug. This will allow PSA to cleave between Gln and Leu followed by subsequent cyclisation to release the drug (Scheme 59).

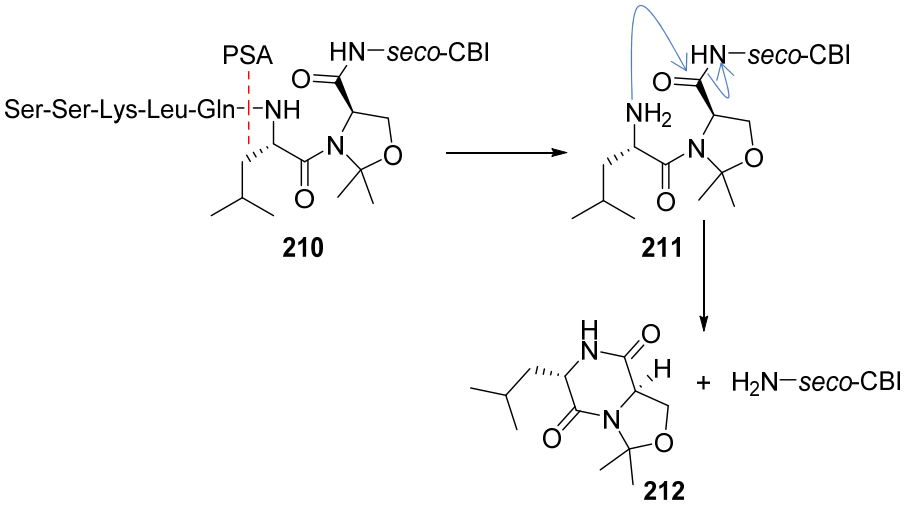


**Scheme 59:** Proposed mechanism for the release of *seco*-CBIs by PSA-cleavage and spontaneous cyclisation.

The rate of cyclisation of dipeptide linkers is based on the proportion in the *cis*-amide conformation.[83, 104] 5,5-Dimethyl-4-oxaproline (Dmo) have been found to force peptides into a 100% *cis*-amide conformation allowing rapid cyclisation to form diketopiperazine.[106, 108] Insertion of a molecular clip containing the Dmo unit between the PSA-cleavable peptide and the model drug will allow rapid intra-molecular cyclisation of the dipeptide linker to release the drug once the peptide is cleaved by PSA.[83] The *pseudo*proline dipeptide linker, Leu-*R*-Dmo was selected as the molecular clip to investigate due to the proven ability to generate the Dmo unit within a growing peptide.[109] The Dmo will initially be introduced as a C-terminal D-Ser in the heptapeptide (SSKLQLS). Intraresidual N,O-acetalisation of the side-chain hydroxy group and the preceding amide nitrogen of D-Ser with 2,2-dimethoxypropane should

generate the *R*-Dmo unit. L-Leu-*R*-Dmo corresponds to the L,*S* series of Dmt (5,5-dimethyl-4-thiaprolin) *pseudo*proline. The L,*S*-Dmt molecular clips have been shown to cyclise at a faster rate than the L,*R*-Dmt series.[105, 106] The rate of cyclisation of the *cis*-*pseudo*proline dipeptide molecular clips further depends on the conformation about the $C^{\alpha}$ of the N-terminal amino-acids (Scheme 60).

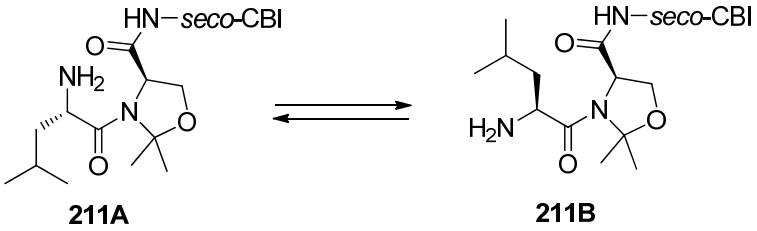


**211A** **211B**

**Scheme 60:** Confromations of Leu-*R*-Dmo molecular clip.

Dipeptide molecular clips must adopt conformer **211A** rather than other conformers such as **211B** where the reacting amine is pointing away from the target carbonyl. Conformer **221A** was shown to be more sterically accessible in the L,*S* series of Aaa-Dmt (corresponding to L-Aaa-*R*-Dmo) facilitating rapid cyclisation and expulsion of drug.[106] Use of Leu-*R*-Dmo should therefore lead to rapid release of drug. Leu has been chosen as part of the proposed dipeptide molecular clip because it has been shown to be essential for cleavage by PSA at the appropriate site. For instance, replacement of Leu with Val in the synthesis of the PSA-cleavable peptide, Ser-Ser-Lys-Leu-Gln-Val-Dmt caused PSA to release Gln-Val-Dmt rather than the desired Val-Dmt. This meant rapid cyclisation to release drug attached to the C-terminal was not possible.[105]

## 3.19 Synthesis of Fmoc-Ser(Bn)-Ser(Bn)-Lys(Cbz)-Leu-Gln-Leu-D-Ser-OH

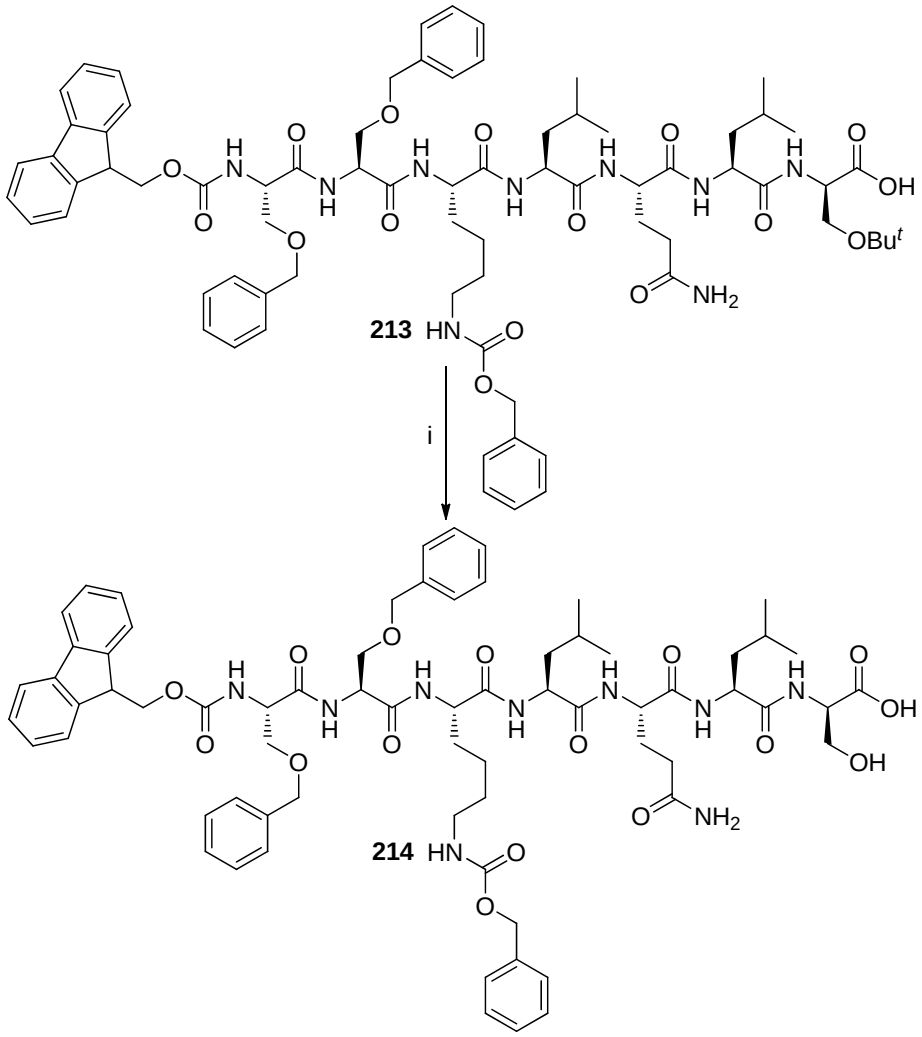


**Scheme 61:** Synthesis of heptapeptide **214**. *Reagents and conditions:* i. $CF_3CO_2H$ / $CH_2Cl_2$ (1:1), r.t., 2 h.

The heptapeptide (Scheme 61) was made by solid-phase synthesis. Cleavage from the 2-chlorotrityl chloride linker with trifluoroacetic acid (1% v/v) led to **213** (89%) with the *tert*-butyl protecting group intact whilst cleavage with trifluoroacetic acid (50%) gave **214** without loss of other protecting groups.

## 3.20 The synthesis of 5,5-dimethyl-4-oxaproline (Dmo) molecular clip

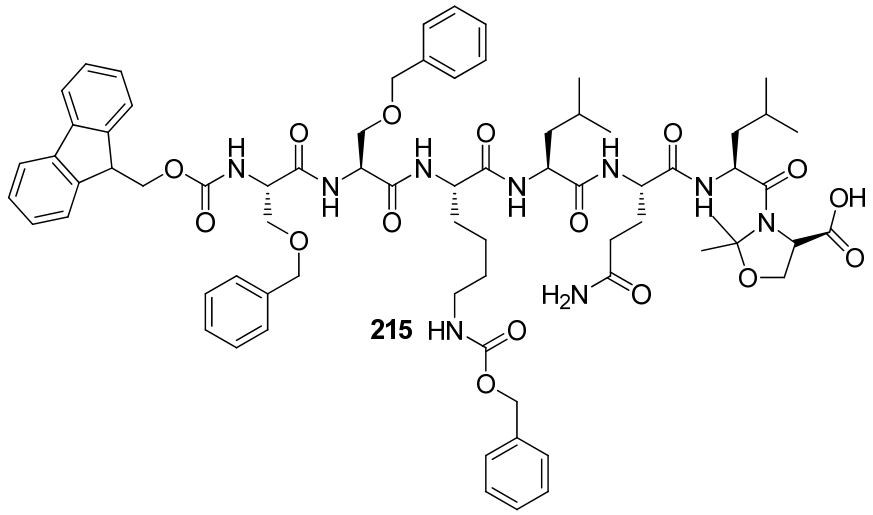


**Figure 56:** Structure of Fmoc-Ser(Bn)-Ser(Bn)-Lys(Cbz)-Leu-Gln-Leu-*R*-Dmo.

The C-terminal D-Ser of **214** had been introduced as a precursor to Leu-*R*-Dmo molecular clip. The next steps studied conversion of the D-Ser into the *R*-Dmo *pseudo*proline in the protected heptapeptide **214** to give **215**. Intraresidual N,O-acetalisation of the side-chain hydroxy group and the preceding amide nitrogen of D-Ser was attempted with 2,2-dimethoxypropane (DMP) applying catalytic amounts of *para*-toluenesulfonic acid (pTsOH). The first attempt was carried out in toluene under microwave conditions but this resulted in decomposition of the peptide. The same result was obtained when the reaction was repeated under reflux using a Dean-Stark apparatus. One possibility for this failure was thought to be the poor solubility of **215** in the solvent used (toluene). The solvent was changed to dimethylformamide / dichloromethane and the reaction repeated for longer periods of time (up to 96 h). This, however, gave only decomposed products as well as starting materials. Aggregation of the peptide was thought to be one of the reasons why this reaction was unsuccessful. This means the site of reaction is sterically hindered and therefore the 2,2-dimethoxypropane molecule does not get access.

The tetrapeptide **216** was synthesised to ascertain the ability to generate Dmo within a shorter peptide chain (Scheme 62).

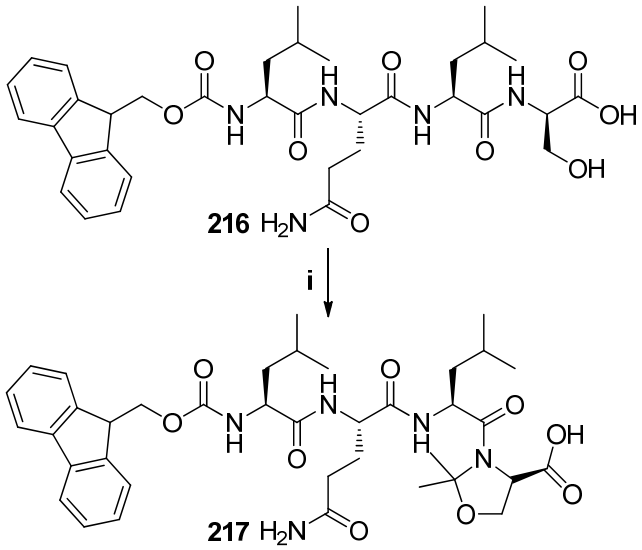


MS (ES$^+$) *m/z* 744.3534 (M + Na) ($C_{38}H_{51}N_5NaO_9$ requires 744.3579), 722.3715 (M+H) ($C_{38}H_{52}N_5O_9$ requires 722.3760)

**Scheme 62:** Synthsis of the Dmo motif. *Reagents and conditions:* i. Dimethoxypropane, pTSOH, DMF, 40°C, 72 h.

Intraresidual N,O-acetalisation was tested on this compound using 2,2-dimethoxypropane and *para*-toluensulfonic acid. At 40°C for 3 d, traces of the desired product **217** were observed by mass spectrometry, together with decomposed products. Repeating this reaction at a higher temperature (70°C) led to no detectable product. This suggests that the peptide is not stable at higher temperatures and, therefore, this reaction should be tested at lower temperatures. Using a shorter peptide chain in the synthesis of the molecular clip might also be advantageous. Although regioselective insertion of *pseudo*proline systems into complex peptides such as cyclosporine C has been achieved,[189] most *pseudo*prolines have been synthesised as dipeptides. One way of dealing with this will therefore be to synthesise the Dmo unit on a shorter peptide chain with protection at the C-terminal carboxyl group.[109] The synthesis of the molecular clip as the dipeptide (Leu-*R*-Dmo) to be coupled to the remaining amino-acids should, however, be avoided. This is because rapid cyclisation into the diketopiperazine is likely to occur making it difficult to couple to other amino-acids.[106] Synthsising the molecular clip within a tripeptide as in **177** or a tetrapeptide as in **175** (Scheme 49) will allow one to couple the remaining amino-acids employing solution-phase synthesis. In this instance since Gln is not a terminal amino-acid, it can be masked as the nitrile to aid solubility. The nitrile can be hydrated to the amide without running the risk of over hydration to the carboxylate.[178] Synthesis of **215** will be followed by coupling to the model drug **200** and removal of the

protecting groups to test the peptide-molecular clip-drug conjugate for enzymatic cleavage. This peptide-molecular clip-drug-conjugate will further be coupled to poly(ethylene glycol) and then subjected to more *in vitro* assays.

The total synthesis of an analogue of the anti-tumour antibiotics has been achieved and biological evalution undertaken to confirm its potency. The development of the polymeric prodrug system saw the synthesis of the model drug **200** which was coupled to the proposed PSA-cleavable peptide **189**. The peptide-model drug conjugate was further coupled to poly(ethylene glycol) to form the polymeric prodrug system. Enzymatic assay to test the ability of PSA to cleave the drug directly from the peptide, however, faced various challenges. This led to the synthesis of the heptapeptide **214** with the intention of inserting a molecular clip between the PSA-cleavable peptide and the drug. Insertion of the *pseudo*proline molecular clip (Leu-*R*-Dmo) into the heptapeptide **214** to give **215**, however, failed. This has mainly been attributed to the steric bulk of the heptapeptide with a plan to synthesise the Dmo motif on a shorter peptide chain. Future synthesis of **215** will allow coupling to the model drug **200** followed by deprotection to give a peptide-Dmo-drug conjugate that can be investigated as to whether PSA can cleave. A successful cleavage by PSA will lead to the synthesis of polymer-peptide-molecular clip-drug conjugate and subsequent testing against PSA. Once the polymeric-peptide prodrug system is proven, the *seco*-CBI drug **136** will be conjugated with the peptide and the polymer and investigated for PSA triggered release from the polymeric prodrug system.

# 4 Conclusion

Conventional chemotherapeutic agents have significant limitations which impedes their ability to control tumour growth in patients. These limitations have been mainly attributed to their lack of selective targeting of cancerous cells over normal cells. CBI anti-tumour antibiotics represent synthetically accessible chemotherapeutic agents with high potency and novel mode of action.[70, 78, 156, 190] The ability to deliver these drugs selectively to prostate tumours will not only address the limitations of current chemotherapeutic agents but will also present a new mode of targeting cancerous cells.

Synthesis of the proposed *seco*-CBI drug **136** was addressed in two parts, namely, synthesis of the alkylating subunit and synthesis of the non-alkylating subunit. The key naphthalene intermediate, *tert*-butyl N-(1-iodo-2-(trifluoroacetamidonaphthalen-4-yl) carbamate **67** with iodo at C1 and orthogonally protected $N^2$- and $N^4$-amines was essential for the synthesis of the alkylating subunit. One of the main challenges faced in the synthesis of **67** was unintended de-iodination of 1-iodo-2,4-naphthalendiamines. Attempted acidic removal of the *tert*-butoxycarbonyl groups of N,N'-bis(*tert*-butoxycarbonyl)-1-iodonaphthalene-2,4-diamine **25** led to either selective de-iodination to give **59** or de-iodination with deprotection to give naphthalene-1,3-diamine **58** (Scheme 21). This observation triggered an extensive NMR studies to ascertain the reason for de-iodination. At 0°C, it was observed that 1-iodonaphthalene-2,4-diamine was stable in trifluoroacetic acid whilst, at 20°C, an unexpected Wheland-like intermediate in the de-iodination process was observed. It was also observed that the source of the new proton in the Wheland-like intermediate had an intra-molecular origin. The findings that 1-iodonaphthalen-2,4-diamine was stable in trifluoroacetic acid at 0°C led to an effort to trap this compound as the salt and then protect the $N^4$-amino group with *tert*-butoxycarbonyl (Boc). This, however, led to the isolation of the de-iodinated product, *tert*-butyl N-(1-aminonaphthalen-3-yl) carbamate **62**, with Boc-protection at the $N^2$-amino group (Scheme 21).

This result showed that preventing de-iodination in these compounds was too difficult and also gave a new direction in the synthesis of **67**. It was thought that de-iodination occurred first to give naphthalene-1,3-diamine, which then underwent selective protection at the $N^2$-amino group to give **62**. This suggested that the $N^2$-amino group was more reactive than the $N^4$-amino group, probably due its higher steric accessibility. Besides, it was found that naphthalene-1,3-diamine **58** could be monoprotected with 2-(*tert*-butoxycarbonyloxyimino)-

2-phenylacetonitrile to give **62** but at a low yield of 8%.[142] Introduction of trifluoroacetyl protection at the $N^2$-amino group of **58** and *tert*-butoxycarbonyl at the $N^4$-amino group was followed by electrophilic iodination to give **67**. Selective alkylation at the $N^2$-amide of **67** followed by free-radical cyclisation with TEMPO trap and basic removal of the trifluoroacetyl group allowed coupling to the 5-(2-dimethylaminoethoxy)indole-2-carboxylic acid non-alkylating subunit **127**. Reductive removal of 2,2,6,6-tetramethylpiperidine followed by substitution of the exposed hydroxy group with chlorine gave the Boc-protected CBI drug **135**. Acidic removal of the Boc group gave the final *seco*-CBI drug as its dihydrochloride salt **136**.

Calf-thymus DNA melting assay of the synthesised CBI drug **136** was carried out. This confirmed that **136** binds and alkylates double stranded DNA very efficiently to bring about its cytotoxic effects. This effect was observed as an increase in the melting temperature ($T_m$) of dsDNA by as much as 13 deg. C, comparable to the $T_m$ of the known cytotoxic agent, doxorubicin ($T_m$ = 18 deg. C). This was despite **136** being the racemate. The (−)-unnatural enantiomers of the anti-tumour antibiotics tend to have a reduced DNA alkylation efficiency compared to the (+)-natural enantiomers.[61] The significant elevation of the $T_m$ of calf-thymus DNA by **136** therefore suggests that this compound is highly efficient at DNA alkylation.

Preliminary MTS assay of the racemic *seco*-CBI drug **136** demonstrated that it was a potent cytotoxin, with an $IC_{50}$ of 18 nM in LNCaP cells. The cytotoxic effect of the Boc-protected *seco*-CBI-drug **135** was measured as a rough prediction of the effect of conjugating the *seco*-CBI drug **136** to the PSA-cleavable peptide to form a prodrug. The observed preliminary $IC_{50}$ was 218 nM showing an approximate ten-fold reduction in cytotoxicity compared to the unprotected drug. This suggested that the prodrug concept is viable. The high $IC_{50}$ of **135** was attributed to the labile Boc-protection at $N^4$. This meant that Winstein cyclisation was probably occurring to form the highly reactive cyclopropane ring, essential for cytotoxicity. The proposed peptide prodrug will form a more stable amide prodrug and therefore avoid unintended cyclisation of the *seco*-CBI. This should in turn reduce the cytotoxicity of the prodrug and increase the $QIC_{50}$.[87]

Investigation into a polymeric prodrug system involved firstly the synthesis of the proposed PSA-cleavable peptide SSKLQ. Initial attempts to synthesise this peptide *via* solution phase was met with solubility problems mainly due to the presence of the unprotected amide side-chain of glutamine. This group was successfully masked as the nitrile to improve solubility

and reduce the chance of side-reactions. Although this effort proved effective in situations in which the glutamine is not a terminal amino-acid, attempted hydration of the nitrile when the glutamine is a terminal amino-acid resulted in conversion to glutamic acid rather than glutamine. This proved that this technique of masking the amide side-chain of glutamine as a nitrile in the synthesis of the pentapeptide, SSKLQ, was not going to work. Solid-phase peptide synthesis was therefore adopted in the synthesis of the pentapeptide **189**. 4-Methoxynaphthalen-1-amine **200** was coupled to the C-terminal of the pentapeptide as a model peptide-drug conjugate. A model polymer-peptide-drug conjugate was also synthesised by coupling of the model drug **200** to the C-terminal of the pentaptide followed by coupling to poly(ethylene glycol) at the N-terminal. Testing of the ability of PSA to cleave the amide bond between glutamine and the model drug was carried out with the peptide-model drug conjugate. Preliminary results from his assay, however, showed that cleavage did not occur and suggested the need to optimise the assay.

In order to deal with a situation whereby PSA is unable to cleave the drug directly from the peptide, investigations were made into the insertion of self-immolative molecular clip between the drug and the peptide. The heptapeptide SSKLQLS was synthesised to investigate this proposal. Intra-residual N,O-acetalisation of the side-chain hydroxy group and the preceding amide nitrogen of the C-terminal D-Ser to generate the L-Leu-*R*-Dmo molecular clip, however, proved difficult. This was attributed to the bulky nature of the peptide and the possibility of aggregation leading to steric hinderance. Investigation into the use of a shorter peptide chain to generate the Dmo unit showed great promise as the desired product was detected by mass spectrometry. Dmo synthesis is quite problematic since though it requires acid catalysis, the cleavage of this molecular clip is also effected by acidic conditions. 5,5-Dimethyl-L-proline (dmP)[191] might be an alternative if the synthesis of Dmo becomes problematic. This *pseudo*proline (dmP) acts in similar fashion to Dmo but its carbocyclic framework renders it completely stable to acidic conditions. Synthesis of the molecular clip and its incorporation into the peptide will give a PSA-cleavable peptide that can be coupled to the model drug and polymer. PSA cleavage assays of the polymeric prodrug with the molecular clip and that without the molecular clip will be compared to assess the best system for efficient drug release. The most efficient system will then be adopted to synthesise the polymeric prodrug of the *seco*-CBI **136**. Further biological evaluations will then be carried out with PSA-producing prostate cells to check the efficiency of activation of the polymeric prodrug system. The results from such studies will then be used as a guide in optimising the polymeric prodrug system.

# 5 Experimental

## 5.1 General

Chemical reagents were purchased from Sigma-Aldrich, Fluka, and Novabiochem. TLC was carried out on Merck aluminium backed TLC plates Silicagel 60 $F_{254}$ and viewed using UV light ($\lambda$ = 254 nm). Reverse phase (RP) TLC was performed with RP-18 F254s pre-coated aluminium sheets (0.27 mm thickness). Column chromatography was carried on silica gel 60 (35 – 70 micron). Reverse phase chromatography was carried out using VersaPak C18 (spherical) 23 × 110 mm (bed. wt., 30 g) cartridge. NMR data were obtained on either a Varian Mercury VX (400 MHz for $^{1}H$ and 100 MHz for $^{13}C$) or a Bruker Avance III spectrometer (500 MHz for $^{1}H$, 125 MHz for $^{13}C$ and 470 MHz for $^{19}F$). The chemical shifts are recorded in parts per million (ppm). A single mean value of chemical shift is given for multiplets arising from proton(s) in the same chemical environment whilsts a range value is given for the chemical shift of multiplets arising from protons of different chemical environments. Mass spectrometry was carried out on a micrOTOF$^{TM}$ from Bruker Daltonics (Bremen, Germany) using an electrospray source (ESI-TOF). Melting points were obtained using a Reichert-Jung heated-stage microscope. Optical rotations were measured at ambient temperature using an Optical Activity Ltd AA-10 polarimeter in a cell volume of 5 mL and specific rotations are given in $10^{-1}$ deg. mL $g^{-1}$. IR spectra were recorded on a Perkin-Elmer 782 infra-red spectrometer using liquid films between NaCl discs or solids as KBr discs and values are given in $cm^{-1}$. Analytical RP-HPLC was performed on a Dionex HPLC system (system 1) equipped with a Dionex UltiMate 3000 HPLC system with a Phenomenex Gemini 5µm C-18 (150 × 4.6 mm) column with a flow rate of 1.0 mL $min^{-1}$. Detecting was at $\lambda$ = 214, 220, 254, 280 nm. Mobile phase A was 0.1% (v/v) TFA in water and mobile phase B was 0.1% TFA in acetonitrile. Gradient 1 was T = 0 min, A = 95%; T = 10 min, A = 5%. Gradient 2 was T = 0 min, A = 95%; T = 20 min, A = 5%. Preparative RP-HPLC was performed on a Dionex HPLC system equipped with a Phenomenex Gemini 5µm C-18 (250 x 30 mm) with a flow rate of 22.5 mL $min^{-1}$. Mobile phase A was 0.1% TFA in water and mobile phase B was 0.1% TFA in acetonitrile. Gradient was T = 0 min, A = 95%; T = 20 min, A = 5%. Centrifugation was carried out using Eppendorf MiniSpin centrifuge at 13400 rpm unless otherwise specified. Experiments were conducted at room temperature unless otherwise stated. Solvents were evaporated under reduced pressure. Solutions in organic solvents were dried with $MgSO_4$.

Reagents for biological experiments were obtained from the Sigma-Aldrich Chemical Co. Fisher Ltd or Invitrogen and were of at least biochemical grade. Aqueous solutions were made in 18.2 Mega-Ω.cm$^{-1}$ Milli-Q water and pH adjusted with HCl or NaOH solutions as appropriate. The pH was monitored using a Corning pH meter 240 and Corning general purpose combination pH electrode, calibrated at pH 7.0 and 10.0 or 4.0 at ambient room temperature. Reagents and plasticware were sterilised where required by autoclaving at 121°C for 15 minutes or were purchased already sterilised. Temperature-sensitive reagents were filtered through a 0.2 μ filter. Tissue culture experiments were carried out in a sterile hood.

The human prostate cancer cell line LNCaP (Sigma-Aldrich) was cultured in Dulbecco's Modified Eagle's Medium (DMEM) supplemented with high glucose (4.5 g L$^{-1}$), 20% (v/v) foetal bovine serum (FBS), penicillin (100 U mL$^{-1}$) and streptomycin sulfate (100 μg mL$^{-1}$) at 37°C in humidified atmosphere containing 5% (v/v) $CO_2$. The MTS assay is based on the reagent: Promega 'Cell Titer 96® Aqueous One Solution Cell Proliferation Assay'.[192] Centrifugation was carried out using Jouan B3.11 centrifuge at 1300 rpm unless otherwise specified. Perkin Elmer Lambda 40 UV/VIS spectrometer fitted with Perkin Elmer PTP-6 (Peltier Temperature Programmer) was used to monitor DNA melting temperature.

## 5.2 Benzyl N-(4-hydroxynaphthalen-1-yl)carbamate (32)

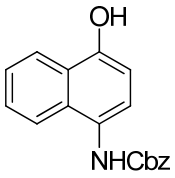


A suspension of 4-amino-1-naphthol hydrochloride **31** (224 mg, 1.1 mmol) in THF (30 mL) was stirred at −70°C under $N_2$. Potassium *tert*-butoxide (1.1 mL of 1.0 M solution in THF, 1.1 mmol) was added dropwise over a 10 min period. The resulting mixture was warmed to −10°C and stirred for 1 h. The mixture was cooled again to −70°C and benzyl chloroformate (216 mg, 1.3 mmol) was added. The mixture was warmed gradually to 20°C and was stirred overnight. The solvent was evaporated. The residue was dissolved in EtOAc and washed with water and brine. Drying, evaporation and chromatography (petroleum ether / EtOAc 1:1) gave **32** (207 mg, 62%) as a purple solid: $R_f$ = 0.2 (petroleum ether / EtOAc 1:1); $^1$H NMR [$(CD_3)_2SO$) (COSY / NOESY)] δ 5.20 (2 H, s, Ph $CH_2$), 6.90 (1 H, d, *J* = 8.0 Hz, Naph 3-H), 7.33 (1 H, d, *J* = 8.0 Hz, Naph 2-H), 7.37-7.58 (7 H, m, Naph 6,7-$H_2$ + Ph $H_5$), 7.93 (1 H, d, *J* = 7.8 Hz, Naph 8-H), 8.20 (1 H, dd, *J* = 8.7, 1.5 Hz, Naph 5-H), 9.29 (1 H, brs, NH), 10.15 (1 H, s, OH); $^{13}$C NMR [$(CD_3)_2SO$) (HSQC / HMBC)] δ 65.63 (Ph $CH_2$), 107.31 (Naph 3-C), 122.25 (Naph 5-C), 122.68 (Naph 8-C), 123.66 (Naph 2-C), 124.59 (Naph 1-C or 7-C or Ph 4-C), 124.69 (Naph 7-C or 1-C or Ph 4-C), 124.73 (Ph 4-C or Naph 1-C or 7-C), 126.09 (Naph 6-C),

127.84 (Ph 3,5-$C_2$), 128.38 (Ph 2,6-$C_2$), 130.18 (Naph 4a,8a-$C_2$), 137.05 (Ph 1-C), 151.33 (Naph 4-C), 155.32 (C=O).

### 5.3 Naphthalene-1,4-dione (35)

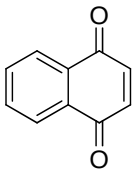

4-Amino-1-naphthol hydrochloride **31** (67.6 mg, 0.35 mmol) was dissolved in trifluoroacetic acid (10 mL) and stirred at −20°C. Potassium nitrate (35.5 mg, 0.35 mmol) was added dropwise over 5 min. The mixture was then allowed to stir at −20°C for 30 min and then poured onto ice. Extraction with EtOAc, drying and chromatography ($CH_2Cl_2$ / EtOAc 3:2) gave **35** (41.4 mg, 75%) as a buff solid: $R_f$ = 0.8 ($CH_2Cl_2$ / EtOAc 6:1); mp 124-126°C (lit.[193] 125-127°C); $^1$H NMR [$(CD_3)_2SO$) (COSY)] δ 7.14 (2 H, s, 2,3-$H_2$), 7.93 (2 H, m, 6,7-$H_2$), 8.04 (2 H, m, 5,8-$H_2$); $^{13}$C NMR [$(CD_3)_2SO$) (HSQC / HMBC)] δ 125.83 (5,8-$C_2$), 131.53 (4a,8a-$C_2$), 134.18 (6,7-$C_2$), 138.70 (2,3-$C_2$), 184.80 (1,4-$C_2$); MS ($ES^+$) *m/z* 159.0446 (M + 1) ($C_{10}H_7O_2$ requires 159.0446).

### 5.4 4-Amino-2-nitronaphthalen-1-ol (40)

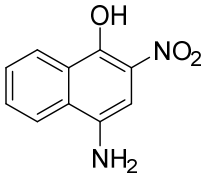

2,4-Dinitronaphthalen-1-ol **24** (5.04 g, 22 mmol) was stirred in conc. aq. HCl (20 mL) and EtOH (10 mL) for 1 h during the addition of $SnCl_2.2H_2O$ (15.04 g, 66.64 mmol) in EtOH (20 mL), keeping the temperature < 30°C. The mixture was stirred for 17 h at 20°C. The suspension was filtered and and the collected solid washed with EtOH / aq. conc. HCl (3:2). The yellow solid was partitioned between EtOAc and water and extracted several times with EtOAc. The organic layer was washed with brine and dried. Evaporation and chromatography ($CH_2Cl_2$) gave **40** (3.11 g, 71%) as a pale red solid: $R_f$ = 0.5 ($CH_2Cl_2$); mp 160-161°C (lit.[130] mp 160°C); IR $\nu_{max}$ 3418, 3337 (OH, NH); $^1$H NMR ($CDCl_3$) δ 3.98 (2 H, s, $NH_2$), 7.26 (1 H, s, 3-H), 7.64 (1 H, ddd, *J* = 8.2, 7.0, 1.1 Hz, 7-H), 7.74 (1 H, ddd, *J* = 8.2, 6.9, 1.3 Hz, 6-H), 7.83 (1 H, d, *J* = 8.4 Hz, 5-H), 8.53 (1 H, dd, *J* = 8.3, 0.6 Hz, 8-H), 11.92 (1 H, s, OH); $^{13}$C NMR ($CDCl_3$) (HSQC / HMBC) δ 100.54 (3-C), 121.42 (5-C), 125.65 (8a-C), 125.92 (8-C), 127.15 (7-C), 127.90 (2-C), 129.56 (4a-C), 130.87 (6-C), 135.18 (4-C), 150.11 (1-C); MS ($ES^+$) *m/z* 203.0466 (M - H) ($C_{10}H_7N_2O_3$ requires 203.0457).

### 5.5 4-Amino-2-nitronaphthalen-1-yl *tert*-butyl carbonate (41)

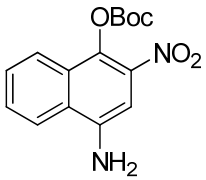


4-Amino-2-nitronaphthalene-1-ol **40** (53.8 mg, 0.26 mmol) was dissolved in $CH_2Cl_2$ (10 mL) and stirred under $N_2$. $Boc_2O$ (60.2 mg, 0.28 mmol) in $CH_2Cl_2$ (5 mL) was added, followed by addition of DMAP (24.6 mg, 0.20 mmol) in $CH_2Cl_2$ (2 mL); the mixture was stirred at 20°C for 30 min. The mixture was washed with water, brine and dried. Evaporation and chromatography ($CH_2Cl_2$) gave **41** (13.6 mg, 17%) as a yellow solid: $R_f$ = 0.4 ($CH_2Cl_2$); $^1$H NMR ($CDCl_3$) δ 1.60 (9 H, s, $Bu^t$), 4.34 (2 H, s, $NH_2$), 7.29 (1 H, s, 3-H), 7.62-7.66 (2 H, m, 6,7-$H_2$), 7.79-7.82 (1 H, m, 5-H), 8.13-8.16 (1 H, m, 8-H); $^{13}$C NMR [($CDCl_3$) (HSQC / HMBC)] δ 27.60 (C*Me*$_3$), 84.87 (*C*Me$_3$), 102.48 (3-C), 121.22 (5-C), 124.15 (8-C), 126.12 (4a-C), 128.14 (6-C), 128.20 (8a-C), 128.67 (7-C), 133.79 (4-C), 137.91 (2-C), 141.07 (1-C), 150.94 (C=O).

### 5.6 *tert*-Butyl (4-hydroxy-3-nitronaphthalen-1-yl)carbamate (42)

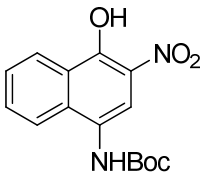


4-Amino-2-nitronaphthalen-1-ol **40** (0.56 g, 2.7 mmol) was stirred in dry THF (20 mL) under $N_2$. $Boc_2O$ (3.04 g, 14 mmol) in dry THF (5 mL) was added and the mixture was boiled under reflux for 20 h. The mixture was cooled and the solvent was evaporated. The residue was partitioned between $CH_2Cl_2$ and water and extracted with $CH_2Cl_2$, followed by washing with brine and drying. Evaporation and chromatography (petroleum ether / EtOAc 9:1) gave **42** (0.74 g, 89%) as an orange solid: $R_f$ = 0.4 (EtOAc / petroleum ether 1 : 4); mp 175-177ºC; IR $\nu_{max}$ 3338 (NH, OH), 3259 (NH, OH), 1687 (C=O), 1525 ($NO_2$); $^1$H NMR [($CDCl_3$) (NOESY)] δ 1.55 (9 H, s, $Bu^t$), 6.59 (1 H, br s, NH), 7.65 (1 H, ddd, *J* = 8.2, 7.0, 1.1 Hz, 6-H), 7.77 (1 H, ddd, *J* = 8.2, 6.9, 1.2 Hz, 7-H), 7.87 (1 H, d, *J* = 8.4 Hz, 8-H), 8.33 (1 H, s, 2-H), 8.56 (1 H, dd, *J* = 8.4, 0.5 Hz, 5-H), 12.11 (1 H, s, OH); $^{13}$C NMR [($CDCl_3$) (HSQC / HMBC)] δ 28.31 (C*Me*$_3$), 81.31 (*C*Me$_3$), 112.82 (2-C), 121.46 (8-C), 125.45 (8a-C), 125.83 (4-C), 125.91 (4a-C), 127.25 (6-C), 127.55 (3-C), 131.56 (7-C), 152.98 (1-C), 153.50 (C=O); MS ($ES^+$) *m/z* 327.0966 (M + Na) ($C_{15}H_{16}N_2NaO_5$ requires 327.0957).

## 5.7 4-(*tert*-Butoxycarbonyl)amino-2-nitronaphthalen-1-yl trifluoromethanesulfonate (43)

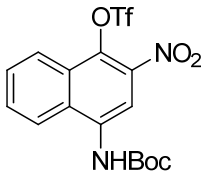


Compound **42** (808 mg, 2.7 mmol), was stirred in dry pyridine (20 mL) under $N_2$ at 0°C for 15 min. Trifluoromethanesulfonic anhydride (0.70 mL, 1.2 g, 4.2 mmol) was added dropwise during 45 min and the mixture was stirred for 30 min at 0°C. The mixture was then allowed to warm to 20°C during 10 min. Water was added and the mixture extracted with EtOAc. Drying, evaporation and chromatography ($CH_2Cl_2$ → $CH_2Cl_2$ / EtOAc 1:1→ EtOAc) gave **43** (942 mg, 81%) as a yellow solid: $R_f$ = 0.8 ($CH_2Cl_2$); mp 110-111°C; IR $\nu_{max}$ 3435 (NH), 1737 (C=O); $^1$H NMR [($CDCl_3$) (NOESY)] δ 1.59 (9 H, s, Bu$^t$), 7.19 (1 H, s, NH), 7.78-7.82 (2 H, m, 6,7-$H_2$), 7.96 (1 H, dd, *J* = 6.5, 3.0 Hz, 5-H), 8.29 (1 H, dd, *J* = 6.5, 3.3 Hz, 8-H), 8.73 (1 H, s, 3-H); $^{13}$C NMR [($CDCl_3$) (HSQC / HMBC)] δ 28.20 (C*Me*$_3$), 82.54 (*C*Me$_3$), 110.52 (3-C), 118.42 (q, *J* = 321.2 Hz, $CF_3$), 121.34 (5-C), 125.19 (8-C), 127.13 (8a-C), 127.51 (4a-C), 129.35 (6-C or 7-C), 130.12 (7-C or 6-C), 132.72 (2-C), 134.61 (4-C), 143.02 (1-C), 152.20 (C=O); $^{19}$F NMR ($CDCl_3$) δ -72.55 (s, $CF_3$); MS ($ES^+$) *m/z* 459.0484 (M + Na) ($C_{16}H_{15}F_3N_2NaO_7S$ requires 459.0450).

## 5.8 Attempted nucleophilic displacement of the triflate group of 43 with iodide

Compound **43** (89.9 mg, 0.21 mmol) was stirred in DMF (20 mL) and NaI (63.1 mg, 0.46 mmol) was added. The mixture was stirred at 80°C overnight and then at 90°C for 2 h. The solvent was evaporated and the residue was suspended in water. Extraction with EtOAc, washing with sat. aq. $Na_2S_2O_3$, drying and evaporation gave **42** (50.2 mg, 80%) with properties as above.

## 5.9 Attempted reduction of the triflate group of 43

METHOD A

Compound **43** (41.9 mg, 96 µmol), magnesium (4.1 mg, 0.17 mmol) and Pd/C (10%, 4.5 mg) were placed in a flask and placed under Ar. Dry MeOH (10 mL) was introduced *via* a syringe and the reaction was stirred at 20°C for 16 h. Filtration through Celite®, evaporation and chromatography ($CH_2Cl_2$) gave **42** (13.1 mg, 45%) as an orange solid with properties as above.

METHOD B

Compound **43** (122 mg, 0.28 mmol) in DMF (5 mL) was treated with $Ph_3P$ (3.66 mg, 14 μmol), palladium acetate (1.70 mg, 7.6 μmol), $Et_3N$ (0.12 mL, 87 mg 0.84 mmol) and formic acid (0.02 mL, 24 mg, 0.56 mmol). The mixture was stirred at 65°C for 16 h, diluted with water, extracted with EtOAc, dried and evaporated. Chromatography ($CH_2Cl_2$) gave **42** (66 mg, 78%) as an orange solid with properties as above.

## 5.10 (*E*)-*tert*-Butyl (3-amino-4-oxonaphthalen-1(4H)-ylidene)carbamate (50)

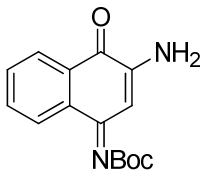


Compound **42** (66 mg, 0.22 mmol) was stirred vigorously with Pd/C (10%, 36.5 mg) in MeOH (20 mL) under $H_2$ for 1.5 h. The suspension was filtered through Celite® and the solvent was evaporated to give **50** (51 mg, 84%) as a dark brown solid: $R_f$ = 0.3 ($CH_2Cl_2$); mp 155-156°C; IR $\nu_{max}$ 3331 (NH), 1704 (C=O); $^1$H NMR ($CDCl_3$) δ 1.61 (9 H, s, Bu$^t$), 5.06 (2 H, s, $NH_2$), 6.10 (1 H, s, 2-H), 7.58 (1 H, t, *J* = 7.2 Hz, 6-H), 7.65 (1 H, t, *J* = 6.9 Hz, 7-H), 8.09 (1 H, d, *J* = 7.6 Hz, 5-H), 8.29 (1 H, d, *J* = 7.7 Hz, 8-H); $^{13}$C NMR [($CDCl_3$) (HSQC / HMBC)] δ 28.23 (C*Me*$_3$), 82.26 (*C*Me$_3$), 99.01 (2-C), 125.78 (8-C), 126.33 (5-C), 130.41 (4a-C), 131.27 (6-C), 133.62 (7-C), 134.84 (8a-C), 144.84 (3-C), 157.13 (1-C), 162.94 (Boc C=O), 180.70 (4-C); MS ($ES^+$) *m/z* 567.2262 (2 M + Na) ($C_{15}H_{16}N_2NaO_3$ requires 567.2220), 295.1052 (M + Na) ($C_{15}H_{16}N_2NaO_3$ requires 295.1059).

## 5.11 *tert*-Butyl N-(4-oxo-3-(2,2,2-trifluoroacetamido)naphthalen-1-ylidene)-carbamate (52)

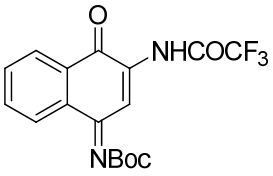


$K_2CO_3$ (178 mg 1.3 mmol) and sodium dithionite (198 mg, 1.1 mmol) in water (4 mL) were added dropwise to **42** (75 mg, 0.25 mmol) in $CH_2Cl_2$ (8 mL) and water (1 mL) under $N_2$. Stirring was continued for 16 h at 35°C. The mixture was dried and filtered. The filtrate was cooled to 0°C. $Pr^i_2NEt$ (580 mg, 4.5 mmol) was added followed by dropwise addition of trifluoroacetic anhydride (315 mg, 1.5 mmol). The mixture was stirred at 0°C for 15 min then allowed to warm to 20°C. Stirring was continued for 2 h. The mixture was washed with water and brine and dried. Evaporation and chromatography (petroleum ether / EtOAc 9:1) gave **52** (39 mg, 42%) as a yellow solid: $R_f$ = 0.6 (petroleum ether / EtOAc 4:1); mp 122-123°C; IR $\nu_{max}$ 3290, 3097 (NH), 1744 (C=O); $^1$H NMR ($CDCl_3$) δ 1.66 (9 H, s, Bu$^t$), 7.71 (1 H, ddd, *J* = 9.0, 7.7, 1.9 Hz, 6-H), 7.78 (1 H, ddd, *J* = 8.9, 7.4, 1.5 Hz, 7-H), 8.13 (1 H,

s, 2-H), 8.19 (1 H, dd, *J* = 7.7, 1.1, Hz, 5-H), 8.36 (1 H, dd, *J* = 7.8, 0.9 Hz, 8-H), 9.17 (1H, s, NH); $^{13}$C NMR [($CDCl_3$) (HSQC / HMBC)] δ 28.13 (C*Me*$_3$), 84.22 (*C*Me$_3$), 114.57 (2-C), 114.72 (q, *J* = 288.4 Hz, $CF_3$), 126.11 (8-C), 127.12 (5-C), 129.40 (4a-C), 132.45 (6-C), 133.67 (3-C), 134.80 (7-C), 135.00 (8a-C), 155.28 (Boc C=O), 155.57 (q, *J* = 39.2 Hz, $CF_3$C=O), 161.36 (1-C), 178.63 (4-C); $^{19}$F NMR ($CDCl_3$) δ -75.76 (s, $CF_3$); MS ($ES^-$) *m/z* 367.0941 (M - H) ($C_{17}H_{14}F_3N_2O_4$ requires 367.0906).

### 5.12 2,4-Dinitronaphthalen-1-yl trifluoromethanesulfonate (53)

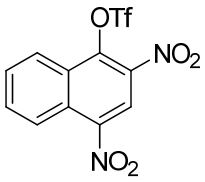


2,4-Dinitronaphthalen-1-ol **24** (501 mg, 2.14 mmol) and $Et_3N$ (562 mg, 5.6 mmol) in $CH_2Cl_2$ (10 mL) were cooled in an ice bath and treated dropwise with trifluoromethanesulfonic anhydride (784 mg, 2.8 mmol). The mixture was stirred at 20°C for 2 h under $N_2$. Aq. HCl (0.5 M, 10 mL) was added in one portion and the mixture was stirred for 30 min. The aqueous phase was separated and extracted with $CH_2Cl_2$. The combined organic phases were washed with sat. aq. $NaHCO_3$ and brine. Drying, evaporation and chromatography ($CH_2Cl_2$) gave **53** (484 mg, 62%) as a yellow solid: $R_f$ = 0.9 ($CH_2Cl_2$); mp 117-119°C (lit.[79] mp 105-107°C); IR $\nu_{max}$ 1532 ($NO_2$), 1365 ($SO_2$-O-), 1349 ($NO_2$); $^1$H NMR [$(CD_3)_2SO$] δ 7.72 (1 H, ddd, *J* = 8.2, 7.1, 1.0 Hz, 7-H), 7.91 (1 H, ddd, *J* = 8.4, 7.0, 1.4 Hz, 6-H), 8.51 (1 H, d, *J* = 8.4 Hz, 8-H), 8.57 (1 H, d, *J* = 8.6 Hz, 5-H), 8.87 (1 H, s, 3-H); $^{13}$C NMR [$(CD_3)_2SO$) (HSQC / HMBC)] δ 120.65 (q, *J* = 322.3 Hz, $CF_3$), 122.31 (3-C), 123.32 (5-C), 125.58 (8-C), 127.49 (2-C), 127.76 (8a-C, 7-C), 128.00 (4a-C), 133.09 (6-C), 134.75 (4-C), 158.70 (1-C); $^{19}$F NMR ($CDCl_3$) δ -71.85 (s, $CF_3$).

### 5.13 1-Iodo-2,4-dinitronaphthalene (54)

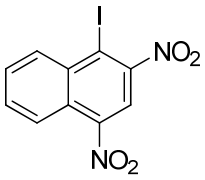


2,4-Dinitronaphthalen-1-yl trifluoromethanesulfonate **53** (4.28 g, 11.7 mmol) was heated under reflux with NaI (5.99 g, 40 mmol) in acetone (170 mL) for 2 h. The evaporation residue, in EtOAc, was washed with sat. aq. $Na_2S_2O_3$ and dried. Evaporation and chromatography ($CH_2Cl_2$) gave **54** (2.98 g, 74%) as yellow solid: $R_f$ = 0.8 ($CH_2Cl_2$ / petroleum ether 1:1); mp 183-186°C (lit.[79] mp 194-195°C); IR $\nu_{max}$ 1530 ($NO_2$), 1333($NO_2$); $^1$H NMR [$(CD_3)_2SO$)] δ 7.98 (2 H, m, 6-H, 7-H), 8.32 (1 H, dd, *J* = 7.1, 1.7 Hz, 5-H), 8.52 (1 H, dd, *J* = 7.7, 2.0 Hz, 8-H), 8.73 (1 H, s, 3-H); $^{13}$C NMR [$(CD_3)_2SO$) (HSQC / HMBC)] δ 102.55 (1-C), 117.53 (3-C), 123.35 (5-C), 124.01 (4a-C), 131.39 (6-C), 132.32 (7-C), 135.07 (8-C), 135.12 (8a-C), 147.21 (4-C), 151.91 (2-C).

### 5.14 Naphthalene-1,3-diamine (58)

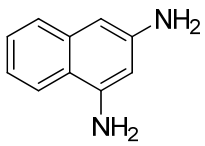

1,3-Dinitronaphthalene **57** (44.1 mg, 0.20 mmol) was stirred in THF (10 mL) and 10 % Pd-C (10 mg) added. The mixture was stirred under $H_2$ for 16 h. The mixture was filtered through Celite® and the solvent evaporated to give **58** (32 mg, 100%) as a dark solid: $R_f$ = 0.3 (EtOAc / $CH_2Cl_2$ 1:4); $^1$H NMR ($CDCl_3$) δ 3.71 (2 H, s, $NH_2$), 4.08 (2 H, s, $NH_2$), 6.23 (1 H, d, *J* = 2.1 Hz, 2-H), 6.50 (1 H, d, *J* = 1.9 Hz, 4-H), 7.18 (1 H, ddd, *J* = 8.2, 6.8, 1.2 Hz, 7-H), 7.34 (1 H, ddd, *J* = 8.0, 6.8, 1.0 Hz, 6-H), 7.53 (1 H, d, *J* = 8.2 Hz, 5-H), 7.64 (1 H, d, *J* = 8.4 Hz, 8-H); $^{13}$C NMR [($CDCl_3$) (HSQC / HMBC)] δ 100.67 (4-C), 100.58 (2-C), 118.65 (8a-C), 120.67 (8-C), 121.36 (7-C), 126.39 (5-C or 6-C), 126.42 (6-C or 5-C), 136.01 (4a-C), 143.28 (1-C), 144.71 (3-C).

### 5.15 N,N'-Bis(*tert*-butoxycarbonyl)naphthalene-1,3-diamine (59)

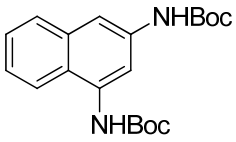

1-Iodo-2,4-dinitronaphthalene **54** (1.05 g, 2.9 mmol) and $SnCl_2.2H_2O$ (9.84 g, 44 mmol) in EtOAc (100 mL) were heated under reflux for 17 h. The mixture was added to ice and $NaHCO_3$ was added until the aqueous layer was basic. The mixture was extracted with EtOAc, washed with water and dried. Evaporation gave crude naphthalene-1,3-diamine **58**. This material was boiled under reflux with $Boc_2O$ (3.11 g, 14.2 mmol) in THF (30 mL) for 17 h. Evaporation and chromatography ($CH_2Cl_2$) gave **59** (769 mg, 74%) as a pale buff solid: $R_f$ = 0.7 ($CH_2Cl_2$); mp 127-130°C (lit.[79] mp 129-131°C); IR $\nu_{max}$ 3254 (NH), 1716 (C=O), 1685 (C=O); $^1$H NMR [($CDCl_3$) (NOESY)] δ 1.54 (9 H, s, $Bu^t$), 1.56 (9 H, s, $Bu^t$), 6.63 (1 H, s, NH), 6.91 (1 H, s, NH), 7.34 (1 H, ddd, *J* = 8.1, 6.8, 1.3 Hz, 7-H), 7.44 (1 H, ddd, *J* = 7.9, 6.9, 1.1 Hz, 6-H), 7.73 (1 H, d, *J* = 8.2, 8-H), 7.77 (2 H, m, 4,5-$H_2$), 7.93 (1 H, s, 2-H); $^{13}$C NMR [($CDCl_3$) (HSQC / HMBC)] δ 28.37 (2 × C*Me*$_3$), 80.63 (*C*Me$_3$), 80.92 (*C*Me$_3$), 110.65 (2-C, 5-C), 119.69 (8-C), 122.5 (8a-C), 124.41 (7-C), 126.49 (6-C), 128.52 (4-C), 133.76 (1-C), 134.82 (5a-C), 135.81 (3-C), 152.76 (C=O), 153.13 (C=O).

### 5.16 N,N'-Bis(*tert*-butoxycarbonyl)-1-iodonaphthalene-2,4-diamine (25)

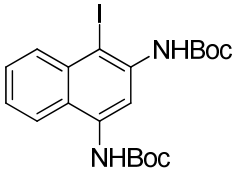

Compound **59** (417 mg, 1.28 mmol) was treated with N-iodosuccinimide (431 mg, 1.9 mmol) and TsOH.$H_2O$ (457 mg, 2.4 mmol) in THF / MeOH (14 mL, 1:1) at −78°C. The mixture was allowed to slowly warm to 20°C over 4 h and was then diluted with aq. $Na_2S_2O_3$ (5%) and stirred at 20°C for 15 min. The mixture was extracted with EtOAc. The

combined organic extracts were dried and the solvents were evaporated. Chromatography ($CH_2Cl_2$) gave **25** (400 mg, 71%) as a pale buff solid: $R_f$ = 0.4 ($CH_2Cl_2$); mp 166-168°C (lit.[79] mp 154-156°C); IR $\nu_{max}$ 3384 (NH), 3229 (NH), 1733(C=O), 1683 (C=O); $^1$H NMR [($CDCl_3$)] δ 1.55 (9 H, s, Bu$^t$), 1.57 (9 H, s, Bu$^t$), 6.86 (1 H, s, 4-NH), 7.17 (1 H, s, 2-NH), 7.43 (1 H, dd, *J* = 6.9, 1.1 Hz, 6-H), 7.51 (1 H, dd, *J* = 6.8, 1.1 Hz, 7-H), 7.76 (1 H, d, *J* = 8.2 Hz, 5-H), 8.09 (1 H, d, *J* = 8.4 Hz, 8-H), 8.62 (1 H, s, 3-H); $^{13}$C NMR [($CDCl_3$) (HSQC / HMBC)] δ 28.38 (2 × C*Me*$_3$), 81.03 (*C*Me$_3$), 81.28 (*C*Me$_3$), 87.36 (1-C), 113.71 (3-C), 121.40 (5-C), 124.88 (4a-C), 125.32 (6-C), 128.15 (7-C), 132.58 (8-C), 134.65 (4-C or 8a-C), 134.82 (8a-C or 4-C), 138.22 (2-C), 152.68 (C=O), 153.21 (C=O).

## 5.17 Selective de-iodination of N,N'-Bis(*tert*-butoxycarbonyl)-1-iodonaphthalene-2,4-diamine (25)

Compound **25** (51.9 mg, 0.11 mmol) in $CH_2Cl_2$ (10 mL) was stirred with $CF_3CO_2H$ in $CH_2Cl_2$ (1.0 mL, 8.5μL mL$^{-1}$, 0.11 mmol). The mixture was stirred for 7 d. Additional $CF_3CO_2H$ in $CH_2Cl_2$ (1.0 mL, 8.5μL mL$^{-1}$, 0.11 mmol) was added at 48 h, 72 h, 96 h and 120 h. The mixture was diluted with water and extracted with $CH_2Cl_2$. Drying, evaporation and chromatography ($CH_2Cl_2$) gave **59** (28.2 mg, 72%) as a pale buff solid with properties as above.

## 5.18 *tert*-Butyl N-(1-aminonaphthalen-3-yl)carbamate (62)

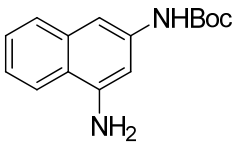


Compound **25** (287 mg, 0.56 mmol) was stirred with HCl in dioxane (4.0 M, 10 mL) for 45 min. The solid was collected by filtration, washed with HCl in dioxane (4.0 M) and dried to give a brown solid (157 mg). This material (54 mg) was suspended in dry THF (2 mL) and stirred under $N_2$. Pr$^i_2$NEt (0.10 mL, 77 mg, 0.60 mmol) was added, followed by dropwise addition of $Boc_2O$ (34 mg, 0.16 mmol) in dry THF (1.0 mL) during 15 min. The reaction was stirred under $N_2$ for 10 d. Water was added and the mixture was concentrated under reduced pressure. The mixture was extracted with EtOAc. The extract was washed with water and sat. aq. $Na_2S_2O_3$. Drying, evaporation and chromatography ($CH_2Cl_2$ / EtOAc 9:1) gave **62** (8.1 mg, 6%) as a yellow solid: $^1$H NMR [($CDCl_3$) (NOESY)] δ 1.54 (9 H, s, Bu$^t$), 6.57 (1 H, s, NH), 6.90 (1 H, s, 2-H), 7.29 (1 H, s, 4-H), 7.32 (1 H, ddd, *J* = 8.2, 6.9, 1.2 Hz, 7-H), 7.40 (1 H, ddd, *J* = 7.9, 6.9, 1.0 Hz, 6-H), 7.68 (1 H, d, *J* = 8.1 Hz, 5-H), 7.71 (1 H, d, *J* = 8.4 Hz, 8-H); $^{13}$C NMR [($CDCl_3$) (HSQC / HMBC)] δ 28.35 (C*Me*$_3$), 80.52 (*C*Me$_3$), 102.52 (2-C),

105.75 (4-C), 120.50 (8a-C), 120.58 (8-C), 122.39 (7-C), 126.48 (6-C), 127.88 (5-C), 134.94 (4a-C), 136.41 (3-C), 142.81 (1-C), 152.78 (C=O); MS ($ES^+$) *m/z* 281.1269 (M + Na) ($C_{15}H_{18}N_2NaO_2$ requires 281.1266), 259.1443 (M + H) ($C_{15}H_{19}N_2O_2$ requires 259.1447).

### 5.19 1,3-Bis(trifluoroacetamido)naphthalene (63)

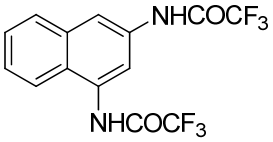


Compound **58** (32.0 mg, 0.20 mmol) was stirred in dry THF (2 mL) under $N_2$ at 0°C. $Pr^i_2NEt$ (0.14 mL, 104 mg, 0.81 mmol) was added followed by dropwise addition of trifluoroacetic anhydride (0.03 mL, 45.3 mg, 0.20 mmol) during 30 min. The reaction was stirred at 0°C and allowed to warm slowly to 20°C over 16 h. Water was added to the reaction and the solvent was evaporated. The residue was dissolved in EtOAc. This solution was washed with water and brine. Drying, evaporation and chromatography ($CH_2Cl_2$ / EtOAc 19:1) gave **63** (19 mg, 26%) as a yellow solid: $R_f$ 0.8 ($CH_2Cl_2$); mp 214-216ºC; IR $\nu_{max}$ 3345, 3258 (NH), 1716 (C=O); $^1$H NMR [$(CD_3)_2SO$) (NOESY)] δ 7.66 (2 H, m, 6,7-$H_2$), 7.91 (2 H, m, 2,8-$H_2$), 8.06 (1 H, m, 5-H), 8.40 (1 H, d, *J* = 1.8 Hz, 4-H), 11.62 (2 H, s, NH); $^{13}$C NMR [$(CD_3)_2SO$) (HSQC / HMBC)] δ 115.73 (q, *J* = 288.7 Hz, $CF_3$), 116.12 (q, *J* = 288.7 Hz, $CF_3$), 118.18 (4-C), 118.73 (2-C), 122.41 (8-C), 126.33 (8a-C), 126.46 6-C or 7-C), 127.39 (7-C or 6-C), 128.28 (5-C), 131.40 (4a-C), 133.39 (3-C), 133.59 (1-C), 154.82 (q, *J* = 37.1 Hz, C=O), 156.03 (q, *J* = 36.7 Hz, C=O); $^{19}$F NMR [$(CD_3)_2SO$] δ -73.85 (3 F, s, $CF_3$), -73.72 (3 F, s, $CF_3$); MS ($ES^-$) *m/z* 349.0442 (M - H) ($C_{14}H_7F_6N_2O_2$ requires 349.0412).

### 5.20 N-(1-aminonaphthalen-3-yl)-2,2,2-trifluoroacetamide (65)

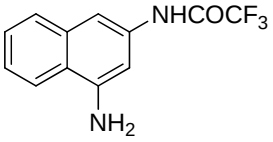


Compound **58** (1.29 g, 8.16 mmol) was stirred in dry THF (100 mL) under $N_2$ at 0°C. $Pr^i_2NEt$ (5.70 mL, 4.23 g, 32.6 mmol) was added followed by dropwise addition of a solution of trifluoroacetic anhydride (1.13 mL, 1.71 g, 8.16 mmol) in dry THF (100 mL) during 2 h. The mixture was allowed to slowly warm to 20°C during 16 h. The solvent was evaporated and the residue dissolved in EtOAc. This solution was washed with water and brine. Drying, evaporation and chromatography (petroleum ether / EtOAc 9:1 → 1:1) gave **65** (309 mg, 15%) as a buff solid: $R_f$ = 0.5 ($CH_2Cl_2$ / EtOAc 4:1); mp 168-169°C; IR $\nu_{max}$ 3482, 3374, 3324 (NH), 1721, 1706 (C=O); $^1$H NMR [$(CD_3)_2SO$)] δ 5.99 (2 H, s, $NH_2$), 7.01 (1 H, d, *J* = 2.0 Hz, 2-H), 7.39 (1 H, ddd, *J* = 8.2, 6.8, 1.3 Hz, 7-H), 7.47 (1 H, ddd, *J* = 8.1, 6.8, 1.2 Hz, 6-H), 7.49 (1 H, d, *J* = 1.4 Hz, 4-H), 7.75 (1 H, d, *J* = 7.7 Hz, 5-H), 8.10 (1 H, d, *J* = 8.4

Hz, 8-H), 11.17 (1 H, s, NH); $^{13}$C NMR [$(CD_3)_2SO$) (HSQC / HMBC)] δ 101.31 (2-C), 106.51 (4-C), 115.88 (q, *J* = 289.0 Hz, $CF_3$), 120.89 (8a-C), 122.24 (8-C), 123.46 (7-C), 126.34 (6-C), 127.78 (5-C), 134.09 (4a-C), 134.67 (3-C), 145.56 (1-C), 154.41 (q, *J* = 36.6 Hz, C=O); $^{19}$F NMR [$(CD_3)_2SO$] δ -73.69 (s, $CF_3$); MS ($ES^+$) *m/z* 277.0554 (M + Na) ($C_{12}H_9F_3N_2NaO$ requires 277.0565).

### 5.21 *tert*-Butyl N-(3-trifluoroacetamidonaphthalen-1-yl)carbamate (66)

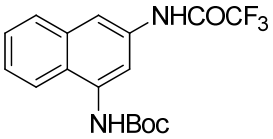


Compound **65** (330 mg, 1.30 mmol) was boiled under reflux with $Boc_2O$ (1.43 g, 6.55 mmol) in dry THF (10 mL) under $N_2$ for 16 h. Evaporation and chromatography (petroleum ether → petroleum ether / EtOAc 19:1) gave **66** (381 mg, 83%) as a pale buff solid.

$R_f$ = 0.4 (petroleum ether / EtOAc 4:1); mp 206-208ºC; IR $\nu_{max}$ 3297 (NH), 3244 (NH), 1711 (C=O), 1683 (C=O); $^1$H NMR [$(CD_3)_2SO$) (NOESY)] δ 1.57 (9 H, s, $Bu^t$), 7.54 (1 H, td, *J* = 6.8, 1.4 Hz, 7-H), 7.58 (1 H, td, *J* = 6.8, 1.2 Hz, 6-H), 7.94 (1 H, d, *J* = 8.1 Hz, 5-H), 8.00 (1 H, d, *J* = 2.0 Hz, 2-H), 8.13 (1 H, d, *J* = 8.2 Hz, 8-H), 8.20 (1 H, d, *J* = 1.8 Hz, 4-H), 9.39 (1 H, s, NHBoc), 11.50 (1 H, s, $NHCOCF_3$); $^{13}$C NMR [$(CD_3)_2SO$) (HSQC / HMBC)] δ 28.13 (C*Me*$_3$), 79.26 (*C*$Me_3$)), 114.63 (2-C), 114.73 (4-C), 115.79 (q, *J* = 288.8 Hz, $CF_3$), 122.64 (8-C), 125.27 (8a-C), 125.33 (7-C), 126.75 (6-C), 128.03 (5-C), 133.52 (4-C), 133.56 (3-C), 134.92 (1-C), 153.76 (Boc C=O), 154.68 (q, *J* = 37.1 Hz, $CF_3$*C*=O); $^{19}$F NMR [$(CD_3)_2SO$] δ -73.76 (s, $CF_3$); MS ($ES^+$) *m/z* 377.1120 (M + Na) ($C_{17}H_{17}F_3N_2NaO_3$ requires 377.1089).

### 5.22 *tert*-Butyl N-(1-iodo-2-(trifluoroacetamidonaphthalen-4-yl)carbamate (67)

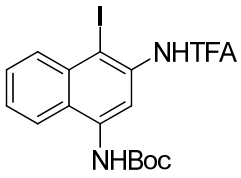


Compound **66** (336 mg, 0.95 mmol) in dry THF (10 mL) was cooled to −78°C and stirred under $N_2$. NIS (309 mg, 1.4 mmol) in dry THF (2.0 mL) was added followed by $TsOH.H_2O$ (370 mg, 1.9 mmol) in dry THF (2.0 mL). The temperature of the mixture was allowed to rise slowly to 20°C over 20 h. The reaction was quenched by addition of sat. aq. $NaHCO_3$. The mixture was diluted with water and extracted with EtOAc. Drying, evaporation and chromatography (petroleum ether → petroleum ether / EtOAc 4:1) gave **67** (344 mg, 75%) as a pale buff solid: $R_f$ = 0.6 ($CH_2Cl_2$); mp 198-199°C; IR $\nu_{max}$ 3323, 3209 (NH), 1721 (C=O), 1698 (C=O); $^1$H NMR [($CDCl_3$) (NOESY)] δ 1.57 (9 H, s, $Bu^t$), 6.95 (1 H, s, Boc NH), 7.54-7.61 (2 H, m, 6,7-$H_2$), 7.82 (1 H, d, *J* = 8.1 Hz, 5-H), 8.14 (1 H, d, *J* = 8.6 Hz, 8-H), 8.58 (1 H, s, $NHCOCF_3$), 8.71 (1 H, s, 3-H); $^{13}$C NMR [($CDCl_3$) (HSQC / HMBC)] δ 28.31 (C*Me*$_3$),

81.63 (*C*$Me_3$), 89.87 (1-C), 113.26 (3-C), 115.77 (q, *J* = 289.3 Hz, $CF_3$), 121.09 (5-C), 125.43 (4a-C), 126.86 (6-C), 128.73 (7-C), 133.17 (8-C), 134.52 (8a-C), 134.90 (4-C), 135.20 (2-C), 152.82 (Boc C=O), 155.05 (q, *J* = 38.0 Hz, $CF_3$*C*=O); $^{19}$F NMR [$(CD_3)_2SO$] δ -74.13 (s, $CF_3$); MS ($ES^+$) *m/z* 503.0100 (M + Na) ($C_{17}H_{16}F_3IN_2NaO_3$ requires 503.0055), 498.0542 (M + $^+NH_4$) ($C_{17}H_{20}F_3IN_3O_3$ requires 498.0500).

## 5.23 Wheland-like intermediates in the de-iodination of N,N'-Bis(*tert*-butoxycarbonyl)-1-iodonaphthalene-2,4-diamine (25) in acidic media

To compound **25** (14.7 mg, 28 μmol) was added a mixture of $CDCl_3$ (0.15 mL) and $CF_3CO_2H$ (0.45 mL) at 0°C. The sample was transferred to an NMR spectrometer, with the probe pre-cooled to 0°C. The mixture was kept at 0°C for 2 h to give **68**. The mixture was allowed to slowly warm to 20°C and kept at this temperature for 2 h to give **69**.

### 5.23.1 1-Iodonaphthalene-2,4-diammonium (68)

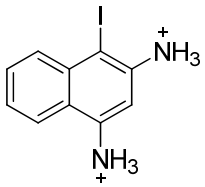


$^1$H NMR ($CF_3CO_2H$ / $CDCl_3$ 3:1) δ 7.95 (1 H, t, *J* = 8.5 Hz, 6-H), 7.98 (1 H, t, *J* = 7.0 Hz, 7-H), 8.05 (1 H, d, *J* = 8.0 Hz, 5-H), 8.11 (1 H, s, 3-H), 8.48 (1 H, d, *J* = 8.5 Hz, 8-H); $^{13}$C NMR [($CF_3CO_2H$ / $CDCl_3$ 3:1) (HSQC / HMBC)] δ 101.74 (1-C), 116.88 (3-C), 120.91 (5-C), 126.58 (4a-C), 127.73 (4-C), 129.30 (2-C), 131.75 (6-C), 132.30 (7-C), 134.69 (8-C), 135.92 (8a-C).

### 5.23.2 2-Imino-1-iodo-1,2-dihydronaphthalen-4-ammonium (69)

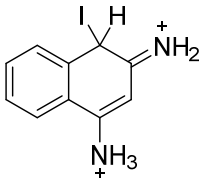


$^1$H NMR ($CF_3CO_2H$ / $CDCl_3$ 3:1) δ 6.05 (1 H, s, 3-H), 6.51 (1 H, s, 1-H), 7.58 (1 H, t, *J* = 7.4 Hz, 6-H), 7.70 (1 H, t, *J* = 7.4 Hz, 7-H), 7.75 (1 H, d, *J* = 7.8 Hz, 8-H), 7.84 (1 H, d, *J* = 8.0 Hz, 5-H); $^{13}$C NMR [($CF_3CO_2H$ / $CDCl_3$ 3:1) (HSQC / HMBC)] δ 9.76 (1-C), 91.48 (3-C), 121.68 (4a-C), 124.18 (5-C), 129.94 (6-C), 131.47 (8-C), 134.99 (7-C), 141.24 (8a-C), 164.01 (4-C), 173.43 (2-C).

The above reaction was repeated using $CF_3CO_2D$ to investigate the source of proton in the Wheland-like intermediate **69**. To compound **25** (14.7 mg, 28 μmol) was added a mixture of $CDCl_3$ (0.15 mL) and $CF_3CO_2D$ (0.45 mL) at 0°C. The sample was transferred to an NMR spectrometer, with the probe pre-cooled to 0°C. The mixture was kept at 0°C for 2 h to give **70**. The mixture was allowed to slowly warm to 20°C and kept at this temperature for 2 h to

give **71**. An attempt to undertake mass spectrometry on sample **71** resulted in the identification of **72**.

### 5.23.3 Deuterated 1-iodonaphthalene-2,4-diammonium (70)

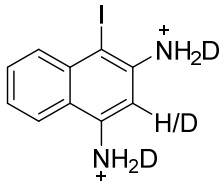


$^1$H NMR ($CF_3CO_2D$ / $CDCl_3$ 3:1) δ 7.95 (1 H, t, *J* = 8.5 Hz, 6-H), 7.98 (1 H, t, *J* = 7.0 Hz, 7-H), 8.05 (1 H, d, *J* = 8.0 Hz, 5-H), 8.11 (0.3 H / 0.7 D, s, 3-H), 8.48 (1 H, d, *J* = 8.5 Hz, 8-H); $^{13}$C NMR [($CF_3CO_2D$ / $CDCl_3$ 3:1) (HSQC / HMBC)] δ 101.62 (1-C), 116.88 (3-C), 120.95 (5-C), 126.66 (4a-C), 127.75 (4-C), 129.38 (2-C), 131.78 (6-C), 132.29 (7-C), 134.73 (8-C), 136.03 (8a-C).

### 5.23.4 Deuterated 2-imino-1-iodo-1,2-dihydronaphthalen-4-ammonium (71)

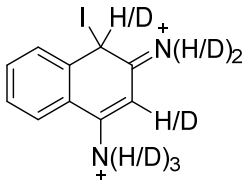


$^1$H NMR ($CF_3CO_2D$ / $CDCl_3$ 3:1) δ 6.06 (0.07 H / 0.93 D , s, 3-H), 6.50 (0.2 H / 0.8 D, s, 1-H), 7.59 (1 H, t, J = 7.8 Hz, 6-H), 7.70 (1 H, t, *J* = 7.5 Hz, 7-H), 7.76 (1 H, d, *J* = 7.8 Hz, 8-H), 7.84 (1 H, d, *J* = 8.0 Hz, 5-H); $^{13}$C NMR [($CF_3CO_2D$ / $CDCl_3$ 3:1) (HSQC / HMBC)] δ 9.55 (t, *J* = 22.9 Hz, 1-C), 90.64 (m, 3-C), 121.66 (4a-C), 124.19 (5-C), 129.98 (6-C), 131.48 (8-C), 135.02 (7-C), 141.18 (8a-C), 163.75 (4-C), 173.09 (2-C).

### 5.23.5 Deuterated naphthalene-1,3-diamine (72)

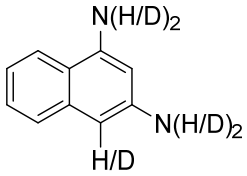


MS ($ES^+$) *m/z* 159.0921 (32.8%) (M + H) ($C_{10}H_{11}N_2$ requires 159.0922), 160.0991 (M + H) (86.1%) ($C_{10}H_{10}DN_2$ requires 160.0985), 161.1054 (M + H) (100%) ($C_{10}H_9D_2N_2$ requires 161.1048), 162.1114 (M + 1) (55%) ($C_{10}H_8D_3N_2$ requires 162.1111).

## 5.24 Wheland-like intermediates from naphthalene-1,3-diamine in acidic media

To naphthalene-1,3-diamine **58** (14.7 mg, 67 μmol) was added a mixture of $CDCl_3$ (0.15 mL) and $CF_3CO_2H$ (0.45 mL) at 0°C. The sample was transferred to an NMR spectrometer, with the probe pre-cooled to 0°C. The mixture was kept at 0°C for 20 min to give **73**. The reaction was then allowed to slowly rise from 0°C → 20°C and kept at 20°C for 2 d to give **74**.

### 5.24.1 Naphthalene-1,3-diammonium (73)

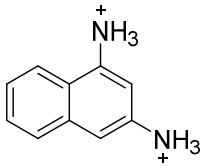

$^1$H NMR ($CF_3CO_2H$ / $CDCl_3$ 3:1) δ 7.87 (1 H, t, *J* = 8.8 Hz, 6-H), 7.91 (1 H, t, *J* = 7.7 Hz, 7-H), 7.98 (1 H, d, *J* = 2.0 Hz, 2-H), 8.04 (1 H, d, *J* = 8.1 Hz, 8-H), 8.10 (1 H, d, *J* = 8.8 Hz, 5-H), 8.21 (1 H, d, *J* = 1.6, 4-H); $^{13}$C NMR [($CF_3CO_2H$ / $CDCl_3$ 3:1) (HSQC / HMBC)] δ 116.65 (2-C), 119.99 (8-C), 125.51 (3-C), 125.96 (4-C), 126.64 (8a-C), 127.33 (1-C), 129.90 (5-C), 130.56 (6-C), 131.20 (7-C), 134.27 (4a-C).

### 5.24.2 3-Imino-3,4-dihydronaphthalen-1-ammonium (74)

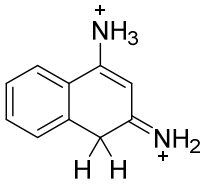

$^1$H NMR ($CF_3CO_2H$ / $CDCl_3$ 3:1) δ 4.13 (2 H, s, 4-$H_2$), 6.02 (1 H, s, 2-H), 7.51 (1 H, d, *J* = 7.8 Hz, 5-H), 7.57 (1 H, t, *J* = 7.7 Hz, 7-H), 7.71 (1 H, t, *J* = 7.6 Hz, 6-H), 7.82 (1 H, d, *J* = 8.1 Hz, 8-H); $^{13}$C NMR [($CF_3CO_2H$ / $CDCl_3$ 3:1) (HSQC/ HMBC)] δ 33.28 (4-C), 93.53 (2-C), 123.03 (8a-C), 123.15 (8-C), 128.83 (7-C), 129.27 (5-C), 134.33 (6-C), 136.63 (4a-C).165.70 (1-C), 171.90 (3-C).

The above procedure was repeated using $CF_3CO_2D$. To naphthalene-1,3-diamine **58** (14.7 mg, 67 µmol) was added a mixture of $CDCl_3$ (0.15 mL) and $CF_3CO_2D$ (0.45 mL) at 20°C for 6 d to give a mixture of **75** and **76**. NMR showed deuterium exchange at 2-C and 4-C.

### 5.24.3 Deuterated naphthalene-1,3-diammonium (75)

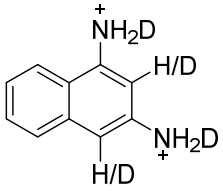

$^1$H NMR ($CF_3CO_2D$ / $CDCl_3$ 3:1) δ 7.90 (1 H, t, *J* = 7.0 Hz, 6-H), 7.94 (1 H , t, *J* = 7.0 Hz, 7-H), 8.05 (0.2 H / 0.8 D, s, 2-H/D), 8.10 (1 H, d, *J* = 8.3 Hz, 8-H), 8.14 (1 H, d, *J* = 8.0 Hz, 5-H), 8.28 (0.2 H / 0.8 D, s, 4-H/D); $^{13}$C NMR [($CF_3CO_2D$ / $CDCl_3$ 3:1) (HSQC / HMBC)] δ 116.63 (2-C), 120.07 (8-C), 125.17-125.31 (3-C), 125.75 (brt, 4-CD), 126.04 (4-CH), 126.74 (8a-C), 127.11-127.18 (1-C), 129.90-129.95 (5-C), 130.59 (6-C), 131.27 (7-C), 134.30, 134.35 (4a-C).

### 5.24.4 Deuterated 3-imino-3,4-dihydronaphthalen-1-ammonium (76)

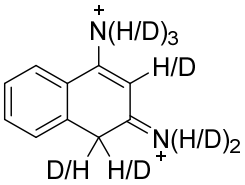

$^1$H NMR ($CF_3CO_2D$ / $CDCl_3$ 3:1) δ 4.11 (0.4 H / 1.6 D, s, 4-CHD), 6.04 (0.25 H / 0.75 D, s, 2-H/D), 7.55 (1 H, d, *J* = 7.8 Hz, 5-H), 7.61 (1 H, t, *J* = 7.8 Hz, 7-H), 7.74 (1 H, t, *J* = 7.6 Hz, 6-H), 7.87 (1 H, d, *J* = 8.2 Hz, 8-H); $^{13}$C NMR [($CF_3CO_2D$ / $CDCl_3$ 3:1) (HSQC / HMBC)] δ

32.74 (sextet, *J* = 20.0 Hz, 4-C), 92.98 (t, *J* = 24.5 Hz, 2-CD), 93.21 (t, *J* = 24.5 Hz, 2-CH), 123.04 (8a-C), 123.21 (8-C), 128.84 (7-C), 129.29 (5-C), 134.42 (6-C), 136.66 (m, 4a-C), 165.72 (1-C), 171.84 (3-C).

## 5.25 De-iodination of *tert*-butyl (4-iodo-3-(2,2,2-trifluoroacetamido)naphthalen-1-yl)carbamate (67) in acidic media

To compound **67** (16.2 mg, 34 µmol) was added a mixture of $CDCl_3$ (0.15 mL) and $CF_3CO_2H$ (0.45 mL) at 0°C. The sample was transferred to an NMR spectrometer, with the probe pre-cooled to 0°C. The mixture was kept at 0°C for 2 h to give **77**.

### 5.25.1 N-(4-Ammonium-1-iodonaphthalen-2-yl)-2,2,2-trifluoroacetamide (77)

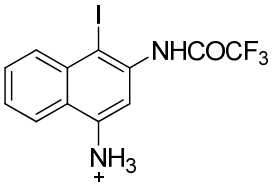


$^1$H NMR ($CF_3CO_2H$ / $CDCl_3$) δ 7.84 (1 H, t, *J* = 7.5 Hz, 6-H), 7.88 (1 H, t, *J* = 7.5 Hz, 7-H), 7.97 (1 H, d, *J* = 8.2 Hz, 5-H), 8.44 (1 H, d, *J* = 8.6 Hz, 8-H), 8.57 (1 H, s, 3-H), 9.24 (1 H, s, NH); $^{13}$C NMR [($CF_3CO_2H$ / $CDCl_3$) (HSQC / HMBC)] δ 99.94 (1-C), 116.71 (3-C), 120.59 (5-C), 125.47 (4a-C), 126.84 (4-C), 130.40 (6-C), 131.41 (7-C), 133.68 (2-C), 134.58 (8-C), 135.78 (8a-C), 158.21 (q, *J* = 39.5 Hz, $CF_3$*C*=O).

The above procedure was repeated with $CF_3CO_2D$ to give **79** at 0°C. The temperature of the reaction was allowed to rise from 0°C → 20ºC and kept at 20°C for 7 d to give **80** with deuterium exchange at 2-C and 4-C.

### 5.25.2 Deuterated N-(4-ammonium-1-iodonaphthalen-2-yl)-2,2,2-trifluoroacetamide (79)

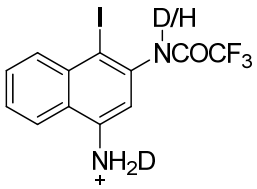


$^1$H NMR ($CF_3CO_2D$ / $CDCl_3$ 3:1) δ 7.84 (1 H, t, *J* = 7.3 Hz, 6-H), 7.88 (1 H, t, *J* = 7.2 Hz, 7-H), 7.96 (1 H, d, J = 8.2 Hz, 5-H), 8.44 (1 H, d, *J* = 8.4 Hz, 8-H), 8.59 (1 H, s, 3-H); $^{13}$C NMR [($CF_3CO_2D$ / $CDCl_3$ 3:1) (HSQC / HMBC)] δ 99.79 (1-C), 116.64 (3-C), 120.56 (5-C), 125.41 (4a-C), 126.49 (4-C), 130.39 (6-C), 131.42 (7-C), 133.64 (2-C), 134.58 (8-C), 135.79 (8a-C).

### 5.25.3 Deuterated N-(1-ammoniumnaphthalen-3-yl)-2,2,2-trifluoroacetamide (80)

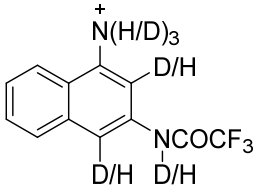


$^1$H NMR ($CF_3CO_2D$ / $CDCl_3$ 3:1) δ 7.76-7.80 (2 H, m, 6,7-$H_2$), 7.95 (1 H, m, 8-H), 8.04 (1 H, m, 5-H), 8.20 (0.2 H / 0.8 D, s 2-H), 8.29 (0.1 H / 0.9 D, s, 4-H), 9.31 (0.05 H / 0.95 D, s, NH); $^{13}$C NMR [($CF_3CO_2H$ / $CDCl_3$ 3:1) (HSQC / HMBC)] δ 116.48 (brt, 2-C), 119.63 (8-C), 122.32-122.90 (brt, 4-C), 125.15 (8a-C), 125.91 (1-C), 129.74 (6-C), 129.79 (5-C), 129.80 (7-C), 131.42 (3-C), 134.81 (4a-C), 157.58 (q, *J* = 39.1 Hz, $CF_3C$=O).

## 5.26 Entrapment of *tert*-butyl cation by trifluoroacetic acid

In each case where deprotection of Boc occurred in the NMR experiments described above, NMR showed that the Bu$^t$ group of **25** and **67** was trapped by the acid to give Bu$^t$ trifluoroacetate **81**. When $CF_3CO_2D$ was used, it was observed that incorporation of deuterium in Bu$^t$ occurred to give **82**.

### 5.26.1 *tert*-Butyl 2,2,2-trifluoroacetate (81)

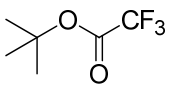


$^1$H NMR ($CF_3CO_2H$ / $CDCl_3$ 3:1) δ 1.63 (9 H, s, Bu$^t$); $^{13}$C NMR [($CF_3CO_2H$ / $CDCl_3$ 3:1) (HSQC)] δ 27.02 (C*Me*$_3$), 90.67 (C*Me*$_3$), 159.45 (q, *J* = 41.9 Hz, C=O).

### 5.26.2 Deuterated *tert*-butyl 2,2,2-trifluoroacetate (82)

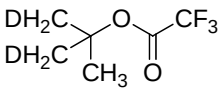


$^1$H NMR ($CF_3CO_2D$ / $CDCl_3$ 3:1) δ 1.61 ($CH_2D$), 1.63 ($CH_3$); $^{13}$C NMR [($CF_3CO_2D$ / $CDCl_3$ 3:1) (HSQC)] δ 26.76 (tt, *J* = 19.9, 3.5 Hz, $CH_2D$), 27.03 (t, *J* = 3.5 Hz, $CH_3$), 90.64 (t, *J* = 5.4 Hz, *C*$CH_3(CH_2D)_2$), 159.53 (q, *J* = 42.0 Hz, C=O).

## 5.27 (2*R*,3*R*)-3-Methyloxiran-2-yl)methanol (90)


Dry $CH_2C1_2$ (200 mL) was stirred at −23°C under $N_2$. To this was added titanium tetraisopropoxide (5.94 mL, 5.68 g, 20 mmol) and (−)-diethyl D-tartrate (3.42 mL, 4.12 g, 20 mmol). The mixture was stirred for 5 min and buten-2-ol **89** (1.7 mL, 1.44 g, 20 mmol) and anhydrous *tert*-butyl hydroperoxide (7.3 mL, 5.5 M in decane, 40 mmol) were added. The mixture was kept at −20°C for 20 h. To this cold mixture was added $Et_2O$ (200 mL) and the mixture was stirred until a homogeneous solution was obtained. Sat. aq. $Na_2SO_4$ (6 mL) was added with vigorous stirring. The resulting slurry was filtered through

Celite® and the solvent was evaporated from the filtrate at 20°C. Chromatography ($Et_2O$ / petroleum ether 1:1 → 4:1) gave **90** (872 mg, 50%) as a colourless oil: $R_f$ = 0.5 ($Et_2O$ / petroleum ether 1:4); IR $\nu_{max}$ 3412 (OH), 3020 (ring CH), 1255 (C-O). $^1$H NMR ($CDCl_3$) δ 1.20 (3 H, d, *J* = 5.2 Hz, Me), 2.76 (1 H, dt, *J* = 5.0, 2.6 Hz, 2-H), 2.89 (1 H, dq, *J* = 10.5, 2.3 Hz, 3-H), 3.21 (1 H, br, OH), 3.45 (1 H, dd, *J* = 12.5, 4.7 Hz, 1-H), 3.72 (1 H, dd, *J* = 12.5, 2.1 Hz, 1-H).

### 5.28 2*R*,3*S* (3-Methyloxiran-2-yl)methyl 4-nitrobenzenesulfonate (91)

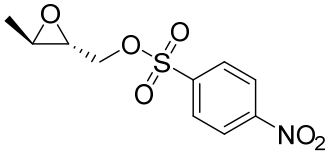

4-Nitrobenzene-1-sulfonyl chloride (903 mg, 4.1 mmol) was added portionwise to a stirred solution of **90** (367 mg, 4.2 mmol) and $Et_3N$ (0.6 mL, 436 mg, 4.3 mmol) in toluene (10 mL) at 0°C. Stirring was continued for 30 min at 20°C and then the mixture was filtered through Celite®. The solvent was evaporated and the residue was purified by column chromatography (petroleum ether / $Et_2O$ 1:1) to give **91** (688 mg, 61%) as a mixture of diastereoisomers. This was dissolved in $Et_2O$ (60 mL) and after removal of about 50% solvent, the white precipitate (the racemate) was filtered off and the solvent was evaporated from the mother liquor. Two crystallisation from $Et_2O$ afforded **91** (121.6 mg, 11%) as a white solid: $R_f$ = 0.6 (petroleum ether / $Et_2O$ 1:1); mp 65-66°C (lit.[81] 65-65.5°C); $[\alpha]^{18}_D$ +26.9° (*c* = 0.41%, $CHCl_3$, 67.7% ee), (lit.[81] $[\alpha]^{25}_D$ +39.68° (*c* = 0.8, $CHCl_3$, 99.8% ee); $^1$H NMR ($CDCl_3$) δ 1.31 (3 H, d, *J* = 5.2 Hz, Me), 2.88-2.95 (2 H, m, 2 × CH), 4.05 (1 H, dd, *J* = 11.4 , 6.2 Hz, SOCH), 4.40 (1 H, dd, *J* = 11.4, 3.2 Hz, SOCH), 8.11 (2 H, d, *J* = 8.7 Hz, Ar 2,6-$H_2$), 8.40 (2 H, d, *J* = 8.7 Hz, Ar 3,5-$H_2$); $^{13}$C NMR [($CDCl_3$) (HSQC / HMBC)] δ 16.84 (Me), 52.60 (CH), 55.23 (CH), 71.23 ($CH_2$), 124.40 (Ar 3,5-$C_2$), 129.22 (Ar 2,6-$C_2$), 141.66 (Ar 1-C), 150.82 (Ar 4-C); MS ($ES^+$) *m/z* 296.0213 (M + Na) ($C_{10}H_{11}NNaO_6S$ requires 296.0205).

### 5.29 (*S*)-Oxiran-2-ylmethyl 4-nitrobenzenesulfonate (93)

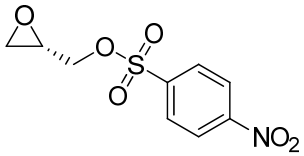

$Et_3N$ (2.3 mL, 1.67 g, 16 mmol) was stirred with *R*-oxiranylmethanol **92** (0.90 mL, 1.00 g, 14 mmol) in toluene at 0°C. This was followed by portionwise addition of 4-nitrobenzenesulfonyl chloride (3.16 g, 14 mmol). The mixture was then stirred at 20°C for 30 min. The suspension was filtered through Celite®. The solvent was evaporated and the residue was dissolved in $CH_2Cl_2$. This solution was washed with aq.

$H_2SO_4$ (2%), sat. aq. $NaHCO_3$ and brine. Drying and evaporation gave a pale yellow solid. The solid was dissolved in dry toluene (20 mL) and the resulting suspension warmed to ~55°C. Hexane was added dropwise till the solution turned cloudy. The resulting solution was cooled to 20°C overnight and then cooled to 0°C for 2 h with stirring. The suspension was filtered through sintered funnel and the precipitate was washed with hexane. Drying gave **93** (1.69 g, 40%) as a white solid: $R_f$ = 0.7 ($Et_2O$); mp 82-83°C (lit.[154] mp 84-86°C); $[\alpha]^{18}_D$ + 33.3°(*c* = 0.65%, $CHCl_3$, > 99% ee), (lit.[154] $[a]^{25}_D$ + 26.5° (*c* = 2.45, $CHCl_3$, 82 % ee]; IR $\nu_{max}$ 3107, 3074 (ring CH); $^1$H NMR ($CDCl_3$) δ 2.60 (1 H, dd, *J* = 4.7, 2.5 Hz, 3-H), 2.83 (1 H, t, *J* = 4.4 Hz, 3-H), 3.20 (1 H, m, 2-H), 4.02 (1 H, dd, *J* =11.6, 6.4 Hz, SOCH), 4.46 (1 H, dd, *J* = 11.6, 2.9 Hz, SOCH), 8.12 (2 H, m, Ph 2,6-$H_2$), 8.40 (2 H, m, Ph 3,5-$H_2$); $^{13}$C NMR [($CDCl_3$) (HSQC / HMBC)] δ 44.42 (3-C), 48.61 (2-C), 71.62 ($SOCH_2$), 124.43 (Ph 3,5-$C_2$), 129.24 (Ph 2,6-$C_2$), 141.59 (Ph 1-C), 150.84 (Ph 4-C).

## 5.30 *tert*-Butyl N-(*R*-1-iodo-2-(N-(oxiranylmethyl)-2,2,2-trifluoroacetamido)naphthalen-4-yl)carbamate (95)

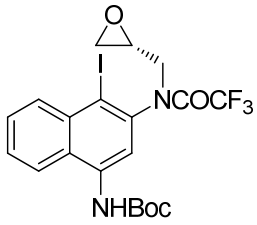


Compound **67** (21 mg, 43 µmol), $K_2CO_3$ (26 mg, 0.19 mmol) and *R*-oxiran-2-ylmethyl 4-nitrobenzenesulfonate **93** (17 mg, 66 µmol) were stirred in acetone (20 mL) at 50°C and stirred under $N_2$ for 3 d. Sat. aq. $NaHCO_3$ was added to the mixture, which was extracted with EtOAc. The organic phase was washed with brine and dried. Evaporation and chromatography (petroleum ether / EtOAc 19:1 → 9:1) gave **95** as two seperable diastereoisomers. Diastereoisomer 1, (7.8 mg, 34%) as a yellow oil: $R_f$ = 0.4 (petroleum ether / EtOAc 4:1). Diastereoisomer 2, (9.08 mg, 39%) as a pale yellow oil: $R_f$ = 0.5 petroleum ether / EtOAc 4:1). With diastereoisomer 2, two rotamers about the $F_3COC$—N were evident by NMR in the ratio 1.3:1 (A:B).

MS ($ES^+$) *m/z* 537.0504 (M +H) ($C_{20}H_{21}F_3IN_2O_4$ requires 537.0498).

**Diastereoisomer 1**

$^1$H NMR [($CDCl_3$) (NOESY)] δ 1.55 (9 H, s, $Bu^t$), 2.78 (1 H, dd, *J* = 4.7, 2.6 Hz, oxirane 3-H), 2.95 (1 H, *t*, J = 4.5 Hz, oxirane 3-H), 3.49 (1 H, m, oxirane 2-H), 4.30 (1 H, dd, *J* = 12.2, 6.2 Hz, $CHNCOCF_3$), 4.71 (1 H, dd, *J* = 12.2, 2.8 Hz, $CHNCOCF_3$), 6.70 (1 H, s, NH), 7.47 (1 H, t, *J* = 7.7 Hz, 6-H), 7.57 (1 H, m, 7-H), 7.63 (1 H, s, 3-H), 7.76 (1 H, d, *J* = 8.4 Hz, 5-H), 8.19 (1 H, d, *J* = 8.5 Hz, 8-H); $^{13}$C NMR [($CDCl_3$) (HSQC / HMBC)] δ 28.29 (C*Me*$_3$),

44.85 (oxirane 3-C), 48.89 (oxirane 2-C), 69.29 (*C*$H_2$NCO$CF_3$), 81.25 (*C*$Me_3$), 85.75 (1-C), 110.89 (3-C), 115.72 (q, *J* = 284.6 Hz, $CF_3$), 120.33 (5-C), 123.42 (4a-C), 125.48 (6-C), 128.25 (7-C), 132.53 (8-C), 134.43 (4-C), 134.95 (8a-C), 145.08 (2-C), 152.71 (C=O Boc); $^{19}$F NMR ($CDCl_3$) δ -75.62 (s, $CF_3$).

**<u>Diastereoisomer 2</u>**

**Rotamer A**

$^1$H NMR [($CDCl_3$) (NOESY)] δ 1.56 (9 H, s, $Bu^t$), 2.56 (1 H, dd, *J* = 4.8, 2.5 Hz, oxirane 3-H), 2.84 (1 H, m, oxirane 3-H), 3.17 (1 H, dd, *J* = 14.3, 7.1 Hz, CHNCO$CF_3$), 3.44 (1 H, m, oxirane 2-H), 4.63 (1 H, dd, *J* = 14.3, 3.9 Hz, CHNCO$CF_3$), 6.99 (1 H, s, NH), 7.63-7.67 (2 H, m, 6,7-$H_2$), 7.85-7.87 (1 H, m, 5-H), 8.18 (1 H, s, 3-H), 8.31 (1 H, m, 8-H); $^{13}$C NMR [($CDCl_3$) (HSQC / HMBC)] δ 28.33 (C*Me*$_3$), 45.67 (oxirane 3-C), 49.31 (oxirane 2-C), 54.66 (*C*$H_2$NCO$CF_3$), 81.64 (*C*$Me_3$), 99.03 (1-C), 115.88 (q, *J* = 288.4 Hz, $CF_3$), 118.47 (3-C), 120.59 (5-C), 125.80 (4a-C), 128.05 (6-C), 128.78 (7-C), 134.42 (8-C), 135.06 (8a-C), 135.09 (4-C), 140.80 (2-C), 152.43 (Boc C=O), 157.09 (q, *J* = 36.5 Hz, $F_3$C*C*=O); $^{19}$F NMR ($CDCl_3$) δ -68.52 (s, $CF_3$).

**Rotamer B**

$^1$H NMR [($CDCl_3$) (NOESY)] δ 1.56 (9 H, s, $Bu^t$), 2.45 (1 H, dd, *J* = 4.6, 2.4 Hz, oxirane 3-C), 2.84 (1 H, m, oxirane 3-H), 3.34 (1 H, m, oxirane 2-H), 3.38 (1 H, dd, *J* = 13.6, 5.8 Hz, CHNCO$CF_3$), 4.55 (1 H, dd, *J* = 13.8, 4.6 Hz, CHNCO$CF_3$), 6.99 (1 H, s, NH), 7.63-7.67 (2 H, m, 6,7-$H_2$), 7.86 (1 H, m, 5-H), 8.06 (1 H, s, 3-H), 8.31 (1 H, m, 8-H); $^{13}$C NMR [($CDCl_3$) (HSQC / HMBC)] δ 28.30 (C*Me*$_3$), 46.70 (oxirane 3-C), 48.02 (oxirane 2-C), 53.29 (*C*$H_2$NCO$CF_3$), 81.68 (*C*$Me_3$), 99.45 (1-C), 115.88 (q, *J* = 288.4 Hz, $CF_3$),), 118.47 (3-C), 120.55 (5-C), 125.80 (4a-C), 128.13 (6-C), 128.86 (7-C), 134.55 (8-C), 135.09 (4-C), 135.11 (8a-C), 140.32 (2-C), 152.43 (Boc C=O), 157.20 (q, *J* = 38.1 Hz, $F_3$C*C*=O); $^{19}$F NMR ($CDCl_3$) δ -68.40 (s, $CF_3$).

## 5.31 (*S*)-*tert*-Butyl N-(1-iodo-2-((oxiran-2-ylmethyl)amino)-naphthalen-4-yl)-carbamate (97)

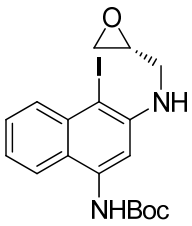


MeLi in $Et_2O$ (1.6 M, 0.24 mL, 0.39 mmol) was added dropwise (~5 min) to a stirred suspension of CuCN (17.4 mg, 0.19 mmol) in dry THF (0.6 mL) at −78°C under $N_2$ and the mixture was stirred for 5 min. The mixture was brought to −40°C and stirred for 30 min. After cooling again to −78°C, compound **95** (65.6 mg, 0.12 mmol) in dry THF (0.6 mL) was added dropwise and stirring was continued at −78°C. The mixture was allowed to warm gradually and was stirred at 25°C for 3 d. Water was added to the mixture and EtOAc was used to extract product. The organic phase was washed with brine. Drying, evaporation and chromatography (petroleum ether / EtOAc 9:1) gave **97** (Conformer A:B 1:1.4) (39.4 mg, 73%) as a yellow solid: $R_f$ = 0.7 (EtOAc / petroleum ether 1:4); mp 127-128°C; IR $\nu_{max}$ 3389, 3336 (NH), 3082 (ring CH ), 1699 (C=O); MS ($ES^+$) *m/z* 463.0522 (M + Na) ($C_{18}H_{21}IN_2NaO_3$ requires 463.0495).

**Conformer A**

$^1$H NMR [($CDCl_3$) (NOESY)] δ 1.56 (9 H, s, $Bu^t$), 2.78 (1 H, d, *J* = 2.7 Hz, $NHCH_2CHOCH$), 2.86 (1 H, d, *J* = 4.0 Hz, $NHCH_2CHOCH$), 3.27 (1 H, m, $NHCH_2CHOCH_2$), 3.51 (1 H, dd, *J* = 6.2, 4.6 Hz, $NHCHCHOCH_2$), 3.75 (1 H, dd, *J* = 5.7, 3.5 Hz, $NHCHCHOCH_2$), 4.87 (1 H, t, *J* = 5.8 Hz, oxirane NH), 6.93 (1 H, s, Boc NH), 7.26 (1 H, ddd, *J* = 8.1, 6.8, 1.1 Hz, 6-H), 7.45 (1 H, ddd, *J* = 8.1, 6.8, 1.2 Hz, 7-H), 7.62 (1 H, d, *J* = 8.2 Hz, 5-H), 7.74 (1 H, s, 3-H), 7.99 (1 H, dd, *J* = 8.6, 0.6 Hz, 8-H); $^{13}$C NMR [($CDCl_3$) (HSQC / HMBC)] δ 28.32 ($CMe_3$), 45.38 ($NHCH_2CHOCH_2$), 45.44 ($NHCH_2CHOCH_2$), 50.82 ($NHCH_2CHOCH_2$), 78.88 (1-C), 80.91 ($CMe_3$), 105.08 (3-C), 120.13 (5-C), 120.74 (4a-C), 122.63 (6-C), 128.10 (7-C), 131.02 (8-C), 135.03 (4-C), 135.59 (8a-C), 145.84 (2-C), 152.84 (C=O).

**Conformer B**

$^1$H NMR [($CDCl_3$) (NOESY)] δ 1.56 (9 H, s, $Bu^t$), 2.77 (1 H, d, *J* = 2.6 Hz, $NHCH_2CHOCH$), 2.84 (1 H, d, *J* = 4.0 Hz, $NHCH_2CHOCH$), 3.25-3.29 (1 H, m, $NHCH_2CHOCH_2$), 3.55 (1 H, dd, *J* = 6.2, 4.6 Hz, $NHCHCHOCH_2$), 3.71 (1 H, dd, *J* = 5.7, 3.5 Hz, $NHCHCHOCH_2$), 4.87 (1 H, t, *J* = 5.8 Hz, oxirane NH), 6.93 (1 H, s, Boc NH), 7.26 (1 H, ddd, *J* = 8.1, 6.8, 1.1 Hz, 6-H), 7.45 (1 H, ddd, *J* = 8.1, 6.8, 1.2 Hz, 7-H), 7.62 (1 H, d, *J* = 8.2 Hz, 5-H), 7.74 (1 H, s, 3-H), 7.99 (1 H, dd, *J* = 8.6, 0.6 Hz, 8-H); $^{13}$C NMR [($CDCl_3$) (HSQC / HMBC)] δ 28.32 ($CMe_3$), 45.38 ($NHCH_2CHOCH_2$), 45.44 ($NHCH_2CHOCH_2$), 50.82 ($NHCH_2CHOCH_2$), 78.88

(1-C), 80.91 (*C*Me$_3$), 105.08 (3-C), 120.13 (5-C), 120.74 (4a-C), 122.63 (6-C), 128.10 (7-C), 131.02 (8-C), 135.03 (4-C), 135.59 (8a-C), 145.84 (2-C), 152.84 (C=O).

## 5.32 Preliminary study using $Bu^t_4ZnLi_2$ as a reagent for cyclisation of terminal epoxides

### 5.32.1 4-(Prop-2-enyl)phenol (99)

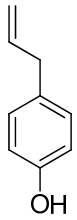


$ZnCl_2$ in THF (0.7 M, 4.10 mL, 2.9 mmol) was added to dry THF (5 mL) under $N_2$. $Bu^tLi$ in pentane (1.7 M, 6.70 mL, 11 mmol) was added dropwise to the solution at −78°C; the solution was brought to 0°C and stirred for 30 min. 4-Iodophenol **98** (285 mg, 1.3 mmol) in dry THF (5 mL) was added dropwise to the solution at −78°C. The mixture was warmed to 20°C and stirred for 2 h. 3-Bromopropene (780 mg, 6.45 mmol) was added and the mixture was stirred at 40°C for 3 d. After cooling to 20°C, the reaction was quenched with sat. aq. $NH_4Cl$ and the mixture was diluted with aq. HCl (2 M). The mixture was extracted with $Et_2O$. The organic layer was washed with brine and dried. Evaporation gave crude **99** as a brown oil (200 mg). NMR showed a mixture of product (66%) and starting material (33%): $^1$H NMR ($CDCl_3$) δ 3.32 (2 H, d, *J* = 6.6 Hz, Pr 1-$H_2$), 5.05 (2 H, m, Pr 3-$H_2$), 5.93 (1 H, ddt, *J* = 16.6, 11.9, 6.7 Hz, Pr 2-H), 6.77 (2 H, d, *J* = 9.4 Hz, Ph 2,6-$H_2$), 7.05 (2 H, d, *J* = 9.4 Hz, Ph 3,5-$H_2$); $^{13}$C NMR [($CDCl_3$) (HSQC / HMBC)] δ 38.30 (Pr 1-C), 114.27 (Ph 2,6-$C_2$), 114.41 (Pr 3-C), 128.67 (Ph 3,5-$C_2$), 131.17 (4-C), 136.84 (Pr 2-C), 152.86 (Ph 1-C).

## 5.33 *tert*-Butyl N-(1-iodo-2-(N-(prop-2-enyl)-2,2,2-trifluoroacetamido)naphthalene4-yl)-N-(prop-2-enyl)carbamate (103)

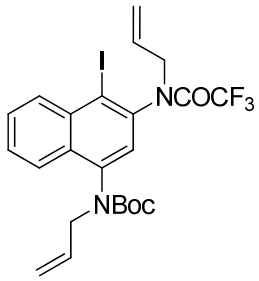


Compound **67** (99.4 mg, 0.21 mmol), $K_2CO_3$ (119 mg, 0.83 mmol) and 3-bromopropene (0.06 mL, 84 mg, 0.69 mmol) in acetone (15 mL) were stirred at 50°C under $N_2$ for 16 h. Sat. aq. $NaHCO_3$ was added and mixture was extracted with EtOAc. Washing with brine, drying and evaporation gave **103** (diastereoisomers A / B 1.4:1) (115 mg, 99%) as a yellow oil: $R_f$ = 0.7 (petroleum ether / EtOAc 4:1); IR $\nu_{max}$ 1698 (C=O); MS ($ES^+$) *m/z* 583.0804 (M + Na) ($C_{23}H_{24}F_3IN_2NaO_3$ requires 583.0681).

**Diasteroisomer A**

$^1$H NMR [($CDCl_3$) (COSY)] δ 1.23 (9 H, br, $Bu^t$), 3.71 (1 H, dd, *J* = 14.4, 8.3 Hz, $CF_3CONCH$), 3.83 (1 H, dd, *J* = 14.9, 7.4 Hz, BocNC*H*), 4.64 (1 H, m, BocNC*H*), 4.98-5.21 (5 H, m, 2 × propenyl 3-H, $CF_3CONCH$), 5.85-5.94 (2 H, m, 2 × propenyl 2-H), 7.11 (1 H, s, 3-H), 7.61-7.68 (2 H, m, 6,7-$H_2$), 7.80-7.85 (1 H, m, 5-H), 8.29-8.32 (1 H, m, 8-H); $^{13}$C NMR [($CDCl_3$) (HSQC / HMBC)] δ 27.88 (C*Me*$_3$), 52.45 (BocN*C*$H_2$), 53.69 ($CF_3CON$*C*$H_2$), 80.78 (*C*$Me_3$), 105.48 (1-C), 115.94 (q, *J* = 289.4 Hz, $CF_3$), 118.46 (BocNCH$_2$CH*C*$H_2$), 120.92 ($CF_3CONCH_2CH$*C*$H_2$), 123.57 (5-C), 128.11 (3-C), 128.52 (6-C or 7-C), 128.91 (7-C or 6-C), 130.31 ($CF_3CONCH_2$*C*$HCH_2$), 130.99 (4a-C), 133.37 (BocNCH$_2$*C*$HCH_2$), 133.87 (8-C), 135.71 (8a-C), 139.39 (2-C), 139.86 (4-C), 154.53 (Boc C=O), 156.50 (q, *J* = 35.0 Hz, $CF_3$*C*=O); $^{19}$F NMR ($CDCl_3$) δ -68.65 (s, $CF_3$).

**Diastereoisomer B**

$^1$H NMR [($CDCl_3$) (COSY)] δ 1.23 (9 H, br, $Bu^t$), 3.76 (1 H, dd, *J* = 14.4, 8.0 Hz, $CF_3CONCH$), 3.95 (1 H, dd, *J* = 14.7, 7.1 Hz, BocNC*H*), 4.4.53 (1 H, m, BocNC*H*), 4.98-5.21 (5 H, m, 2 × propenyl 3-H, $CF_3CONCH$), 5.85-5.94 (2 H, m, 2 × propenyl 2-H), 7.11 (1 H, s, 3-H), 7.61-7.68 (2 H, m, 6,7-$H_2$), 7.80-7.85 (1 H, m, 5-H), 8.29-8.32 (1 H, m, 8-H); $^{13}$C NMR [($CDCl_3$) (HSQC / HMBC)] δ 28.11 (C*Me*$_3$), 52.45 (BocN*C*$H_2$), 53.69 ($CF_3CON$*C*$H_2$), 80.78 (*C*$Me_3$), 105.48 (1-C), 115.94 (q, *J* = 289.4 Hz, $CF_3$), 118.46 (BocNCH$_2$CH*C*$H_2$), 120.92 ($CF_3CONCH_2CH$*C*$H_2$), 123.42 (5-C), 127.79 (3-C), 128.52 (6-C or 7-C), 128.91 (7-C or 6-C), 130.31 ($CF_3CONCH_2$*C*$HCH_2$), 130.99 (4a-C), 133.37 (BocNCH$_2$*C*$HCH_2$), 133.87 (8-C), 135.71 (8a-C), 139.39 (2-C), 139.86 (4-C), 154.39 (Boc C=O), 156.42 (q, *J* = 36.0 Hz, $CF_3$*C*=O); $^{19}$F NMR ($CDCl_3$) δ -68.58 (s, $CF_3$).

## 5.34 *tert*-Butyl N-(1-iodo-2-(N-(prop-2-enyl) 2,2,2-trifluoroacetamido)naphthalen-4-yl)carbamate (104)

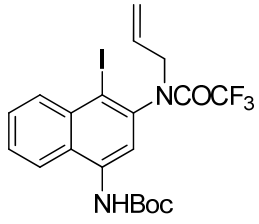


Compound **67** (1.22 mg, 2.5 mmol) was stirred in THF (10 mL) and potassium *tert*-butoxide (318 mg, 2.8 mmol) added. This was stirred at 20°C under $N_2$ for 30 min followed by addition of 3-bromopropene (0.700 mL, 973 mg, 8.04 mmol). The mixture was stirred for 2 h and heated to 50°C overnight. Sat. aq. $NaHCO_3$ was added. Extraction with EtOAc, drying, evaporation and chromatography (petroleum ether → petroleum ether / EtOAc 19:1) gave **104** as diastereoisomer A (yellow oil, 750 mg, 57%): $R_f$ = 0.4 (petroleum

ether / EtOAc 4:1), and diastereoisomer B (yellow solid, 200 mg, 15%): $R_f$ = 0.5 (petroleum ether / EtOAc 4:1); mp 146-147°C.

**Diastereoisomer A**

$^1$H NMR [($CDCl_3$) (NOESY)] δ 1.55 (9 H, s, $Bu^t$), 3.82 (1 H, dd, *J* = 14.5, 7.6 Hz, propenyl 1-H), 4.96 (1 H, dd, *J* = 14.5, 5.6 Hz, propenyl 1-H), 5.18 (1 H, dq, *J* = 18.0, 1.3 Hz, propenyl 3-H $_{TRANS}$) 5.22 (1 H, dq, *J* = 11.0, 1.0 Hz, propenyl 3-H $_{CIS}$), 5.92-5.98 (1 H, m, propenyl 2-H), 7.01 (1 H, s, NH), 7.7.61-7.67 (2 H, m, 6,7-H), 7.83-7.87 (1 H, m, 5-H), 7.93 (1 H, s, 3-H), 8.28-8.32 (1 H, m, 8-H); $^{13}$C NMR [($CDCl_3$) (HSQC / HMBC)] δ 28.27 (C*Me*$_3$), 54.00 (propenyl 1-C), 81.56 (*C*$Me_3$), 115.89 (q, *J* = 288.7 Hz, $CF_3$), 118.90 (3-C), 120.59 (propenyl 3-C), 120.66 (5-C), 127.92 (6-C or 7-C), 128.67 (7-C or 6-C), 130.30 (propenyl 3-C), 134.38 (8-C), 134.70 (8a-C), 135.39 (4-C), 140.14 (2-C), 152.45 (Boc C=O), 156.53 (q, *J* = 36.5 Hz, $F_3C$*C*=O); $^{19}$F NMR ($CDCl_3$) δ -68.55 (s, $CF_3$); MS ($ES^+$) *m/z* 559.0154 (M + K) ($C_{20}H_{20}F_3IN_2KO_3$ requires 559.0107); 543.0437 (M + Na) ($C_{20}H_{20}F_3IN_2NaO_3$ requires 543.0368); 521.0516 (M + H) ($C_{20}H_{21}F_3IN_2O_3$ requires 521.0549); 486.9814 [(M-$Bu^t$) + Na)] ($C_{16}H_{12}F_3IN_2NaO_3$ requires 486.9742).

**Diastereoisomer B**

$^1$H NMR [($CDCl_3$) (NOESY)] δ 1.56 (9 H, s, $Bu^t$), 3.95 (1 H, dd, *J* = 14.2, 7.4 Hz, propenyl 1-H), 4.84 (1 H, dd, *J* = 14.2, 6.1 Hz, propenyl 1-H), 5.12 (1 H, dd, *J* = 17.0, 1.3 Hz, propenyl 3-H $_{TRANS}$), 5.21 (1 H, dd, *J* = 10.1, 1.1 Hz, propenyl 3-H $_{CIS}$), 5.91-5.97 (1 H, m, propenyl 2-H), 7.27 (1 H, s, NH), 7.51 (1 H, dd, *J* = 8.2, 6.9, 1.2 Hz, 6-H), 7.60 (1 H, dd, *J* = 8.3, 6.9, 1.3 Hz, 7-H), 7.67 (1 H, d, *J* = 8.3 Hz, 5-H), 8.17 (1 H, d, *J* = 8.1 Hz, 8-H), 8.27 (1 H, s, 3-H); $^{13}$C NMR [($CDCl_3$) (HSQC / HMBC)] δ 27.30 (C*Me*$_3$), 53.30 (propenyl 1-C), 80.76 (*C*$Me_3$), 91.92 (1-C), 115.16 (q, *J* = 288.6 Hz, $CF_3$), 119.84 (3-C), 120.03 (propenyl 3-C), 121.93 (5-C), 125.63 (6-C), 126.43 (4a-C), 127.97 (7-C), 129.49 (propenyl 2-C), 131.56 (8-C), 134.31 (4-C), 135.26 (8a-C), 136.78 (2-C), 151.32 (Boc C=O), 156.35 (q, *J* = 36.3 Hz, $CF_3$*C*=O); $^{19}$F NMR ($CDCl_3$) δ -68.20 ($CF_3$); MS ($ES^+$) *m/z* 559.0149 (M + K) ($C_{20}H_{20}F_3IN_2KO_3$ requires 559.0107); 543.0371 (M + Na) ($C_{20}H_{20}F_3IN_2NaO_3$ requires 543.0368); 538.0828 (M + $NH_4^+$) ($C_{20}H_{24}F_3IN_3O_3$ requires 538.0809).

## 5.35 *tert*-Butyl N-(1-(2,2,6,6-tetramethylpiperidin-1-yloxy)methyl)-3-(trifluoro-acetyl-2,3-dihydro-1*H*-benzo[*e*]indol-5-yl)carbamate (105)

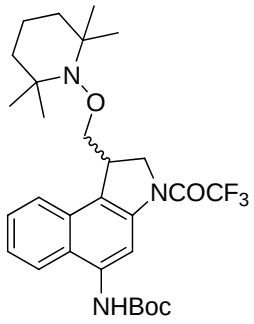


Compound **104** (38.1 mg, 73 µmol) in benzene (2.0 mL) was treated sequentially with TEMPO (35.7 mg, 0.23 mmol) and $Bu_3SnH$ (0.020 mL, 21 mg, 73 µmol). The mixture was heated to 60°C and stirred at this temperature for 135 min. Additional $Bu_3SnH$ (0.020 mL, 21 mg, 73 µmol) was added at 30 min, 60 min and 90 min. Evaporation and chromatography (petroleum ether / EtOAc 49:1 → 19:1) gave **105** (24.1 mg, 60%) as a yellow solid: $R_f$ = 0.6 (petroleum ether / EtOAc 19:1); mp 160-161°C; IR $\nu_{max}$ 3364, 3129, 3266 (NH), 1700 (C=O); $^1$H NMR [($CDCl_3$) (NOESY)] δ 0.90 (3 H, s, piperidine Me), 1.00 (3 H, s, piperidine Me), 1.07 (3 H, s, piperidine Me), 1.20 (3 H, s, piperidine Me), 1.25, (1 H, m, piperidine 4-H), 1.29 (1 H, m, piperidine 3-H or 5-H), 1.35 (1 H, m, piperidine 3-H or 5-H), 1.42 (1 H, m, piperidine 3-H or 5-H), 1.54 (1 H, m, piperidine 4-H), 1.54 (9 H, s, $Bu^t$), 1.66 (1 H, m, piperidine 3-H or 5-H), 3.83 (1 H, t, *J* = 8.8 Hz, NOCH), 3.99 (1 H, m, 1-H), 4.08 (1 H, dd, *J* = 8.9, 4.3 Hz, NOCH), 4.30 (1 H, t, *J* = 8.7 Hz, 2-H), 4.61 (1 H, d, *J* = 10.9 Hz, 2-H), 6.10 (1 H, s, NH), 7.47 (1 H, t, *J* = 7.8 Hz, 7-H), 7.53 (1 H, t, *J* = 7.6 Hz, 8-H), 7.81 (1 H, d, *J* = 8.3 Hz, 9-H), 7.90 (1 H, d, *J* = 8.4 Hz, 6-H), 8.79 (1 H, s, 4-H); $^{13}$C NMR [($CDCl_3$) (HSQC / HMBC)] δ 16.97 (piperidine 4-C), 19.97 (piperidine Me), 20.05 (piperidine Me), 28.30 (C*Me*$_3$), 32.92 (piperidine Me), 32.96 (piperidine Me), 39.52 (piperidine 3-C or 5-C), 39.60 (piperidine 5-C or 3-C), 39.86 (1-C), , 52.42 (2-C), 59.88 (piperidine 2,6-$C_2$), ~77.26 ($NOCH_2$), 81.05 (*C*$Me_3$), 111.17 (4-C), 116.20 (q, *J* = 288.1 Hz, $CF_3$), 122.15 (6-C), 123.13 (9b-C), 124.01 (9-C), 125.36 (7-C), 125.52 (5a-C), 127.06 (8-C), 129.77 (9a-C), 134.19 (5-C), 139.56 (3a-C), 153.34 (Boc C=O), 154.28 (q, *J* = 37.5 Hz, $CF_3$*C*=O); $^{19}$F NMR ($CDCl_3$) δ -72.21 (s, $CF_3$); MS ($ES^+$) *m/z* 572.2804 (M + Na) ($C_{29}H_{38}F_3N_3NaO_4$ requires 572.2712), 550.2937 (M + H) ($C_{29}H_{39}F_3N_3O_4$ requires 550.2893), 516.2095 [(M-$Bu^t$) + Na)] ($C_{25}H_{30}F_3N_3NaO_4$ requires 516.2086).

### 5.36 *tert*-Butyl N-(1-((2,2,6,6-tetramethylpiperidin-1-yloxy)methyl)-2,3-dihydro-1*H*-benzo[*e*]indol-5-yl)carbamate (106)

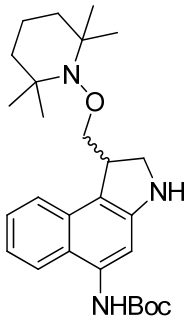


Compound **105** (70.4 mg, 0.13 mmol) was dissolved in THF (4 mL) and aq. NaOH (5 M, 4 mL) added. The mixture was stirred at 20°C for 105 min. Water was added to the mixture and extracted with EtOAc. Washing with brine, drying and evaporation gave **106** (60.7 mg, 100%) as a yellow oil: $R_f$ = 0.35 (petroleum ether / EtOAc 9:1); IR $\nu_{max}$ 3376 (NH), 1715 (C=O); $^1$H NMR [($CDCl_3$) (NOESY)] δ 1.06 (3 H, s, piperidine Me), 1.14 (6 H, s, piperidine Me), 1.16 (3 H, s, piperidine Me), 1.16-1.42 (6 H, m, piperidine 3,4,5-$H_6$), 1.54 (9 H, s, $Bu^t$), 3.70-3.75 (2 H, m, 2-$H_2$), 3.80-3.90 (2 H, m, 1-H, NOCH), 4.00 (1 H, dd, *J* = 7.6, 4.2 Hz, NOCH), 6.86 (1 H, s, Boc NH), 7.20 (1 H, t, *J* = 7.5 Hz, 7-H or 8-H), 7.38 (1 H, t, *J* = 7.1 Hz, 8-H or 7-H), 7.51 (1 H, s, 4-H), 7.69 (2 H, d, *J* = 8.6 Hz, 6,9-$H_2$); $^{13}$C NMR [($CDCl_3$) (HSQC / HMBC)] δ 17.07 (piperidine 4-C), 20.07 (piperidine Me), 20.26 (piperidine Me), 28.33 (C*Me*$_3$), 32.93 (piperidine Me), 33.34 (piperidine Me), 39.45 (piperidine 3-C or 5-C), 39.59 (piperidine 5-C or 3-C), 41.05 (1-C), 51.29 (2-C), 59.63 (piperidine 2-C or 6-C), 59.72 (piperidine 6-C or 2-C), 76.68-77.32 ($NOCH_2$), 80.54 (*C*$Me_3$), 105.52 (4-C), 116.77 (5a,9b-$C_2$), 120.98 (6-C or 9-C), 121.52 (7-C or 8-C), 123.23 (9-C or 6-C), 126.29 (8-C or 7-C), 131.41 (9a-C), 133.52 (5-C), 149.40 (3a-C), 153.34 (C=O); MS ($ES^+$) *m/z* 476.2924 (M + Na) ($C_{27}H_{39}N_3NaO_3$ requires 476.2810), 454.3107 (M + H) ($C_{27}H_{40}N_3O_3$ requires 454.3070).

### 5.37 N,N-Dimethyl-2-(4-nitrophenoxy)ethylamine (108)

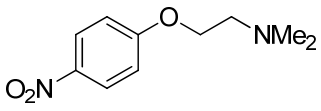


KOH (5.17 g, 92 mmol) in dry EtOH (40 mL) was added to 4-nitrophenol **107** (14.2 g, 0.10 mol) in dry EtOH (30 mL). Filtration, washing (cold dry EtOH) and drying gave potassium 4-nitrophenoxide (16.1 g, 89%) as an orange solid. NaOH (4.28 g, 73 mmol) in water (25 mL) was added to 2-chloro-N,N-dimethylethylammonium chloride (12.6 g, 88 mol) in water (50 mL). The mixture was saturated with NaCl and extracted with toluene (5 × 50 mL). The combined toluene fractions were dried over KOH and added to a suspension of potassium 4-nitrophenoxide (14.0 g, 83 mmol) in toluene (80 mL). The mixture was heated under reflux for 17 h. Cooling, filtration and evaporation gave **108** (10.4 g, 63%) as a yellow oil: $R_f$ = 0.2 (EtOAc / petroleum ether 1:1); IR $\nu_{max}$ 1517.34 ($NO_2$); $^1$H NMR ($CDCl_3$) δ 2.26 (6 H, s, $NMe_2$), 2.69 (2 H, t, *J* = 5.6 Hz, $NCH_2$), 4.08 (2 H, t, *J* = 5.6 Hz, $OCH_2$), 6.88 (2 H, d, *J* = 9.3 Hz, Ph 2,6-$H_2$), 8.08 (2 H, d, *J* = 9.3 Hz, Ph 3,5-$H_2$); $^{13}$C NMR ($CDCl_3$) δ 45.76 ($NMe_2$),

57.87 ($NCH_2$), 66.65 ($OCH_2$), 114.78 (Ph-$C_2$), 125.75 (Ph-$C_2$), 141.48 (Ph-$C_q$), 163.88 (Ph-$C_q$). A sample was converted to the HCl salt and recrystallised ($Pr^iOH$): mp 165-166°C (lit.[194] mp $Pr^iOH$ 166-167°C); $^1H$ NMR [$(CD_3)_2SO$] δ 2.81 (6 H, s, $NMe_2$), 3.53 (2 H, t, *J* = 5.1 Hz, $NCH_2$), 4.51 (2 H, t, *J* = 5.1, $OCH_2$), 7.20 (2 H, d, *J* = 9.2 Hz, Ph 2,6-$H_2$), 8.20 (2 H, d, *J* = 9.2 Hz, Ph 3,5-$H_2$); $^{13}C$ NMR [$(CD_3)_2SO$) (HSQC / HMBC)] δ 42.68 ($NMe_2$), 54.91 ($NCH_2$), 63.17 ($OCH_2$), 115.34 (Ph 2,6-$C_2$), 125.81 (Ph 3,5-$C_2$), 141.36 (Ph 1-C), 162.72 (Ph 4-C).

### 5.38 2-(4-Aminophenoxy)-N,N-dimethylethylamine (109)

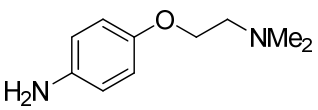

Compound **108** (160 mg, 0.76 mmol) was added dropwise to conc. aq. HCl (2.0 mL, 66 mmol) and $SnCl_2.2H_2O$ (626 mg, 2.8 mmol). The mixture was stirred at 0°C for 30 min and then at room temperature for 19 h. The mixture was made basic by addition of conc. aq. NaOH, then extracted four times with $CH_2Cl_2$. The combined organic phase was washed with water and dried and the solvent was evaporated to give **109** (120 mg, 88%) as a buff oil: $R_f$ = 0.6 (MeOH / $CH_2Cl_2$ 1:9); IR $\upsilon_{max}$ 3397 (NH), 3302 (NH), 3204 (NH); $^1H$ NMR ($CDCl_3$) δ 2.29 (6 H, s, $NMe_2$), 2.65 (2 H, t, *J* = 5.8 Hz, $NCH_2$), 3.96 (2 H, t, *J* = 5.8 Hz, $OCH_2$), 6.58 (2 H, d, *J* = 8.8 Hz, Ph 3,5-$H_2$), 6.72 (2 H, d, *J* = 8.8 Hz, Ph 2,6-H); $^{13}C$ NMR ($CDCl_3$) δ 45.83 (2 C, 2 × Me), 58.43 ($NCH_2$), 66.74 ($OCH_2$), 115.82 (Ph 2,6-C), 116.36 (Ph 3,5-C), 140.22 ( Ph 4-C), 151.78 (Ph 1-C).

### 5.39 Ethyl 5-(2-dimethylaminoethoxy)-1*H*-indole-2-carboxylate (110)

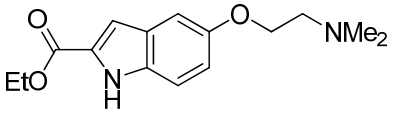

Compound **109** (1.07 g, 5.9 mmol) in water (10 mL) and conc. aq. HCl (3.0 mL) was diazotised at −20°C with $NaNO_2$ (476 mg, 6.9 mmol) in water (2.0 mL). The cold solution was added in one portion to a vigorously stirred ice-cold mixture of ethyl 2-methyl-3-oxobutanoate (895 mg, 6.2 mmol), NaOAc (5.18 g, 63 mmol), EtOH (8.0 mL) and ice (7.0 g). The mixture was stirred at 20°C for 16 h and then cooled to 0°C, basified by slow addition of $Na_2CO_3$ and extracted with $CH_2Cl_2$. The organic layers were combined and washed with water and dried. The evaporation residue was extracted with hot hexanes in the presence of decolourising charcoal and the solvent was evaporated from the clarified solution. The residue, in EtOH (4.0 mL), was treated with sat. ethanolic HCl (3.0 mL) and heated under reflux for 30 min. The evaporation residue was partitioned between dilute aq. $Na_2CO_3$ and $CH_2Cl_2$. The organic layer was washed with water and sat. brine and dried. Evaporation and

recrystallisation gave **110** (25 mg, 15%): $R_f$ = 0.3 (EtOAc / MeOH 1:1); mp 108-109 (lit.[80] mp 110°C); IR $\nu_{max}$ 3315 (NH), 1687 (C=O); $^1$H NMR ($CDCl_3$) δ 1.39 (3 H, t, *J* = 7.1 Hz, $OCH_2$*Me*), 2.35 (6 H, s, $NMe_2$), 2.76 (2 H, t, *J* = 5.8 Hz, $(Me)_2NCH_2CH_2$), 4.10 (2 H, t, *J* = 5.8 Hz, $(Me)_2NCH_2CH_2$), 4.39 (2 H, q, *J* = 7.1 Hz, $OCH_2Me$), 6.99 (1 H, dd, *J* = 8.9, 2.4 Hz, 6-H), 7.07 (1 H, d, *J* = 2.4 Hz, 4-H), 7.12 (1 H, dd, *J* = 2.1, 0.8 Hz, 3-H), 7.28 (1 H, d, *J* = 8.9 Hz, 7-H), 9.30 (1 H, s, NH); $^{13}$C NMR [($CDCl_3$) (HSQC / HMBC)] δ 14.32 ($OCH_2$*Me*), 45.83 ($NMe_2$)), 58.38 $(Me)_2NCH_2CH_2$), 60.82 ($OCH_2Me$), 66.57 $(Me)_2NCH_2CH_2$), 103.67 (4-C), 108.13 (3-C), 112.69 (7-C), 117.37 (6-C), 127.74 (2-C), 127.89 (3a-C), 132.42 (7a-C), 153.83 (5-C), 162.01 (C=O).

## 5.40 Preliminary test of the use of ethanolic HCl for esterification

### 5.40.1 Ethyl 2-(1*H*-indol-3-yl)acetate (123).

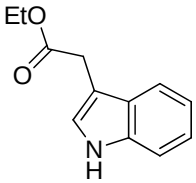


Indole-3-acetic acid **122** (122 mg, 0.70 mmol), was stirred in conc. ethanolic HCl (20 mL) and heated under reflux for 1 h. The solvent was evaporated and the mixture was dissolved in EtOAc. This solution was washed with sat. aq. $NaHCO_3$ and brine. Drying and evaporation yielded **123** (116 mg, 82%) as a pale buff oil: $^1$H NMR ($CDCl_3$) δ 1.28 (3 H, t, *J* = 7.0 Hz, Me), 3.78 (2 H, s, indole $CH_2$), 4.19 (2 H, q, *J* = 7.1 Hz, $OCH_2$), 7.08 (1 H, s, indole 2-H), 7.15 (1 H, t, *J* = 7.5 Hz, indole 6-H), 7.21 (1 H, t, *J* = 7.5 Hz, indole 5-H), 7.31 (1 H, d, *J* = 8.0 Hz, indole 7-H), 7.60 (1 H, d, *J* = 7.8 Hz, indole 4-H), 8.14 (1 H, br, NH); $^{13}$C NMR [($CDCl_3$) (HSQC / HMBC)] δ 14.19 (Me), 31.39 (indole $CH_2$), 60.77 ($OCH_2$), 108.38 (indole 3-H), 111.19 (indole 7-H), 118.81 (indole 4-H), 119.54 (indole 5-H), 122.06 (indole 6-H), 123.11 (indole 2-H), 127.21 (indole 3a-C), 136.12 (indole 7a-C), 172.21 (C=O).

## 5.41 Ethyl 5-hydroxy-1*H*-indole-2-carboxylate (125)

<u>METHOD A</u>

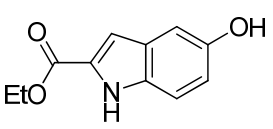


$SOCl_2$ (1 mL, 1.64 g, 14 mmol) was added dropwise to 5-hydroxy-1*H*-indole-2-carboxylic acid **124** (116mg, 0.66 mmol) in absolute ethanol (10 mL). This mixture was boiled under reflux at 80°C for 1 h. The mixture was allowed to cool to room temperature. The solvent was evaporated and the crude mixture, in EtOAc, was washed with aq. $NaHCO_3$ (5%) and with brine. Drying and evaporation gave **125** (4.1 mg, 3%) as a buff solid with properties below.

METHOD B

5-Hydroxy-1*H*-indole-2-carboxylic acid **124** (1.53 g, 8.6 mmol) was heated under reflux in conc. ethanolic HCl (100 mL) under $N_2$ for 4 h. The solvent was evaporated and the residue dissolved in EtOAc. This was washed with water and brine. Drying, evaporation and chromatography ($CH_2Cl_2$ → $CH_2Cl_2$ / EtOAc 4:1) gave **125** (1.64, 92%) as a white solid:

$R_f$ = 0.8 (EtOAc); mp 152-154°C (lit.[195] 146-148°C); IR $\nu_{max}$ 3316, 3209 (OH, NH), 1696 (C=O); $^1$H NMR [$(CD_3)_2SO$] δ 1.38 (3 H, t, *J* = 7.1 Hz, Me), 4.37 (2 H, q, *J* = 7.1 Hz, $CH_2$), 6.86 (1 H, dd, *J* = 8.8, 2.4 Hz, 6-H), 6.97 (1 H, d, *J* = 2.3 Hz, 4-H), 7.00 (1 H, dd, *J* = 2.1, 0.8 Hz, 3-H), 7.32 (1 H, d, *J* = 8.8Hz, 7-H), 8.93 (1 H, s, OH), 11.60 (1 H, s, NH). $^{13}$C NMR [$(CD_3)_2SO$] δ 14.29 (Me), 60.17 ($CH_2$), 104.43 (4-C), 106.66 (3-C), 113.07 (7-C), 116.15 (6-C), 127.36 (2-C or 3a-C), 127.44 (3a-C or 2-C), 132.21 (7a-C), 151.34 (5-C), 161.30 (C=O).

## 5.42 Ethyl 5-ethoxy-1*H*-indole-2-carboxylate (126)

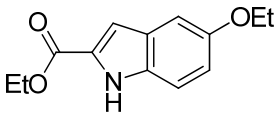


5-Hydroxy-1*H*-indole-2-carboxylic acid **124** (2.00 g, 11 mmol) was boiled under reflux in conc. ethanolic HCl (25 mL) under $N_2$ for 16 h. The solvent was evaporated and the residue in EtOAc was washed with water and brine. Drying, evaporation and chromatography ($CH_2Cl_2$ → $CH_2Cl_2$ / EtOAc 4:1) gave **126** ( 236 mg, 10%) as a white solid: $R_f$ = 0.7 (petroleum ether / EtOAc 1:1) ; mp 147-148°C; $^1$H NMR ($CDCl_3$) δ 1.41 (3 H, t, *J* = 7.2 Hz, ester Me), 1.43 (3 H, t, *J* = 7.0 Hz, ether Me), 4.06 (2 H, q, *J* = 7.0 Hz, ether $CH_2$), 4.40 (2 H, q, *J* = 7.1 Hz, ester $CH_2$), 6.99 (1 H, dd, *J* = 8.9, 2.4 Hz, 6-H), 7.07 (1 H, d, *J* = 2.4 Hz, 4-H), 7.13 (1 H, dd, *J* = 2.1, 0.9 Hz, 3-H), 7.30 (1 H, d, *J* = 9.0 Hz, 7-H), 8.89 (1 H, s, NH); $^{13}$C NMR [($CDCl_3$) (HSQC / HMBC)] δ 14.33 (ester Me), 14.87 (ether Me), 60.31 (ester $CH_2$), 63.93 (ether $CH_2$), 103.65 (4-C), 108.13 (3-C), 112.60 (7-C), 117.34 (6-C), 127.81 (2-C), 127.85 (3a-C), 132.16 (7a-C), 153.92 (5-C), 161.89 (C=O); MS ($ES^+$) *mz* 256.0957 (M + Na) ($C_{13}H_{15}NNaO_3$ requires 256.0950), 234.1125 (M + H) ($C_{13}H_{16}NO_3$ requires 234.1130).

## 5.43 Ethyl 5-(2-dimethylaminoethoxy)-1*H*-indole-2-carboxylate (110)

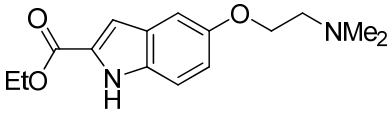


To a solution of ethyl-5-hydroxy-1*H*-indole-2-carboxylate **125** (1.68 g, 8.2 mmol) in $CHCl_3$ (40 mL) was added 2-chloro-N,N-dimethylamine hydrochloride (1.77 g, 12.0 mmol), $K_2CO_3$ (3.40 g, 25 mmol) and water (8 mL) in sequence. The stirred solution was

placed in an oil bath at 65°C and the temperature was slowly raised to 80.5°C (~1°C per 5min) over 65 min and the mixture was stirred for 16 h. The reaction mixture was cooled to room temperature and the phases were separated. The volume of the organic phase was reduced to 25% of its original volume by evaporation. The residue was combined with the aqueous phase and diluted with water and toluene. The organic layer was separated and washed with water and extracted with aq. HCl (1.0 M). The acidic phase was washed with toluene, cooled to 0°C, basified (~pH 12) by addition of aq. NaOH (4.0 M) and extracted with toluene. The organic extract was washed with water and brine and dried and the solvent was evaporated to give **110** as a white solid (1.81 g, 80%) with properties as above (Section 5.39).

### 5.44 5-(2-(Dimethylamino)ethoxy)-1*H*-indole-2-carboxylic acid (127)

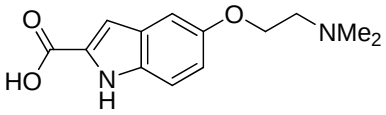


A mixture of **110** (609 mg, 2.2 mmol) and $Cs_2CO_3$ (2.50 g, 7.7 mmol) in MeOH (12 mL) and water (6 mL) was heated at reflux for 2 h. The mixture was evaporated to dryness. The residue was dissolved in water, and adjusted to pH 6.5 with aq. HCl (1.0 M). The mixture was placed in a refrigerator overnight and then in ice for 2 h. The resulting crystalline solid was collected, washed with ice-cold water and acetone to give **127** (419 mg, 77%) as a white crystalline solid: $R_f$ = 0.1 (EtOAc / MeOH 1:1); A portion of the product was treated with HCl in 1,4-dioxane (4.0 M) and EtOAc. Filtration gave the HCl salt of the product as a white solid: mp 238-239°C (lit.[166] mp 237-239°C); IR $\nu_{max}$ 3380, 3240 (OH, NH), 1593 (C=O); $^1$H NMR [$(CD_3)_2SO$] δ 2.37 (6 H, s, $NMe_2$), 2.81 (2 H, t, *J* = 5.7 Hz, $(Me)_2NCH_2CH_2$), 4.12 (2 H, t, *J* = 5.8 Hz, $(Me)_2NCH_2CH_2$), 6.91 (1 H, dd, *J* = 8.9, 2.4 Hz, 6-H), 6.95 (1 H, d, *J* = 1.5 Hz, 3-H), 7.14 (1 H, d, *J* = 2.3 Hz, 4-H), 7.35 (1 H, d, *J* = 8.9 Hz, 7-H), 11.50 (1 H, s, NH); $^{13}$C NMR [$(CD_3)_2SO$) (HSQC / HMBC)] δ 45.04 ($NMe_2$), 57.39 $(Me)_2NCH_2CH_2$), 65.66 $(Me)_2NCH_2CH_2$), 103.18 (4-C), 106.06 (3-C), 113.21 (7-C), 115.50 (6-C), 127.27 (3a-C), 130.33 (2-C), 132.39 (7a-C), 152.69 (5-C), 163.30 (C=O).

## 5.45 *tert*-Butyl N-(3-(5-(2-(dimethylaminoethoxy)indole-2-carbonyl)-1-((2,2,6,6-tetramethylpiperidin-1-yloxy)methyl)-2,3-dihydro-1*H*-benzo[*e*]indol-5-yl)carbamate (128)

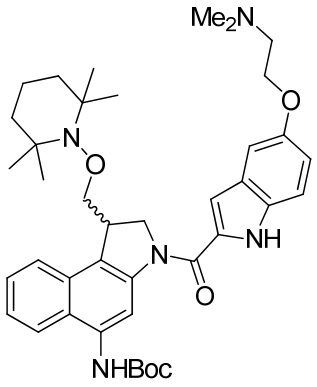


Compound **127** (101 mg, 0.41 mmol) and HOBt (125 mg, 0.81 mmol) were stirred in dry DMF (10 mL) at 0°C under $N_2$. N,N-diisopropylcarbodiimide (0.13 mL, 106 mg, 0.81 mmol) was added *via* a syringe and the mixture was stirred for 1 h at 0°C. Compound **106** (203 mg, 0.37 mmol) in dry DMF (10 mL) was added. The reaction mixture was allowed to warm slowly to 20°C overnight and heated at 40°C for 2 h. Sat. aq. $NaHCO_3$ was added and the mixture was extracted with EtOAc. The extract was washed with water and brine. Drying, evaporation and chromatography (EtOAc → EtOAc / MeOH / $Et_3N$ 90:10:0.1) gave **128** (163 mg, 64%) as a yellow oil: IR $\nu_{max}$ 3447 (NH), 1727, 1693 (C=O); $^1$H NMR [($CDCl_3$) (NOESY)] δ 0.88 (3 H, s, piperidine Me), 1.00 (3 H, s, piperidine Me), 1.04 (3 H, s, piperidine Me), 1.17 (3 H, s, piperidine Me), 1.24-1.50 (6 H, m, piperidine 3,4,5-$H_6$), 1.54 (9 H, s, $Bu^t$), 2.45 (6 H, s, $NMe_2$), 2.88 (2 H, t, *J* = 5.5 Hz, $OCH_2CH_2N(CH_3)_2$), 3.87 (1 H, t, *J* = 8.8 Hz, NOCH), 4.03-4.07 (1 H, m, 1-H), 4.13 (1 H, dd, *J* = 9.0, 4.8 Hz, NOCH), 4.17 (2 H, t, *J* = 5.6 Hz, $OCH_2CH_2N(CH_3)_2$), 4.60 (1 H, t, *J* = 9.1 Hz, 2-H), 4.81 (1 H, dd, *J* = 10.2, 1.2 Hz, 2-H), 6.90 (1 H, s, Boc NH), 7.00 (1 H, s, indole 7-H), 7.02 (1 H, dd, *J* = 8.9, 2.4 Hz, indole 6-H), 7.13 (1 H, d, *J* = 2.1 Hz, indole 3-H), 7.36 (1 H, d, *J* = 8.9 Hz, indole 7-H), 7.42 (1 H, t, *J* = 7.5 Hz, 7-H), 7.50 (1 H, t, *J* = 7.2 Hz, 8-H), 7.84 (1 H, d, *J* = 8.2 Hz, 9-H), 7.89 (1 H, d, J = 8.5 Hz, 6-H), 8.90 (1 H, s, 4-H), 9.52 (1 H, s, indole NH); $^{13}$C NMR [($CDCl_3$) (HSQC / HMBC)] δ 16.94 piperidine 4-C), 20.01 (piperidine Me), 20.16 (piperidine Me), 28.30 ($CMe_3$), 33.02 (piperidine Me), 33.07 piperidine Me), 39.48 (piperidine 3-C or 5-C), 39.53 (piperidine 5-C or 3-C), 40.20 (1-C), 45.51 ($NCH_3)_2$), 54.66 (2-C), 58.06 ($OCH_2CH_2N(CH_3)_2$), 59.77 (piperidine 2-C or 6-C), 59.82 (piperidine 6-C or 2-C), 66.14 ($OCH_2CH_2N(CH_3)_2$), 77.64 ($NOCH_2$), 80.69 ($CMe_3$), 103.71 (indole 3-C), 105.58 (indole 4-C), 111.95 (4-C), 112.61 (indole 7-C), 116.79 (indole 6-C), 122.13 (6-C), 122.62 (9b-C), 123.91 (9-C), 124.47 (7-C), 126.60 (8-C), 128.31 (indole 3a-C), 130.07 (9a-C), 130.99 (5a-C), 131.26 (indole 7a-C), 133.71 (5-C), 141.39 (3a-C), 153.50 (indole 5-C + indole C=O), 160.23 (Boc C=O); MS ($ES^+$) *m/z* 706.3970 (M + Na) ($C_{40}H_{53}N_5NaO_5$ requires 706.3944).

## 5.46 Reductive removal of the 2,2,6,6-tetramethylpiperidine protecting group

To compound **128** (123.28 mg, 0.18 mmol) was added THF (2 mL), AcOH (6 mL), $H_2O$ (2 mL) and activated zinc dust (353.52 mg, 5.41 mmol) in a pressure tube equipped with magnetic stir bar. The reaction mixture was heated to 70°C for 2 h followed by a further addition of activated zinc dust (354 mg, 5.4 mmol) and heated to 70°C for 21 h. After cooling to room temperature and diluted with THF, the organics were filtered through Celite® and concentrated *in vacuo*. Chromatography (EtOAc → EtOAc / MeOH / $Et_3N$ 95:5:0.1) gave two fractions each with a mixture of compounds. First fraction (14.01 mg) consisted of **130** and **131** whilst the second fraction (41.28 mg) consisted of **132** and **133**.

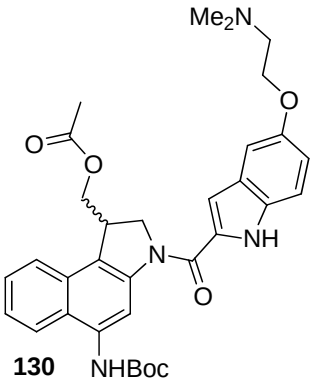


**130**

MS (ES$^+$) *m/z* 587.2945 (M + 1)
($C_{33}H_{39}N_4O_6$ requires 587.2870)

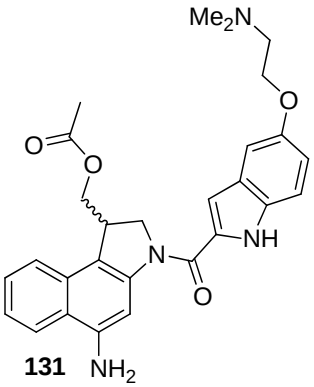


**131**

MS (ES$^+$) *m/z* 487.2432 (M + 1)
($C_{28}H_{31}N_4O_4$ requires 487.2345)

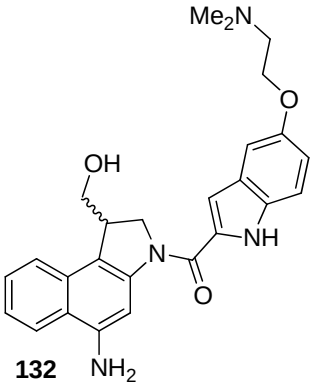


**132**

MS (ES$^+$) *m/z* 445.2328 (M + 1)
($C_{26}H_{29}N_4O_3$ requires 445.2240)

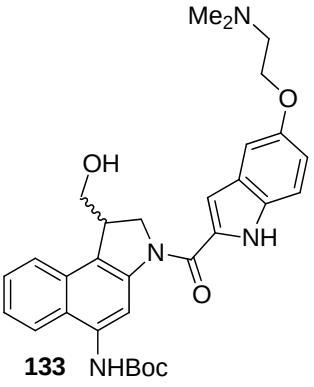


**133**

MS (ES$^+$) *m/z* 545.2815 (M + 1)
($C_{31}H_{37}N_4O_5$ requires 545.2764)

### 5.47 (5-(*tert*-Butoxycarbonylamino)-3-(5-(2-dimethylaminoethoxy) indole-2-carbonyl)-2,3-dihydro-1*H*-benzo[*e*]indol-1-yl)methyl acetate (130)

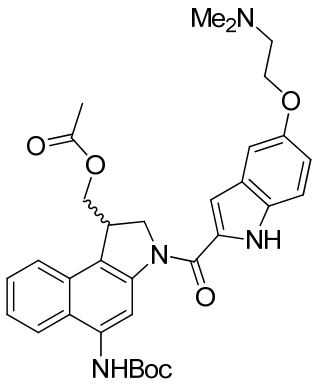

The mixture of **130** and **131** (14.0 mg) and $Boc_2O$ (62.8 mg) were boiled under reflux in dry THF (10 mL) under $N_2$ overnight. Evaporation and chromatography (EtOAc → EtOAc / MeOH / $Et_3N$ 90:10:0.1) gave **130** as a pale buff solid (14.53 mg): mp 170-171°C; $R_f$ = 0.3 (EtOAc / MeOH 1:1); $^1$H NMR [(MeOD) (NOESY)] δ 1.61 (9 H, s, $Bu^t$), 2.03 (3 H, s, OAc), 2.46 (6 H, s, $NMe_2$), 2.88 (2 H, t, *J* = 5.4 Hz, C*H*$_2$$NMe_2$), 4.10 (1 H, dd, *J* = 10.8, 8.0 Hz, C*H*OAc), 4.19 (2 H, t, *J* = 5.4 Hz, OC*H*$_2$$CH_2NMe_2$), 4.16-4.22 (1 H, m, 1-H), 4.59 (1 H, dd, *J* = 10.8, 3.6 Hz, C*H*OAc), 4.68 (2 H, d, *J* = 4.4 Hz, 2-H), 7.04 (1 H, dd, *J* = 9.0, 2.4 Hz, indole 6-H), 7.11 (1 H, s, indole 3-H), 7.23 ( 1 H, d, *J* = 2.1 Hz, 4-H), 7.45 (1 H, d, *J* = 8.9 Hz, indole 7-H), 7.51 (1 H, ddd , *J* = 8.2, 6.8, 1.0 Hz, 7-H), 7.60 (1 H, ddd, *J* = 8.0, 6.8, 1.0 Hz, 8-H), 8.01 (1 H. d, *J* = 8.3 Hz, 9-H), 8.08 (1 H, d, *J* = 8.5 Hz, 6-H); $^{13}$C NMR [(MeOD) (HSQC / HMBC)] δ 20.73 (OAc), 28.78 (C*Me*$_3$), 41.13 (1-C), 45.82 ($NMe_2$), 56.45 (2-C), 59.27 (*C*$H_2$$NMe_2$), 66.48 (*C*$H_2$OAc), 67.12 (O*C*$H_2$$CH_2NMe_2$), 81.30 (*C*$Me_3$), 104.65 (indole 4-C), 107.35 (indole 3-C), 114.01 (indole 7-C), 115.05 (4-C), 117.67 (indole 6-C), 123.93 (9b-C), 124.64 (6-C, or 9-C), 124.71 (9-C or 6-C), 125.87 (7-C), 127.90 (5a-C), 128.21 (8-C), 129.37 (indole 3a-C), 131.54 (9a-C), 132.06 (indole 2-C), 133.70 (indole 7a-C), 135.96 (indole 5-C), 142.52 (indole 3a-C), 154.91 (indole 5-C), 156.70 (Boc C=O), 162.89 (indole C=O), 172.77 (OAc C=O); MS ($ES^+$) *m/z* 587.2945 (M + H) ($C_{33}H_{39}N_4O_6$ requires 587.2870).

### 5.48 *tert*-Butyl N-(3-(5-(2-dimethylaminoethoxy) indole-2-carbonyl)-1-(hydroxymethyl)-2,3-dihydro-1*H*-benzo[*e*]indol-5-yl)carbamate (133)

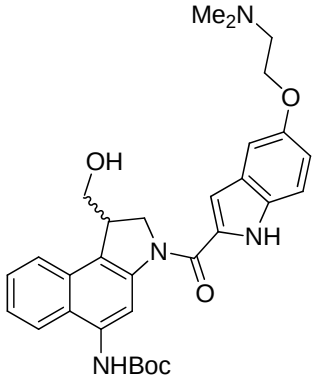

To compound **128** (122.7 mg, 0.18 mmol) were added sequentially, THF (3.0 mL), $H_2O$ (1.0 mL), activated Zn dust (934 mg, 14.4 mmol, 80 eq.) and AcOH (1.0 mL). The mixture was heated at 70°C in a sealed pressure tube overnight. After cooling to room temperature, the mixture was filtered through Celite® and the solvents were evaporated from the filtrate. Sat aq. $NaHCO_3$ was added to the mixture and the suspension was extracted with EtOAc. The organic phase was washed with water and brine. Drying, evaporation and chromatography (EtOAc → EtOAc / MeOH / $Et_3N$

90:10:0.1) gave **133** as an off-white solid (69.3 mg, 71%): $R_f$ = 0.2 (EtOAc / MeOH 1:1); mp 219-220°C; IR $\nu_{max}$ 3567, 3423, 3293 (OH, NH), 1684 (C=O); $^1$H NMR [$(CD_3)_2SO$ (NOESY)] δ 1.56 (9 H, s, Bu$^t$), 2.36 (6 H, s, $NMe_2$), 2.79 (2 H, t, *J* = 5.7 Hz, C*H*$_2$$NMe_2$), 3.23 (1 H, m, C*H*OH), 3.84-3.87 (1 H, m, C*H*OH), 4.02 (1 H, m, 1-H), 4.15 (2 H, t, *J* = 5.8 Hz, OC*H*$_2$$CH_2NMe_2$), 4.74 (2 H, m, 2-H), 5.11 (1 H, br, OH), 6.98 (1 H, dd, *J* = 8.9, 2.4 Hz, indole 6-H), 7.18 (1 H, d, *J* = 1.7 Hz, indole 3-H), 7.24 (1 H, d, *J* = 2.3 Hz, indole 4-H), 7.46 (1 H, d, *J* = 8.8 Hz, indole 7-H), 7.48 (1 H, t, *J* = 8.2 Hz, 7-H), 7.8 (1 H, t, *J* = 7.8 Hz, 8-H), 7.96 (1 H, d, *J* = 8.3 Hz, 9-H), 8.06 (1 H, d, *J* = 8.4 Hz, 6-H), 8.58 (1 H, s, 4-H), 9.29 (1 H, s, Boc NH), 11.66 (1 H, s, indole NH); $^{13}$C NMR [$(CD_3)_2SO$) (HSQC / HMBC)] δ 28.16 (C*Me*$_3$), 42.81 (1-C), 45.35 ($NMe_2$), 54 (2-C), 57.65 (*C*$H_2NMe_2$), 62.81 ($CH_2OH$), 65.95 (O*C*$H_2CH_2NMe_2$), 78.95 (*C*$Me_3$), 103.31 (indole 4-C), 105.35 (indole 3-C), 113.13 (indole 7-C), 113.61 (4-C), 115.78 (indole 6-C), 123.38 (9b-C), 123.65 (9-C), 123.88 (6-C), 124.01 (7-C), 125.78 (5a-C), 126.62 (indole 2-C), 129.72 (9a-C), 131.08 (indole 3a-C), 131.66 (indole 7a-C), 134.20 (5-C), 141.01 (3a-C), 152.90 (indole 5-C), 154.07 (Boc C=O), 160.26 (indole C=O); MS (ES$^+$) *m/z* 567.2608 (M + Na) ($C_{31}H_{36}N_4NaO_5$ requires 567.258340), 545.2829 (M + H) ($C_{31}H_{37}N_4O_5$ requires 545.2764).

### 5.49 N'-(1-(Chloromethyl)-3-(5-(2-dimethylaminoethoxy) indole-2-carbonyl)-2,3-dihydro-1*H*-benzo[*e*]indol-5-yl)-N,N-dimethylformimidamide (134)

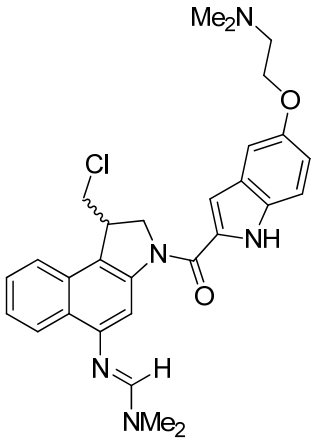


Compound **133** (29.6 mg, 54 µmol) was stirred in dry DMF (0.4 mL) under $N_2$ at 0°C. $Et_3N$ (38.0 µL, 27.6 mg, 0.27 mmol) was added dropwise, followed by dropwise addition of MsCl (13.0 µL, 19.2 mg, 0.16 mmol). The mixture was stirred at 0°C for 1 h. LiCl (134 mg, 3.2 mmol) was added to the mixture which was stirred at 20°C for 3 d. Water was added and the solvent was evaporated (< 30°C). Chromatography (EtOAc → EtOAc / MeOH / $Et_3N$ 95:5:0.1) gave **134** (21.3 mg, 76%) as a yellow solid: $R_f$ = 0.2 (EtOAc / MeOH 1:1); mp 229-230°C; $^1$H NMR [($CDCl_3$) (NOESY)] δ 2.42 (6 H, s, $OCH_2CH_2N$*Me*$_2$), 2.84 (2 H, t, *J* = 5.6 Hz, C*H*$_2$$NMe_2$), 3.04 (3 H, br, NCHN*Me*), 3.10 (3 H, br, NCHN*Me*), 3.45 (1 H, t, *J* = 10.9 Hz, CHCl), 3.98 (1 H, dd, *J* = 11.4, 3.1 Hz, CHCl), 4.10-4.18 (1 H, m, 1-H), 4.16 (2 H, t, *J* = 5.6 Hz, OC*H*$_2$$CH_2NMe_2$), 4.63 (1 H, t, *J* = 8.6 Hz, 2-H), 4.78 (1 H, dd, *J* = 10.8, 1.5 Hz, 2-H), 7.00 (1 H, d, *J* = 2.4 Hz, indole 6-H), 7.02 (1 H, d, *J* = 2.3 Hz, indole 3-H), 7.14 (1 H, d, *J* = 2.2 Hz, indole 4-H), 7.35 (1 H, d, *J* = 8.9 Hz, indole 7-H), 7.38 (1 H, t, *J* = 7.3 Hz, 7-H), 7.50 (1 H,

dd, *J* = 8.0, 1.1 Hz, 8-H), 7.67-7.69 (2 H, m, 9-H + NC*H*N(Me)$_2$), 7.70 (1 H, s, 4-H), 8.47 (1 H, d, *J* = 8.3 Hz, 6-H), 9.59 (1 H, s, indole NH). $^{13}$C NMR [(CDCl$_3$) (HSQC / HMBC)] δ ~35.0 (NCHN*Me*), ~40.0 (NCHN*Me*), 43.30 (1-C), 45.63 (OCH$_2$CH$_2$N*Me$_2$*), 46.08 (CH$_2$Cl), 55.05 (2-C), 58.21 (OCH$_2$*C*H$_2$NMe$_2$), 66.30 (O*C*H$_2$CH$_2$NMe$_2$), 103.70 (indole 4-C), 104.68 (4-C), 105.97 (indole 3-C), 112.63 (indole 7-C), 117.10 (indole 6-C), 118.26 (9b-C), 121.97 (9-C), 123.64 (7-C), 125.76 (6-C), 127.26 (8-C), 127.81 (5a-C), 128.25 (indole 3a-C), 129.75 (9a-C), 130.81 (indole 7-C), 131.36 (indole 7a-C), 142.03 (3a-C), 150.91 (5-C), 153.03 (N*C*HNMe$_2$), 153.66 (indole 5-C), 160.49 (indole C=O). Ms (ES$^+$) *m/z* 520.2375 (M + H) (C$_{29}$H$_{32}$$^{37}$ClN$_5$O$_2$ requires 520.2293), 518.2341 (M + H) (C$_{29}$H$_{32}$$^{35}$ClN$_5$O$_2$ requires 518.2323).

### 5.50 *tert*-Butyl N-(1-chloromethyl-3-(5-(2-dimethylaminoethoxy)indole-2-carbonyl)-2,3-dihydro-1*H*-benzo[*e*]indol-5-yl)carbamate (135)

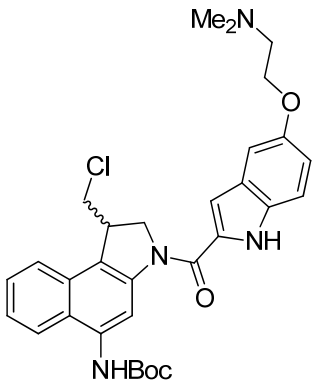


Compound **133** (23.8 mg, 44 μmol) was stirred in dry pyridine (0.7 mL) under N$_2$ at 0°C. Methanesulfonyl chloride (5.0 μL, 7.0 mg, 61 μmol) was added dropwise and the mixture was stirred at 0°C for 1 h. LiCl (92 mg, 2.2 mmol) was added and the mixture was warmed to 20°C and was stirred for 7 d. EtOAc was added followed by sat. aq. NaHCO$_3$. The mixture was extracted with EtOAc; the extract was washed with water and brine. Drying, evaporation and chromatography (EtOAc → EtOAc / MeOH / Et$_3$N 980:20:1) gave **135** (16.3 mg, 66%) as a yellow solid: R$_f$ = 0.3 (MeOH / EtOAc 1:1); mp > 250°C; $^1$H NMR [(CDCl$_3$) (COSY / NOESY)] δ 1.55 (9 H, s, Bu$^t$), 2.37 (6 H, s, NMe$_2$), 2.78 (2 H, t, *J* = 5.7 Hz, C*H$_2$*NMe$_2$), 3.47 (1 H, t, *J* = 10.7 Hz, ClCH), 3.96 (1 H, dd, *J* = 11.2, 2.9 Hz, , ClCH), 4.13 (2 H, t, *J* = 5.8 Hz, OC*H$_2$*CH$_2$NMe$_2$), 4.14 (1 H, m, 1-H), 4.66 (1 H, t, *J* = 8.6 Hz, 2-H), 4.82 (1 H, dd, *J* = 10.7, 1.7 Hz, 2-H), 6.91 (1 H, s, Boc NH), 7.01 (1 H, d, *J* = 1.4 Hz, indole 3-H), 7.04 (1 H, dd, *J* = 8.9, 2.4 Hz, indole 6-H), 7.14 (1 H, d, *J* = 2.2 Hz, indole 4-H), 7.35 (1 H, d, *J* = 8.9 Hz, indole 7-H), 7.45 (1 H, ddd, *J* = 8.3, 7.0, 1.1 Hz, 7-H), 7.55 (1 H, ddd, *J* = 7.9, 6.8, 0.9 Hz, 8-H), 7.77 (1 H, d, *J* = 8.2 Hz, 9-H), 7.90 (1 H, d, *J* = 8.4 Hz, 6-H), 8.92 (1 H, s, 4-H), 9.42 (1 H, s, indole NH). $^{13}$C NMR [(CDCl$_3$) δ (HSQC / HMBC)] 28.28 (C*Me$_3$*), 43.40 (1-C), 45.84 (NMe$_2$ + CH$_2$Cl), 54.94 (2-C), 58.37 (*C*H$_2$NMe$_2$), 66.59 (O*C*H$_2$CH$_2$NMe$_2$), 80.92 (*C*Me$_3$), 103.64 (indole 4-C), 105.90 (indole 3-C), 111.46 (4-C), 112.59 (indole 7-C), 117.32 (indole 6-C), 120.77 (9b-C), 122.37 (6-C), 123.04 (9-C), 124.71 (5a,7-C$_2$), 127.23 (8-C), 128.24 (indole 3a-C), 129.68 (9a-C), 130.49 (indole 2-C), 131.32 (indole 7a-C), 134.75 (5-C), 141.66 (3a-C), 153.28 (Boc C=O), 153.86 (indole 5-C),

160.41 (indole C=O); MS ($ES^+$) *m/z* 565.2382 (M + H) ($C_{31}H_{36}{}^{37}ClN_4O_4$ requires 565.2396), 563.2443 (M + H) ($C_{31}H_{36}{}^{35}ClN_4O_4$ requires 563.2425), 427.2157 [(M – (Boc + Cl) + H] ($C_{26}H_{27}N_4O_2$ requires 427.2134).

### 5.51 5-Amino-1-chloromethyl-3-(5-(2-dimethylaminoethoxy)indole-2-carbonyl)-2,3-dihydro-1*H*-benzo[*e*]indole dihydrochloride (136)

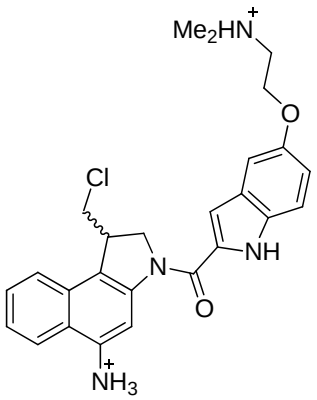


HCl in 1,4-dioxane (4.0 M, 2mL) was added to **135** and the mixture stirred at 20°C for 2 h. The solvent and excess HCl were evaporated at 20°C. The residue was triturated with acetonitrile and $Et_2O$. Drying gave **136** (15.3 mg, 100%) as a buff solid: mp > 250°C. A sample in EtOAc was washed with sat. aq. $NaHCO_3$ and brine. Drying and evaporation gave the free base as a yellow solid: $R_f$ = 0.3 (EtOAc / MeOH 1:1); mp > 250 °C; $^1H$ NMR [$(CD_3)_2SO$) (NOESY)] δ 2.90 (6 H, d, *J* = 3.3 Hz, $NMe_2$), 3.55 (2 H , t, *J* = 4.2 Hz, C*H*$_2$$NMe_2$), 3.77 (1 H, dd, *J* = 11.0, 8.2 Hz, ClCH), 3.99 (1 H, dd, *J* = 11.1, 3.1 Hz, ClCH), 4.15 (1 H, m, 1-H), 4.33 (2 H, t, *J* = 4.9 Hz, OC*H*$_2$$CH_2NMe_2$), 4.52 (1 H, dd, *J* = 10.8, 1.5 Hz, 2-H), 4.75 (1 H, t, *J* = 10.7 Hz, 2-H), 7.00 (1 H, d, *J* = 8.8 Hz, indole 6-H), 7.10 (1 H, d, *J* = 1.7 Hz, indole 3-H), 7.26 (1 H, d, *J* = 1.9 Hz, indole 4-H), 7.32 (1 H, t, *J* = 7.9 Hz, 7-H), 7.45 (1 H, d, *J* = 8.9 Hz, indole 7-H), 7.48 (1 H, t, *J* = 7.4 Hz, 8-H), 7.75-7.80 (2 H, m, 4,9-$H_2$), 8.08 (1 H, d, *J* = 8.5 Hz, 6-H), 11.66 (1 H, s, indole NH); $^{13}C$ NMR [$(CD_3)_2SO$) (HSQC / HMBC)] δ 41.40 (1-C), 42.89 ($NMe_2$), 47.51 ($ClCH_2$), 55.04 (2-C), 55.67 (*C*$H_2NMe_2$), 62.70 (O*C*$H_2CH_2NMe_2$), 99.50 (4-C), 104.01 (indole 4-C), 105.00 (indole 3-C), 113.30 (indole 7-C), 115.54 (indole 6-C), 117.55 (9b-C), 120.67 (4a-C), 122.46 (7-C), 123.05 (9-C), 123.37 (6-C), 126.91 (8-C), 127.11 (indole 2-C), 130.01 (9a-C), 131.52 (indole 3a-C), 131.95 (indole 7a-C), 142.78 (5-C), 151.97 (indole 5-C), 157.90 (3a-C), 158.17 (C=O); MS ($ES^+$) *m/z* 465.1910 (M + H) ($C_{26}H_{28}{}^{37}ClN_4O_2$ requires 465.1871), 463.1874 (M + H) ($C_{26}H_{28}{}^{35}ClN_4O_2$ requires 463.1901).

## 5.52 (9*H*-Fluoren-9-yl)methyl *S*-(2,6-dioxopiperidin-3-yl)carbamate (157)

Method A

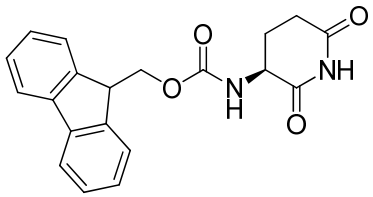

Dry pyridine (15 mL) was stirred with Fmoc-L-Gln-OH **155** (2.01 g, 5.46 mmol) under $N_2$ for 20 min. DCC (1.73 g, 8.40 mmol) in dry pyridine (5 mL) was added during 30 min and the mixture was stirred for 3 h. The reaction was filtered through Celite®. The solvent was evaporated to approximately half the volume and the mixture was filtered again (Celite®). The solvent was evaporated and water was added. The suspension was kept at 4°C for 1 h. The suspension was filtered. Aq. HCl (6 M, 50 mL) was added and the suspension was extracted with EtOAc. The extract was washed with brine and dried. The solvent was evaporated to yield **157** (914 mg, 48%) as a white solid with properties as below.

Method B

Fmoc-L-Gln-OH **155** (1.55 g, 4.2 mmol) was suspended in dry THF (20 mL) and placed under $N_2$. Dry pyridine (2.0 mL) was added and the mixture was stirred at 0°C. Trifluoroacetic anhydride (2.0 mL) was added dropwise during 45 min (keeping the temperature ≤ 5°C). The mixture was then stirred at 0°C for 6 h. The solvent was evaporated and the residue was suspended in water and EtOAc. Extraction with EtOAc, drying and chromatography (petroleum ether / EtOAc 1:1 → EtOAc) gave **157** (867 mg, 59 %) as a white solid:

$R_f$ = 0.7 (EtOAc); mp 125-127ºC; IR $\nu_{max}$ 3290 (NH), 3185(NH), 3083(NH), 1690 (C=O); $^1$H NMR [$(CD_3)_2SO$] δ 1.98-2.04 (2 H, m, Gln γ-$H_2$), 2.56 (1 H, m, Gln β-H), 2.80 (1 H, dt, *J* = 17.6, 6.2 Hz, β-H), 4.32 (1 H, t, *J* = 6.7 Hz, fluorene 9-H), 4.38-4.40 (3 H, m, Fmoc-$CH_2$, Gln α-H), 7.40 (2 H, t, *J* = 7.4 Hz, fluorene 2,7-$H_2$), 7.48 (2 H, t, *J* = 7.4 Hz, fluorene 3,6-$H_2$), 7.72 (1 H, d, *J* = 8.7 Hz, Fmoc NH), 7.78 (2 H, d, *J* = 7.3 Hz, fluorene 4,5-$H_2$), 8.02 (2 H, d, *J* = 7.5 Hz, fluorene 1,8-$H_2$), 10.87 (1 H, brs, NH). $^{13}$C NMR [$(CD_3)_2SO$) (HSQC / HMBC)] δ 24.28 (Gln γ-C), 30.94 (Gln β-C), 46.58 (fluorene 9-C), 50.71 (Gln α-C), 65.63 (Fmoc $CH_2$), 120.13 (fluorene 1,8-$C_2$), 125.20 (fluorene 4,5-$C_2$), 127.07 (fluorene 2,7-$C_2$), 127.63 (fluorene 3,6-$C_2$), 140.73 (fluorene 4a,4b-$C_2$), 143.81 (fluorene 8a,9a-$C_2$), 156.08 (C=O), 172.37 (C=O), 172.97 (C=O); MS ($ES^+$) *m/z* 373.1174 (M + Na) ($C_{20}H_{18}N_2NaO_4$ requires 373.1164), 351.1347 (M + H) ($C_{20}H_{19}N_2O_4$ requires 351.1345).

### 5.53 *S*-2-(Benzyloxycarbonylamino)-4-cyanobutanoic acid (163)

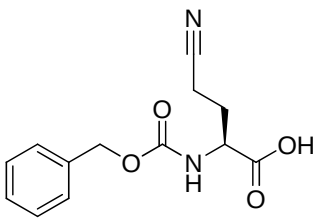

Cbz-L-Gln-OH **162** (4.11 g, 14.3 mmol) in dry pyridine (15 mL) was treated with DCC (3.03 g, 14.7 mmol) in dry pyridine (15 mL), added in portions during 30 min. The mixture was stirred for 16 h and was then filtered through Celite®. Most of the solvent was evaporated and the suspension was filtered again. The remaining solvent was evaporated. Water was added to the residue followed by aq. HCl (2 M) until the pH was *ca*. 1. The mixture was extracted with EtOAc (3 ×) and dried. Evaporation and chromatography (EtOAc) gave **163** (3.06 g, 82%) as a colourless oil: $R_f$ = 0.3 (EtOAc); IR $\nu_{max}$ 3320 $cm^{-1}$ (NH, OH), 2251 $cm^{-1}$ (C≡N), 1710 $cm^{-1}$ (C=O); $^1$H NMR ($CDCl_3$) δ 2.06 (1 H, m, 3-H), 2.29 (1 H, m, 3-H), 2.44 (2 H, t, *J* = 6.6 Hz, 4-$H_2$), 4.43 (1 H, t, *J* = 6.7 Hz, 2-H), 5.10 (2 H, s, $PhCH_2$), 5.62 (1 H, d, *J* = 7.2 Hz, NH), 7.34 (5 H, m, Ph-$H_5$); $^{13}$C NMR [($CDCl_3$) (HMBC / HMQC)] δ 13.57 (4-C), 21.01 (3-C), 52.62 (2-C), 67.46 ($PhCH_2$), 118.65 (CN), 128.14 (Ph 2,6-$C_2$), 128.37 (Ph 3,5-$C_2$), 128.58 (Ph 4-C), 135.68 (Ph 1-C), 156.24 (N-C=O), 174.01 ($CO_2H$); MS ($ES^+$) *m/z* 285.0837 (M + Na) ($C_{13}H_{14}N_2NaO_4$ requires 285.0851), 263.1022 (M + H) ($C_{13}H_{15}N_2O_4$ requires 263.1031).

### 5.54 *tert*-Butyl N-(N-phenylmethoxycarbonyl-L-leucyl)-D-serine methyl ester (168)

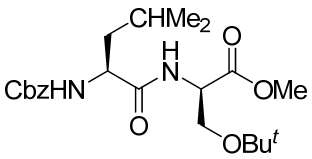

Cbz-L-Leu-OH **167** (670 mg, 2.5 mmol) and D-Ser(OBu$^t$)-OMe (1.00 g, 2.5 mmol) were stirred with benzotriazol-1-yl-oxytri-pyrrolidinophosphonium hexafluorophosphate (PyBOP) (1.60 g, 3.0 mmol) and $Et_3N$ (1.01 g, 10 mmol) in $CH_2Cl_2$ (30 mL) for 24 h. The solution was washed with water, aq. citric acid (5%), aq. $NaHCO_3$ and water. Drying, evaporation and chromatography (petroleum ether / EtOAc 7:3) afforded **168** (1.00 g, 95%) as a white powder: mp 83-84°C; $^1$H NMR ($CDCl_3$) δ 0.94 (6 H, d, *J* = 6.0 Hz, 2 × Leu Me), 1.18 (9 H, s, Bu$^t$), 1.52 (1 H, dd, *J* = 16.5, 8.5 Hz, Leu β-H), 1.63-1.72 (2 H, m, Leu β,γ-$H_2$), 3.55 (1 H, dd, *J* = 9.2, 2.7 Hz, Ser β-H), 3.73 (3 H, s, OMe), 3.79 (1 H, dd, *J* = 9.2, 2.7 Hz, Ser β-H), 4.25 (1 H, m, Leu α-H), 4.68 (1 H, td, *J* = 8.3, 2.7 Hz, Ser α-H), 5.12 (2 H, s, $PhCH_2$), 5.21 (1 H, d, *J* = 7.3 Hz, NH), 6.77 (1 H, d, *J* = 7.3 Hz, NH), 7.35 (5 H, s, Ph-$H_5$); $^{13}$C-NMR [($CDCl_3$) (HMBC / HMQC)] δ 22.85 (Leu Me), 22.85 (Leu Me), 24.70 (Leu γ-C), 27.25 (C*Me*$_3$), 41.78 (Leu β-C), 52.39 (OMe), 52.75 (Ser α-C), 53.50 (Leu α-C), 61.70 (Ser β-C), 67.04 ($PhCH_2$), 72.83 (*C*$Me_3$), 128.06 (Ph), 128.16 (Ph), 128.52 (Ph), 136.19 (Ph 1-C),

170.65 (Ser C=O), 171.13 (Cbz C=O), 171.81 (Leu C=O); MS ($ES^+$) *m/z* 445.2314 (M + Na) ($C_{22}H_{34}N_2NaO_6$ requires 445.2314), 423.2455 (M + H) ($C_{22}H_{35}N_2O_6$ requires 423.2495).

### 5.55 *tert*-Butyl N-(L-leucyl)-D-serine methyl ester (169)

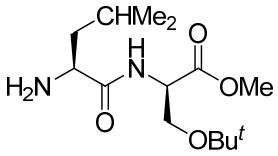


Compound **168** (280 mg, 0.66 mmol) was stirred vigorously under $H_2$ with Pd/C (10%, 30 mg) in MeOH (30 mL) for 16 h. Filtration (Celite®) and evaporation gave **169** (250 mg, quant.) as a white powder: mp 145-146°C; $^1$H NMR ($CDCl_3$) δ 0.92 (3 H, t, *J* = 6.9 Hz, Leu Me), 0.93 (3 H, t, *J* = 6.9 Hz, Leu Me), 1.11 (9 H, s, $Bu^t$), 1.39 (1 H, d heptet, *J* = 9.1, 4.1 Hz, Leu γ-H), 1.53 (2 H, br, $NH_2$), 1.62-1.77 (2 H, m, Leu β-$H_2$), 3.39 (1 H, dd, *J* = 9.3, 4.1 Hz, Leu α-H), 3.53 (1 H, dd, *J* = 9.1, 3.3 Hz, Ser β-H), 3.71 (3 H, s, OMe), 3.80 (1 H, dd, *J* = 9.1, 3.0 Hz, Ser β-H), 4.66 (1 H, td, *J* = 8.5, 3.0 Hz, Ser α-H), 7.78 (1 H, d, *J* = 8.0 Hz, NH); $^{13}$C NMR ($CDCl_3$) δ 21.50 (Leu Me), 23.44 (Leu Me), 24.88 (Leu γ-C), 27.39 (C*Me*$_3$), 44.03 (Leu β-C), 52.37(OMe), 52.58 (Ser α-C), 53.61 (Leu α-C), 62.12 (Ser β-C), 73.42 (*C*$Me_3$), 171.17 (Ser C=O), 175.71 (Leu C=O).

### 5.56 *tert*-Butyl N-(N-(*S*-2-phenylmethoxycarbonylamino-4-cyanobutanoyl)-L-leucyl)-D-serine methyl ester (170)

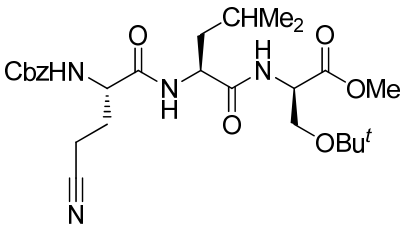


Compound **163** (900 mg, 3.43 mmol) and L-Leu-D-Ser($Bu^t$)-OMe **169** (1.00 g, 3.43 mmol) were stirred with 2-(1*H*-7-azabenzotriazol-1-yl)-1,1,3,3-tetramethyluronium hexafluorophosphate (HATU) (1.43 g, 3.77 mmol) and $Pr^i_2$NEt (885 mg, 6.86 mmol) in $CH_2Cl_2$ (80 mL) for 20 h. The solution was washed with water, aq. citric acid (5%), aq. $NaHCO_3$ and water. Drying, evaporation and chromatography (EtOAc) gave **170** (1.14 g, 77%) as a white powder: mp 95-96°C; $^1$H NMR ($CDCl_3$) δ 0.89 (3 H, d, *J* = 6.3 Hz, Leu Me), 0.92 (3 H, d, *J* = 6.3 Hz, Leu Me), 1.12 (9 H, s, $Bu^t$), 1.53 (1 H, t, *J* = 7.8 Hz, Leu β-H), 1.61-1.68 (2 H, m, Leu β,γ-$H_2$), 2.03 (1 H, ddd, *J* = 13.6, 7.6, 5.8 Hz, Gln(CN) β-H), 2.17 (1 H, ddd, *J* = 13.6, 7.6, 5.8 Hz, Gln(CN) β-H), 2.40 (2 H, t, *J* = 7.6 Hz, Gln(CN) γ-$H_2$), 3.55 (1 H, dd, *J* = 9.0, 3.1 Hz, Ser β-H), 3.71 (3 H, s, OMe), 3.77 (1 H, dd, *J* = 9.0, 3.1 Hz, Ser β-H), 4.45 (1 H, dd, *J* = 13.7, 7.5 Hz, Gln(CN) α-H), 4.55 (1 H, dd, *J* = 14.0, 7.5 Hz, Leu α-H), 4.65

(1 H, dt, *J* = 8.2, 3.1 Hz, Ser α-H), 5.88 (1 H, d, *J* = 7.6 Hz, CbzNH), 7.0 (1 H, d, *J* = 8.2 Hz, Ser NH), 7.18 (1H, d, *J* = 7.5 Hz, Leu NH); $^{13}$C NMR [($CDCl_3$) (HMBC / HMQC)] δ 13.35 (Gln(CN) γ-C), 22.18 (Leu Me), 22.61 (Leu Me), 24.62 (Leu γ-C), 27.17 (C*Me*$_3$), 28.44 (Gln(CN) β-C), 40.64 (Leu β-C), 51.61 (Leu α-C), 52.46 (OMe), 52.95 (Ser α-C), 53.23 (Gln(CN) α-C), 61.49 (Ser β-C), 67.19 ($PhCH_2$), 73.40 (O*C*$Me_3$), 119.19 (CN), 128.01 (Ph), 128.18 (Ph), 128.48 (Ph), 135.95 (Ph 1-C), 156.07 (Cbz C=O), 170.38 (Gln(CN) C=O), 170.61 (Leu C=O), 171.58 (Ser C=O); MS ($ES^+$) *m/z* 533.2941 (M + H) ($C_{27}H_{41}N_4O_7$ requires 533.2975).

## 5.57 N-(N-(*S*-2-Amino-4-cyanobutanoyl)-L-leucyl)- *tert*-butoxycarbonyl-D-serine methyl ester (171)

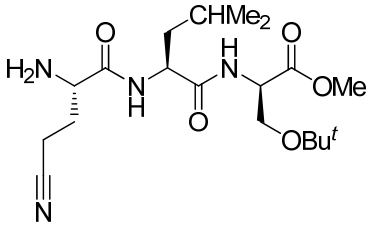


Compound **170** (820 mg, 1.54 mmol) was stirred vigorously under $H_2$ with Pd/C (10%, 80 mg) in MeOH (80 mL) for 16 h. Filtration (Celite®) and evaporation gave **171** (640 mg, quant.) as a pale yellow oil: $^1$H NMR ($CDCl_3$) δ 0.94 (3 H, d, *J* = 6.2 Hz, Leu Me), 0.96 (3 H, d, *J* = 6.2 Hz, Leu Me), 1.14 (9 H, s, Bu$^t$), 1.57 (1 H, m, Leu β-H), 1.65 (1 H, sextet, *J* = 6.2 Hz, Leu γ-H), 1.72 (1 H, m, Leu β-H), 1.88 (1 H, m, Gln(CN) β-H), 2.13 (1 H, m, Gln(CN) β-H), 2.54 (2 H, dt, *J* = 10.2, 6.6 Hz, Gln(CN) γ-H), 2.55 (2 H, dt, *J* = 10.2, 6.6 Hz, Gln(CN) γ-H), 3.49 (1 H, dd, *J* = 7.4, 5.8 Hz, Gln(CN) α-H), 3.56 (1 H, dd, *J* = 9.0, 3.5 Hz, Ser β-H), 3.74 (3 H, s, OMe), 3.79 (1 H, dd, *J* = 8.9, 3.1, Ser β-H), 4.51 (1 H, ddd, *J* = 14.4, 8.6, 2.4 Hz, Leu α-H), 4.65 (1 H, dt, *J* = 8.2, 3.1 Hz, Ser α-H), 6.88 (1 H, d, *J* = 8.2 Hz, Ser NH), 7.47 (1 H, d, *J* = 8.2 Hz, Leu NH); $^{13}$C-NMR [($CDCl_3$) (HMBC / HMQC)] δ 13.98 (Gln(CN) γ-C), 22.14 (Leu Me), 22.74 (Leu Me), 27.21 (C*Me*$_3$), 30.80 (Gln(CN) β-C), 40.76 (Leu β-C), 51.23 (Leu α-C), 52.41 (OMe), 52.83 (Ser α-C), 53.92 (Gln(CN) α-C), 61.58 (Ser βC), 73.42 (*C*$Me_3$), 119.41 (CN), 170.69 (Ser C=O), 171.63 (Leu C=O), 173.72 (Gln(CN) C=O).

## 5.58 *tert*-Butyl N-(N-(*S*-2-((N-phenylmethoxycarbonyl-L-leucyl)amino)-4-cyano-butanoyl)-L-leucyl)-D-serine methyl ester (172)

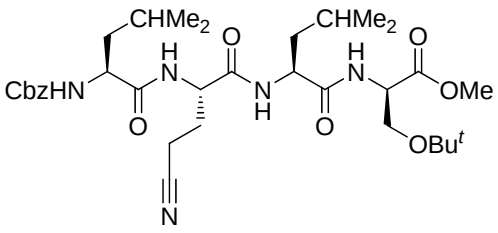

Cbz-L-Leu-OH **167** (210 mg, 0.80 mmol) and **171** (320 mg, 0.80 mmol) were stirred with benzotriazol-1-yl-oxytripyrrolidinophosphonium hexafluorophosphate (PyBOP) (500 mg, 0.96 mmol) and $Et_3N$ (323 mg, 3.20 mmol) in $CH_2Cl_2$ (15 mL) for 2 d. The solution was washed with water, aq. citric acid (5%), aq. $NaHCO_3$ and water. Drying, evaporation and chromatography (petroleum ether / EtOAc 7:3) afforded **172** (390 mg, 75%) as a white powder: mp 152-154ºC; IR (Nujol) $\nu_{max}$ 3304, 2239, 1758, 1705, 1629 $cm^{-1}$; $^1H$ NMR ($CDCl_3$) δ 0.91 (6 H, d, *J* = 6.2 Hz, 2 × Leu Me), 0.94 (6 H, d, *J* = 6.2 Hz, 2 × Leu Me), 1.14 (9 H, s, $Bu^t$), 1.51-1.70 (6 H, m, 2 × Leu γ-H + 2 × Leu β-$H_2$), 2.02 (1 H, m, Gln(CN) β-H), 2.23 (1 H, m, Gln(CN) β-H), 2.39 (2 H, t, *J* = 7.6 Hz, Gln(CN) γ-$H_2$), 3.57 (1 H, dd, *J* = 8.9, 3.1, Ser β-H), 3.73 (3 H, s, OMe), 3.79 (1 H, dd, *J* = 38.9, 3.1, Ser β-H), 4.19 (1 H, m, Gln(CN) α-H), 4.53 (1 H, dd, *J* = 14.0, 7.6 Hz, Leu α-H), 4.60 (1 H, m, Leu α-H), 4.65 (1H, dt, *J* = 8.0, 3.2 Hz, Ser α-H), 5.12 (2 H, s, $PhCH_2$), 5.30 (1 H, d, *J* = 7.6 Hz, NH), 6.80-6.89 (3 H, br m, 3 × NH), 7.35 (5 H, s, Ph-$H_5$); $^{13}C$ NMR [($CDCl_3$) (HMBC / HMQC)] δ 13.51 (Gln(CN) γ-C), 21.82 (Leu Me), 22.12 (Leu Me), 22.75 (Leu Me), 22.91 (Leu Me), 24.71 (2 × Leu γ-C), 27.25 (C*Me*$_3$), 28.07 (Gln(CN) β-C), 40.62 (2 × Leu β-C), 51.65 (Leu α-C), 51.91 (Leu α-C), 52.48 (OMe), 52.99 (Ser α-C), 53.72 (Gln(CN) α-C), 61.53 (Ser β-C), 67.28 ($PhCH_2$), 73.48 (*C*$Me_3$), 119.28 (CN), 128.09 (Ph), 128.28 (Ph), 128.57 (Ph), 136.04 (Ph 1-C), 156.46 (Cbz C=O), 169.79 (Ser C=O Ser), 170.60 (Gln(CN) C=O), 171.28 (Leu C=O), 172.56 (Leu C=O); MS ($ES^+$) *m/z* 668.3610 (M + Na) ($C_{33}H_{51}N_5Na_1O_8$ requires 668.3635).

## 5.59 *tert*-Butyl N-(N-(N-(N-phenylmethoxycarbonyl-L-leucyl)-L-glutamyl)-L-leucyl)-D-serine methyl ester (173)

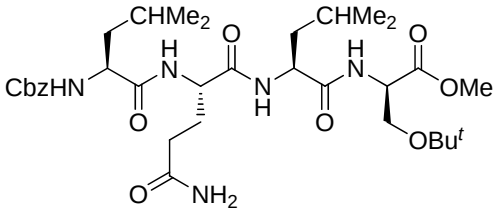

Aq. $H_2O_2$ (35%, 0.30 mL) was added to **172** (20 mg, 30 μmol) in aq. NaOH (0.5 M, 2.7 mL), followed by aq. NaOH (2.0 M, 0.2 mL). The mixture was stirred for 1 h at room temperature. The mixture was cooled to 0°C and the pH was adjusted to 2.0 with aq. HCl (1.0 M).

Extraction ($CH_2Cl_2$, thrice), drying and evaporation gave **173** (18.8 mg, 90%) as a white powder: mp 193-194°C; IR (Nujol) 3292, 1623, 1540 $cm^{-1}$; $^1H$ NMR ($CDCl_3$) δ 0.82 (6 H, d, *J* = 6.7 Hz, 2 × Leu Me), 0.86 (6 H, d, *J* = 6.7 Hz, 2 × Leu Me), 1.09 (9 H, s, $Bu^t$), 1.39-1.45 (4 H, m, 2 × Leu β-$H_2$), 1.59-1.60 (2 H, m, 2 × Leu γ-H), 1.75 (1 H, m, Gln β-H), 1.84-1.90 (1 H, m, Gln β-H), 2.08 (2 H, t, *J* = 7.2 Hz, Gln γ-H), 3.33 (3 H, s, OMe), 3.49 (1 H, dd, *J* = 9.0, 3.9 Hz, Ser β-H), 3.58 (1 H, dd, *J* = 9.4, 5.5 Hz, β-H), 4.03 (1 H, m Leu α-H), 4.25 (1 H, m, Gln α-H), 4.33 (1 H, dd, *J* = 7.8, 3.9 Hz, Ser α-H), 4.40 (1 H, m, Leu α-H), 5.01 (1 H, d, *J* = 13.0 Hz, PhCH), 5.02 (1 H, d, *J* = 13.0 Hz, PhCH), 6.74 (1 H, br, Gln γ-CONH), 7.20 (1 H, br, Gln γ-CONH), 7.31 (1 H, d, *J* = 8.6 Hz, Gln α-NH), 7.35 (5 H, s, Ph-$H_5$), 7.37 (1 H, d, *J* = 8.8 Hz, Leu NH), 7.93 (1 H, d, *J* = 9.0 Hz, Leu NH), 7.97 (1 H, d, *J* = 7.8 Hz, Ser NH); $^{13}C$ NMR [($CD_3OD$) (HMBC / HMQC)] δ 21.43 (Leu Me), 21.63 (Leu Me), 23.05 (2 × Leu Me), 24.04 (Leu γ-H), 24.16 (Leu γ-H), 27.13 (C*Me*$_3$), 27.79 (Gln β-C), 31.47 (Gln γ-C), 40.69 (Leu β-C), 41.18 (Leu β-C), 50.78 (Leu α-C), 51.87 (OMe), 52.00 (Gln α-C), 52.74 (Ser α-C), 53.07 (Leu α-C), 61.55 (Ser β-C), 65.37 ($PhCH_2$), 72.66 (*C*$Me_3$), 127.63 (Ph 2,6-$C_2$), 127.76 (Ph 4-C), 128.34 (Ph 3,5-$C_2$), 137.04 (Ph 1-C), 155.95 (Cbz C=O), 170.86 (Ser C=O), 171.55 (Gln α-C=O), 171.79 (Leu C=O), 172.31 (Leu C=O), 173.77 (Gln γ-C=O); MS ($ES^+$) *m/z* 664.3968 (M + H) ($C_{33}H_{54}N_5O_9$ requires 664.3916).

## 5.60 N-(N-(*S*-2-((N-Phenylmethoxycarbonyl-L-leucyl)amino)-4-cyanobutanoyl)-L-leucyl)-D-serine methyl ester (174)

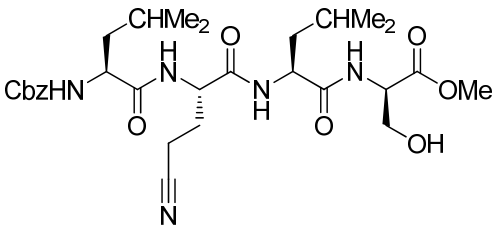


Compound **172** (33 mg, 51 μmol) was stirred with $CF_3CO_2H$ (1.0 mL) and $CH_2Cl_2$ (1.0 mL) for 1 h. Evaporation gave **174** (41 mg, quant.) as a pale yellow oil: $^1H$ NMR ($CDCl_3$) δ 0.89 (6 H, d, *J* = 6.9 Hz, 2 × Leu Me), 0.90 (6 H, d, *J* = 6.9 Hz, 2 × Leu Me),1.55-1.70 (6 H, m, 2 × Leu β-$H_2$ + 2 × Leu γ-H), 1.89-2.19 (2 H, m, Gln(CN) β-$H_2$), 2.35-2.42 (2 H, m, Gln(CN) γ-$H_2$), 3.72 (3H, s, OMe), 3.91 (1H, d, *J* = 11.0 Hz, Ser β-H), 4.05 (1H, dd, *J* = 12.1, 3.5 Hz, Ser β-H), 4.26 (1 H, m, Gln(CN) α-H), 4.60 (2 H, s, $PhCH_2$), 4.70 (1 H, dd, *J* = 11.3, 3.3 Hz, Leu α-H), 4.99-5.16 (2 H, m, Leu α-H + Ser α-H), 5.82 (1 H, d, *J* = 5.2 Hz, NH), 7.32 (5 H, m, Ph-$H_5$), 7.59 (1 H, br, NH), 7.78 (1 H, br, NH), 7.91 (1 H, br, NH); MS ($ES^-$) *m/z* 588.3053 (M - H) ($C_{29}H_{42}N_5O_8$ requires 588.3033).

### 5.61 Methyl *R*-2,2-dimethyl-3-(*S*-N-(4-cyano-2-(N-phenylmethoxycarbonyl-L-leucylamino)butanoyl)-L-leucyl)oxazolidine-4-carboxylate (175)

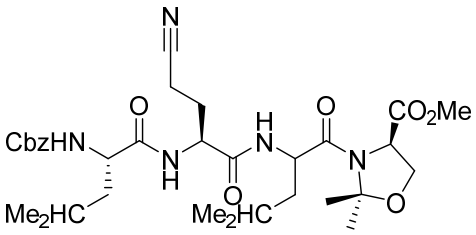

Compound **174** (32 mg, 54 μmol) was boiled under reflux with 2,2-dimethoxypropane (28 mg, 0.27 mmol) and TsOH (1.2 mg, 6 μmol) in $CH_2Cl_2$ (2.0 mL) under $N_2$ for 19 h. Evaporation and chromatography (petroleum ether / EtOAc 1:4) gave **175** (7.5 mg, 22%) as a pale yellow oil: $^1$H NMR ($CDCl_3$) δ 0.88 (6 H, d, *J* = 6.0 Hz, 2 × Leu Me), 0.91 (6 H , d, *J* = 5.5 Hz, 2 × Leu Me), 1.49 (3 H, s, Dmo 2-Me), 1.52-1.57 (4 H, m, 2 × Leu β-$H_2$), 1.59-1.69 (2 H, m, 2 × Leu γ-H), 1.64 (3 H, s, Dmo 2-Me), 1.98 (1 H, m, Gln(CN) β-H), 2.14 (1 H, m, Gln(CN) β-H), 2.30 (2 H, t, *J* = 7.2 Hz, Gln(CN) γ-$H_2$), 2.72 (1 H, t, *J* = 2.5 Hz, α-H), 3.78 (3 H, s, OMe), 4.07-4.25 (3 H, m, Dmo 4,5-$H_3$), 4.34 (1 H, t, *J* = 7.9 Hz, α-H), 4.61 (1 H, dd, *J* = 11.6, 5.8 Hz, α-H), 5.04 (1 H, d, *J* = 5.8 Hz, NH), 5.10 (2 H, s, $PhCH_2$), 5.59 (1 H, d, *J* = 8.0 Hz, NH), 6.85 (1 H, d, *J* = 8.3 Hz, NH), 7.33 (5 H, s, Ph-$H_5$); $^{13}$C NMR [($CD_3OD$) (HMBC / HMQC)] δ 13.29 (Gln(CN) γ-C), 21.21 (Leu Me), 21.83 (Leu Me), 22.85 (Dmo 2-Me), 22.87 (Leu Me), 23.43 (Leu Me), 24.38 (Leu γ-C), 24.68 (Leu γ-C), 24.85 (Dmo 2-Me), 27.81 (Gln(CN) β-C), 40.42 (Leu β-C), 40.34 (Leu β-C), 50.73 (α-C), 51.64 (α-C), 52.82 (OMe), 53.72 (Dmo 5-C), 59.46 (α-C), 67.07 (Dmo 4-C), 67.26 ($PhCH_2$), 96.73 (Dmo 2-C), 118.99 (CN), 128.15 (Ph 2,6-$C_2$), 128.28 (Ph 4-C), 128.55 (Ph 3,5-$C_2$), 136.07 (Ph 1-C), 156.57 (C=O), 169.57 (C=O), 169.98 (C=O), 169.98 (C=O), 171.05 (C=O), 172.57 (C=O); MS ($ES^+$) *m/z* 652.3282 (M + Na) ($C_{32}H_{47}N_5Na_1O_8$ requires 652.3322), 630.3464 (M + H) ($C_{32}H_{48}N_5O_8$ requires 630.3502).

### 5.62 N-(N-(*S*-4-Cyano-2-(phenylmethoxycarbonylamino)butanoyl)-L-leucyl)-D-serine methyl ester (176)

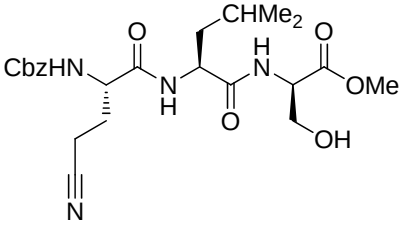

Compound **170** (200 mg, 0.37 mmol) was stirred with $CF_3CO_2H$ (2.0 mL) and $CH_2Cl_2$ (2 mL) for 2 h. Evaporation afforded **176** (220 mg, quant.) as a yellow oil: $^1$H NMR ($CDCl_3$) δ 0.87 (3 H, d, *J* = 5.2 Hz, Leu Me), 0.88 (3 H, d, *J* = 5.2 Hz, Leu Me), 1.55-1.60 (3 H, m, Leu β,γ-$H_3$), 1.95 (1 H, m, Gln(CN) β-H), 2.14 (1 H, m, Gln(CN) β-H), 2.40 (2 H, t, *J* = 6.9 Hz, Gln(CN) γ-$H_2$), 3.70 (3 H, s, OMe), 3.86 (1 H, dd, *J* =

11.3, 6.0 Hz, Ser β-H), 3.99 (1 H, ddd, *J* = 11.3, 6.0, 3.6 Hz, Ser β-H), 4.43 (1 H, t, *J* = 6.9 Hz, Gln(CN) α-H), 4.57-4.72 (2 H, m, Leu α-H + Ser α-H), 5.07 (2 H, s, $PhCH_2$), 6.29 (2 H, br, 2 × NH), 7.31 (5 H, s, Ph-$H_5$), 7.55 (1 H, t, *J* = 6.0 Hz, OH); $^{13}C$ NMR ($CDCl_3$) δ 13.46, 14.12, 21.64, 22.69, 24.78, 28.75, 40.74, 50.97, 52.40, 53.24, 67.27, 119.01, 128.00, 128.12, 128.27, 128.53, 135.84, 156.08, 170.15, 172.92; MS ($ES^+$) *m/z* 477.2327 (M + H) ($C_{23}H_{33}N_4O_7$ requires 477.2349).

## 5.63 Methyl *R*-2,2-dimethyl-3-(*S*-N-(4-cyano-2-(phenylmethoxycarbonylamino)-butanoyl)-L-leucyl)oxazolidine-4-carboxylate (177).

Compound **176** (220 mg, 0.46 mmol) was boiled under reflux with 2,2-dimethoxypropane (240 mg, 2.3 mmol) and TsOH (9.6 mg, 50 μmol) in $CH_2Cl_2$ (5.0 mL) under $N_2$ for 19 h. Evaporation and chromatography (petroleum ether / EtOAc 1:4) gave **177** (120 mg, 50%) as a pale yellow oil:

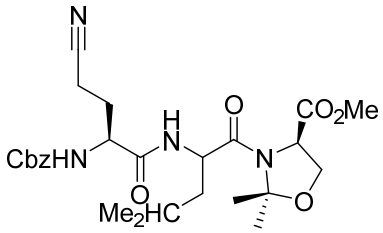


$^1H$ NMR ($CDCl_3$) δ 0.81 (3 H, d, *J* = 5.8 Hz, Leu Me), 0.90 (3 H, d, *J* = 6.3 Hz, Leu Me), 1.54 (3 H, s, Dmo 2-Me), 1.44-1.64 (3 H, m, Leu β,γ-$H_3$), 1.66 (3 H, s, Dmo 2-Me), 1.92 (1 H, m, Gln(CN) β-H), 2.18 (1 H, m, Gln(CN) β-H), 2.40 (2 H, t, *J* = 7.0 Hz, Gln(CN) γ-$H_2$), 3.80 (3 H, s, OMe), 4.18 (2 H, dd, *J* = 9.4, 6.2 Hz, Dmo 5-H), 4.24 (1 H, d, *J* = 9.4 Hz, Dmo 5-H), 4.32 (1 H, t, *J* = 8.6 Hz, Leu α-H), 4.37 (1 H, m, Gln(CN) α-H), 5.05 (1 H, d, *J* = 5.8 Hz, Dmo 4-H), 5.11 (2 H, s, $PhCH_2$), 5.49 (1 H, d, *J* = 7.4 Hz, CbzNH), 6.60 (1 H, d, *J* = 6.6 Hz, Leu NH), 7.35 (5 H, s, Ph-$H_5$); $^{13}C$ NMR [($CDCl_3$) (HMBC / HMQC)] δ 13.31 (Gln(CN) γ-C), 21.10 (Leu Me), 22.90 (Dmo 2-Me), 23.43 (Leu Me), 24.39 (Leu γ-C), 24.88 (Dmo 2-Me), 28.52 (Gln(CN) β-C), 40.39 (Leu β-C), 50.90 (Gln(CN) α-C), 52.82 (OMe), 53.20 (Leu α-C), 59.44 (Dmo 4-C), 67.10 (Dmo 5-C), 67.42 ($PhCH_2$), 96.76 (Dmo 2-C), 118.70 (CN), 128.17 (Ph 2,6-$C_2$), 128.39 (Ph 4-C), 128.60 (Ph 3,5-$C_2$), 135.78 (Ph 1-C), 155.83 (Cbz C=O), 169.56 (Gln C=O), 170.10 (Leu C=O), 171.01 (Dmo C=O); MS ($ES^+$) *m/z*: 539.2450 (M + Na) ($C_{26}H_{36}N_4O_7Na$ requires 539.2476).

## 5.64 Methyl *S*-2-(2-(benzyloxycarbonylamino)-4-cyanobutanamido)propanoate (178)

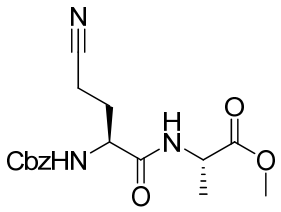

Cbz-L-Gln(CN)-OH **163** (3.06 g, 11.7 mmol) was stirred with DMF (200 mL) and $Pr^{i}_{2}NEt$ (12 mL, 8.90 g, 69 mmol) and PyBOP (9.10 g, 17.5 mmol) for 5 min. L-Ala-OMe.HCl (2.50 g, 17.9 mmol) was added and the mixture was stirred for 3 d. The DMF was evaporated and the residue was extracted with EtOAc. The extract was washed with aq. $NaHCO_3$ (5%) and brine, and was dried. Evaporation and chromatography (petroleum ether / EtOAc 1:1 → EtOAc) gave **178** (3.52 g, 87%) as a white solid: $R_f$ = 0.9 (EtOAc / MeOH 1:1); mp 157-158ºC; $[\alpha]^{18}_{D}$ -10.2º (c = 1.6%, DMF); IR $\nu_{max}$ 3303 (NH), 2244 (C≡N), 1750 (C=O), 1693 (C=O), 1657 (C=O); $^1$H NMR [$(CD_3)_2SO$] δ 1.29 (3 H, d, *J* = 7.5 Hz, Ala Me), 1.82 (1 H, m, Gln(CN) β-H), 1.96 (1 H, m, Gln(CN) β-H), 2.52 (2 H, m, Gln(CN) γ-$H_2$), 3.62 (3 H, s, OMe), 4.11 (1 H, td, *J* = 8.6, 4.8 Hz , Gln(CN) α-H), 4.26 (1 H, qn, *J* = 7.3 Hz, Ala α-H), 5.03 (2 H, s, $PhCH_2$), 7.34 (5 H, m, Ph-$H_5$), 7.52 (1 H, d, *J* = 8.0 Hz Gln(CN) NH), 8.50 (1 H, d, *J* = 7.0 Hz, Ala NH). $^{13}$C NMR [$(CD_3)_2SO$) (HSQC / HMBC)] δ 13.14 (Gln(CN) γ-C), 16.68 (Ala-Me), 27.63 (Gln(CN) β-C), 47.67 (Ala α-C), 51.95 (OMe), 53.03 (Gln(CN) α-C), 65.57 ($PhCH_2$), 119.94 (CN), 127.76 (Ph 2,6-$C_2$), 127.85 (Ph 4-C), 128.36 (Ph 3,5-$C_2$), 136.87 (Ph 1-C), 155.93 (Cbz C=O), 170.79 (Gln(CN) C=O), 172.99 (ester C=O); MS ($ES^+$) *m/z* 370.1518 (M + Na) ($C_{17}H_{21}N_3NaO_5$ requires 370.1379).

## 5.65 N-(*S*-4-Cyano-2-(N-(*tert*-butoxycarbonyl)-L-alanyl)butanoyl)-L-alanine (180)

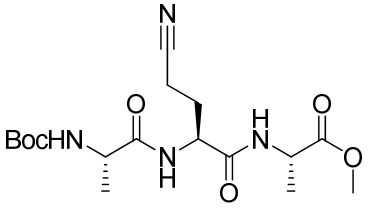

Cbz-L-Gln(CN)-L-Ala-OMe **178** (357 mg, 1.03 mmol) was stirred vigorously with Pd/C (10% 36 mg) in MeOH (25 mL) under hydrogen for 2 h. Filtration (Celite®) and evaporation gave N-(*S*-2-amino-4-cyanobutanoyl)-L-alanine **179**. This was added to Boc-L-Ala-OH (395 mg, 2.1 mmol), $Pr^{i}_{2}NEt$ (0.72 mL, 533 mg, 4.1 mmol) and HATU (822 mg, 2.2 mmol) in DMF (25 mL). The mixture was stirred for 2 h and the solvent was evaporated. The residue in EtOAc was washed with aq. $NaHCO_3$ (5%), water and brine. Evaporation and chromatography (EtOAc / petroleum ether 1:1 → EtOAc) gave **180** (252 mg, 64%) as a white solid: mp 175-176 ºC; $[\alpha]^{18}_{D}$ -24.6° (c = 0.80%, DMF); IR $\nu_{max}$ 3318 (NH), 3279 (NH), 2250 (C≡N), 1673 (C=O); $^1$H NMR ($CDCl_3$) δ 1.37 (3 H, d, *J* = 7.1 Hz, Ala Me), 1.41 (3 H, d, *J* = 7.3 Hz, Ala Me), 1.43 (9 H, s, $Bu^t$), 2.02 (1 H, m, Gln(CN) β-H), 2.26 (1 H, m, Gln(CN) β-H), 2.46 (2 H, m, Gln(CN) γ-$H_2$), 3.71 (3 H,

s, OMe), 4.11 (1 H, m, Ala α-H), 4.51 (1 H, qn, *J* = 7.2 Hz, Ala α-H), 4.62 (1 H, td, *J* = 7.5, 5.5 Hz, Gln (CN) α-H), 5.35 (1 H, br, BocNH), 7.01 (1 H, d, *J* = 7.2 Hz, Ala-OMe NH), 7.07 (1 H, d, *J* = 8.1 Hz, Gln(CN) NH); $^{13}$C NMR [($CDCl_3$) (HSQC / HMBC)] δ 13.33 (Gln(CN) γ-C), 17.39 (Ala Me), 17.88 (Ala Me), 28.20 (C*Me*$_3$), 28.34 (Gln(CN) β-C), 48.20 (Ala α-C), 50.46 (Ala α-C), 51.62 (Gln(CN) α-C), 52.41 (OMe), 80.25 (*C*Me$_3$), 119.28 (C≡N), 155.63 (Boc C=O), 169.79 (Gln(CN) C=O), 172.84 (N-terminal Ala C=O), 173.42 (C-terminal Ala C=O): MS (ES$^+$) *m/z* 407.2052 (M + Na) ($C_{17}H_{28}N_4NaO_6$ requires 407.1907).

### 5.66 N-(N-(*tert*-Butoxycarbonyl)-L-alanyl)-L-glutaminyl)-L-alanine (181).

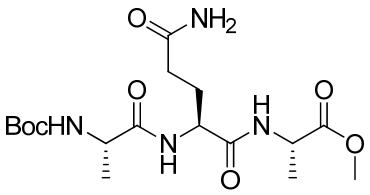


Boc-L-Ala-L-Gln(CN)-L-Ala-OMe **180** (1.00 g, 2.6 mmol) in MeOH (50 mL) at 0°C was stirred with aq. $H_2O_2$ (35% w/w, 1.6 mL, 18.2 mmol) and aq. NaOH (1.0 M, 2.6 mL, 2.6 mmol) for 6 h. The reaction was quenched by addition of aq. $Na_2S_2O_3$ (20%, 30 mL) and the methanol was evaporated. The residue was extracted with EtOAc; the organic solution was washed with brine and dried. Evaporation and chromatography (EtOAc → EtOAc / MeOH 4:1) gave **181** (243 mg, 23%) as a white solid: mp 193-194°C; $[\alpha]^{18}_D$ -26.4° (c = 0.85%, DMF); IR $\nu_{max}$ 3420 (NH), 3306 (NH), 1747 (C=O), 1660 (C=O); $^1$H NMR [$(CD_3)_2SO$] δ 1.16 (3 H, brd, *J* = 7.0 Hz, N-terminal Ala Me), 1.27 (3 H, d, *J* = 7.5 Hz, C-terminal Ala Me), 1.37 (9 H, s, Bu$^t$), 1.72 (1 H, m, Gln β-H), 1.86 (1 H, m, Gln β-H), 2.10 (2 H, t, *J* = 7.0 Hz, Gln γ-$H_2$), 3.62 (3 H, s, OMe), 3.96 (1 H, qn, *J* = 7.1 Hz, N-terminal Ala α-H), 4.28-4.35 (2 H, m, C-terminal Ala α-H + Gln α-H), 6.75 (1 H, s, Gln δ-NH), 6.97 (1 H, d, *J* = 7.3 Hz, N-terminal Ala-NH), 7.21 (1 H, s, Gln δ-NH), 7.80 (1 H, d, *J* = 8.0 Hz, Gln α-NH), 8.35 (1 H, d, *J* = 6.5 Hz, C-terminal Ala NH); $^{13}$C NMR ($(CD_3)_2SO$) (HSQC / HMBC) δ 16.79 (C-terminal Ala-Me), 18.05 (N-terminal Ala-Me), 28.17 (C*Me*$_3$ + Gln β-C), 31.13 (Gln γ-C), 47.50 (C-terminal Ala α-C), 49.73 (N-terminal Ala α-C), 51.52 (Gln α-C), 51.86 (OMe), 78.11 (*C*Me$_3$), 155.09 (Boc C=O), 171.10 (Gln α-C=O), 172.48 (N-terminal Ala C=O), 172.86 (C-terminal Ala C=O), 173.72 (Gln δ-C=O); $^{15}$N NMR [$(CD_3)_2SO$) (HSQC / HMBC)] δ 63.83 (BocN), 79.33 (Gln γ-$CONH_2$), 85.20 (Gln α-N), 91.03 (C-terminal Ala-N); MS (ES$^+$) *m/z* 425.2166 (M + Na) ($C_{17}H_{30}N_4NaO_7$ requires 425.2012), 403.2183 (M + H) ($C_{17}H_{31}N_4O_7$ requires 403.2193).

### 5.67 N-Phenylmethoxycarbonyl-L-glutamic acid (188)

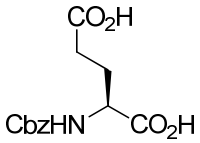


Aq. $H_2O_2$ (35%, 1.5 mL) was added to **163** (110 mg, 0.42 mmol) in aq. NaOH (0.5 M, 15 mL), followed by aq. NaOH (2 M, 1.0 mL) and the mixture was stirred for 30 min. The mixture was cooled to 0ºC and the pH was adjusted to 2.0 with aq. HCl (1.0 M). Extraction ($CH_2Cl_2$, thrice), drying and evaporation gave **188** (120 mg, quant.) as a colourless viscous oil: IR (liquid film) $\nu_{max}$ 3290, 1697 $cm^{-1}$; $^1H$ NMR ($CD_3OD$) $\delta$ 1.96 (1 H, m, β-H), 2.19 (1 H, m, β-H), 2.32 (1 H, m, γ-H), 2.40 (1 H, m, γ-H), 4.18 (1 H, m, α-H), 4.88 (2 H, s, $PhCH_2$), 5.09 (1 H, br, OH), 7.32 (5 H, s, Ph-$H_5$); MS ($ES^+$) *m/z* 282.1023 (M + H) ($C_{13}H_{16}NO_6$ requires 282.0972).

### 5.68 Solid phase peptide synthesis

The Kaiser test was used to test for the presence / absence of free amino groups during deprotection or coupling. The resin is treated with ninhydrin in ethanol, phenol in ethanol and potassium cyanide in pyridine. A positive test (presence of free amino group) is indicated by a purple colour. To determine the resin loading after coupling the first amino-acid, the resin is treated with piperidine in DMF (1:4) (4 ×) for 3 min each time to cleave the Fmoc group. The absorbance of the dibenzofulvene-piperidine adduct is recorded at 301 nm against DMF and the loading of the first amino-acid on the resin calculated using Beer Lambert equation:

$A = C.\ \varepsilon.\ L$, $C = A / \varepsilon$, $C = n / v$, $n = (v \times 10^{-3}) \times C$

Therefore loading of resin (mol) = $[(A_{301} \times v \times 10^{-3}) / (\varepsilon_{301})] \times F$

Where $A_{301}$ is the absorbance at 301 nm minus the control reading, V is the volume (mL), $\varepsilon_{301}$ is the extinction coefficient at 301 nm (7800 $M^{-1}$ $cm^{-1}$) and F is the dilution factor.

Peptides were synthesised using standard Fmoc solid-phase peptide synthetic protocols. The resin used was 2-chlorotrityl chloride polystyrene. Before starting a peptide synthesis, the resin was swollen in $CH_2Cl_2$ for about 5 min. Loading of the resin involved reaction with the appropriate $N^{\alpha}$-Fmoc amino-acids (2 - 4 equiv.) in $CH_2Cl_2$ in the presence of $^iPr_2NEt$ (6 equiv.) for 2 h. The mixture was rinsed with DMF (5 ×) and $CH_2Cl_2$ (5 ×) followed by treatment with $CH_2Cl_2$ / MeOH / $Pr^i_2NEt$ (17:2:1) (3 × 15 min) to cap unreacted resin. Washing with DMF (5 ×) and $CH_2Cl_2$ (5 ×) followed by Fmoc deprotection by treating resin with piperidine in DMF (1:4) (4 ×) for 3 min each time, yielded the desired loaded resin. Determination of the absorbance of the dibenzofulvene-piperidine adduct allowed estimation

of the percentage loading of the resin. The peptide chains were then assembled by sequential couplings of preactivated $N^{\alpha}$-Fmoc amino-acids (2 - 3 equiv.) for 2 h. The preactivation was carried out manually in DMF by treatment with benzotriazol-1-yl-oxytrispyrrolidinophosphonium hexafluorophosphate (PyBOP) (2 equiv.) and $Pr^{i}_{2}NEt$ (6 equiv.) for 5 min. Removal of the Fmoc-protection was carried out by treatment with piperidine (20% in DMF) (5 × 3 min). The completeness of each coupling and Fmoc deprotection were verified by Kaiser test. A positive Kaiser test was usually followed by an additional coupling cycle. The protected peptides were cleaved from the resin with $CF_3CO_2H$ (TFA) (1% in $CH_2Cl_2$), concentrated (~5 % of volume) and precipitated with water. Filtration and drying in a freeze drier / oven (40°C) gave the product.

### 5.69 Fmoc-L-Ser(Bn)-L-Ser(Bn)-L-Lys(Cbz)-L-Leu-L-Gln-OH (189)

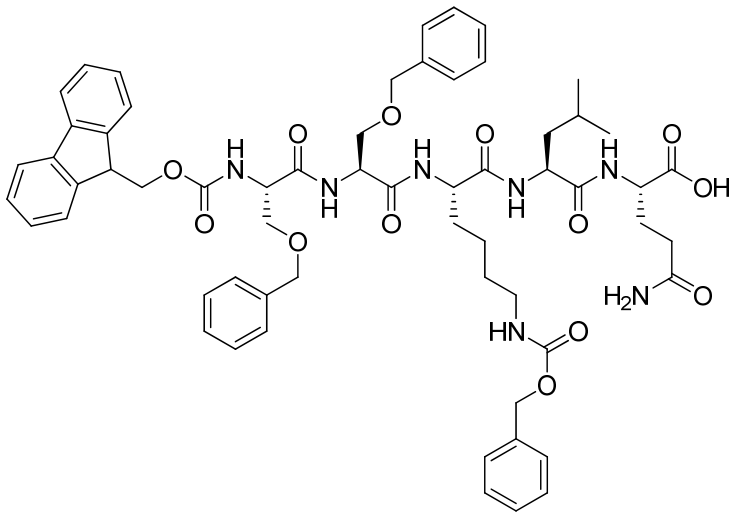

Peptide **189** was synthesised on 2-chlorotrityl chloride polystyrene resin (1.05 g, 1.66 mmol) according to the general procedure (Section 5.68) described above to yield **189** (1.23 g, 93%) as a white solid: $R_f$ = 0.5 (EtOAc / MeOH 1:1); mp 192-195°C; IR $\nu_{max}$ 3295 (NH, OH), 1728-1635 (C=O); $^1$H NMR [$(CD_3)_2SO$) (COSY)] δ 0.83-0.92 (6 H, m, Leu $Me_2$), 1.31-1.36 (2 H, m, Lys γ-$H_2$), 1.41-1.54 (5 H, m, Leu β-$H_2$, + Lys β-$H_1$, δ-$H_2$), 162-1.68 (2 H, m, Leu γ-$H_1$ + Lys β-$H_1$), 1.80-1.89 (1 H, m, Gln β-H), 1.95-2.04 (1 H, m, Gln β-H), 2.13-2.24 (2 H, m, Gln γ-H), 2.99 (2 H, m, Lys ε-$H_2$), 3.62-3.74 (4 H, m, 2 × Ser β-$H_2$), 4.22 ( 1 H, m, Gln α-H), 4.31-4.42 (5 H, m, Fmoc-$CH_2$ + fluorene 9-H + Leu α-H + Lys α-H), 4.47-4.59 (5 H, m, 2 × SerOC*$H_2$*Ph + Ser α-H ), 4.62-4.70 (1 H, m, Ser α-H), 5.05 (2 H, s, Cbz $CH_2$), 6.88 (1 H, br, NH), 7.28-7.41 (18 H, m, 17 × Ar-H + NH), 7.46 (2 H, t, *J* = 7.4 Hz, 2 × Ar-H), 7.76-7.80 (3 H, m, 2 × Ar-H + NH), 7.91-7.96 (3 H, m, 2 × Ar-H + NH), 8.11 (1 H, d, *J* = 7.7 Hz, NH),

8.20 (1 H, d, *J* = 7.4 Hz, Gln NH), 8.33 (1 H, d, *J* = 7.4 Hz, Ser NH), 12.63 (1 H, s, OH); $^{13}$C NMR [$(CD_3)_2SO$) (HSQC / HMBC)] δ 21.56 (Leu Me), 22.52 (Lys γ-C), 23.03 (Leu Me), 24.01 (Leu γ-C), 26.78 (Gln β-C), 29.13 (Lys δ-C), 31.31 (Gln γ-C), 31.73 (Lys β-C), 38.83-40.08 (Lys ε-C), 40.82 (Leu β-C), 46.58 (fluorene 9-C), 50.67 (Leu α-C), 51.52 (Gln α-C), 52.55 (Lys α-C), 52.80 (Ser α-C), 54.67 (Ser α-C), 65.10 (Cbz O*C*$H_2$Ph), 65.83 (Fmoc-$CH_2$), 69.74 (2 × Ser β-C), 71.98 (SerO*C*$H_2$Ph), 72.08 (SerO*C*$H_2$Ph), 120.09 (Ar-C), 125.30 (Ar-C), 127.07 (Ar-C), 127.33 (Ar-C), 127.37 (Ar-C), 127.41 (Ar-C), 127.44 (Ar-C), 127.63 (Ar-C), 127.74 (Ar-C), 128.13 (Ar-C), 128.16 (Ar-C), 128.32 (Ar-C), 137.23 (Cbz Ph 1-C), 138.09 (Bn Ph 1-C), 138.14 (Bn Ph 1-C), 140.68 (2 × Fmoc-$C_q$), 143.74 (Fmoc-$C_q$), 143.80 ((Fmoc-$C_q$), 156.03 (Cbz C=O), 169.09 (Ser 2 × C=O), 169.70 (Fmoc C=O), 171.00 (Lys C=O), 171.92 (Leu C=O), 173.19 ($CO_2H$), 173.49 (Gln δ-C=O); MS ($ES^+$) *m/z* 1120.5117 (M + Na) ($C_{60}H_{71}N_7NaO_{13}$ requires 1120.5008), 1098.5283 (M + H) ($C_{60}H_{72}N_7O_{13}$ requires 1098.5189).

### 5.70 Chloro-5-nitroisoquinoline (191)

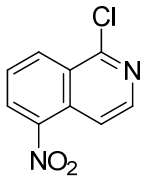


A mixture of conc. $H_2SO_4$ (1.37 g, 13.9 mmol) and conc. aq. $HNO_3$ (70%, 1.20 g, 13.1 mmol) at 0°C was added to 1-chloroisoquinoline **190** (2.14 g, 13.1 mmol) in conc. $H_2SO_4$ (10 mL) at 0°C and the mixture was stirred at 0°C for 2 h and at 20°C for 10 min before being poured onto ice-water. The solid was collected by filtration and dried to give **191** (1.80 g, 66%) as a yellow solid: $R_f$ = 0.4 (MeOH / $CH_2Cl_2$ 1:9); mp 178-181°C (lit.[196] mp 187°C); IR $\nu_{max}$ 1524 ($NO_2$); $^1$H NMR ($CDCl_3$) δ (COSY) δ 7.81 (1 H, t, *J* = 8.1 Hz, 7-H), 8.40 (1 H, dd, *J* = 6.2, 0.9 Hz, 4-H), 8.49 (1 H, d, *J* = 6.1 Hz, 3-H), 8.56 (1 H, dd, *J* = 7.7, 1.1 Hz, 6-H), 8.74 (1 H, d, *J* = 8.5 Hz, 8-H); $^{13}$C NMR [($CDCl_3$) (HSQC / HMBC)] δ 115.80 (4-C), 126.98 (7-C), 127.54 (8a-C), 128.84 (6-C), 130.35 (4a-C), 133.24 (8-C), 144.78 (3-C), 145.43 (5-C), 152.63 (1-C).

### 5.71 1-Benzyloxy-5-nitroisoquinoline (192)

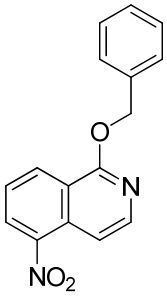


NaH (60% dispersion in mineral oil, 94 mg, 3.9 mmol) was added to benzyl alcohol (445 mg, 4.1 mmol) in dry DMF (10 mL). 1-Chloro-5-nitro-isoquinoline **191** (407 mg, 2.0 mmol) was added and the mixture was stirred under $N_2$ for 15 min at 20°C and at 100°C for 2 h. Water (50 mL) was added to the evaporation residue, which was then extracted with EtOAc (5 × 50 mL). The combined organic phases were washed with brine and dried. Evaporation and chromatography (EtOAc / petroleum ether 1:9) yielded **192** (485 mg, 89%)

as a yellow solid: $R_f$ = 0.9 (EtOAc / petroleum ether 1:9); mp 85-86°C; IR $\nu_{max}$ 1522 ($NO_2$); $^1$H NMR [($CDCl_3$) (COSY)] δ 5.61 (2 H, s, $CH_2$ ), 7.34-7.44 (3 H, m, Ph 3,4,5-$H_3$), 7.53 (2 H, d, *J* = 7.3 Hz, Ph 2,6-$H_2$), 7.61 (1 H, t, *J* = 8.2 Hz, 7-H), 8.02 (1 H, dd, *J* = 6.4, 0.8 Hz, 4-H), 8.23 (1 H, d, *J* = 6.3 Hz, 3-H), 8.47 (1 H, dd, *J* = 7.8, 1.2 Hz, 6-H), 8.67 (1 H, dd, *J* = 8.3, 0.9 Hz, 8-H); $^{13}$C NMR [($CDCl_3$) (HSQC / HMBC)] δ 68.58 ($CH_2$), 110.00 (4-C), 120.89 (8a-C), 125.08 (7-C), 128.12 (Ar-C), 128.18 (Ar-C), 128.30 (Ar-C), 128.60 (Ar-C), 130.69 (4a-C), 131.28 (8-C), 136.67 (Ph 1-C), 143.74 (3-C), 144.82 (5-C), 160.43 (1-C); MS ($ES^+$) *m/z* 303.0729 (M + Na) ($C_{16}H_{12}N_2NaO_3$ requires 303.0746), 281.0895 (M + H) ($C_{16}H_{13}N_2O_3$ requires 281.0926).

### 5.72 1-Benzyloxyisoquinolin-5-amine (193)

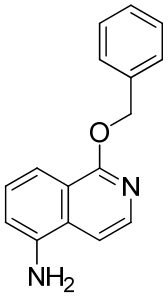


$NaBH_4$ (381 mg, 10.1 mmol) in MeOH (5.0 mL) was added to **192** (698 mg, 2.5 mmol) and Pd/C (10% 692 mg) in MeOH (25 mL) and the mixture was stirred for 30 min. Aq. HCl (1.0 M, 1.0 mL) was added and the mixture was filtered through Celite®. The evaporation residue was partitioned between water and EtOAc. The product was extracted with EtOAc and the solution was dried. Evaporation and chromatography (petroleum ether / EtOAc 1:1) yielded **193** (206 mg, 33%) as a buff oil: $R_f$ = 0.7 (EtOAc / petroleum ether 1:1); $^1$H NMR [($CDCl_3$) (COSY)] δ 5.66 (2 H, s, $CH_2$), 6.95 (1 H, dd, *J* = 7.8, 0.8 Hz, 6-H), 7.17 (1 H, d, *J* =6.0 Hz, 4-H), 7.32-7.36 (2 H, m, 7-H, Ph 4-H), 7.40 (2 H, t, *J* = 7.5 Hz, Ph 3,5-$H_2$), 7.54 (2 H, d, *J* = 7.0 Hz, Ph 2,6-$H_2$), 7.77 (1 H, d, *J* = 8.5 Hz, 8-H), 8.00 (1 H, d, *J* = 6.0 Hz, 3-H); $^{13}$C NMR [($CDCl_3$) (HSQC / HMBC)] δ 67.96 ($CH_2$), 108.64 (4-C), 112.99 (6-C), 114.57 (8-C), 120.49 (8a-C), 127.07 (7-C, Ph 4-C), 127.67 (4a-C), 127.75 (Ph 2,6-$C_2$), 128.44 (Ph 3,5-$C_2$), 137.34 (Ph 1-C), 138.34 (3-C), 141.23 (5-C), 160.67 (1-C); MS ($ES^+$) *m/z* 273.0974 (M + Na) ($C_{16}H_{14}N_2NaO$ requires 273.1004), 251.1161 (M + H) ($C_{16}H_{15}N_2O$ requires 251.1184).

### 5.73 N-(4-Hydroxynaphthalen-1-yl)acetamide (198)

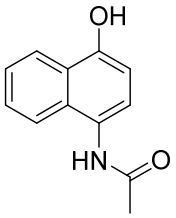


4-Aminonaphthalen-1-ol hydrochloride **31** (1.01 g, 5.15 mmol) was stirred with $Et_3N$ (0.72 mL, 525 mg, 5.2 mmol) and $Ac_2O$ (0.49 mL, 530 mg, 5.2 mmol) in MeOH (25 mL) at 50°C for 1 h. The solvent was evaporated. Chromatography (EtOAc / $CH_2Cl_2$ 1:3) gave **198** (959 mg, 93%) as a pale pink solid: $R_f$ = 0.4 (EtOAc); mp 184-186ºC (lit.[197] mp 186-187°C); IR $\nu_{max}$ 3327, 3258 (OH, NH), 1652 (C=O); $^1$H NMR [($CD_3)_2SO$) (NOESY)] δ 2.18 (3 H, s, Me), 6.89 (1 H, d, *J* = 8.0 Hz, 3-H), 7.36 (1 H, d, *J* = 8.0 Hz, 2-H), 7.51 (1 H, ddd, *J* = 8.2, 6.8, 1.4

Hz, 6-H), 7.56 (1 H, ddd, *J* = 8.2, 6.8, 1.4 Hz, 7-H), 7.94 (1 H, d, *J* = 8.0 Hz, 8-H), 8.20 (1 H, dd, *J* = 8.0, 0.6 Hz, 5-H), 9.66 (1 H, s, NH), 10.11 (1 H, s, OH); $^{13}$C NMR [$(CD_3)_2SO$) (HSQC / HMBC)] δ 23.12 (Me), 107.27 (3-C), 122.23 (5-C), 122.81 (8-C), 123.59 (2-C), 124.51 (6-C), 124.70 (4a-C), 124.98 (1-C), 125.93 (7-C), 129.78 (8a-C), 151.16 (4-C), 168.86 (C=O); MS ($ES^-$) *m/z* 200.0713 (M - H) ($C_{12}H_{10}NO_2$ requires 200.0712).

### 5.74 N-(4-Methoxynaphthalen-1-yl)acetamide (199)

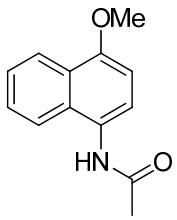


Compound **198** (211 mg, 1.05 mmol), $K_2CO_3$ (158 mg, 1.14 mmol) and MeI (70 μL, 149 mg, 1.05 mmol) in acetone (10 mL) were refluxed for 16 h. The solvent was evaporated. The residue in EtOAc, was washed with water, sat. aq. $Na_2S_2O_3$ and brine. Drying, evaporation and chromatography ($CH_2Cl_2$ / EtOAc 3:2) gave **199** (189 mg, 80%) as a pale pink solid: $R_f$ = 0.3 ($CH_2Cl_2$ / EtOAc 3:2); mp 185-187°C (lit.[198] mp 186-186.5°C); IR $\nu_{max}$ 3270 (NH), 1652 (C=O); $^1$H NMR [$(CD_3)_2SO$) (NOESY)] δ 2.20 (3 H, s, NCOMe), 4.02 (3 H, s, OMe), 7.00 (1 H, d, *J* = 8.2 Hz, 3-H), 7.52 (1 H, d, *J* = 8.2 Hz, 2-H), 7.57 (1 H, ddd, *J* = 8.0, 6.8, 1.2 Hz, 6-H), 7.62 (1 H, ddd, *J* = 8.1, 6.8, 1.3 Hz, 7-H), 8.01 (1 H, d, *J* = 7.9 Hz, 8-H), 8.23 (1 H, dd, *J* = 8.0, 1.2 Hz, 5-H), 9.75 (1 H, s, NH); $^{13}$C NMR [$(CD_3)_2SO$) (HSQC / HMBC)] δ 23.19 (NCO*Me*), 55.66 (OMe), 103.82 (3-C), 121.65 (5-C), 122.89 (8-C), 122.93 (2-C), 125.02 (4a-C), 125.27 (6-C), 126.27 (7-C), 126.46 (1-C), 129.33 (8a-C), 152.63 (4-C), 168.91 (C=O); MS ($ES^-$) *m/z* 214.0890 (M - H) ($C_{13}H_{12}NO_2$ requires 214.0868).

### 5.75 4-Methoxynaphthalen-1-amine (200)

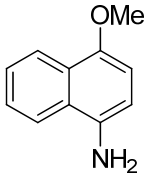


A suspension of **199** (123 mg, 0.57 mmol) in aq. HCl (3.0 M, 9 mL) and MeOH (3 mL) was heated at 90°C for 4 h. The mixture was cooled to 20°C. and sat. aq. $NaHCO_3$ was added until the mixture was basic to universal indicator paper. The suspension was extracted with EtOAc. The extract was washed with water, brine and dried. Evaporation and chromatography (petroleum ether / $CH_2Cl_2$ 1:4 → $CH_2Cl_2$) gave **200** (83 mg, 83%) as a purple oil: $R_f$ = 0.5 ($CH_2Cl_2$); $^1$H NMR [($CDCl_3$) (COSY)] δ 3.70 (2 H, s, $NH_2$), 4.00 (3 H, s, Me), 6.68 (1 H, d, *J* = 8.0 Hz, 3-H), 6.71 (1 H, d, *J* = 8.0 Hz, 2-H), 7.50 (2 H, m, 6-H,7-H), 7.82 (1 H, m, 8-H), 8.28 (1 H, m, 5-H); $^{13}$C NMR [($CDCl_3$) (HSQC / HMBC)] δ 55.78 (Me), 104.50 (3-C), 109.61 (2-C), 120.95 (8-C), 122.51 (5-C), 125.19 (4a-C), 125.21 (6-C or 7-C), 125.58 (7-C or 6-C), 126.14 (8a-C), 135.27 (1-C), 149.17 (4-C); MS ($ES^+$) *m/z* 174.0965 (M + H) ($C_{11}H_{12}NO$ requires 174.0919).

## 5.76 Fmoc-L-Ser(Bn)-L-Ser(Bn)-L-Lys(Cbz)-L-Leu-L-Gln-N-(4-methoxynaphthalen-1-yl)amide (201)

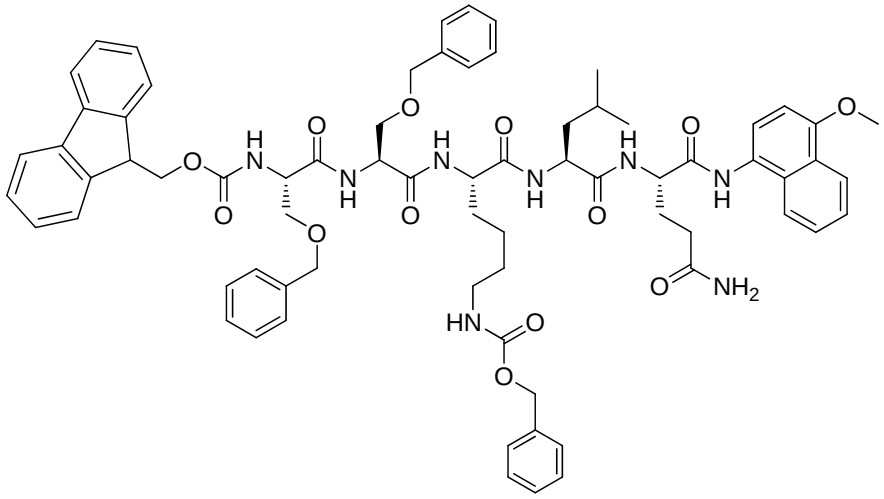

Compound **189** (203 mg, 0.19 mmol) and **200** (67.9 mg, 0.39 mmol) were stirred in dry DMF (10 mL) and at 0°C. HOBt (42.6 mg, 0.28 mmol) and EDC.HCl (56.5 mg, 0.29 mmol) were added and the mixture was stirred for 2 d under $N_2$ at room temperature. The DMF was evaporated and the residue was triturated with hot MeOH. Cooling at 0°C for 30 min, filtration, washing with MeOH and drying gave **201** (181 mg, 78%) as a pale purple solid: $R_f$ = 0.50 (EtOAc / AcOH / MeOH 19:2:1); mp 227-228°C; $^1$H NMR [$(CD_3)_2SO$) (COSY)] δ 0.82-0.93 (6 H, m, Leu $Me_2$), 1.31 (2 H, br, Lys γ-$H_2$), 1.39-1.40 (2 H, m, Lys δ-$H_2$), 1.53-1.56 (3 H, m, Leu β-$H_2$, + Lys β-$H_1$), 1.61-1.68 (2 H, m, Leu γ-$H_1$ + Lys β-$H_1$), 1.99-2.04 (1 H, m, Gln β-$H_1$), 2.11-2.15 (1 H, m, Gln β-$H_1$), 2.27-2.31 (2 H, m, Gln γ-$H_2$), 2.97-2.98 (2 H, m, Lys ε-$H_2$), 3.62-3.73 (4 H, m, Ser β-$H_4$), 4.01 (3 H, s, OMe), 4.27-4.43 (5 H, m, Fmoc $CH_2$, Fmoc CH, Leu α-H, Lys α-H), 4.47-4.58 (6 H, m, 2 × SerOC*H*$_2$, Ser α-H, Gln α-H), 4.64-4.66 (1 H, m, Ser α-H), 5.04 (2 H, s, Cbz $CH_2$), 6.92 (1 H, br, NH), 6.99 (1 H, d, *J* = 8.4 Hz, Naph Ar-H), 7.26-7.50 (21 H, m, Fmoc Ar-H, Bn Ar-H, Naph Ar-H, 3 × NH), 7.53-7.61 (2 H, m, 2 × Ar-H), 7.75-7.80 (3 H, m, 2 × Ar-H, NH), 7.93-8.02 (4 H, m, 3 × Ar-H, NH), 8.08-8.15 (1 H, m, NH), 8.20-8.23 (2 H, m, Ar-H, NH), 8.29-8.33 (1 H, m, NH); $^{13}$C NMR [$(CD_3)_2SO$) (HSQC / HMBC)] δ 21.51 (Leu Me), 22.60 (Lys γ-C), 23.04 (Leu Me), 24.09 (Leu γ-C), 27.44 (Gln β-C), 27.81 (Lys δ-C), 29.22 (Gln γ-C), 31.55 (Lys β-C), 38.82-40.07 (2 C, Lys ε-C, Leu β-C), 46.55 (Fmoc CH), 50.87 (Leu α-C or Lys α-C), 51.14 (Lys α-C or Leu α-C), 52.83 (2 × Ser α-C), 54.66 (Gln α-C), 55.66 (OMe), 65.09 (Cbz $CH_2$), 65.81 (Fmoc $CH_2$), 69.74 (2 × Ser β-C), 72.06 (2 C, 2 × SerO*C*$H_2$Ph), 103.72 (Naph Ar-C), 120.10 (Ar-C), 121.67 (Ar-C), 122.83 (Ar-C), 123.11 (Ar-C), 124.99 (Ar-$C_q$), 125.30 (Ar-C), 125.81 (Ar-$C_q$), 127.07 (Ar-C), 127.44 (Ar-C), 127.63 (Ar-C), 127.73 (Ar-C), 128.15 (Ar-C), 128.32 (Ar-C),

129.39 (Ar-C), 137.22 (Cbz $C_q$), 138.13 (2 × Bn $C_q$), 140.68 (Ar-$C_q$), 145.07 (Fmoc $C_q$), 152.89 (Naph 1-C), 156.02 (Cbz C=O), 169.20 (C=O), 169.75 (C=O), 170.93 (C=O), 171.33 (C=O), 172.07 (C=O), 172.96 (C=O), 173.75 (C=O); MS ($ES^+$) *m/z* 1253.6693 (M + H) ($C_{71}H_{81}N_8O_{13}$ requires 1253.5923), 1031.5964 [(M –Fmoc) +H] ($C_{56}H_{71}N_8O_{11}$ requires 1031.5242).

## 5.77 Fmoc-L-Ser(OAc)-L-Ser(OAc)-L-Lys-L-Leu-L-Gln-N-(4-methoxynaphthalen-1-yl)amide (202)

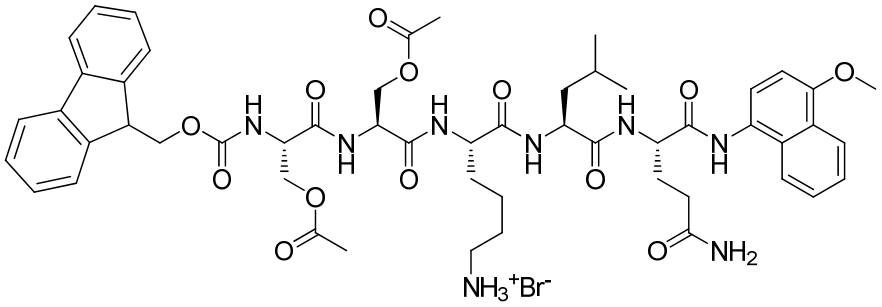

Compound **201** (1.40 g, 1.1 mmol) was stirred with HBr in AcOH (33%, 10 mL) at 20°C for 2 h. $Et_2O$ was added and the precipitate was filtered and washed with $Et_2O$. The solid residue was dried and triturated with hot MeOH. The solvent was cooled to 20°C and placed at 0°C for 30 min. The solid residue was collected by filteration and washed with cold MeOH. Drying gave **202** (0.89 g, 72%) as a white solid: mp 245-246°C; $^1$H NMR [$(CD_3)_2SO$) (COSY)] δ 0.89 (3 H, d, *J* = 6.4 Hz, Leu Me), 0.93 (3 H, d, *J* = 6.4 Hz, Leu Me), 1.35-1.37 (2 H, m, Lys γ-$H_2$), 1.57 (5 H, m, Leu β-$H_2$, Lys β-$H_1$, Lys δ-$H_2$), 1.66-1.73 (2 H, m, Lys β-$H_1$, Leu γ-$H_1$), 2.03 (3 H, s, SerOCOC*H*$_3$), 2.05 (3 H, s, SerOCOC*H*$_3$), 2.03-2.14 (2 H, m, Gln β-$H_2$), 2.29 (2 H, m, Gln γ-$H_2$), 2.79 (2 H, qn, *J* = 2.8 Hz, Lys ε-$H_2$), 4.03 (3 H, s, OMe), 4.11-4.31 (5 H, m, 2 × Ser β-$H_2$, Fmoc CH), 4.34-4.47 (5 H, m, Fmoc $CH_2$, Leu α-H, Lys α-H, Ser α-$H_1$), 4.56 (1 H, dd, *J* = 13.6, 7.5 Hz, Gln α-H), 4.66 (1 H, dd, *J* = 12.8, 7.0 Hz, Ser α-$H_1$), 6.92 (1 H, s, NH), 7.02 (1 H, d, *J* = 8.4 Hz, Naph 2-H), 7.37 (2 H, t, *J* = 7.4 Hz, 2 × Ar-H), 7.41 (1 H, s, NH), 7.48 (3 H, t, *J* = 8.6 Hz, Naph 3-H, 2 × Ar-H), 7.59 (2 H, qn, *J* = 6.9 Hz, 2 × Ar-H), 7.70 (3 H, s, Lys $NH_3^+Br^-$), 7.78 (2 H, dd, *J* = 7.1, 0.31 Hz, 2 × Ar-H), 7.84 (1 H, d, *J* = 8.3 Hz, NH), 7.96 (3 H, d, *J* = 7.3 Hz, 3 × Ar-H), 8.10 (1 H, d, *J* = 7.6 Hz, NH), 8.25 (3 H, m, Ar-H, 2 × NH), 8.41 (1 H, d, *J* = 7.6 Hz, NH), 9.83 (1 H, s, NH); $^{13}$C NMR [$(CD_3)_2SO$)] δ (HSQC / HMBC) 20.63 (2 × SerOCO*C*$H_3$), 21.49 (Leu Me), 22.12 (Lys γ-C), 23.09 (Leu Me), 24.11 (Leu γ-C), 26.56 (Lys δ-C), 27.85 (Gln β-C), 31.26 (Lys β-C), 31.49 (Gln γ-C), 38.67 (Lys ε-C), 40.62 (Leu β-C), 46.57 (Fmoc CH), 51.00 (Leu α-C), 51.68 (Ser α-C), 52.31

(Lys α-C), 52.89 (Gln α-C), 53.58 (Ser α-C), 55.71 (OMe), 63.22 (Ser β-C), 63.33 (Ser β-C), 65.82 (Fmoc $CH_2$), 103.77 (Naph 2-C), 120.14 (2 × Ar-C), 121.69 (Ar-C), 122.79 (Ar-C), 123.11 (Naph 3-C), 125.01 (Ar-$C_q$), 125.23 (2 × Ar-C), 125.41 (Ar-C), 125.79 (Ar-$C_q$), 126.39 (Ar-C), 127.09 (2 × Ar-CH), 127.67 (2 × Ar-CH), 129.38 (Ar-$C_q$), 140.71 (2 × Ar-$C_q$), 143.74 (2 ×Fmoc Ar-$C_q$), 152.89 (Naph 1-C), 155.97 (C=O), 168.20 (C=O), 169.04 (C=O), 170.10 (SerO*C*O$CH_3$), 170.16 (SerO*C*O$CH_3$), 170.88 (C=O), 171.06 (C=O), 172.07 (C=O), 173.72 (Gln δ-C=O); MS ($ES^+$) *m/z* 1045.4515 (M + Na) ($C_{53}H_{66}N_8NaO_{13}$ requires 1045.4647), 1023.4706 (M + H) ($C_{53}H_{67}N_8O_{13}$ requires 1023.4828), 981.4644 (M – OAc + H) ($C_{51}H_{65}N_8O_{12}$ requires 981.4722).

### 5.78 Fmoc-Ser-Ser-Lys-Leu-Gln-N-(4-methoxynaphthalen-1-yl)amide (203)

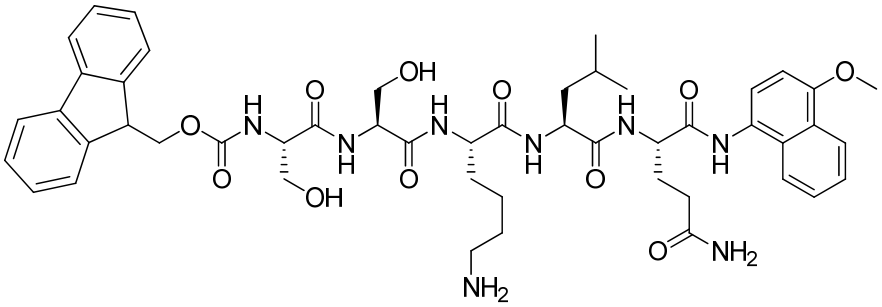

Compound **201** (76.5 mg, 0.061 mmol) was stirred with HBr in AcOH (33%, 5 mL) for 2 h. MeOH was added and excess reagent were evaporated. The solid residue was triturated several times with $Et_2O$ and dried to give a purple solid. Purification (~28.6 mg) by preparative HPLC gave **203** (14.2 mg, 48%) as a buff solid: $R_t$ 11.81 min (0.1% TFA in water / 0.1% TFA in acetonitrile, 95% → 5%, over 20 min); MS ($ES^+$) m/z 961.4453 (M + Na) ($C_{49}H_{62}N_8NaO_{11}$ requires 961.4436), 939.4633 (M + 1) ($C_{49}H_{63}N_8O_{11}$ requires 939.4616).

## 5.79 Ser(Bn)-Ser(Bn)-Lys(Cbz)-Leu-Gln-N-(4-methoxynaphthalen-1-yl)amide (204)

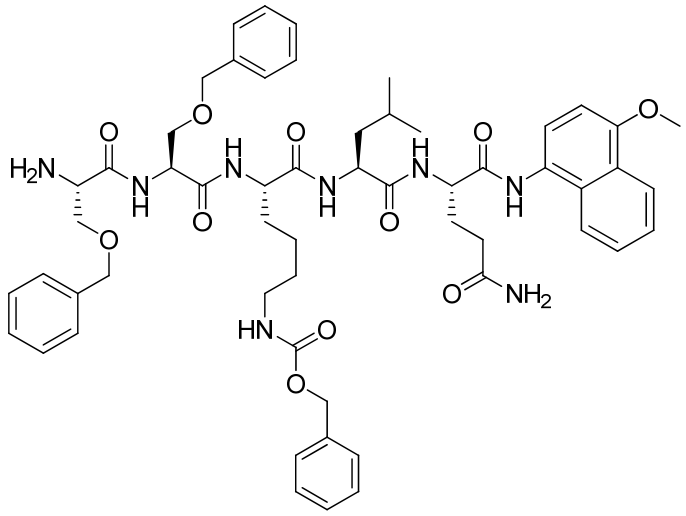

Compound **201** (453 mg, 0.36 mmol) was stirred in piperidine / DMF (20 mL, 1:5) at 20°C for 45 min. The solvent was evaporated and the residue was triturated with hot MeOH. The mixture was cooled to 0°C, filtered and the collected solid washed with cold MeOH. Drying gave **204** (304 mg, 82%) as an off white solid: $R_f$ = 0.5 (EtOAc / MeOH / AcOH 9:1:1); mp 225-226°C; $^1$H NMR [$(CD_3)_2SO$) (COSY)] δ 0.85 (3 H, d, *J* = 6.4 Hz, Leu Me), 0.89 (3 H, d, *J* = 6.4 Hz, Leu Me), 1.29-1.31 (2 H, m, Lys γ-$H_2$), 1.41 (2 H, br, Lys δ-$H_2$), 1.54-1.59 (3 H, m, Leu β-$H_2$ + Lys β-$H_1$), 1.62-1.71 (2 H, m, Leu γ + Lys β-$H_1$), 2.01-2.14 (4 H, m, Gln β-$H_2$ + $NH_2$), 2.26-2.28 (2 H, m, Gln γ-$H_2$), 2.96-3.00 (2 H, m, Lys ε-$H_2$), 3.52-3.71 (5 H, m, 2 × Ser β-$H_2$ + Ser α-$H_1$), 4.02 (3 H, s, OMe), 4.31-4.43 (2 H, m, Leu α-H + Lys α-H), 4.49-4.56 (5 H, m, 2 × SerOC*H*$_2$Ph + Gln α-H), 4.61 (1 H, br, Ser α-H), 5.04 (2 H, s, Cbz OC*H*$_2$Ph), 6.90 (1 H, s, NH), 7.00 (1 H, d, *J* = 8.3 Hz, Naph 2-H), 7.26 (1 H, t, *J* = 5.6 Hz, Cbz NH), 7.33-7.42 (16 H, m, 10 × Bn Ar-CH + 5 × Cbz Ar-CH, NH), 7.49 (1 H, d, *J* = 8.2 Hz, Naph 3-H), 7.56-7.58 (2 H, m, Naph 6,7-$H_2$), 7.95-8.00 (2 H, m, Naph 5-H + NH), 8.19-8.23 (3 H, m, Naph 8-H + 2 × NH), 8.30 (1 H, br, NH), 9.80 (1 H, s, NH); $^{13}$C NMR [$(CD_3)_2SO$) (HSQC / HMBC)] δ 21.51 (Leu Me), 22.33 (Lys γ-C), 23.04 (Leu Me), 27.77 (Gln β-C), 29.07 (Lys δ-C), 31.52 (Gln γ-C + Lys β-C), 38.83-40.09 (Leu β-C + Lys ε-C), 51.00 (Lys α-C or Leu α-C), 52.88 (Ser α-C), 52.61 (Leu α-C or Lys α-C), 52.96 (Gln α-C), 54.63 (Ser α-C), 55.67 (OMe), 65.09 (Cbz O*C*H$_2$Ph), 69.93 (Ser β-C), 72.02 (2 × SerO*C*H$_2$Ph), 72.43 (Ser β-C), 121.65 (Naph 8-C), 122.79 (Naph 5-C), 123.06 (Naph 3-C), 124.99 (Naph 6-C or 7-C), 125.38 (Naph 8a-C), 125.82 (Naph 4-C), 126.38 (Naph 7-C or 6-C), 127.37 (Ar-C), 127.44 (Ar-C), 127.72 (Ar-C), 128.18 (Ar-C), 128.33 (Ar-C), 129.38 (Naph 4a-C), 137.22 (Cbz Ar-$C_q$), 138.09 (Bn Ar-$C_q$), 138.28 (Bn Ar-$C_q$), 152.86 (Naph 1-C), 155.83 (Cbz C=O), 169.32

(C=O), 170.90 (C=O), 171.32 (C=O), 172.12 (C=O), 172.76 (C=O), 173.67 (C=O); MS (ES+) *m/z* 1053.5064 (M + Na) ($C_{59}H_{70}N_8NaO_{11}$ requires 1053.5062, 1031.5296 (M + H) ($C_{59}H_{71}N_8O_{11}$ requires 1031.5242).

### 5.80 Ser-Ser-Lys-Leu-Gln-N-(4-methoxynaphthalen-1-yl)amide (205)

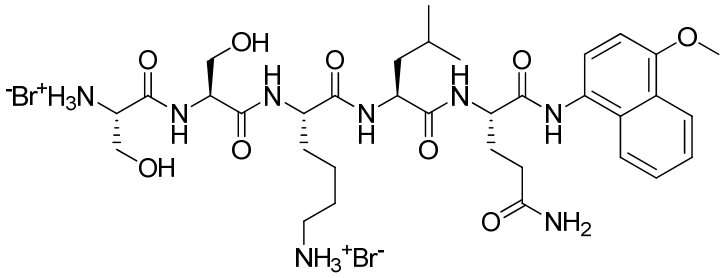

Compound **202** (330 mg, 0.32 mmol) was stirred with HBr in AcOH (33%, 4 mL) for 2 h at 20°C. MeOH was added and the solvent was evaporated. The solid residue was recrystallised (MeOH / EtOAc) to give **205** (176.41 mg, 63%) as a white solid: mp 224-225; $^1$H NMR [($D_2O$) (COSY)] δ 0.80 (3 H, d, *J* = 4.8 Hz, Leu Me), 0.85 (3 H, d, *J* = 5.0 Hz, Leu Me), 1.32 (2 H, br, Lys γ-$H_2$), 1.51-1.54 (2 H, m, Lys δ-$H_2$), 1.59-1.61 (4 H, m, Leu β-$H_2$ + Leu γ + Lys β-$H_1$), 1.71 (1 H, m, Lys β-$H_1$), 2.11 (1 H, m, Gln β-$H_1$), 2.25 (1 H, m, Gln β-$H_1$), 2.41-2.44 (2 H, m, Gln γ-$H_2$), 2.83-2.85 (2 H, m, Lys ε-$H_2$), 3.80-3.81 (2 H, m, Ser β-$H_2$), 3.92 (2 H, m, Ser β-$H_2$), 3.96 (3 H, s, OMe), 4.14 (1 H, m, Ser α-H), 4.24 (1 H, t, *J* = 6.8 Hz, Lys α-H), 4.30-4.32 (1 H, m, Leu α-H), 4.46 (1 H, m, Ser α-H), 4.51 (1 H, m, Gln α-H), 6.92 (1 H, d, *J* = 8.1 Hz, Naph 2-H), 7.29 (1 H, d, *J* = 8.2 Hz, Naph 3-H), 7.52 (1 H, t, *J* = 7.0 Hz, Naph 7-H), 7.56 (1 H, t, *J* = 6.7 Hz, Naph 6-H), 7.70 (1 H, d, *J* = 8.1 Hz, Naph 5-H), 8.20 (1 H, d, *J* = 8.1 Hz, Naph 8-H); $^{13}$C NMR [($D_2O$) (HSQC / HMBC)] δ 20.88 (Leu Me), 21.96 (Leu Me), 24.34 (Leu γ-C), 26.20 (Lys δ-C), 30.22 (Lys β-C), 31.26 (Gln γ-C), 39.09 (Lys ε-C), 39.57 (Leu β-C), 52.71 (Leu α-C), 53.70 (Lys α-C + Gln α-C), 54.40 (Ser α-C), 55.42 (Ser α-C), 55.79 (OMe), 60.14 (Ser β-C), 61.12 (Ser β-C), 104.21 (Naph 2-C), 122.06 (Naph 8-C), 122.17 (Naph 5-C), 123.91 (Naph 4-C), 125.14 (Naph 8a-C), 125.39 (Naph 3-C) 126.13 (Naph 7-C), 127.55 (Naph 6-C), 129.99 (Naph 4a-C), 154.61 (Naph 1-C), 168.00 (Ser C=O), 171.40 (Ser C=O), 173.40 (Gln C=O), 173.74 (Lys C=O), 174.81 (Leu C=O), 177.81 (Gln δ-C=O); Ms ($ES^+$) *m/z* 739.3718 (M + Na) ($C_{34}H_{52}N_8NaO_9$ requires 739.3755).

### 5.81 α-Methoxy-ω-(4-nitrophenoxy carbonyl)-polyoxyethylene (207)

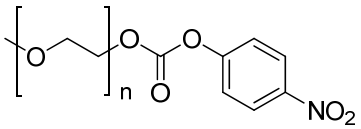

Monomethoxy-PEG-OH (Mw ~5000 g $mol^{-1}$) **206** (1.0 g, 0.20 mmol) was dissolved in toluene (20 mL) and dried by water-toluene distillation. 1,2-Dichloroethane (2 mL), 4-nitrophenyl chloroformate (81.3 mg, 0.40 mmol) and $Et_3N$ (60 µL, 43.6 mg, 0.43 mmol) were added sequentially. The mixture was stirred overnight at 20°C. $Et_2O$ was added to form a white precipitate. Filtration and drying gave **207** (1.0 g, 97%) as a white solid: $R_f$ = 0.3 (EtOAc / MeOH 1:1); $^1H$ NMR ($CDCl_3$) δ 3.35 (3 H, s, OMe), 3.43 (2 H, t, *J* = 5.2 Hz, mPEG $CH_2$), 3.52 (2 H, m, mPEG $CH_2$), 3.61-3.72 (~434 H, m, mPEG $CH_2$), 3.77-3.78 (4 H, m, mPEG $CH_2$), 4.41 (2 H, t, *J* = 4.5 Hz, mPEG $CH_2$), 7.36 (2 H, d, *J* = 9.1 Hz, Ar 2,6-H), 8.25 (2 H, d, *J* = 9.1 Hz, Ar 3, 5-H).

### 5.82 mPEG-L-Ser(Bn)-L-Ser(Bn)-L-Lys(Cbz)-L-Leu-L-Gln-methoxynaphthalenamide (208)

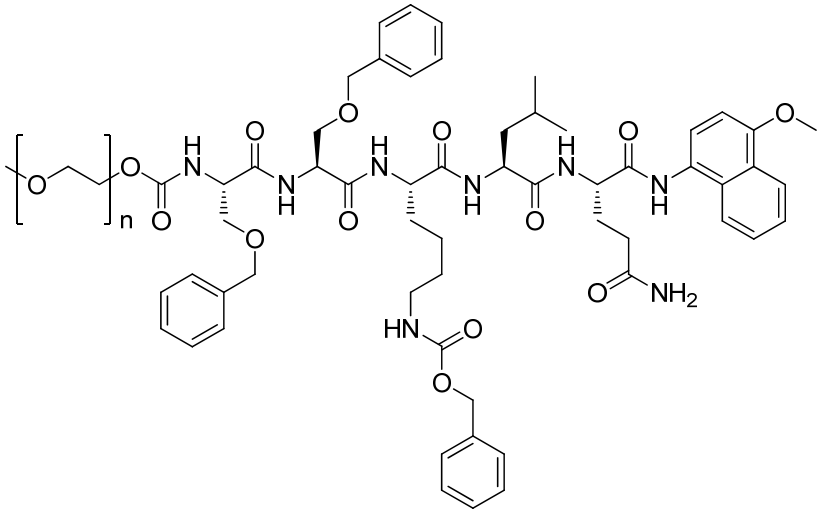

Compound **204** (45.8 mg, 44 µmol) was stirred in dry DMF (1.0 mL) and $Et_3N$ (0.05 mL) added, followed by addition of mPEG-nitrophenyl ester **207** (205mg, 0.040 mmol). The mixture was stirred under $N_2$ at 20°C for 8 d. The solvent was evaporated. Reverse-phase chromatography ($H_2O$ / MeCN 99:1 → 5:95) and freeze drying gave **208** (123 mg, 52%) as a white solid: $R_f$ = 0.7 (MeCN / MeOH 4:1); $^1H$ NMR [$(CD_3)_2SO$) (COSY)] δ 0.85 (3 H, d, *J* = 6.4 Hz, Leu Me), 0.89 (3 H, d, *J* = 6.4 Hz, Leu Me), 1.23-1.30 (2 H, m, Lys γ-$H_2$), 1.39-1.41 (Lys δ-$H_2$), 1.51-1.59 (3 H, m, Leu β-$H_2$ + Lys β-$H_1$), 1.66-1.71 (2 H, m, Leu γ-H + Lys β-$H_1$), 1.96-2.04 (1 H, m, Gln β-$H_1$), 2.12-2.16 (1 H, m, Gln β-$H_1$), 2.27-2.31 (2 H, m, Gln γ-$H_2$), 2.97-2.99 (2 H, m, Lys ε-$H_2$), 3.30 (3 H, s, mPEG OMe), 3.39 (2 H, t, *J* = 5.0 Hz, mPEG

$CH_2$), 3.47-3.68 (~444 H, m, 2 × Ser β-$H_2$ + mPEG 220 × $CH_2$), 3.74 (2 H, t, *J* = 4.6 Hz, mPEG $CH_2$), 4.02 (3 H, s, Naph OMe), 4.10-4.13 (1 H, Ser α-H), 4.31-4.45 (2 H, m, Leu α-H + Lys α-H), 4.52-4.58 (5 H, m, Gln α-H + 2 × SerOC*H*$_2$Ph), 4.63-4.64 (1 H, m, Ser α-H), 5.05 (2 H, s, Cbz OC*H*$_2$Ph), 6.85 (1 H, s, NH), 6.99 (1 H, d, *J* = 9.0 Hz, Naph 2-H), 7.16-7.19 (1 H, br, NH), 7.28-7.42 (15 H, m, 10 × Bn Ar-H, 5 × Cbz Ar-H), 7.50 (2 H, m, Naph 3-H, NH), 7.56-7.58 (2 H, m, Naph 6,7-$H_2$), 7.96-7.98 (2 H, m, Naph 5-H, NH), 8.07 (1 H, d, *J* = 7.1 Hz, NH), 8.15-8.23 (3 H, m, Naph 8-H, 2 × NH), 8.36 (1 H, br, NH), 9.74 (1 H, s, NH).

## 5.83 Fmoc-L-Ser(Bn)-L-Ser(Bn)-L-Lys(Cbz)-L-Leu-Gln-L-Leu-L-D-Ser(Bu$^t$)-OH (213)

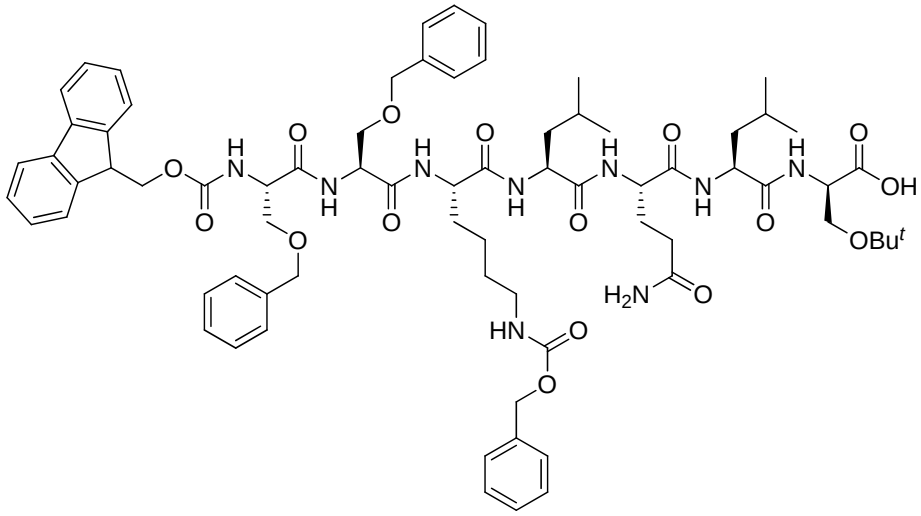

Peptide **213** was synthesised on 2-chlorotrityl chloride polystyrene resin (1.09 g, 1.64 mmol) according to the general procedure (Section 5.68) as described above to yield **213** (1.27 g, 89%) as a white solid: $R_f$ = 0.7 (EtOAc / MeOH 1 :1); mp 243-245°C; IR $\nu_{max}$ 3287 (NH, OH), 1634 (C=O); $^1$H NMR [$(CD_3)_2SO$) (COSY)] δ 0.79-0.86 (12 H, m, 2 × Leu $Me_2$), 1.10 (9 H, s, Bu$^t$), 1.24 (2 H, m, Lys γ-$H_2$), 1.36-1.46 (7 H, m, 2 × Leu β-$H_2$ + Lys β-$H_1$, δ-$H_2$), 1.57-1.62 (3 H, m, 2 × Leu γ-H + Lys β-$H_1$), 1.75-1.77 (1 H, m, Gln β-H), 1.85-1.89 (1 H, m, Gln β-H), 2.09 (2 H, t, *J* = 7.7 Hz, Gln γ-$H_2$), 2.94-2.95 (2 H, m, Lys ε-$H_2$), 3.49-3.51 (1 H, m, D-Ser β-$H_1$), 3.58-3.69 (5 H, m, 2 × L-Ser β-$H_2$ + D-Ser β-$H_1$), 4.22-4.37 (7 H, m, Fmoc-$CH_2$, fluorene 9-H, Gln α-H, Leu α-H, D-Ser α-H, Lys α-H), 4.42-4.51 (6 H, m, 2× SerOC*H*$_2$Ph, Leu α-H, L-Ser α-H), 4.60 (1 H, m, L-Ser α-H), 5.00 (2 H, s, Cbz $CH_2$), 6.77 (1 H, br, NH), 7.18-7.43 (20 H, m, 19 × Ar-H + NH), 7.63-7.74 (3 H, m, Fmoc Ar-$H_2$ + NH), 7.89-7.90 (4 H, m, Fmoc Ar-$H_2$ + 2 × NH), 7.99-8.06 (3 H, m, 3 × NH), 8.23-8.34 (2 H, m, 2 × NH); $^{13}$C NMR [$(CD_3)_2SO$) δ (HSQC / HMBC)] δ 21.58 (2 × Leu Me), 22.55 (Lys γ-C),

22.96 (Leu Me), 23.02 (Leu Me), 23.99 (Leu γ-C), 24.04 (Leu γ-C), 27.08 (C*Me*$_3$), 27.75 (Gln β-C), 29.13 (Lys δ-C), 31.48 (Gln γ-C), 31.68 (Lys β-C), 40.19 (Lys ε-C), 40.75 (Leu β-C), 41.20 (Leu β-C), 46.57 (fluorene 9-C), 50.72 (Leu α-C), 50.89 (Leu α-C), 51.98 (Gln α-C), 52.56 (Lys α-C), 52.64 (Ser α-C), 52.76 (Ser α-C), 54.67 (L-Ser α-C), 61.51 (D-Ser β-C), 65.09 (Cbz O*C*H$_2$Ph), 65.82 (Fmoc CH$_2$), 69.73 (2 × L-Ser β-C), 71.97 (SerO*C*H$_2$Ph), 72.08 (SerO*C*H$_2$Ph), 72.65 (*C*Me$_3$), 120.07 (Fmoc Ar-C), 125.28 (Fmoc Ar-C), 127.05 (Ar-C), 127.30 (Ar-C), 127.35 (Ar-C), 127.39 (Ar-C), 127.42 (Ar-C), 127.61 (Ar-C), 127.70 (Ar-C), 128.11 (Ar-C), 128.13 (Ar-C), 128.30 (Ar-C), 137.22 (Cbz Ph 1-C), 138.07 (Bn Ph 1-C), 138.13 (Bn Ph 1-C), 140.67 (2 × Fmoc-C$_q$), 143.72 (Fmoc-C$_q$), 143.78 (Fmoc-C$_q$), 156.02 (Cbz C=O), 169.10 (C=O), 169.67 (C=O), 170.21 (C=O), 170.73 (C=O), 171.12 (C=O), 171.53 (C=O), 171.76 (C=O), 171.82 (C=O), 173.77 (Gln δ-C=O); (MS (ES$^+$) *m/z* 1376.6879 (M + Na) (C$_{73}$H$_{95}$N$_9$NaO$_{16}$ requires 1376.6795).

## 5.84 Calf-thymus DNA melting assay[199]

### 5.84.1 Buffer preparation

NaH$_2$PO$_4$ (1.17 g, 9.75 mM), ethylenediaminetetraacetic acid (EDTA) disodium salt dihydrate (372 mg, 1.0 mM) and NaCl (438 mg, 7.5 mM) were dissolved in MilliQ water (0.8 L). The pH was adjusted to pH 7.0 using aq. NaOH (0.1 M) or aq. HCl (0.1 M) as required and Milli-Q water added to produce 1 L.

### 5.84.2 Calf thymus DNA solution preparation

Calf thymus DNA stock solution was prepared by dissolving DNA in 9.75 mM phosphate buffer to a concentration of 1 mg mL$^{-1}$. Once fully dissolved, the stock was diluted down until an absorbance of 0.6 at 256 nm was obtained. This was found to be approximately 1.6 mL of DNA stock made up to 50 mL with phosphate buffer (*i.e.* ~0.032 mg mL$^{-1}$).

### 5.84.3 Calculations

The DNA concentration of the diluted DNA (9.06 × 10$^{-5}$ M) was calculated using the following Beer-Lambert equation:

Equation 1: $A = \varepsilon cl$

Where: A = the absorbance of diluted calf thymus DNA at 256 nm

ε = molar extinction of DNA (6600 M$^{-1}$ cm$^{-1}$);[200, 201]

c = molar concentration of DNA solution;
l = path length in cm (in this case 1 cm cuvette).

The volume of the drug sample solution needed to obtain the required molar equivalent (0.01 → 0.6) could be worked out using the following equation:

Equation 2: Volume of sample = Molar concentration of diluted DNA × Volume of diluted DNA × MW of drug sample × Molar equivalent required

### 5.84.4 Procedure

Compound **136** (1.04 mg, 1.94 µmol) was dissolved in DMSO (1 mL) to make a stock solution (1.94 mM). Different volumes of the stock solution (corresponding to the range of molar equivalents given above (Equation 2) were added to the DNA (3 mL, $9.06 \times 10^{-5}$ M) in the appropriate cells and incubated at room temperature for 1 h to allow alkylation of DNA.

Samples in quartz cells consisted of:

- Cell 1 (blank) → Buffer + DMSO (40 µL);
- Cells 2 and 3 (positive control) → DNA + buffer + DMSO (40 µL);
- Cells 4 and 5→Test compound + DNA + buffer + DMSO.

All cells contained the same total volume of DMSO (40 µL). Since the test compound solution was prepared in DMSO, this had to be taken into account. The absorbance at 256 nm was monitored for each sample over the range of 40-95°C at a rate of 0.5°C per minute in a 1 cm quartz cell using a complete PC controlled spectrometer system by Perkin Elmer: Lambda BioDNA Melt system including PTP-6 temperature controlled programmer for simultaneous curves, UVTemplab software and in-cuvette temperature sensor. The thermal melting ($T_m$) of the calf thymus DNA was determined for samples in cells 2-5. $\Delta T_m$ = $T_m$ of DNA-drug complex (cells 4 and 5) – $T_m$ of DNA alone (cells 2 and 3). $T_m$ values were calculated from the midpoint of the first derivative plots.

## 5.85 Anti-proliferative assay

### 5.85.1 Preparation of cell suspension

Medium was poured off the cells and the cells washed with PBS (5 mL). Trypsin/EDTA [(0.05% (w/v), 5 mL)] was added and the mixture placed at 37°C until the cells detached. Medium (8 mL) was added to suspend the cells which were transferred to a Universal tube. The suspension was centrifuged at ~1300 rpm for 7 min using Jouvan B3.11 centrifuge at room temperature. The supernatant was removed and the cells re-suspended in medium (5 mL). This was then diluted (~1 in 10) and the cells counted using a haemocytometer. Further dilution was made to give a suspension with the required number of cells per well for the experiment (2000 cells per well to be added in 50 µL). These seed densities had been determined previously to give an acceptable optical density value after 3 d incubation.

### 5.85.2 Procedure[202]

Cells (2000 per well) were seeded onto 96-well microtitre plates, allowed to attach for 2-4 h at 37$^{o}$C, in humidified atmosphere containing 5% (v/v) $CO_2$ and then treated with various concentrations of test compounds (1 µM → 1 nM for **136** and 100 µM → 100 nM for **135**).

Quadruplicate samples were run by adding the following reagents:

- Culture medium only (negative control) → 100 µL medium per well;
- Cells suspension only (positive control) → 50 µL medium + 50 µL cell suspension;
- Cells + 1% (v/v) DMSO vehicle → 50 µL of 2% (v/v) DMSO in medium + 50 µL cell suspension;
- Cells + test compound in 1% (v/v) DMSO vehicle → 50 µL of drug at 2 × concentration with 2% (v/v) DMSO in medium + 50 µL cell suspension.

Each well contained a final volume of 100 µL medium containing final vehicle concentration of 1% (v/v) DMSO and was incubated at 37°C, in a humidified atmosphere containing 5% (v/v) $CO_2$ for 3 d. Cell viability was measured by chemical treatment with MTS reagent as recommended by the manufacturer (Promega, U.S.A),[192] followed by incubation at 37°C, in humidified atmosphere containing 5% (v/v) $CO_2$ for 2-4 hours after which the absorbance of each well was measured at 490 nm using a VERSAmax microplate reader. The determination of $IC_{50}$ data was calculated using a four parameter logistic curve and SigmaPlot 12 software

for windows. Means and standard deviations were calculated from background corrected absorbance. (MTS procedure was adopted from a protocol developed by Dr Pauline Wood.[202])

## 5.86 PSA-Cleavage Assay

### 5.86.1 Buffer preparation

Tris.HCl (788 mg, 50 mM), NaCl (818 mg, 140 mM) and were dissolved in Milli-Q water (80 mL). The pH was adjusted to pH 7.4 using aq. NaOH (0.1 M) or aq. HCl (0.1 M) as required and Milli-Q water added to produce 100 mL.

### 5.86.2 Procedure[98, 100]

The peptide-model drug conjugate **203** or **205** (~2 mM) was incubated with PSA (10 μg $mL^{-1}$) at 37°C in 50 mM Tris.HCl and 140 mM NaCl, pH 7.4 buffer (500 μL). A control experiment without the enzyme was also set up. Samples (50 μL) were taken at different time intervals (up to 7 d) and added to $ZnCl_2$ solution (final concentration 10 mM) to quench the reaction. Centrifugation (Eppendorf Mini-Spin centrifuge, 13400 rpm, 10 min) was followed by HPLC analysis of the supernatant on reverse-phase Phenomenex Gemini 5μm C-18 (150 × 4.6 mm) analytical column with gradient and flow-rate as described in Section 5.1. Detection was monitored at λ = 220 nm and 280 nm using a Dionex HPLC system (Section 5.1).

# 6 References


1. Timms, B. G. Prostate development: A historical perspective. *Differentiation* **2008,** *76*, 565-577.

2. Wood, C. K.; Lockhart, J. S. Prostate cancer. *Am. J. Nurs.* **2000,** *100*, 47-51.

3. Amin, M.; Khalid, A.; Tazeen, N.; Yasoob, M. Zonal anatomy of prostate. *Annals* **2010,** 16, 138-142.

4. Laczko, I.; Hudson, D. L.; Freeman, A.; Feneley, M. R.; Masters, J. R. Comparison of the zones of the human prostate with the seminal vesicle: Morphology, immunohistochemistry, and cell kinetics. *Prostate* **2005,** *62*, 260-266.

5. Kumar, V. L.; Majumder, P. K. Prostate gland: Structure, functions and regulation. *Int. J. Urol. Nephrol.* **1995,** *27*, 231-243.

6. NHS Choices. Prostate disease-Introduction. http://www.nhs.uk/conditions/Prostate-disease/Pages/Introduction.aspx (7 January 2013).

7. Tindall, D. J.; Scardino, P. T. *Recent advances in prostate cancer: basic science discoveries and clinical advances*. World Scientific Publishing Co. Pte. Ltd: Singapore, **2011**.

8. NHS Choices. Prostate enlargement-Introduction. http://www.nhs.uk/Conditions/-Prostate-enlargement/Pages/Introduction.aspx (7 January 2013).

9. Chen, Y.; Zhang, X.; Hu, X.; Deng, Y.; Chen, J.; Li, S.; Zhang, C.; Wang, J.; Liu, Z.; Hao, Y.; Xiao, Y.; Yuan, J.; Xu, T.; Wang, X. The potential role of a self-management intervention for benign prostate hyperplasia. *Urology* **2012,** *79*, 1385-1389.

10. Yoo, T. K.; Cho, H. J. Benign prostatic hyperplasia: From bench to clinic. *Korean J. Urol.* **2012,** *53*, 139-148.

11. NHS Choices. Prostatitis-introduction. http://www.nhs.uk/Conditions/Prostatitis/-Pages/Introduction.aspx (07 January 2013).

12. Pluta, R. M.; Lynm, C.; Golub, R. M. Prostatitis. *J. Am. Med. Assoc.* **2012,** *307*, 527.

13. Naber, K. G. Prostatitis. *Nephrol. Dial. Transpl.* **2001,** *16*, 132-134.

14. Clark, C. Protatitis. *Pharm. J.* **2004,** 272, 511-514.

15. Bott, S. R.; Birtle, A. J.; Taylor, C. J.; Kirby, R. S. Prostate cancer management: (1) An update on localised disease. *Postgrad. Med. J.* **2003,** 79, 575-580.

16. Heidenreich, A.; Bastian, P. J.; Bellmunt, J.; Bolla, M.; Joniau, S.; Mason, M. D.; Matveev, T.; Mottet, N.; van der Kwast, T. H.; Wiegel, T.; Zattoni, F. The updated EAU guidelines on prostate cancer. http://www.uroweb.org/fileadmin/guidelines/-2012_Guidelines_large_text_print_total_file.pdf (8 January 2013).

17. Damber, J.; Aus, G. Prostate cancer. *Lancet* **2008,** *371*, 1710-1721.

18. Mazhar, D.; Waxman, J. Review: Prostate cancer. *Postgrad. Med. J.* **2002,** 78, 590-595.

19. Hsing, A.; Chokkalingam, A. Prostate cancer epidemiology. *Frontiers Biosci.* **2006,** *11*, 1388-1413.

20. Crawford, E. D. Epidemiology of prostate cancer. *Urology* **2003,** 62, 3-12.

21. Eeles, R. A.; Olama, A. A. A.; Benlloch, S.; Saunders, E. J.; Leongamornlert, D. A.; Tymrakiewicz, M.; Ghoussaini, M.; Luccarini, C.; Dennis, J.; Jugurnauth-Little, S.; Dadaev, T.; Neal, D. E.; Hamdy, F. C.; Donovan, J. L.; Muir, K.; Giles, G. G.; Severi, G.; Wiklund, F.; Gronberg, H.; Haiman, C. A.; Schumacher, F.; Henderson, B. E.; Le Marchand, L.; Lindstrom, S.; Kraft, P.; Hunter, D. J.; Gapstur, S.; Chanock, S. J.; Berndt, S. I.; Albanes, D.; Andriole, G.; Schleutker, J.; Weischer, M.; Canzian, F.; Riboli, E.; Key, T. J.; Travis, R. C.; Campa, D.; Ingles, S. A.; John, E. M.; Hayes, R. B.; Pharoah, P. D. P.; Pashayan, N.; Khaw, K.-T.; Stanford, J. L.; Ostrander, E. A.; Signorello, L. B.; Thibodeau, S. N.; Schaid, D.; Maier, C.; Vogel, W.; Kibel, A. S.; Cybulski, C.; Lubinski, J.; Cannon-Albright, L.; Brenner, H.; Park, J. Y.; Kaneva, R.; Batra, J.; Spurdle, A. B.; Clements, J. A.; Teixeira, M. R.; Dicks, E.; Lee, A.; Dunning, A. M.; Baynes, C.; Conroy, D.; Maranian, M. J.; Ahmed, S.; Govindasami, K.; Guy, M.; Wilkinson, R. A.; Sawyer, E. J.; Morgan, A.; Dearnaley, D. P.; Horwich, A.; Huddart, R. A.; Khoo, V. S.; Parker, C. C.; Van As, N. J.; Woodhouse, C. J.; Thompson, A.; Dudderidge, T.; Ogden, C.; Cooper, C. S.; Lophatananon, A.; Cox, A.; Southey, M. C.; Hopper, J. L.; English, D. R.; Aly, M.; Adolfsson, J.; Xu, J.; Zheng, S. L.; Yeager, M.; Kaaks, R.; Diver, W. R.; Gaudet, M. M.; Stern, M. C.; Corral, R.; Joshi, A. D.; Shahabi, A.; Wahlfors, T.; Tammela, T. L. J.; Auvinen, A.; Virtamo, J.; Klarskov, P.; Nordestgaard, B. G.; Roder, M. A.; Nielsen, S. F.; Bojesen, S. E.; Siddiq, A.; FitzGerald, L.

M.; Kolb, S.; Kwon, E. M.; Karyadi, D. M.; Blot, W. J.; Zheng, W.; Cai, Q.; McDonnell, S. K.; Rinckleb, A. E.; Drake, B.; Colditz, G.; Wokolorczyk, D.; Stephenson, R. A.; Teerlink, C.; Muller, H.; Rothenbacher, D.; Sellers, T. A.; Lin, H.-Y.; Slavov, C.; Mitev, V.; Lose, F.; Srinivasan, S.; Maia, S.; Paulo, P.; Lange, E.; Cooney, K. A.; Antoniou, A. C.; Vincent, D.; Bacot, F.; Tessier, D. C.; Kote-Jarai, Z.; Easton, D. F. Identification of 23 new prostate cancer susceptibility loci using the iCOGS custom genotyping array. *Nat. Genet.* **2013,** *45*, 385-391.

22. The breast cancer linkage consortium. Cancer risks in BRCA2 mutation carriers. *J. Natl. Cancer Inst.* **1999,** *91*, 1310-1316.

23. Francis, J. C.; McCarthy, A.; Thomsen, M. K.; Ashworth, A.; Swain, A. Brca2 and Trp53 deficiency cooperate in the progression of mouse prostate tumourigenesis. *PLoS Genetics* **2010,** *6*, 1-9.

24. Nelson, W. G.; De Marzo, A. M.; Isaacs, W. B. Review: Mechanisms of disease-prostate cancer. *N. Engl. J. Med.* **2003,** *349*, 366-381.

25. Kirby, R.; Madhavan, S. G. Prostate cancer. *Surgery* **2010,** *28*, 594-598.

26. Coffey, D. S. Similarities of prostate and breast cancer: Evolution, diet, and estrogens. *Urology* **2001,** *57*, 31-38.

27. Kumar, V.; Anderson, J. Prostate cancer. *Surgery* **2002,** *20*, 297-300.

28. Lee, W. H.; Morton, R. A.; Epstein, J. I.; Brooks, J. D.; Campbell, P. A.; Bova, G. S.; Hsieh, W. S.; Isaacs, W. B.; Nelson, W. G. Cytidine methylation of regulatory sequences near the pi-class glutathione *S*-transferase gene accompanies human prostatic carcinogenesis. *Proc. Natl. Acad. Sci. USA* **1994,** *91*, 11733-11737.

29. Bastian, P. J.; Yegnasubramanian, S.; Palapattu, G. S.; Rogers, C. G.; Lin, X.; De Marzo, A. M.; Nelson, W. G. Molecular biomarker in prostate cancer: The role of CpG Island hypermethylation. *Eur. Urol.* **2004,** *46*, 698-708.

30. Meeker, A. K.; Hicks, J. L.; Platz, E. A.; March, G. E.; Bennett, C. J.; Delannoy, M. J.; De Marzo, A. M. Telomere shortening is an early somatic DNA alteration in human prostate tumorigenesis. *Cancer Res.* **2002,** *62*, 6405-6409.

31. Meeker, A. K.; Hicks, J. L.; Iacobuzio-Donahue, C. A.; Montgomery, E. A.; Westra, W. H.; Chan, T. Y.; Ronnett, B. M.; De Marzo, A. M. Telomere length abnormalities occur early in the initiation of epithelial carcinogenesis. *Clin. Cancer Res.* **2004,** *10*, 3317-3326.

32. Sommerfeld, H. J.; Meeker, A. K.; Piatyszek, M. A.; Bova, G. S.; Shay, J. W.; Coffey, D. S. Telomerase activity: A prevalent marker of malignant human prostate tissue. *Cancer Res.* **1996,** *56*, 218-222.

33. Iwata, T.; Schultz, D.; Hicks, J.; Hubbard, G. K.; Mutton, L. N.; Tamara L. Lotan, T. L.; Bethel, C.; Lotz, M. T.; Yegnasubramanian, S.; Nelson, W. G.; Dang, C. V.; Xu, M.; Anele, U.; Koh, C. M.; Bieberich, C. J.; De Marzo, A. M. MYC overexpression induces prostatic intraepithelial neoplasia and loss of Nkx3.1 in mouse luminal epithelial cells. *PLoS ONE* **2010,** *5*, 1-16.

34. Nationl Institute for Health and Care Excellence (NICE). *Prostate cancer: Diagnosis and treatment.* National Collaborating Centre for Cancer: Cardiff, 2008; pp 1-186.

35. Jain, S.; Bhojwani, A.; Mellon, J. Improving the utility of prostate specific antigen (PSA) in the diagnosis of prostate cancer: The use of PSA derivatives and novel markers. *Postgrad. Med. J.* **2002,** *78*, 646-650.

36. Wood, N. Understanding treatment of prostate cancer. *Pharm. J.* **2009**, 35-38.

37. Zhang, T. Y.; Agarwal, N.; Sonpavde, G.; DiLorenzo, G.; Bellmunt, J.; Vogelzang, N. J. Management of castrate resistant prostate cancer-Recent advances and optimal sequence of treatments. *Curr. Urol. Rep.* **2013**, 1-10.

38. National Institute for Health and Care Excellence (NICE). *Abiraterone for castration-resistant metastatic prostate cancer previously treated with a docetaxel-containing regimen.* Centre for Health Technology Evaluation: **2012**; pp 1-51.

39. Suárez, C.; Morales-Barrera, R.; Ramos, V.; Núñez, I.; Valverde, C.; Planas, J.; Morote, J.; Maldonado, X.; Carles, J. Role of immunotherapy in castration-resistant prostate cancer (CRPC). *Brit. J. Urol. Int.* **2013**, 1-10.

40. Mukherji, D.; Temraz, S.; Wehbe, D.; Shamseddine, A. Angiogenesis and anti-angiogenic therapy in prostate cancer. *Crit. Rev. Oncol. Hematol.* **2013,** *87*, 122-131.

41. Lajiness, J., P.; Boger, D., L. Asymmetric synthesis of 1,2,9,9a-tetrahydrocyclopropa[*c*]benzo[*e*]indol-4-one (CBI). *J. Org. Chem* **2011,** *76*, 583-587.

42. Wrasidlo, W.; Douglas, S.; Boger, D. Introduction of endonucleolytic DNA fragmentation and apoptosis by the duocarmycins. *Bioorg. Med. Chem.* **1994,** *2* 631-636.

43. Li, L. H.; Swenson, D. H.; Schpok, S. L. F.; Kuentzel, S. L.; Dayton, B. D.; Krueger, W. C. CC-1065 (NSC298223), a novel antitumour agent that interacts strongly with double-stranded DNA. *Cancer Res.* **1982,** *42*, 999-1004.

44. Atwell, G. J.; Tercel, M.; Boyd, M.; Wilson, W. R.; Denny, W. A. Synthesis and cytotoxicity of 5-amino-1-(chloromethyl)-3-[(5,6,7-trimethoxyindol-2-yl)carbonyl]-1,2-dihydro-3*H*-benz[*e*]indole (amino-*seco*-CBI-TMI) and related 5-alkylamino analogues: New DNA minor groove alkylating agents. *J. Org. Chem.* **1998,** *63*, 9414-9420.

45. Baraldi, P. G.; Cacciari, B.; Guiotto, A.; Romagnoli, R.; Zaid, A. N.; Spalluto, G. DNA minor-groove binders: Results and design of new antitumor agents. *Farmaco* **1999,** *54*, 15-25.

46. Mohamadi, F.; Spees, M. M.; Staten, G. S.; Marder, P.; Kipka, J. K.; Johnson, D. A.; Boger, D. L.; Zarrinmayeh, H. Total synthesis and biological properties of novel antineoplastic (chloromethyl)furanoindolines: An asymmetric hydroboration mediated synthesis of the alkylation subunits. *J. Med. Chem.* **1994,** *37*, 232-239.

47. Nagamura, S.; Asai, A.; Kobayashi, E.; Gomi, K.; Saito, H. Studies on duocarmycin SA and its derivatives. *Bioorg. Med. Chem.* **1997,** *5*, 623-630.

48. Tercel, M.; Atwell, G. J.; Yang, S.; Ashoorzadeh, A.; Stevenson, R. J.; Botting, K. J.; Gu, Y.; Mehta, S. Y.; Denny, W. A.; Wilson, W. R.; Pruijn, F. B. Selective treatment of hypoxic tumor cells *in vivo*: Phosphate pre-prodrugs of nitro analogues of the duocarmycins. *Angew. Chem. Int. Ed.* **2011,** *50*, 2606-2609.

49. Wang, Y.; Jiang, J.; Jiang, X.; Cai, S.; Han, H.; Li, L.; Tian, Z.; Jiang, W.; Zhang, Z.; Xiao, Y.; Wright, S. C.; Larrick, J. W. Synthesis and antitumor activity evaluations of albumin-binding prodrugs of CC-1065 analog. *Bioorg. Med. Chem.* **2008,** *16*, 6552-6559.

50. Parrish, J. P.; Kastrinsky, D. B.; Stauffer, F.; Hedrick, M. P.; Hwang, I.; Boger, D. L. Establishment of substituent effects in the DNA binding subunit of CBI analogues of the duocarmycins and CC-1065. *Bioorg. Med. Chem.* **2003,** *11*, 3815-3838.

51. Boger, D. L. The duocarmycins: Synthetic and mechanistic studies. *Acc. Chem. Res.* **1995,** *28*, 20-29.

52. Cacciari, B.; Romagnoli, R.; Baraldi, P. G.; DaRos, T. D.; Spalluto, G. CC-1065 and the duocarmycins: Recent developments. *Expert Opin. Ther. Pat.* **2000,** *10*, 1853-1871.

53. Bhuyan, B. K.; Newell, K., A.; Crampton, S. L.; Von Hoff, D. D. CC-1065 (NSC 298223), a most potent antitumor agent: Kinetics of inhibition of growth, DNA synthesis, and cell survival. *Cancer Res.* **1982,** *42*, 3532-3537.

54. Pecere, T.; Gazzola, M. V.; Mucignat, C.; Parolin, C.; Vecchia, F. D.; Cavaggioni, A.; Basso, G.; Diaspro, A.; Salvato, B.; Carli, M.; Palù, G. Aloe-emodin is a new type of anticancer agent with selective activity against neuroectodermal tumors. *Cancer Res.* **2000,** *60*, 2800-2804.

55. Purnell, B.; Sato, A.; O'Kelley, A.; Price, C.; Summerville, K.; Hudson, S.; O'Hare, C.; Kiakos, K.; Asao, T.; Lee, M.; Hartley, J. A. DNA interstrand crosslinking agents: Synthesis, DNA interactions, and cytotoxicity of dimeric achiral *seco*-amino-CBI and conjugates of achiral *seco*-amino-CBI with pyrrolobenzodiazepine (PBD). *Bioorg. Med. Chem. Lett.* **2006,** *16*, 5677-5681.

56. Howard, T. T.; Lingerfelt, B. M.; Purnell, B. L.; Scott, A. E.; Price, C. A.; Townes, H. M.; McNulty, L.; Handl, H. L.; Summerville, K.; Hudson, S. J.; Bowen, J. P.; Kiakos, K.; Hartleyd, J. A.; Leea, M. Novel furano analogues of duocarmycin C1 and C2: Design, synthesis, and biological evaluation of *seco*-iso-cyclopropylfurano[2,3-*e*]indoline (*seco*-iso-CFI) and *seco*-cyclopropyltetrahydrofurano[2,3-*f*]quinoline (*seco*-CFQ) analogues. *Bioorg. Med. Chem.* **2002,** *10*, 2941-2952.

57. Sato, A.; McNulty, L.; Cox, K.; Kim, S.; Scott, A.; Daniell, K.; Summerville, K.; Price, C.; Hudson, S.; Kiakos, K.; Hartley, J. A.; Asao, T.; Lee, M. A novel class of *in vivo* active anticancer agents: Achiral *seco*-amino- and *seco*-hydroxycyclopropylbenz[*e*]indolone (*seco*-CBI) analogues of the duocarmycins and CC-1065. *J. Med. Chem.* **2005,** *48*, 3903-3918.

58. Kupchinsky, S.; Centioni, S.; Howard, T.; Trzupek, J.; Roller, S.; Carnahan, V.; Townes, H.; Purnell, B.; Price, C.; Handl, H.; Summerville, K.; Johnson, K.; Toth, J.; Hudson, S.; Kiakos, K.; Hartley, J. A.; Lee, M. A novel class of achiral seco-analogs of CC-

1065 and the duocarmycins: Design, synthesis, DNA binding, and anticancer properties. *Bioorg. Med. Chem.* **2004,** *12*, 6221-6236.

59. Darzynkiewicz, Z.; Juan, G.; Li, X.; Gorczyca, W.; Murakami, T.; Traganos, F. Cytometry in cell necrobiology: Analysis of apoptosis and accidental cell death (necrosis). *Cytometry* **1997,** *27*, 1-20.

60. Boger, D. L.; Johnson, D. S. CC-1065 and the duocarmycins: Unraveling the keys to a new class of naturally derived DNA alkylating agents. *Proc. Natl. Acad. Sci. USA* **1995,** *92*, 3642-3649.

61. Boger, D. L.; Johnson, D. S. CC- 1065 and the duocarmycins : understanding their biological function through mechanistic studies. *Angew. Chem. Int. Ed. Engl.* **1996,** *35*, 1438-1474.

62. Wang, Y.; Yuan, H.; Wright, S. C.; Wang, H.; Larrick, J. W. Synthesis and cytotoxicity of a biotinylated CC-1065 analogue. *BMC. Chem. Biol.* **2002,** *2*, 1-4.

63. Hurley, L. H.; Warpehoski, M. A.; Lee, C. S.; McGovren, J. P.; Scahill, T. A.; Kelly, R. C.; Mitchell, M. A.; Wicnienski, N. A.; Gebhard, I.; Johnson, P. D.; Bradford, V. S. Sequence specificity of DNA alkylation by the unnatural enantiomer of CC-1065 and its synthetic analogues. *J. Am. Chem. Soc.* **1990,** *112*, 4633-4649.

64. Remers, W. A. The chemistry of antitumour antibiotics. John Wiley & Sons, Inc.: Canada, 1988; Vol. 2, p 154-161.

65. Huang, W.; Xu, H.; Li, Y.; Zhang, F.; Chen, X.; He, Q.; Igarashi, Y.; Tang, G. Characterization of yatakemycin gene cluster revealing a radical *S*-adenosylmethionine dependent methyltransferase and highlighting spirocyclopropane biosynthesis. *J. Am. Chem. Soc.* **2012,** *134*, 8831-8840.

66. Boger, D. L.; Mbini, P.; Tarby, C. M. Chemical and structural comparison of N-Boc-CBQ and N-Boc-CBI: Identification and structural origin of an unappreciated but productive stability of the CC-1065 and duocarmycin SA alkylation subunits. *J. Am. Chem. Soc.* **1994,** *116*, 6461-6462.

67. Boger, D. L.; Garbaccio, R. M.; Jin, Q. Synthesis and evaluation of CC-1065 and duocarmycin analogues incorporating the Iso-CI and Iso-CBI alkylation subunits: Impact of relocation of the C-4 carbonyl. *J. Org. Chem.* **1997,** *62*, 8875-8891.

68. MacMillan, K. S.; Boger, D. L. Fundamental relationships between structure, reactivity, and biological activity for the duocarmycins and CC-1065. *J. Med. Chem.* **2009,** *52*, 5771-5780.

69. Boger, D. L.; Turnbull, P. Synthesis and evaluation of CC-1065 and duocarmycin analogs incorporating the 1,2,3,4,11,11a-hexahydrocyclopropa[*c*]naphtho[2,1-b]azepin-6-one (CNA) alkylation aubunit: structural features that govern reactivity and reaction regioselectivity. *J. Org. Chem.* **1997,** *62*, 5849-5863.

70. Lajiness, J. P.; Boger, D. L. Synthesis and characterization of a cyclobutane duocarmycin derivative incorporating the 1,2,10,11-tetrahydro-9*H*-cyclobuta[*c*]benzo[*e*]indol-4-one (CbBI) alkylation subunit. *J. Am. Chem. Soc.* **2010,** *132*, 13936-13940.

71. Boger, D. L.; Santillán, J., A.; Searcey, M.; Jin, Q. Synthesis and evaluation of duocarmycin and CC-1065 analogues containing modifications in the subunit linking amide. *J. Org. Chem.* **1999,** *64*, 5241-5244.

72. Boger, D. L.; Santillán, A.; Searcey, M.; Jin, Q. Critical role of the linking amide in CC-1065 and the duocarmycins: Implications on the source of DNA alkylation catalysis. *J. Am. Chem. Soc.* **1998,** *120*, 11554-11557.

73. Warpehoski, M. A.; Harper, D. E.; Mitchell, M. A.; Monroe, T. J. Reversibility of the covalent reaction of CC-1065 and analogs with DNA. *Biochemistry* **1992,** *31*, 2502-2508.

74. Lee, C.; Gibson, N. W. DNA interstrand cross-links induced by the cyclopropylpyrroloindole antitumor agent bizelesin are reversible upon exposure to alkali. *Biochemistry* **1993,** *32*, 9108-9114.

75. McGovren, J. P.; Clarke, G. L.; Pratt, E. A.; Dekoning, T. F. Preliminary toxicity studies with the DNA-binding antibiotic, CC-1065. *J. Antibiot.* **1984,** *37*, 63-70.

76. Aristoff, P. A.; Johnson, P. D.; Sun, D.; Hurleyt, L. H. Synthesis and biochemical evaluation of the CBI-PDE-I-dimer, a benzannelated analog of (+)-CC-1065 that also produces delayed toxicity in mice. *J. Med. Chem.* **1993,** *36*, 1956-1963.

77. Boger, D. L.; Boyce, C.; Garbaccio, R.; Searcey, M.; Jin, Q. CBI prodrug analogs of CC-1065 and the duocarmycins. *Synthesis* **1999**, 1505-1509.

78. Boger, D. L.; Ishizaki, T.; Sakya, S. M.; Munk, S. A.; Kitos, P. A.; Jin, Q.; Besterman, J. M. Synthesis and preliminary evaluation of (+)-CBI-indole2: An enhanced functional analog of (+)-CC-1065. *Bioorg. Med. Chem. Lett.* **1991,** *1*, 115-120.

79. Yang, S.; Denny, W. A. A new short synthesis of 3-substituted 5-amino-1-(chloromethyl)-1,2-dihydro-3*H*-benzo[*e*]indoles (amino-CBIs). *J. Org. Chem.* **2002,** *67*, 8958-8961.

80. Milbank, J. B. J.; Tercel, M.; Atwell, G. J.; Wilson, W. R.; Hogg, A.; Denny, W. A. Synthesis of 1-substituted 3-(chloromethyl)-6-aminoindoline (6-amino-*seco*-CI) DNA minor groove alkylating agents and structure-activity relationships for their cytotoxicity. *J. M. Chem.* **1999,** *42*, 649-658.

81. Tietze, L. F.; Schuster, H. J.; Hampel, S. M.; Rühl, S.; Pfoh, R. Enantio- and diastereoselective synthesis of duocarmycine-based prodrugs for a selective treatment of cancer by epoxide opening. *Chem. Eur. J.* **2008,** *14*, 895-901.

82. Atkinson, J. M.; Siller, C. S.; Gill, J. H. Tumour endoproteases: The cutting edge of cancer drug delivery? *Brit. J. Pharmacol.* **2008,** *153*, 1344-1352.

83. Tranoy-Opalinski, I.; Fernandes, A.; Thomas, M.; Gesson, J. P.; Papot, S. Design of self-Immolative linkers for tumour-activated prodrug therapy. *Anticancer Agents Med. Chem.* **2008,** *8*, 618-637.

84. Papot, S.; Tranoy, I.; Tillequin, F.; Florent, J. C.; Gesson, J. P. Design of selectively activted anticancer prodrugs: Elimination and cyclisation strategies. *Curr. Med. Chem. Anticancer Agents* **2002,** *2*, 155-185.

85. Kamal, A.; Tekumalla, V.; Raju, P.; Naidu, V. G. M.; Diwan, P. V.; Sistla, R. Pyrrolo[2,1-c][1,4]benzodiazepine-β-glucuronide prodrugs with a potential for selective therapy of solid tumors by PMT and ADEPT strategies. *Bioorg. Med. Chem. Lett.* **2008,** *18*, 3769-3773.

86. Bagshawe, K. D. Antibody directed enzymes revive anti-cancer prodrugs concept. *Brit. J. Cancer* **1987,** *56*, 531-532.

87. Tietze, L. F.; Krewer, B. Antibody-Directed Enzyme Prodrug Therapy: A promising approach for a selective treatment of cancer based on prodrugs and monoclonal antibodies. *Chem. Biol. Drug Des.* **2009,** 74, 205-211.

88. Tietze, L. F.; Schuster, H. J.; Schmuck, K.; Schuberth, I.; Alves, F. Duocarmycin-based prodrugs for cancer prodrug monotherapy. *Bioorg. Med. Chem.* **2008,** *16*, 6312-6318.

89. Niculescu-Duvaz, I.; Springer, C. J. Introduction to the background, principles, and state of the art in suicide gene therapy. *Mol. Biotechnol.* **2005,** *30*, 71-88.

90. Singh, P.; LeBeau, A. M.; Lilja, H.; Denmeade, S. R.; Isaacs, J. T. Molecular insights into substrate specificity of prostate specific antigen through structural modeling. *Proteins* **2009,** *77*, 984-993.

91. Choi, K. Y.; Swierczewska, M.; Lee, S.; Chen, X. Protease-activated drug development. *Theranostics* **2012,** *2*, 156-178.

92. Denmeade, S. R.; Nagy, A.; Gao, J.; Lilja, H.; Schally, A. V.; Isaacs, J. T. Enzymatic activation of a doxorubicin-peptide prodrug by prostate-specific antigen. *Cancer Res.* **1998,** *58*, 2537-2540.

93. Ferrieu-Weisbuch, C.; Michel, S.; Collomb-Clerc, E.; Pothion, C.; Deléage, G.; Jolivet-Reynaud, C. Characterization of prostate-specific antigen binding peptides selected by phage display technology. *J. Mol. Recogn.* **2006,** *19*, 10-20.

94. Kumar, S. K.; Williams, S. A.; Isaacs, J. T.; Denmeade, S. R.; Khan, S. R. Modulating paclitaxel bioavailability for targeting prostate cancer. *Bioorg. Med. Chem.* **2007,** *15*, 4973-4984.

95. Michel, S.; Collomb-Clerc, E.; Geourjon, C.; Charrier, J. P.; Passagot, J.; Courty, Y.; Deléage, G.; Jolivet-Reynaud, C. Selective recognition of enzymatically active prostate-specific antigen (PSA) by anti-PSA monoclonal antibodies. *J. Mol. Recogn.* **2005,** *18*, 225-235.

96. DiPaola, R. S.; Rinehart, J.; Nemunaitis, J.; Ebbinghaus, S.; Rubin, E.; Capanna, T.; Ciardella, M.; Doyle-Lindrud, S.; Goodwin, S.; Fontaine, M.; Adams, N.; Williams, A.; Schwartz, M.; Winchell, G.; Wickersham, K.; Deutsch, P.; Yao, S.-L. Characterization of a novel prostate-specific antigen-activated peptide-doxorubicin conjugate in patients with prostate cancer. *J. Clin. Oncol.* **2002,** *20*, 1874-1879.

97. DeFeo-Jones, D.; Garsky, V. M.; Wong, B. K.; Feng, D. M.; Bolyar, T.; Haskell, K.; Kiefer, D. M.; Leander, K.; McAvoy, E.; Lumma, P.; Wai, J.; Senderak, E. T.; Motzel, S. L.; Keenan, K.; Van Zwieten, M.; Lin, J. H.; Freidinger, R.; Huff, J.; Oliff, A.; Jones, R. E. A

peptide-doxorubicin 'prodrug' activated by prostate-specific antigen selectively kills prostate tumor cells positive for prostate-specific antigen *in vivo*. *Nat. Med.* **2000,** *6*, 1248-52.

98. Mhaka, A.; Denmeade, S. R.; Yao, W.; Isaacs, J. T.; Khan, S. R. A 5-fluorodeoxyuridine prodrug as targeted therapy for prostate cancer. *Bioorg. Med. Chem. Lett.* **2002,** *12*, 2459-2461.

99. Denmeade, S. R.; Lou, W.; Lövgren, J.; Malm, J.; Lilja, H.; Isaacs, J. T. Specific and efficient peptide substrates for assaying the proteolytic activity of prostate-specific antigen. *Cancer Res.* **1997,** *57*, 4924-4930.

100. Denmeade, S. R.; Jakobsen, C. M.; Janssen, S.; Khan, S. R.; Garrett, E. S.; Lilja, H.; Christensen, S. B.; Isaacs, J. T. Prostate-specific antigen-activated thapsigargin prodrug as targeted therapy for prostate cancer. *J. Natl. Cancer Inst.* **2003,** *95*, 990-1000.

101. Lee, D. I.; Sumbilla, C.; Lee, M.; Natesavelalar, C.; Klein, M. G.; Ross, D. D.; Inesi, G.; Hussain, A. Mechanisms of resistance and adaptation to thapsigargin in androgen-independent prostate cancer PC3 and DU145 cells. *Arch. Biochem. Biophy.* **2007,** *464*, 19-27.

102. Schuster, H. J.; Krewer, B.; von Hof, J. M.; Schmuck, K.; Schuberth, I.; Alves, B.; Tietze, L. F. Synthesis of the first spacer containing prodrug of a duocarmycin analogue and determination of its biological activity. *Org. Biomol. Chem.* **2010,** *8*, 1833-1842.

103. Ge, Y.; Wua, X.; Zhang, D.; Hua, L. 3-Aminoxypropionate-based linker system for cyclization activation in prodrug design. *Bioorg. Med. Chem. Lett.* **2009,** *19*, 941-944.

104. Manabe, S.; Machida, H.; Aihara, Y.; Yasunaga, M.; Itoa, Y.; Matsumur, Y. Development of a diketopiperazine-forming dipeptidyl Gly-Pro spacer for preparation of an antibody–drug conjugate. *Med. Chem. Commun.* **2013,** *4*, 792-796.

105. Suaifan, G. A. R. Y.; Arafat, T.; Threadgill, M. D. Synthetic approaches to peptides containing the L-Gln-L-Val-D(S)-Dmt motif. *Bioorg. Med.Chem.* **2007,** *15*, 3474-3488.

106. Suaifan, G. A. R. Y.; Mahon, M. F.; .; Arafat, T.; Threadgill, M. D. Effects of steric bulk and stereochemistry on the rates of diketopiperazins formation from N-aminoacyl-2,2-dimethylthiazolidine-4-carboxamides (Dmt dipeptide amides)-a model for a new prodrug linker system. *Tetrahedron* **2006,** *62*, 11245-11266.

107. Brady, S. F.; Pawluczyk, J. M.; Lumma, P. K.; Feng, D.-M.; Wai, J. M.; Jones, R.; DeFeo-Jones, D.; Wong, B. K.; Miller-Stein, C.; Lin, J. H.; Oliff, A.; Freidinger, R. M.; Garsky, V. M. Design and synthesis of a pro-drug of vinblastine targeted at treatment of prostate cancer with enhanced efficacy and reduced systemic toxicity. *J. Med. Chem.* **2002,** *45*, 4706-4715.

108. Han, S.; Choi, K. N-Arylcarbonyl*pseudo*prolines as tunable chiral derivatizing agents for the determination of the absolute configuration of secondary alcohols. *Eur. J. Org. Chem.* **2011,** *2011*, 2920-2923.

109. Wöhr, T.; Mutter, M. *Pseudo*-prolines in peptide synthesis: Direct insertion of serine and threonine derived oxazolidines in dipeptides. *Tetrahedron Lett.* **1995,** *36*, 3847-3848.

110. Abedini, A.; Raleigh, D. P. Incorporation of *pseudo*proline derivatives allows the facile synthesis of human IAPP, a highly amyloidogenic and aggregation-arone polypeptide. *Org. Lett.* **2005,** *7*, 693-696.

111. Wöhr, T.; Wahl, F.; Nefzi, A.; Rohwedder, B.; Sato, T.; Sun, S.; Mutter, M. *Pseudo*-prolines as a solubilizing, structure-disrupting protection technique in peptide synthesis. *J. Am. Chem. Soc.* **1996,** *118*, 9218-9227.

112. Maeda, H.; Wu, J.; Sawa, T.; Matsumura, Y.; Hori, K. Tumor vascular permeability and the EPR effect in macromolecular therapeutics: A review. *J. Control. Release* **2000,** *65*, 271-284.

113. Arias, J. L. Drug targeting strategies in cancer treatment. *Mini-Rev. Med. Chem.* **2011,** *11*, 1-17.

114. Bisht, S.; Maitra, A. Dextran–doxorubicin/chitosan nanoparticles for solid tumor therapy. *Wiley Interdisciplinary Reviews: Nanomedicine and Nanobiotechnology* **2009,** *1*, 415-425.

115. Cao, N.; Feng, S.-S. Doxorubicin conjugated to D-α-tocopheryl polyethylene glycol 1000 succinate (TPGS): Conjugation chemistry, characterization, *in vitro* and *in vivo* evaluation. *Biomaterials* **2008,** 29, 3856-3865.

116. Marcus, Y.; Sasson, K.; Fridkin, M.; Shechter, Y. Turning low-molecular-weight drugs into prolonged acting prodrugs by reversible pegylation: A study with gentamicin. *J. Med. Chem.* **2008,** *51*, 4300-4305.

117. Seymour, L. W.; Ulbrich, K.; Steyger, P. S.; Brereton, M.; Subr, V.; Strohalm, J.; Duncan, R. Tumour tropism and anti-cancer efficacy of polymer-based doxorubicin prodrugs in the treatment of subcutaneous murine B16F10 melanoma. *Brit. J. Cancer* **1994,** *70*, 636-641.

118. Vasey, P.; Kaye, S.; Morrison, R.; Twelves, C.; Wilson, P.; Duncan, R.; Thomson, A.; Murray, L.; Hilditch, T.; Murray, T.; Burtles, S.; Fraier, D.; Frigerio, E.; Cassidy, J. Phase I clinical and pharmacokinetic study of PK1 [N-(2- hydroxypropyl)methacrylamide copolymer doxorubicin]: First member of a new class of chemotherapeutic agents-Drug-polymer conjugates. *Clin. Cancer Res.* **1999,** *5*, 83-94.

119. Chandran, S. S.; Nan, A.; Rosen, D. M.; Ghandehari, H.; Samuel R. Denmeade, S. R. A prostate-specific antigen–activated N-(2-hydroxypropyl) methacrylamide copolymer prodrug as dual-targeted therapy for prostate cancer. *Mol. Cancer Ther.* **2007,** *6*, 2928-2937.

120. Roberts, M. J.; Bentley, M. D.; Harris, J. M. Chemistry for peptide and protein PEGylation. *Adv. Drug Deliver. Rev.* **2002,** *54*, 459-476.

121. Choi, H.; Chuna, M.; Lee, S. H.; Jang, M. H.; Kimb, H. D.; Jung, C. S.; Oh, S. Y. *In vitro* and *in vivo* study of poly(ethylene glycol) conjugated ketoprofen to extend the duration of action. *Int. J. Pharmaceutics* **2007,** *341*, 50-57.

122. Greenwald, R. B.; Choe, Y. H.; McGuire, J.; Conover, C. D. Effective drug delivery by PEGylated drug conjugates. *Adv. Drug Deliver. Rev.* **2003,** *55*, 217-250.

123. Veronese, F. M.; Schiavon, O.; Pasut, G.; Mendichi, R.; Andersson, L.; Tsirk, A.; Ford, J.; Wu, G.; Kneller, S.; Davies, J.; Duncan, R. PEG-doxorubicin conjugates: Influence of polymer structure on drug release, *in vitro* cytotoxicity, biodistribution, and antitumor activity. *Bioconjugate Chem.* **2005,** *16*, 775-784.

124. Tietze, L. F.; Major, F.; Schuberth, I.; Dirk A. Spiegl, D. A.; Krewer, B.; Maksimenka, K.; Bringmann, G.; Magull, J. Selective treatment of cancer: Synthesis, biological evaluation and structural elucidation of novel analogues of the antibiotic CC-1065 and the duocarmycins. *Chem. Eur. J.* **2007,** *13*, 4396-4409.

125. Tietze, L. F.; Herzig, T.; Fecher, A.; Haunert, F.; Schuberth, I. Highly selective glycosylated prodrugs of cytostatic CC-1065 analogues for antibody-directed enzyme tumor therapy. *Chem. Biochem.* **2001,** *2*, 758-765.

126. Boger, D. L.; Yun, W.; Teegarden, B. R. An improved synthesis of 1,2,9,9a-tetrahydrocyclopropa[*c*]benz[*e*]indol-4-one (CBI): A simplified analogue of the CC-1065 alkylation subunit. *J. Org. Chem.* **1992,** *57*, 2813-287.

127. Boger, D. L.; Ishizaki, T. Synthesis of *N*-(*tert*-butyloxycarbonyl)-CBI, CBI, CBI-$CDPI_1$, and CBI-$CDPI_2$: Enhanced functional analogues of CC-1065 incorporating the 1,2,9,9a tetrahydrocyclopropa[*c*]benz[*e*]indol-4-one (CBI) left-hand subunit. *J. Org. Chem.* **1990,** *55*, 5823-5832.

128. Boger, D. L.; McKie, J. A. An eficient synthesis of 1,2,9,9a-tetrahydrocyclo-propa[*c*]benz[*e*]indol-4-one (CBI): An enhanced and simplified analogue of the CC-1065 and duocarmycin alkylation subunits. *J. Org. Chem.* **1995,** *60*, 1271-1275.

129. Tietze, L. F.; Major, F.; Schuberth, I. Antitumor agents: Development of highly potent glycosidic guocarmycin analogues for selective cancer therapy. *Angew. Chem. Int. Ed.* **2006,** *45*, 6574–6577.

130. Hodgson, H. H.; Smith, E. W. The mononitration of α-naphthol and of α-naphthyl methyl ether, and the monoreduction of 2,4-dinitro-1-naphthol. *J. Chem. Soc.* **1935**, 671-674.

131. Clayden, R.; Greeves, N.; Warren, S.; Wothers, P. *Organic chemistry*. Oxford university press: New York, 2001.

132. Mori, A.; Mizusaki, T.; Ikawa, T.; T., M.; Monguchi, Y.; Sajiki, H. Mechanistic study of a Pd/C-catalyzed reduction of aryl sulfonates using Mg-MeOH-$NH_4$OAc system. *Chem. Eur. J.* **2007,** *13*, 1432-1441.

133. Peterson, G. A.; Kunng, F.-A.; McCallum, J. S.; Wulffe, W. D. Palladium catalyzed reduction of aryl triflates-Utilization in the synthesis of angelicin, olivin and chromomycinone from phenolsproduced in the benzannulation reaction of chromium carbenecomplexes. *Tetrahedron Lett.* **1987,** *28*, 1381-1384.

134. Cacchi, S.; Ciattini, P. G.; Morera, E.; Ortar, G. Palladium-catalysed triethylammonium formate reduction of aryl triflates. A selective method for deoxygenation of phenols. *Tetrahedron. Lett.* **1986,** *27*, 5541-5544,.

135. Morey, J.; Saá, J. M. Solid state redox chemistry of hydroquinones and quinones. *Tetrahedron* **1993,** *49*, 105-112.

136. Oatis, J., J. E.; Walle, T.; Daniell, H. B.; Gaffney, T. E.; Knapp, D. R. Synthesis of 4'-hydroxypropranolol sulfate, a major non-β-blocking propranolol metabolite in man. *J. Med. Chem.* **1985,** *28*, 822-824.

137. Barrero, A. F.; Alvarez-Manzaneda, E. J.; Chahboun, R.; Meneses, R. Raney nickel: An efficient reagent to achieve the chemoselective hydrogenation of α,β-unsaturated carbonyl compounds. *Synlett* **1999,** *10*, 1663-1666.

138. Yang, J.; Xiong, C.; Han, X.; Zhou, L. Liquid phase hydrogenation of chloronitrobenzene to chloroaniline with PtM/CNTs (M=La, Ce, Pr, Nd and Sm) catalyst. *Indian J. Chem.* **2009,** *48A*, 1358-1363.

139. Ben-David, Y.; Gozin, M.; Portnoy, M.; Milstein, D. Reductive dechlorination of aryl chlorides catalyzed by palladium complexes containing basic, chelating phosphines. *J. Mol. Catal.* **1992,** *73*, 173-180.

140. Indra, A.; Rajamohanan, P. R.; Gopinath, C. S.; Bhaduri, S.; Lahiri, G. K. Selective hydrogenation of chloronitrobenzenes with an MCM-41 supported platinum allyl complex derived catalyst. *Appl. Catal. A-Gen.* **2011,** *399*, 117-125.

141. Twum, E. A.; Woodman, T. J.; Wang, W.; Threadgill, M. D. Observation by NMR of cationic Wheland-like intermediates in the deiodination of protected 1-iodonaphthalene-2,4-diamines in acidic media. *Org. Biomol. Chem.* **2013,** *11*, 6208-6214.

142. Hawkings, M. J.; Greco, M. N.; Powell, E.; De Garvilla, L.; Maryanoff, B. E. Novel inhibitors of chymase. 2005.

143. Houle, F. A.; Beauchamp, J. L. Photoelectron spectroscopy of methyl, ethyl, isopropyl, and *tert*-butyl radicals. Implications for the thermochemistry and structures of the radicals and their corresponding carbonium ions. *J. Am. Chem. Soc.* **1979,** *101*, 4067-4074.

144. Rathore, R.; Kochi, J. K. Donor/acceptor organizations and the electron-transfer paradigm for organic reactivity. *Adv. Phys. Org. Chem.* **2000,** *35*, 193-318.

145. Mascal, M.; Hansen, J. Design, synthesis and metal binding properties of a mixed-donor macrobicycle. *Chem. Commun.* **1998**, 355-356.

146. Olah, G. A.; Lin, H. C.; Mo, Y. K. Stable carbocations. CXXXIX. Nitro- and chlorohexamethylbenzeneium ions and 1-nitro- and 1-chloro-2,4,6-trifluoromesitylenium ions. *J. Am. Chem. Soc.* **1972,** *94*, 3667-3669.

147. Reed, C. A.; Fackler, N. L. P.; Kim, K.-C.; Stasko, D.; Evans, D. R.; Boyd, P. D. W.; Rickard, C. E. F. Isolation of protonated arenes (Wheland intermediates) with BArF and carborane anions. A novel crystalline superacid. *J. Am. Chem. Soc.* **1999,** *121*, 6314-6315.

148. Reed, C. A.; Kim, K.-C.; Stoyanov, E. S.; Stasko, D.; Tham, F. S.; Mueller, L. J.; Boyd, P. D. W. Isolating benzenium ion salts. *J. Am. Chem. Soc.* **2003,** *125*, 1796-1804.

149. Boga, C.; Del Vecchio, E.; Forlani, L.; Mazzanti, A.; Lario, C. M.; Todesco, P. E.; Tozzi, S. Meisenheimer-Wheland complexes between 1,3,5-tris(N,N-dialkylamino)benzenes and 4,6-dinitrotetrazolo[1,5-a]pyridine. Evidence of reversible C−C coupling in the $S_EAr/S_NAr$ reaction. *J. Org. Chem.* **2009,** *74*, 5568-5575.

150. Katsuki, T.; Sharpless, K. B. The first practical method for asymmetric epoxidation. *J. Am. Chem. Soc.* **1980,** *102*, 5974-5976.

151. Pickard, S. T.; Smith, H. E.; Polavarapu, P. L.; Black, T. M.; Rat, A.; Yang, D. Synthesis, experimental and *ab initio* theoretical vibrational circular dichroism, and absolute configurations of substituted oxiranes. *J. Am. Chem. Soc.* **1992,** *114*, 6850-6857.

152. Rossiter, B. E.; Katsuki, T.; Sharpless, K. B. Asymmetric epoxidation provides shortest routes to four chiral epoxy alcohols which are key intermediates in syntheses of methymycin, erythromycin, leukotriene C-1, and disparlure. *J. Am. Chem. Soc.* **1981,** *103*, 465-467.

153. White, J. D.; Theramongkol, P.; Kuroda, C.; Engebrecht, J. R. Enantioselective total synthesis of (-)-monk acid C *via* carbosulfenylation of a dihydropyran. *J . Org. Chem.* **1988,** *53*, 5909-5921.

154. Klunder, J. M.; Onami, T.; Sharpless, K. B. Arenesulfonate derivatives of homochiral glycidol: Versatile chiral building blocks for organic synthesis. *J. Org. Chem.* **1989,** *54*, 1295-1304.

155. Tietze, L. F.; Schuster, H. J.; von Hof, J. M.; Hampel, S. M.; Colunga, J. F.; Michael John, M. Atropisomerism of aromatic carbamates. *Chem. Eur. J.* **2010,** *16*, 12678–12682.

156. Boger, D. L.; McKie, J. A.; Boyce, C. W. Asymmetric synthesis of the CBI alkylation subunit of the CC-1065 and duocarmycin analogues. *Synlett* **1997**, 515-517.

157. Furuyama, T.; Yonehara, M.; Arimoto, S.; Kobayashi, M.; Matsumoto, Y.; Uchiyama, M. Development of highly chemoselective bulky zincate complex. $^{t}Bu_4ZnLi_2$: Design, structure, and practical applications in small-/macromolecular synthesis. *Chem. Eur. J.* **2008,** *14*, 10348-10356.

158. Carpino, L. A.; El-Faham, A. The diisopropylcarbodiimide/1-hydroxy-7-azabenzotriazole system: Segment coupling and stepwise peptide assembly. *Tetrahedron* **1999,** *55*, 6813-6830.

159. Valeur, E.; Bradley, M. Amide bond formation: Beyond the myth of coupling reagents. *Chem. Soc. Rev.* **2009,** *38*, 606-631.

160. Reed, G. H.; Kent, J. O.; Wittwer, C. T. High-resolution DNA melting analysis for simple and efficient molecular diagnostics. *Pharmacogenetics* **2007,** *8*, 597-608.

161. David-Cordonnier, M.-H.; Laine, W.; Lansiaux, A.; Rosu, F.; Colson, P.; de Pauw, E.; Michel, S.; Tillequin, F.; Koch, M.; Hickman, J. A.; Pierré, A.; Bailly, C. Covalent binding of antitumor benzoacronycines to double-stranded DNA induces helix opening and the formation of single-stranded DNA: Unique consequences of a novel DNA-bonding mechanism. *Mol. Cancer Ther.* **2005,** *4*, 71-80.

162. Barltrop, J. A.; Owen, T. C.; Cory, A. H.; Cory, J. G. 5-(3-carboxymethoxyphenyl)-2-(4,5-dimethylthiazolyl)-3-(4-sulfophenyl)tetrazolium, inner salt (MTS) and related analogs of 3-(4,5-dimethylthiazolyl)-2,5-diphenyltetrazolium bromide (MTT) reducing to purple water-soluble formazans as cell-viability indicators. *Bioorg. Med. Chem. Lett.* **1991,** *1*, 611-614.

163. Malich, G.; Markovic, B.; Winder, C. The sensitivity and specificity of the MTS tetrazolium assay for detecting the *in vitro* cytotoxicity of 20 chemicals using human cell lines. *Toxicology* **1997,** *124*, 179-192.

164. Wang, P.; Henning, S. M.; Heber, D. Limitations of MTT and MTS-based assays for measurement of antiproliferative activity of green tea polyphenols. *PLoS ONE* **2010,** *5*, 1-10.

165. Reiter, R. J.; Tan, D. X.; Manchester, L. C.; Korkmaz, A.; Fuentes-Broto, L.; Hardman, W. E.; Rosales-Corral, S. A.; Qi, W. A walnut-enriched diet reduces the growth of LNCaP human prostate cancer xenografts in nude mice. *Cancer Invest.* **2013,** *31*, 365–373.

166. Tercel, M.; Lee, H. H.; Yang, S.; Liyanage, H. D. S.; Mehta, S. Y.; Boyd, P. D. W.; Jaiswal, J. K.; Tan, K. L.; Pruijn, F. B. Preparation and antitumour properties of the enantiomers of a hypoxia-selective nitro analogue of the duocarmycins. *Chem. Med. Chem.* **2011,** *6*, 1860-1871.

167. Boger, D. L.; Johnson, D. S.; Yun, W. (+)- And ent-(-)-duocarmycin SA and (+)- and ent-(-)-N-Boc-DSA DNA alkylation properties. Alkylation site models that accommodate the offset AT-rich adenine $N^3$ alkylation selectivity of the enantiomeric agents. *J. Am. Chem. Soc.* **1994,** *116*, 1635-1656.

168. Isidro-Llobet, A.; Alvarez, M.; Albericio, F. Amino acid-protecting groups. *Chem. Rev.* **2009,** *109*, 2455-2504.

169. Pietta, P. G.; Biondi, P. A.; Brenna, O. Comparative acidic cleavage of methoxybenzyl-protected amides of amino acids. *J. Org. Chem.* **1976,** *41*, 703-704.

170. Marshall, G. R.; Pietta, P. G.; Cavallo, P. 2,4-Dimethoxybenzyl as a protecting group for glutamine and asparagine in peptide synthesis. *J. Org. Chem.* **1971,** *36*, 3966-3970.

171. Henkel, B.; Zhang, L.; Goldammer, C.; Bayer, E. Combined solid phase and solution synthesis of the fully protected segment 74-99 of HIV 1-protease with the application of a new trityl-linker. *Z. Naturforsch. B.* **1996,** *51*, 1339-1346.

172. Gita, P. M.; Yusuf, A. O.; Bhatt, B. M. Application of tetralinyls as carboxamide protecting groups in peptide synthesis. *Bull. Chem. Soc. Ethiopia* **1998,** *12*, 35-43.

173. Franzen, H. M.; Nagren, K.; Grehn, L.; Langstrom, B.; Ragnarsson, U. Preparation and $^{11}$C-labelling of a substance P analogue containing D-tryptophan in positions 7 and 9. *J. Chem. Soc. Perkin Trans. 1*. **1988**, 497-502.

174. Sieber, P.; Riniker, B. Protection of carboxamide functions by the trityl residue. Application to peptide synthesis. *Tetrahedron Lett.* **1991,** *32*, 739-742.

175. Lee, J. T.; Chen, D. Y.; Yang, Z.; Ramos, A. D.; Hsieh, J. J. D.; Bogyo, M. Design, syntheses, and evaluation of Taspase1 inhibitors. *Bioorg. Med. Chem. Lett.* **2009,** *19*, 5086-5090.

176. Jelinski, M.; Hamacher, K.; Coenen, H. H. C-Terminal $^{18}$F-fluoroethylamidation exemplified on [Gly-$OH^9$] oxytocin. *J. Label Compd. Radiopharm.* **2002,** *45*, 217-229.

177. Ramesh, D.; Wieboldt, R.; Billington, A. P.; Carpenter, B. K.; Hess, G. P. Photolabile precursors of biological amides: Synthesis and characterization of caged o-nitrobenzyl derivatives of glutamine, asparagine, glycinamide, and γ-aminobutyramide. *J. Org. Chem.* **1993,** *58*, 4599-4605.

178. Beauchard, A.; Twum, E. A.; Lloyd, M. D.; Threadgill, M. D. *S*-2-Amino-4-cyanobutanoic acid (β-cyanomethyl-L-Ala) as an atom-efficient solubilising synthon for L-glutamine. *Tetrahedron Lett.* **2011,** *52*, 5311-5314.

179. Ressler, C.; Ratzkin, H. Synthesis of β-cyano-L-alanine and γ-cyano-α-L-aminobutyric acid, dehydration products of L-asparagine and L-glutamine; A new synthesis of amino acid nitriles. *J. Org. Chem.* **1961,** *26*, 3356-3360.

180. Campagna, F.; Carotti, A.; Casin, G. A convenient synthesis of nitriles from primary amides under mild conditions. *Tetrahedron Lett.* **1977,** *21*, 1813-1816.

181. Merck. *Peptide synthesis*. Novabiochem: 2008-2009.

182. Bollhagen, R.; Schmiedberger, M.; Barlos, K.; Grell, E. A new reagent for the cleavage of fully protected peptides synthesised on 2-chlorotrityl chloride resin. *J. Chem. Soc., Chem. Commun.* **1994**, 2559-2560.

183. Purchase, I. F. H.; Kalinowski, A. E.; Ishmael, J.; Wilson, J.; Gore, C. W.; Chart, I. S. Lifetime carcinogenicity study of 1- and 2-naphthylamine in dogs. *Brit. J. Cancer* **1981,** *44*, 892-901.

184. Sunderland, P. T.; Woon, E. C. Y.; Dhami, A.; Bergin, A. B.; Mahon, M. F.; Wood, P. J.; Jones, L. A.; Tully, S. R.; Lloyd, M. D.; Thompson, A. S.; Javaid, H.; Martin, N. M. B.; Threadgill, M. D. 5-Benzamidoisoquinolin-1-ones and 5-(ω-carboxyalkyl)isoquinolin-1-ones as isoform-selective inhibitors of poly(ADP-ribose) polymerase 2 (PARP-2). *J. Med. Chem.* **2011,** *54*, 2049-2059.

185. McDonald, M. C.; Mota-Filipe, H.; Wright, J. A.; Abdelrahman, M.; Michael D. Threadgill, M. D.; Thompson, A. S.; Thiemermann, C. Effects of 5-aminoisoquinolinone, a water-soluble, potent inhibitor of the activity of poly(ADP-ribose) polymerase on the organ injury and dysfunction caused by haemorrhagic shock. *Brit. J. Pharmacol.* **2000,** *130*, 843-850.

186. Cuzzocrea, S.; Mazzon, E.; Di Paola, R.; Genovese, T.; Patel, N. S. A.; Muià, C.; Michael D. Threadgill, M. D.; De Sarro, A.; Thiemermann, C. 5-Aminoisoquinolinone reduces colon injury by experimental colitis. *N-S. Arch. Pharmacol.* **2004,** *370*, 464-473.

187. Chartterjee, P. K.; Chatterjee, B. E.; Pedersen, H.; Sivarajah, A.; Mcdonald, M. C.; Mota-Filipe, H.; Brown, P. A. J.; Stewart, K. N.; Cuzzocrea, S.; Threadgill, M. D.; Thiemermann, C. 5-Aminoisoquinolinone reduces renal injury and dysfunction caused by experimental ischemia/reperfusion. *Kidney Int.* **2004,** *65*, 499-509.

188. Kesten, S. J.; Johnson, J.; Werbel, L. M. Antimalarial drugs. 61. Synthesis and antimalarial effects of 4-[(7-chloro-4-quinolinyl)amino]-2-[(diethylamino)methyl]-6-alkylphenols and their $N^{\omega}$-oxides. *J. Med. Chem.* **1987,** *30*, 906-911.

189. Keller, M.; Wöhr, T.; Dumy, P.; Patiny, L.; Mutter, M. *Pseudo*prolines in drug design: Direct insertion of *pseudo*proline systems into cyclosporin C. *Chem. Eur. J.* **2000,** *6*, 4358-4363.

190. Boger, D. L.; Boyce, C.; Garbaccio, R.; Searcey, M.; Jin, Q. CBI prodrug analogs of CC-1065 and the duocarmycins. *Synthesis* **1999,** *SI* 1505-1509.

191. van Lierop, B. J.; Jackson, W. R.; Robinson, A. J. 5,5-Dimethylproline dipeptides: An acid-stable class of *pseudo*proline. *Tetrahedron* **2010,** *66*, 5357-5366.

192. CellTiter 96® AQueous One Solution Cell Proliferation Assay. *Promega corporation* **2012,** *TB245*, 1-12.

193. Cui, L.-Q.; Liu, K.; Zhang, C. Effective oxidation of benzylic and alkane C-H bonds catalyzed by sodium O-iodobenzenesulfonate with oxone as a terminal oxidant under phase-transfer conditions. *Org. Biomol. Chem.* **2011,** *9*, 2258-2265.

194. Hunter, D. H.; Aponce, Y. 4-Iodophenylcholine: A potential myocardial imaging agent. *Cancer J . Chem.* **1984,** *62*, 2015-2018.

195. Frecentese, F.; Fiorino, F.; Perissutti, E.; Severino, B.; Magli, E.; Esposito, A.; De Angelis, F.; Massarelli, P.; Nencini, C.; Viti, B.; Santagada, V.; Caliendo, G. Efficient microwave combinatorial synthesis of novel indolic arylpiperazine derivatives as serotoninergic ligands. *Eur. J. Med. Chem.* **2010,** *45*, 752-759.

196. Robinson, R. A. 1-Dialkylaminoalkylaminoisoquinolines. *J. Am. Chem. Soc.* **1947,** *69*, 1939-1942.

197. Jorgensen, E. C.; Slade, P. Thyroxine analogs. 20. Substituted 1- and 2-naphthyl ethers of 3,5-diiodotyrosine. *J. Med. Chem.* **1971,** *14*, 1023-1026.

198. Cablewski, T.; Gurr, P. A.; Raner, K. D.; Strauss, C. R. A new, regioselective, tandem amidation reaction of electron-rich arenes. *J. Org. Chem.* **1994,** 59, 5814-5817.

199. A. Rabbani, A.; Khodabandeh, M. Studies on the binding of the alkylating agent sulfur mustard to calf thymus chromatin. *Med. J. Islamic Rep. Iran.* **1993,** *7*, 43-46.

200. Zhang, P.; Chen, J.; Liang, Y. DNA binding, cytotoxicity, and apoptotic-inducing activity of ruthenium(II) polypyridyl complex. *Acta Biochimica. Biophysica. Sinica.* **2010,** *42*, 440-449.

201. Reichmann, M. E.; Rice, S. A.; Thomas, C. A.; Doty, P. A further examination of the molecular weight and size of desoxypentose nucleic acid. *J. Am. Chem. Soc.* **1954,** *76*, 3047-3053.

202. Ciupa, A.; De Bank, P. A.; Mahon, M. F.; Wood, P. J.; Caggiano, L. Synthesis and antiproliferative activity of some 3-(pyrid-2-yl)-pyrazolines. *Med. Chem. Comm. (Suppl.)* **2013,** *4*, 956-961.